3.3.4 Number of books and chapters in edited volumes / books published, and papers in national/international conference-proceedings per teacher during the last five years (6)

Sl. No.	Name of the teacher	Title of the book/chapters published	Title of the paper	Name of the conference	Year of publication
1	P.Kotteeswaran	NA	Adsorption efficiency of synthetic nano iron oxideand commercial activated carbon towards the removal of the Cu(II) ions comparative study	International Confernce on Advances in New Materials	2013-2014
2	S.Kannan	On-line Economic Dispatch of Distributed Generation Using Artificial Neural Networks.	NA	NA	2014-2015
3	S.Kannan	Multi-objective Generation Scheduling using Modified Non-dominated Sorting Genetic Algorithm-II	NA	NA	2014-2015
4	Balaji Ganesh Rajagopal	NA	Indian Road Traffic Surveillance System using Blob Tracking for ATIS Applications	Secure Knowledge Management	2014-2015
5	K Vijayalakshmi	NA	Detecting contrast enhancement based image forgeries by parallel approach	IEEE International Conference Electronics and Communication Systems	2014-2015
6	S.Kannan	NA	A Production Cost Model for Reactive Power in Electricity Market	National Conference on Innovations in Engineering, Science and Technology	2014-2015
7	S.Kannan	NA	Asset Management in Smart Grids Using Improved Dissolved Gas Analysis	International Conference on Power and Advanced Control Engineering	2015-2016
8	S.Kannan	NA	Electricity Generation Planning for Tamil Nadu by Considering GHG Emission Using LEAP	International Conference on Soft Computing Systems	2015-2016

9	S.Rajakarunakaran	NA	Fuzzy based optimization to reduce the blind spots in heavy transport vehicles	1st National Conference on Technological Advances in Mechanical Engineering	2015-2016
10	J.Jerold John Britto	NA	Damage Detection of Cost Effective CRRP Composite Structure Using Fiber Optic Sensor Under Dynamic Load.	International Conference on Productivity, Efficiency and Competitiveness in Design and Manufacturing	2015-2016
11	C.Subha	NA	Utilization of Dry Solid Waste in Bricks	National Conference on Innovations in Engineering, Science and Technology	2016-2017
12	R.Muruganantham	NA	Thermal Conductive Concrete Using Slags	National Conference on Innovations in Engineering, Science and Technology	2016-2017
13	T.Chockalingam	NA	Laboratory Study of Porosity and Strength Properties of Pervious Concrete	National Conference on Innovations in Engineering, Science and Technology	2016-2017
14	R.Chithradevi	NA	Experimental Investigation on Waste Glass Powder as Partial Replacement of Cement in Concrete	National Conference on Innovations in Engineering, Science and Technology	2016-2017
15	R.Venkatesh	NA	Secure De-Duplication in Hybrid Cloud	Second National Conference on Innovations in Engineering, Science and Technology	2016-2017
16	R.Venkatesh	NA	Career Dendrogram	Second National Conference on Innovations in Engineering, Science and Technology	2016-2017
17	C.Subha	NA	Power production from wastewater using Microbial Fuel Cell	National Conference on Sustainability in Construction	2017-2018
18	R.Muruganantham	NA	Effect of Haritaki as a Retarding a water reducing admixture for Concrete	National Conference on Sustainability in Construction	2017-2018
19	T.Chockalingam	NA	Shape and Size effect on Mechanical Properties of Pervious Concrete	National Conference on Sustainability in Construction	2017-2018
20	G.Mahalakshmi	NA	Network Intrusion Detection using Machine Learning Algorithms	Second International Conference on Electronics Communication and Aerospace Technology	2017-2018

21	M.Swarna Sudha	NA	Data Mining approach for anomaly detection in social network analysis	International Conference on Recent Trends in Engineering, Computers, Information Technology and Applications	2017-2018
22	R. Ramalakshmi	NA	Automatic Gas Leakage Detection, Alerting and Booking System Using GSM	National Conference on Advanced Technologies in Robotics and Industrial Automation	2017-2018
23	T. Ramprakash	NA	Smart Door Lock System Using Quick Response	International Conference on Engineering and Advancement in Technology	2017-2018
24	D. Gopinath	NA	Wireless Health Monitoring System using Mobile phone Accessories	National Conference on Innovation in Communication Technology for social Development	2017-2018

CHE/2013-14/01

Department of Inorganic Chemistry
University of Madras

International Conference on Advances in New materials [ICAN 2014]

20th & 21st June 2014

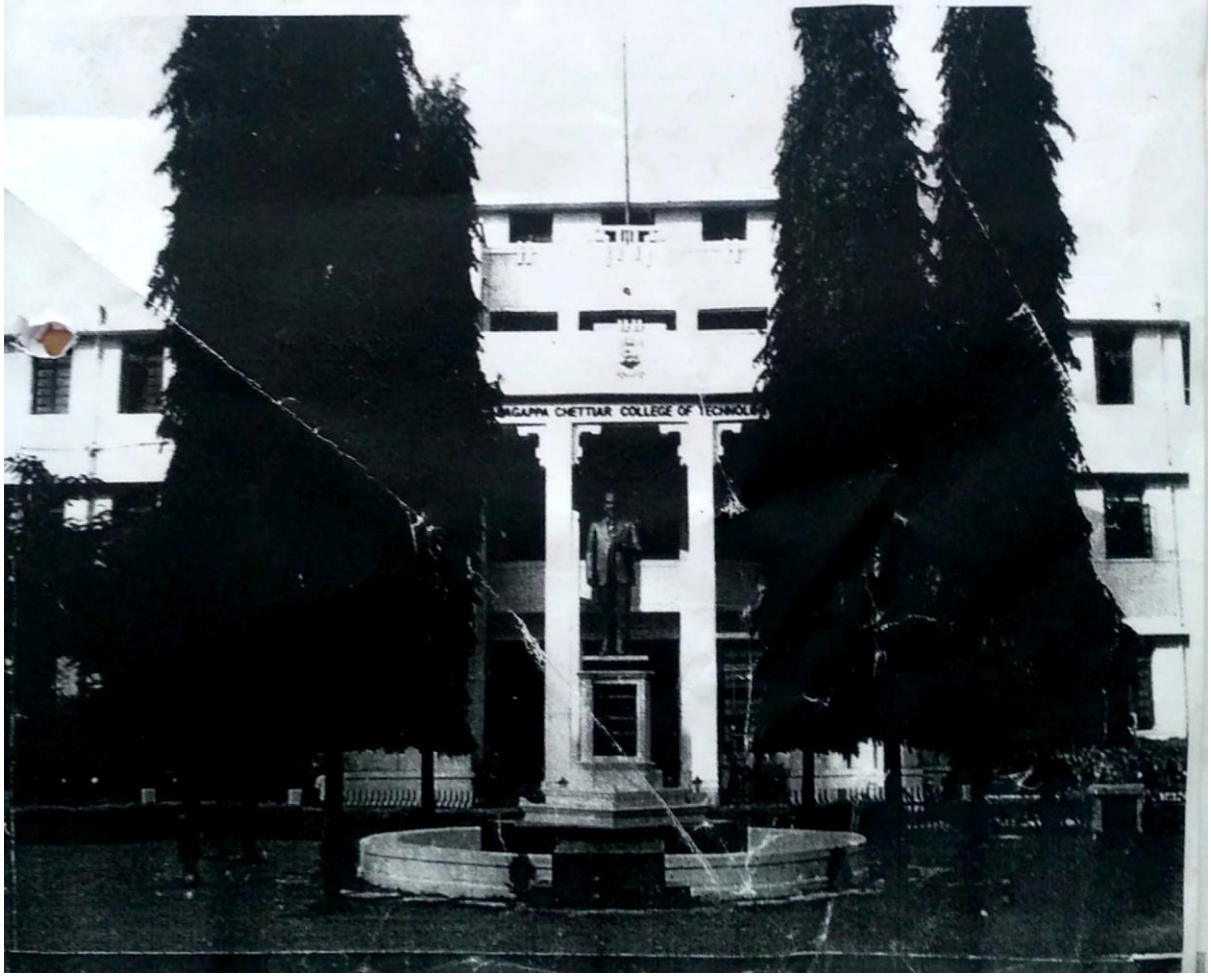

AM-9 **Adsorption Efficiency of Synthetic Nano Iron Oxide and Commercial Activated Carbon Towards the Removal of the Cu(II) Ions-Comparative Study**

G. Kanthimathi*[1], P. Thillai Arasu[1], P. Kotteeswaran[2], and M. Kottaisamy[3]

*[1]Department of Chemistry, Kalasalingam University, Krishnankoil, India – 626 126; [2]Department of Chemistry, Ramco Institute of Technology, Rajapalayam, India – 626 117; [3]Department of Chemistry, Thiagarajar College of Engineering, Madurai India – 625 015; *Email: kanthi_somu@rediffmail.com*

The adsorbent Nano Iron Oxide (SNIO) was synthesized and essential characteristics were ascertained using FT-IR, SEM, and EDAX techniques. Commercially available carbon (CAC) was activated further by acid treatment to enhance its adsorption capacity. Adsorption experiments were carried out by using Batch method to compare the sorption behaviour of SNIO and CAC for the removal of Cu(II) ions. The study was conducted on the basis of parameters such as a function of initial concentration of the adsorbate, adsorbent dosage, contact time and pH. Freundlich and Langmuir isotherm models have been tested. The applicability of various first order kinetic equations like Natarajan-Khalaf, Lagergren, Elovich and Power functions equations were also tested. The optimum conditions of the various factors for the maximum removal of the Cu(II) ions arrived at from this studies.

Bijaya Ketan Panigrahi
Ponnuthurai Nagaratnam Suganthan
Swagatam Das (Eds.)

LNCS 8947

Swarm, Evolutionary, and Memetic Computing

5th International Conference, SEMCCO 2014
Bhubaneswar, India, December 18–20, 2014
Revised Selected Papers

On-line Economic Dispatch of Distributed Generation Using Artificial Neural Networks

M. Arumuga Babu[1(✉)], R. Mahalakshmi[2], S. Kannan[3], M. Karuppasamypandiyan[4], and A. Bhuvanesh[5]

[1] Department of EEE, Tejaa Shakthi Institute of Technology for Women, Coimbatore, India
arumuga1978@gmail.com
[2] Department of EEE, Sri Krishna College of Technology, Coimbatore, India
[3] Department of EEE, Ramco Institute of Technology, Rajapalayam, India
[4] Department of EEE, University College of Engineering, BIT Campus, Trichy, India
[5] Department of EEE, Mepco Schlenk Engineering College, Sivakasi, India

Abstract. In recent years, distributed generators (DG) are most widely installed in distribution system to meet the increasing demand and especially to reduce the losses. According to demand, dispatch of generator should be modified for economic operation. The Economic Dispatch (ED) of DGs are usually solved by conventional methods such as Lambda iteration method, Dynamic Programming etc., or any optimization technique such as Genetic algorithm (GA), Evolutionary Programming (EP) etc., This off-line methods of solving ED problem require comparatively large computation time and are not suitable for on-line applications. Therefore, it is important to estimate Real Power dispatch values within a short period. This paper presents an On-line ED of various non-renewable DGs for various demands using Artificial Neural Networks namely Back Propagation Neural Network (BPNN) and Radial Basis Function Neural Network (RBFNN). The input pattern for Neural Networks (NN) is demand and output is corresponding optimal real power dispatch. The input and output patterns for NN is obtained using evolutionary programming method. In this work two diesel engines and two fuel cells are used as DG. This case study has been illustrated in a distribution system having two types of four numbers of DGs. The test result shows that the proposed method is better for real time ED.

Keywords: Back propagation neural network · Distributed generators · Economic dispatch · Evolutionary programming · Radial basis function neural network

1 Introduction

According to the definition of CIGRE, Distributed Generation (DG) is defined as the generating plant with a capacity of less than 100 MW, usually connected to the distribution networks that are neither centrally planned nor dispatched [1]. One of the drawbacks of using non-renewable DG in distribution system is its fuel cost. Hence, to reduce this fuel cost the DGs should be optimally dispatched.

B.K. Panigrahi et al. (Eds.): SEMCCO 2014, LNCS 8947, pp. 275–283, 2015.
DOI: 10.1007/978-3-319-20294-5_24

Economic dispatch (ED) is one of the most important optimization problems in power system operation and planning. ED economically dispatch the generators according to demand while satisfying physical and operational constraints. Classical methods such as Lambda iteration, Base point Participation factor, Gradient method, Newton's method and Lagrange multiplier method can solve ED problem under the assumption that the incremental cost curves of the generating units are monotonically increasing piecewise-linear functions. However, in reality, the cost curves of generating units are non-convex. Classical based techniques fail to address these types of problems satisfactorily and lead to sub optimal solutions producing huge revenue loss over time. Dynamic programming (DP) can solve ED problem with inherently nonlinear and discontinuous cost curves. But it suffers from the curse of dimensionality or local optimality [2].

ED problems are also solved by many optimization algorithms namely Genetic algorithm (GA) [3, 4], Evolutionary Programming (EP) [5], Particle Swarm Optimization (PSO) [6], Artificial Immune system (AIS) [7], Differential Evolution Algorithm (DE) [8] Biogeography-based optimization (BBO) [9], Simulated Annealing (SA) [10] etc., The main drawbacks of these optimization algorithms are time consuming because for every demand the programs needs to be run to get optimal result. Hence, it is not suitable for on-line application.

This paper presents an online ED of four non-renewable DGs using Neural Network (NN). Two Types of NN has been developed for On-Line Estimation of ED namely Back Propagation Neural Network (BPNN) and Radial Basis Neural Network (RBFNN). The case study has been implemented on a four DGs test system.

2 Problem Formulation

The ED of DGs may be formulated as non-linear optimization problem. Two types of DGs are considered here. They are diesel engines and two fuel stacks. The objective function in a diesel engine consists of the fuel cost function similar to the cost function used for conventional generating plants. The operating cost of fuel cell system takes the fuel costs and includes the efficiency of fuel cell. The constraints include power generation capacity limits.

The objective function is:

$$minF_T = F_{diesel} + F_{fuelcell} \tag{1}$$

where, F_{diesel} is Fuel cost of diesel generator, $F_{Fuel\text{-}cell}$ is Fuel cost Fuel-cell

Subject to,

$$P_D = \sum_{i=1}^{n} P_{Gi} \tag{2}$$

$$P_G^{min} \leq P_G \leq P_G^{max} \tag{3}$$

where, P_D is Demand, P_G is Real power generation of DGs,n is number of DG's and P_G^{min}, P_G^{max} is Minimum and maximum capacity of DGs.

2.1 Diesel Generator

The objective function in a diesel engine consists of the fuel cost function similar to the cost function used for conventional thermal generating plants.

$$F_{diesel} = \sum_{i=1}^{n} \left(a_i * P_{diesel,i}^2 + b_i * P_{diesel,i} + c_i \right) \tag{4}$$

where F_{diesel} is the diesel generator fuel cost; n is the number of diesel generator; $P_{diesel,i}$ is the diesel generation output in kW of unit i. a_i, b_i, c_i are fuel cost coefficient of i^{th} generator.

2.2 Fuel Cell Plant

The operating cost of fuel cell system takes the fuel costs and includes the efficiency of fuel cell. When fuel is transferred into power, the cost function considers the efficiency of fuel cell. The generation cost of fuel cell is as follows:

$$F_{fuelcell} = \sum_{i=1}^{n} b_i \left(\frac{P_{FC,i}}{n_{FC,i}} \right) \tag{5}$$

where $F_{fuelcell}$ is the fuel cell generation cost; b_i is the natural gas cost in \$/kg; $P_{FC,i}$ is fuel cell generation of the ith plant; $n_{FC,i}$ is fuel cell efficiency of unit i.

3 Review of Neural Networks

In this work BPA based ANN and RBF based ANN is used to solve the present problem.

3.1 BPA Based ANN

A multilayer feed forward network trained by back propagation is the most popular and versatile form of neural network for pattern mapping or function approximation problem. The structure of a BPA based multilayer feed forward network is shown in Fig. 1.

The ANN utilized here contains three layers. These are input, hidden, and output layers. During the training phase, the training data is fed into the input layer. The data is propagated to the hidden layer and then to the output layer. This is called the forward pass of the Back Propagation Algorithm. In the forward pass, each node in hidden layer gets input from all the nodes of input layer, which are multiplied with appropriate weights and then summed. The output of the hidden node is the non- linear transformation of the resulting sum. Similarly each node in output layer gets input from all the nodes of hidden layer, which are multiplied with appropriate weights and then summed. The output of this node is the non-linear transformation of the resulting sum.

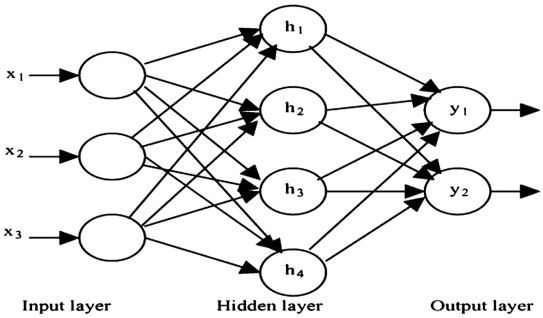

Fig. 1. Structure of BPA based neural network

3.2 RBF Based ANN

RBF networks are feed-forward networks trained using a supervised training algorithm. They are typically configured with a single hidden layer of units whose activation function is selected from a class of functions called basis functions.

Radial Basis Function Neural Network is the three layers feed forward neural network. Figure 2 shows the schematic diagram of a RBF neural network. In RBFNN the input neurons are directly fed to input layer. Then, the output of the input layer is fed to hidden layer without adding any weight. The transfer function of hidden nodes is same as that of multivariate Gaussian density function,

$$\emptyset_j(x) = \exp\left(-\frac{x - u_j^2}{2\sigma_j^2}\right) \tag{6}$$

Where x is the input vector u_j,σ_j are the center and the spread of the corresponding Gaussian function. $\| \cdot \|$ denotes the Euclidean distance between x and u_j. Then, the connections in the second layer is weighted and the output nodes are linear summation units [11].

The value of the k_{th} output node y_k is given by,

$$y_k(x) = \sum_{j=1}^{h} w_{kj}\emptyset_j(x) + w_{k0} \tag{7}$$

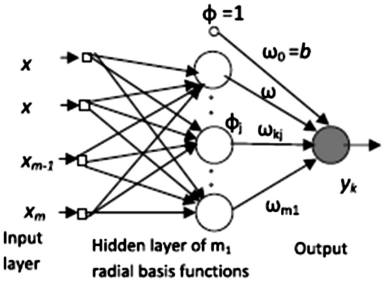

Fig. 2. Structure of RBF neural network

where w_{kj} is the connection weight between the k_{th} output node and j_{th} hidden node and w_{k0} is the bias term.

The training algorithm for RBF neural network is summarized as below.

- Determine the unit centres u_j by the K-means clustering algorithm.
- Determine the unit width σ_j using a heuristic approach that ensures the smoothness and continuity of the fitted function. The width of any hidden node is taken as the maximum Euclidean distance between the identified centres.
- Compute weights of the second layer connections are determined by linear regression using a least-squares objective function.

4 Development of Neural Network for on-Line Power Dispatch of DGs

Many optimization techniques are proposed to solve ED problem [3–10]. However, these methods are needed to solve every time when the system load changes so these methods are not suitable for the on-line power dispatch.

4.1 Training Data Development

The generation of the appropriate training data is an important step in the development of ANN models. For the ANN to accurately predict the output, the training data should represent the complete range of operating conditions of the system under consideration. For model development, a large number of training data is generated through off-line power system simulation. The schematic diagram of proposed approach is given in Fig. 3.

The procedure for generating training data to develop the neural network is as follows:

- First, a range of situations is generated by randomly varying the real power demand between 100 kW to 950 kW.

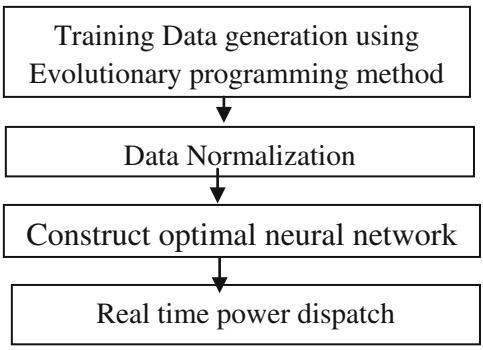

Fig. 3. Schematic diagram of the proposed approach

- For each demand compute real power dispatch of DGs using evolutionary algorithm.

4.2 Data Normalization

During training of the neural network, higher valued input variables may tend to suppress the influence of smaller ones. Also, if the raw data is directly applied to the network, there is a risk of the simulated neurons reaching the saturated conditions. If the neurons get saturated, then the changes in the input value will produce a very small change or no change in the output value. This affects the network training to a great extent. To avoid this, the raw data is normalized before the actual application to the neural network. One way to normalize the data x is by using the expression.

$$x_n = \frac{(x - x_{min})}{(x_{max} - x_{min})} + starting\ value \tag{8}$$

Where x_n is the normalized value, x_{min} and x_{max} are the minimum and maximum values of the variable.

4.3 Network Development

The input after normalization is presented to the ANN networks for training. After training, the networks are evaluated through a different set of input–output data. Once the networks are trained and tested, they are ready for estimating the real power dispatch of DGs.

5 Simulation Results

The proposed NN is implemented on four DGs system under various power demands. Two diesels and two fuel cells are used as DGs. The fuel cost coefficient, generation capacity for diesel, fuel cell and fuel cell efficiency is presented in Table 1. The demand is varied between 100 kW to 950 kW. The simulation studies were carried out by developing program on MATLAB 13.

In the ANN model a sum of 250 input-output pairs are generated in which 200 used for training and 50 used for testing. Based on evolutionary algorithm for each demand the optimum real power dispatch of DGs is obtained. The parameters used for evolutionary programming are population size 200; maximum iteration 100; beta = 0.025.

Table 2 shows the real power dispatch values of four types of DGs obtained using evolutionary programming, BP neural network and RBF neural network.

Figures 4 and 5 shows the testing patterns error for four DGs obtained using BP neural network and RBF neural network respectively.

Figures 6 and 7 shows the Training performance of BP neural network and RBF neural network respectively.

The parameters settings and performance of proposed neural network is presented in Table 3.

Table 1. Parameters of DGs

DG type	Fuel cost coefficient for diesel/natural gas cost for fuel cell			Generation capacity (kW)		Cell efficiency
	c($/hr)	b($/kWh)/($/Kg)	a($/(kW)^2 h)	P_{min}	P_{max}	
Diesel1	0.4333	0.2333	0.0074	25	400	——
Diesel2	0.2731	0.1453	0.0042	15	350	——
Fuel cell1	0	0.05	0	0	100	90 %
Fuel cell2	0	0.05	0	0	150	95 %

Table 2. Dispatch for different load levels in test system

Methods	Demand (kW)	Dispatch of DGs (kW)			
		$P_{Diesel1}$	$P_{Diesel2}$	$P_{Fuel\ Cell1}$	$P_{Fuel\ Cell2}$
EP	810.9502	212.8403	348.4443	99.9234	149.7422
BPNN		212.5039	349.4207	99.9524	149.7422
RBFNN		212.9961	347.3780	99.3582	149.1423
EP	914.5509	317.3113	347.5691	99.9182	149.9298
BPNN		315.1947	349.4319	99.9595	149.7411
RBFNN		316.6144	348.5779	99.9176	149.7411
EP	727.4762	168.2298	309.2145	99.9453	149.8229
BPNN		167.4437	310.0856	99.9801	149.9667
RBFNN		168.5832	309.9683	99.9127	149.5437

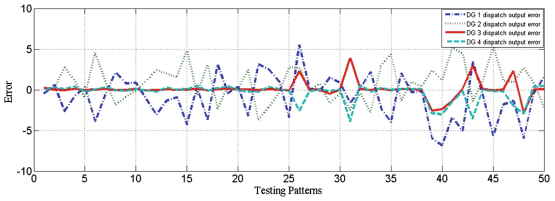

Fig. 4. Error plot for testing patterns of BPNN

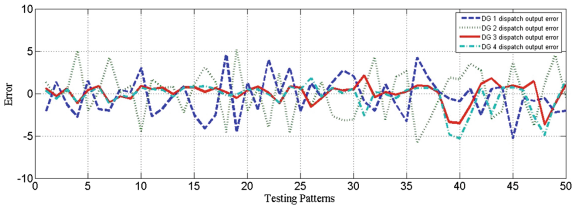

Fig. 5. Error plot for testing patterns of RBFNN

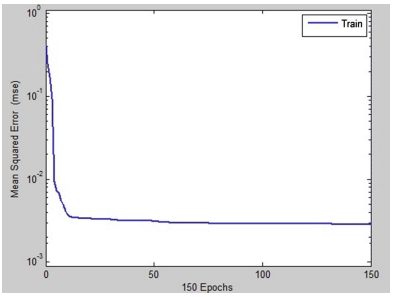

Fig. 6. Training performance of BPNN

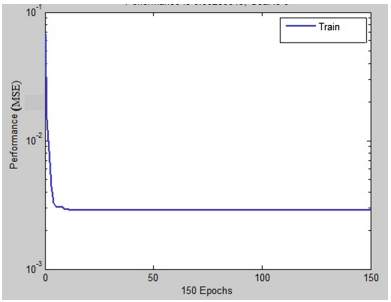

Fig. 7. Training performance of RBFNN

Table 3. Performance of the network

Neural network type	No. of hidden neurons	No. of inputs	No. of outputs	Training time (s)	Training error (mse)	Testing time (s)	Testing error (mse)
BPNN	6	1	4	69	0.00170	0.0936	0.0641
RBFNN	——	1	4	1.62	0.00028	0.046	0.0021

The time taken by the EP for calculating dispatch of DGs for 200 different loading condition is approximately 3854 s. This time may reduce to 69 s when BPNN is chosen. Further the time may reduce to 1.62 s when RBFNN is chosen also from Table 3 it is inferred that the RBFNN testing error is comparatively lower than BP neural network error. Hence, RBFNN is more suitable for on-line ED of DGs.

6 Conclusion

This paper has presented an ANN-based estimation of Real power dispatch of non-renewable DGs for on-line applications. Computer simulation was carried out on the 4 DGs System. Test results show that the proposed BPA based approach and RBF based approach provides accurate estimation of real power dispatch of DGs. In

comparison with BPNN, the RBFNN accurately predict power dispatch of DGs. Hence RBFNN is more suitable for on line ED of DGs in distribution system.

References

1. CIGRE: Impact of increasing contribution of dispersed generation on the power system. Working Group 37.23, (1999)
2. Basu, M., Chowdhury, A.: Cuckoo search algorithm for economic dispatch. Energy **60**, 99–108 (2013)
3. Walter, D.C., Sheble, G.B.: Genetic algorithm solution of economic dispatch with Valve point loading. IEEE Trans. Power Syst. **8**, 1325–1332 (1993)
4. Cheng, P.H., Chang, H.C.: Large scale economic dispatch by genetic algorithm. IEEE Trans. Power Syst. **10**(4), 1919–1926 (1995)
5. Yang, H.T., Yang, P.C., Huang, C.L.: Evolutionary programming based economic dispatch for units with non-smooth fuel cost functions. IEEE Trans. Power Syst. **11**, 112–118 (1996)
6. Gaing, Z.-L.: Particle swarm optimization to solving the economic dispatch considering the generator constraints. IEEE Trans. Power Syst. **18**(3), 1187–1195 (2003)
7. Panigrahi, B.K., Yadav, S.R., Agrawal, S., Tiwari, M.K.: A clonal algorithm to solve economic load dispatch. Electr. Power Syst. Res. **77**(10), 1381–1389 (2007)
8. Wang, S.K., Chiou, J.P., Liu, C.W.: Non-smooth/non-convex economic dispatch by a novel hybrid differential evolution algorithm. IET Gener. Transm. Distrib. **1**(5), 793–803 (2007)
9. Bhattacharya, A., Chattopadhyay, P.K.: Biogeography-based optimization for different economic load dispatch problems. IEEE Trans. Power Syst. **25**(2), 1064–1077 (2010)
10. Wong, K.P., Fung, C.C.: Simulated annealing based economic dispatch algorithm. IEE Proc. Gener. Transmission and Distribution **140**(6), 509–515 (1993)
11. Devaraj, D., Yegnanrayana, B., Ramar, K.: Radial basis function networks for fast contingency ranking. Electr. Power Energy Systems **24**, 387–395 (2002)

Bijaya Ketan Panigrahi
Ponnuthurai Nagaratnam Suganthan
Swagatam Das (Eds.)

LNCS 8947

Swarm, Evolutionary, and Memetic Computing

5th International Conference, SEMCCO 2014
Bhubaneswar, India, December 18–20, 2014
Revised Selected Papers

Multi-objective Generation Scheduling Using Modified Non-dominated Sorting Genetic Algorithm- II

S. Dhanalakshmi[1(✉)], S. Kannan[2], S. Baskar[3], and K. Mahadevan[4]

[1] Velammal College of Engineering and Technology, Viraganoor, Madurai, India
dhanaml26@gmail.com
[2] Ramco Institute of Technology, Rajapalayam, India
kannaneeeps@gmail.com
[3] Thiagarajar College of Engineering, Madurai, Tamilnadu, India
sbeee@tce.edu
[4] PSNA College of Engineering and Technology, Dindugal, India
mahadevand@rediffmail.com

Abstract. This paper presents a Modified Non-dominated Sorting Genetic Algorithm-II (MNSGA-II) solution to Multi-objective Generation Scheduling (MOGS) problem. The MOGS problem involves the decisions with regards to the unit start-up, shut down times and the assignment of the load demands to the committed generating units, considering conflicting objectives such as minimization of system operational cost and minimization of emission release. Through an intelligent encoding scheme, hard constraints such as minimum up/down time constraints are automatically satisfied. For maintaining good diversity in the performance of NSGA-II, the concepts of Dynamic Crowding Distance (DCD) is implemented in NSGA-II algorithm and given the name as MNSGA-II. In order to prove the capability of the proposed approach 10 units, 24-hour test system is considered. The performance of the MNSGA-II are compared with NSGA-II and validated with reference Pareto front generated by conventional weighted sum method using Real Coded Genetic Algorithm (RGA). Numerical results demonstrate the ability of the proposed approach, to generate well distributed pareto front solutions for MOGS problem.

Keywords: Dynamic crowding distance · Emission · Generation scheduling · Multi-objective optimization · Non-dominated sorting genetic Algorithm-II · Real coded genetic algorithm unit commitment

1 Introduction

Generation Scheduling (GS) is used to schedule the generators, in a power system, such that the total system production cost over the given time period is minimized while meeting various plant and system constraints such as the loading levels, the amount of spinning reserve for each unit and satisfying minimum up-time and down-time constraints. GS problem is a nonlinear, mixed integer combinatorial optimization

B.K. Panigrahi et al. (Eds.): SEMCCO 2014, LNCS 8947, pp. 456–470, 2015.
DOI: 10.1007/978-3-319-20294-5_40

problem. The global optimal solution can be obtained by complete enumeration, which is not practicable to large power systems due to its excessive computation time [1, pp. 131–160].

A number of methods have been used previously for solving the above problem and each method has its own difficulties. The various traditional methods used for this problem are Priority List based method, Branch and Bound, Dynamic Programming and Lagrangian Relaxation [2, 3]. In the Priority List method an exhaustive enumeration of all unit combinations are performed at each load level. Hence, it is hard to handle when the dimension of the problem is huge, whereas in the case of Branch-and-Bound method, finding the optimal solution is time consuming, because it can only be obtained by successive elimination of a set of inappropriate solutions [4]. Based on the "Principle of Optimality", Dynamic Programming was suggested for GS problem. But the main drawback of this was that it could not take into account the coupling time constraints and also time dependent start-up costs [5]. Lagrangian Relaxation method is superior to Dynamic Programming due to its higher solution quality and faster computational time [6] but there is no guarantee in getting an optimal solution. In addition, it is very difficult to handle the minimum up and down time constraints unless some heuristic method was used.

Recently, Evolutionary Algorithms(EAs) are having widespread application because of its two important aspects like very simple, function independent and they are not limited by the properties of the function such as continuity, existence of derivates, unimodality etc. Genetic Algorithm (GA) [7–10], Evolutionary Programming (EP) [11], Simulated Annealing (SA) [12], Tabu Search (TS) [13], Fuzzy Logic/expert systems [14–16], and Artificial Neural Networks (ANN) [17] were applied to solve this problem. But the results obtained by these methods required a considerable amount of computational time especially for a large system size. Hence recently, the traditional methods are integrated with these methods to solve this problem more effectively. These hybrid methods are claimed to accommodate more complicated constraints and also claimed to have better quality solutions even though the system under consideration is very large [18–20].

Due to the increasing environmental pollution caused by the fossil-fuelled electric power plants, the U.S. Clean Air Act amendments of 1990 have forced the utilities to reduce the emissions from such power plants [21]. Hence, it is essential to consider the emission as another objective and GS problem becomes Multi-objective Generation Scheduling (MOGS), which is a multi-objective optimization problem (MOOP) due to conflicting nature of operating cost and emission release.

In general, for solving MOOP, Weighted sum method provides a set of Pareto-optimal solutions by varying the weights, which requires multiple runs [22]. Further, the main disadvantage of this method is that it can't be used to find good distribution of pareto-solutions, for non-convex problems [23]. To overcome this, the ε-constraint method of Multi-objective optimization was used. It is based on reformulating the MOOP by keeping one of the most preferred objectives and restricting the rest of the objectives with some user-specified value ε [24]. These values are adjusted to generate the entire Pareto optimal solution. It is obvious that the solution will depends upon the chosen ε value and this method will consume more time. Currently, the ability of Evolutionary Multi-objective Algorithms (EMOAs) to find Pareto-optimal

solutions is an attractive tool to solve these type of problems with multiple and conflicting objectives [25]. Evolutionary multi-objective search using Multi-Objective Genetic Algorithm towards preferred regions of the pareto front has been discussed for power system generation scheduling problem [26, 27].

Among these algorithms, NSGA-II algorithm is very popular and used to solve various power system multi-objective optimization problems, but still NSGA-II algorithm suffers in maintaining diversity among the solutions in the Pareto front. Hence in addition to NSGA-II, this paper makes use of diversity maintenance strategy which is based on Dynamic Crowding Distance (DCD) [27].

The objective of this paper is to solve the MOGS problem as a true multi-objective optimization problem and by using NSGA-II algorithm with DCD. To validate the performance of NSGA-II and MNSGA-II, conventional weighted sum method using RGA is used. In addition, in order to deal hard constraints of MOGS problem effectively intelligent coding [28, 29] is employed in this paper.

The organization of this paper is as follows. Section 2 addresses the MOGS problem formulation. Section 3 deals with basic introduction of MNSGA-II. The MNSGA-II implementation to the MOGS problem and intelligent coding scheme are described in Sect. 4. Section 5 provides test results and finally Sect. 6 concludes.

2 Multi-objective Generation Scheduling (MOGS)

The objective of MOGS problem is to minimize the operating cost and emission release over the scheduled time period, subjected to generator operational and spinning reserve constraints. MOGS problem is formulated as follows:

2.1 Objectives

2.1.1 Operating Cost

The total operating cost can be mathematically represented as in Eq. (1).

$$f_1 = \sum_{i=1}^{N} \sum_{t=1}^{T} \left[F_i(P_i^t) + ST_{i,t}(1 - U_{i,t-1}) \right] U_{i,t} + (1 - U_{i,t})\, SD_{i,t} \quad \$/hr \tag{1}$$

where, $F_i(P_i^t)$ is represented as,

$$F_i(P_i^t) = \sum_{i=1}^{N} a_i + b_i P_i + c_i P_i^2 \tag{2}$$

where, N is the number of generators, T is the number of time periods, a_i,b_i and c_i are fuel cost coefficients of the ith generator; and P_i^t is the real power output of the ith generator at tth hour and $U_{i,t}$ is the ith unit status at tth hour.

2.1.2 Emission

The total emission of atmospheric pollutants, caused by the operation of fossil-fueled thermal power generation can be expressed in terms of (mg/Nm^3) as

$$f_2 = \sum_{i=1}^{N} \sum_{t=1}^{T} (\alpha_i + \beta_i P_i + \gamma_i P_i^2) \tag{3}$$

2.2 Constraints

2.2.1 Generation Capacity Constraint

For stable operation, real power outputs of each generator must be restricted by lower and upper limits as follows:

$$P_{i,\min}\ U_{i,t} \ \leq \ P_{i,t} \ \leq \ P_{i,\max}\ U_{i,t} \tag{4}$$

2.2.2 Power Balance Constraint

By neglecting losses, the total electric power generation must cover the total power demand $P^t{}_{demand.}$ Hence,

$$\sum_{i=1}^{N} P_{i,t}\, U_{i,t} \ = \ P^t_{demand} \tag{5}$$

2.2.3 Spinning Reserve Constraint

$$P^t_{demand} \ + \ R_t \ = \ \sum_{i=1}^{N} P_{i,\max}\ U_{i,t} \tag{6}$$

2.2.4 Minimum up/Down Time Constraints

Minimum Up time

$$U_{i\,,t} = \ 1\,; \ \ \sum_{j=ts}^{t-1} U_{i,j} < MUT_i \ , \ \ for\, i = 1, \ldots\ldots N, \ \ t = t_s + 1, \ldots\ldots T \tag{7}$$

Minimum Down time

$$U_{i\,,t} = \ 0\,; \ \ \sum_{j=td}^{t-1} (1 - U_{i,j}) < MDT_i \ , \ \ for\, i = 1, \ldots\ldots N, \ \ t = t_d + 1, \ldots\ldots T \tag{8}$$

3 Modified Non-dominated Sorting Genetic Algorithm – II (MNSGA – II)

3.1 Introduction

Before describing the non-dominated sorting genetic algorithm-II (NSGA-II), it is necessary to discuss some terminologies related to it. They are termed as non-dominated sorting, crowding distance, elitism and crowded-tournament operator. The first step of an NSGA-II is to sort the population according to non-domination levels. In order to find solutions of the first non-dominated front in a population, each solution can be compared with every other solution in the population, to find if it is dominated. To find the individuals in the next non-dominated front, the first front solutions are discarded temporarily and the same procedure is repeated until all population members are classified.

To get an estimate of the density of solutions surrounding a particular solution in the population, an average distance of the two solutions on either side of the solution along each of the objectives is calculated. This quantity serves as an estimate of the perimeter of the cuboids formed by using the nearest neighbors as the vertices. This is termed as crowding distance. The overall crowding distance value is calculated as the sum of individual distance values corresponding to each objective. Each objective function is normalized before calculating the crowding distance. In NSGA-II once, the non-dominated sorting is over, the new population is filled by solutions of different non-dominated fronts, one at a time. First the best non-dominated front is filled and continues with solutions of the second non-dominated front and so on. All fronts which could not be accommodated are simply deleted. One important thing to be noted is, when the last allowed front is being considered, there may exists more solutions in the last front than the remaining slots in the new population. The crowded-tournament operator guides the selection process at the various stages of the algorithm toward a uniformly spread-out pareto-optimal front. Every population has two attributes: non-domination rank and crowding distance. Between two different populations with differing ranks, the population with better rank is preferred. If both populations belong to the same front, then the population with larger crowding distance is preferred.

3.2 MNSGA – II

In MOEAs, the horizontal diversity of Pareto-front is very important. The horizontal diversity is often realized by removing excess individuals in the non-dominated set (NDS) when the number of non-dominated solutions exceeds population size. NSGA-II uses Crowding Distance (CD) measure as given in (9) to remove excess individuals. The individuals having lower value of CD are preferred over individuals with higher value of CD in removal process.

$$CD_i = \frac{1}{r}\sum_{k=1}^{r} \left| f_{i+1}^{k} - f_{i-1}^{k} \right| \tag{9}$$

where, r is the number of objectives, f_{i+1}^k is the k^{th} objective of the $i+1^{th}$ individual and f_{i-1}^k is the k^{th} objective of the $i-1^{th}$ individual after sorting the population according to crowding distance. The major drawback of crowding distance is lack of uniform diversity in obtained non-dominated solutions as illustrated in Fig. 1.

In Fig. 1, if normal crowding distance method is adopted then the individuals C, D, and E are deleted from NDS, since they have small cd values. Because of that, some parts of paretofront are too crowded and some parts are with sparseness. Also, cd of B is small, because one side of the rectangle is short, while another side is long. However, the cd of F is large because the length of one side almost equal to another side. If one individual must be removed between the individuals B and F, because of small cd value, individual B will be removed and F will be retained in NDS. But, in order to get good horizontal diversity the individual B should be maintained, because the individual B helps to maintain uniform spread. To overcome this problem, dynamic crowding distance (DCD) method is recently suggested [28, 29].

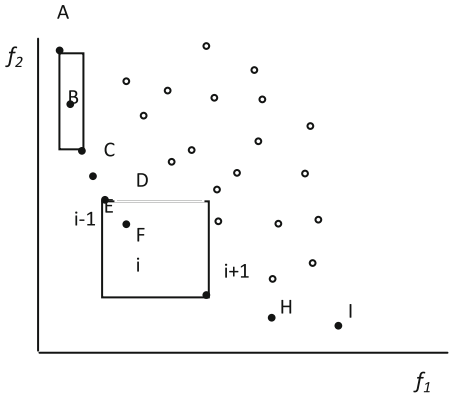

Fig. 1. Crowding distance of individuals

In this approach, one individual with lowest DCD value every time is removed and recalculates DCD for the remaining individuals. The individuals DCD are calculated as follows:

$$DCD_i = \frac{CD_i}{\log\left(\frac{1}{V_i}\right)} \tag{10}$$

Where CD_i is calculated by Eq. (9), V_i is based on Eq. (11),

$$V_i = \frac{1}{r}\sum_{k=1}^{r}\left(\left|f_{i+1}^k - f_{i-1}^k\right| - CD_i\right)^2 \tag{11}$$

V_i is the variance of CDs of individuals which are neighbors of the i^{th} individual. V_i can give information about the difference variations of CD in different objectives. In Fig. 1, the individual B has larger value of V_i than the individual F and DCD of B is larger than F. Therefore, the individuals similar to B in the NDS will have more chance to retain.

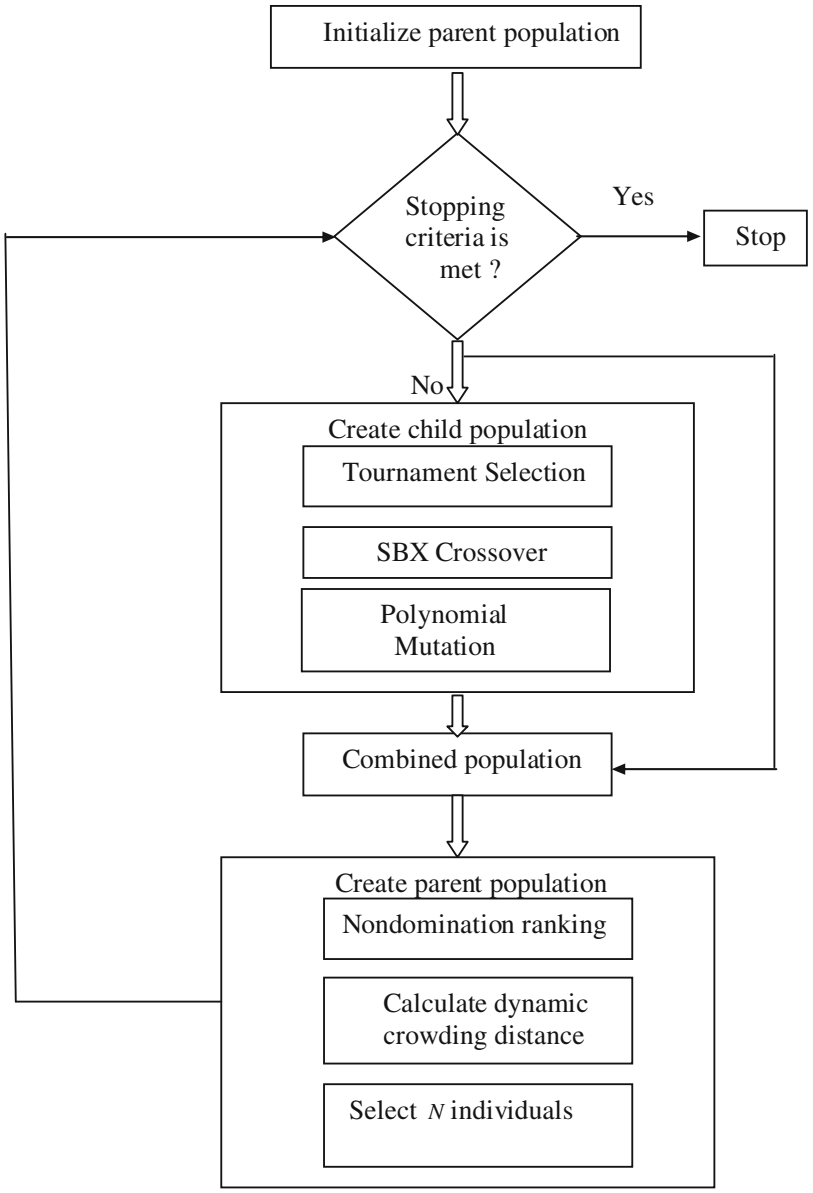

Fig. 2. Computational flow of MNSGA_II

3.3 Computational Flow

The computational flow chart of MNSGA_II is shown in Fig. 2.

4 Implementation of MOGS Problem

In the case of NSGA-II and MNSGA-II the population is generated using real numbers. In fitness function calculation, this real number vector is first rounded to the nearest integer number and then converted to a binary vector of 10 bits. Using intelligent coding scheme [30, 31] this binary vector is converted to a UC schedule without up/down constraint violations.

4.1 Penalty Parameter-Less Constraint-Handling Scheme

In this paper, a constraint-handling method which does not require any penalty parameter is used for handling other than minimum up/down time constraints. In this scheme, all feasible solutions have zero constraint violation and all infeasible solutions are evaluated according to their constraint violation alone. In penalty parameter-less scheme, the fitness function is calculated using (12) [32].

$$F(x) = \begin{Bmatrix} f(x) & \text{if } g_j(x) \geq 0 \ \forall \ j = 1, 2, \ldots\ldots\ldots m \\ f_{\max} + \sum_{j=1}^{m} (g_j(x)) & \text{otherwise} \end{Bmatrix} \tag{12}$$

The advantage of this scheme when compared with the usual penalty parameter based scheme are the tedious process of choosing a suitable penalty parameter can be avoided and no need to evaluate the objective function value for constraint violation, which reduces the computation time. Thus, intelligent coding and penalty parameter-less constraint handling schemes are applied to the MOGS problem to effectively handle the hard and soft constraints.

5 Test Results

The implementation of NSGA-II and MNSGA-II algorithms are carried out using MATLAB Version 7.4 on a Pentium dual core processor desktop computer operating at 2 GHz with 1 GB RAM. The population size is selected as 120. Crossover probability (P_c) and mutation probability (P_m) are fixed at 0.9 and 0.1 respectively. Crossover index (η_c) and mutation index (η_m) are selected as 4 and 18 respectively. The maximum numbers of iterations is fixed at 500 and maximum function evaluations are fixed at 100000. The effectiveness of the algorithm has been tested on a 10 unit 24 h test system. To determine the optimal dispatch for a UC schedule, Quadratic Programming technique is used [33].

5.1 Test System Description

The 10 unit test systems operating cost and emission release function are used in this paper to demonstrate the performance of the proposed method. The demand of the system was divided into 24 intervals. The detailed fuel cost coefficients, emission coefficients, the lower power limits/upper power limits and minimum up/down time are taken from [26].

5.2 Generation of Reference Pareto Front

To compare the performance of MNSGA-II and NSGA-II multiple run generated reference pareto-front is used which is obtained using Real Coded Genetic Algorithm (RGA) with weighted sum approach [23]. The MOGS problem is treated as single objective optimization problem by linear combination of normalized objectives as follows.

$$\text{Minimize } C = w f_{1\_\text{norm}} + (1 - w) f_{2\_\text{norm}} \tag{13}$$

where, C is the combined objective function, f_{1_norm} and f_{2_norm} are the normalized objectives of f_1 and f_2. To generate 25 non-dominated solutions the algorithm is applied 25 times with varying weighting (w) factors as a uniform random number varying between 0 and 1.

5.3 Results and Discussion

The NSGA-II and MNSGA-II are applied to the MOGS problem with and without intelligent coding. Without intelligent coding, NSGA-II and MNSGA-II algorithms are not able to produce even feasible solutions. Whereas with intelligent coding, the NSGA-II and MNSGA-II algorithms have been applied ten times with different initial population, to show the effectiveness of the algorithm. The best results obtained in 10 trails are reported in Tables 1 to 4. From the Tables 1, 2, 3 and 4, it is clear that, all the hard constraints like minimum up/down time and demand constraint are satisfied.

Table 1 gives the hourly dispatch (U1-U10) for best total operating cost and the corresponding total emission release using NSGA-II. From Table 1, it is observed that the best total operating cost is 778470 $/hr and the corresponding total emission release is 874750 mg/Nm^3, using NSGA-II. Similarly Table 2 represents the best total emission release is 700010 mg/Nm^3, and the corresponding total operating cost is 810040 $/hr using NSGA-II.

Table 3 gives the hourly dispatch (U1-U10) for best total operating cost and the corresponding total emission release using MNSGA-II. From Table 3, it is observed that the best total operating cost is 764240 $/hr and the corresponding total emission release is 783240 mg/Nm^3, using MNSGA-II. Similarly Table 4 represents the best total emission release is 585830 mg/Nm^3, and the corresponding total operating cost is 789870 $/hr using MNSGA-II.

Table 1. Hourly dispatch, best total operating cost ($) and corresponding total emission release (mg/Nm^3) using NSGA-II

Hour	Hourly dispatch (MW)										Best total operating cost ($)	Corresponding total emission release (mg/Nm^3)
	U1	U2	U3	U4	U5	U6	U7	U8	U9	U10		
1	54	72	90	108	135	172.13	445.15	94.72	288	0	**778470**	**874750**
2	54	72	90	108	135	158	403.10	63.91	288	0		
3	54	72	90	108	135	146.14	367.81	38.05	288	0		
4	54	72	90	108	135	143.06	358.62	31.32	288	0		
5	52	72	90	108	135	0	435.99	88.01	288	0		
6	54	72	90	108	135	0	445.32	94.85	288	26.84		
7	0	72	90	108	135	0	468	134.10	288	76.90		
8	54	72	90	108	135	0	445	94.85	288	26.84		
9	54	72	90	108	0	0	468	125.32	288	65.68		
10	54	0	90	108	0	0	468	135	288	99		
11	54	0	90	108	0	0	468	124.44	288	64.56		
12	54	0	90	108	0	0	468	117.85	288	56.15		
13	54	72	90	108	0	0	435.94	87.98	288	18.08		
14	54	72	90	108	0	0	429.94	83.58	288	12.48		
15	54	72	90	108	0	0	424.69	79.73	288	7.57		
16	54	72	90	108	0	0	450.93	0	288	32.07		
17	54	72	90	108	0	0	435.93	0	288	18.07		
18	54	72	90	108	0	0	420.94	0	288	4.06		
19	54	72	90	108	0	0	381	0	288	0		
20	54	72	90	108	0	0	366	0	288	0		
21	54	0	90	108	0	0	377.70	45.30	288	0		
22	54	72	90	108	0	0	370.20	39.80	288	0		
23	54	72	90	108	0	0	404.25	64.75	288	0		
24	54	72	90	108	135	0	468	135	288	109		

Table 2. Hourly dispatch, best total emission release (mg/Nm^3) and corresponding total operating cost ($) using NSGA-II

Hour	Hourly dispatch (MW)										Best total emission release (mg/Nm^3)	Corresponding total operating cost ($)
	U1	U2	U3	U4	U5	U6	U7	U8	U9	U10		
1	54	0	90	0	0	244	468	135	288	180	**700010**	**810040**
2	54	0	90	0	0	208.68	468	135	288	128.32		
3	54	0	90	0	0	189.82	468	133.31	288	75.87		
4	54	0	90	0	0	186.63	468	126.36	288	67.01		
5	54	0	90	0	0	185.12	468	123.07	288	62.81		
6	54	0	0	108	0	189.32	468	132.21	288	74.47		
7	0	0	0	108	0	218.21	468	135	288	154.79		
8	0	0	0	108	0	202.86	468	135	288	112.14		
9	0	0	0	108	0	191.49	468	135	288	80.51		
10	0	0	90	108	0	0	468	135	288	153		
11	0	72	90	108	0	0	468	116.53	288	54.47		
12	54	72	90	108	0	0	446.44	95.67	288	27.89		
13	54	72	90	108	0	0	435.94	87.98	288	18.08		
14	54	0	90	108	0	0	456.94	103.36	288	37.69		
15	54	0	90	108	0	0	451.69	99.52	288	32.79		
16	0	0	90	108	0	0	468	0	288	141		
17	0	0	90	108	0	0	468	0	288	112		
18	0	0	90	108	0	0	468	0	288	83		
19	0	0	90	108	0	0	422.82	78.36	288	5.82		
20	0	0	0	108	0	0	450.94	98.97	288	32.09		
21	0	0	0	108	0	0	460.81	106.19	288	0		
22	0	0	90	108	0	0	442.92	93.08	288	0		
23	54	0	90	108	0	0	445.80	95.20	288	0		
24	54	0	90	108	0	203.13	468	135	288	112.87		

Table 3. Hourly dispatch, best total operating cost ($) and corresponding total emission release (mg/Nm^3) using MNSGA-II

Hour	Hourly dispatch (MW)										Best total operating cost ($)	Corresponding total emission release (mg/Nm^3)
	U1	**U2**	**U3**	**U4**	**U5**	**U6**	**U7**	**U8**	**U9**	**U10**		
1	54	72	90	108	135	172.13	445.15	94.72	288	0	**764240**	**783240**
2	54	72	90	108	135	158	403.10	63.91	288	0		
3	54	72	90	108	135	146.14	367.81	38.05	288	0		
4	54	72	90	108	135	143.06	358.62	31.32	288	0		
5	0	72	90	108	135	150.36	380.38	47.26	288	0		
6	54	72	90	108	135	159.48	407.52	0	288	0		
7	54	72	90	108	135	174.07	450.93	0	288	0		
8	54	72	90	108	135	159.48	407.52	0	288	0		
9	54	72	90	108	135	148.67	375.33	0	288	0		
10	54	72	90	108	135	141.38	353.62	0	288	0		
11	54	72	90	108	135	131.86	325.31	0	280.83	0		
12	54	72	90	108	135	198..90	0	135	288	101.1		
13	54	0	90	108	135	210.53	0	135	288	133.47		
14	54	72	90	108	135	188.48	0	130.38	288	72.14		
15	54	72	90	108	135	186.13	0	125.26	288	65.61		
16	0	72	90	108	135	190.32	0	134.41	288	77.27		
17	0	72	90	108	135	185.46	0	123.80	288	63.74		
18	0	72	90	108	135	180.59	0	113.19	288	50.22		
19	0	72	90	108	135	182.55	0	117.45	288	0		
20	54	72	90	0	0	0	407.13	66.87	288	0		
21	54	72	90	0	0	0	459	0	288	0		
22	54	72	90	108	0	0	410	0	288	0		
23	54	72	90	108	0	0	443.69	0	288	25.31		
24	54	72	90	108	0	219.79	468	0	288	159.21		

Table 4. Hourly dispatch, total best emission release (mg/Nm^3) and corresponding total operating cost ($) using MNSGA-II

Hour	Hourly dispatch (MW)										Total best emission release (mg/Nm^3)	Corresponding total operating cost ($)
	U1	**U2**	**U3**	**U4**	**U5**	**U6**	**U7**	**U8**	**U9**	**U10**		
1	54	0	90	108	135	177.20	460.24	105.78	288	40.78	**585830**	**789870**
2	54	0	90	108	135	180.12	467.98	0	288	48.90		
3	54	0	90	108	135	169.17	436.36	0	288	18.47		
4	54	0	0	108	135	179.69	467.61	0	288	47.70		
5	0	0	0	108	135	191.49	468	0	288	80.51		
6	0	0	0	108	135	202.86	468	0	288	112.14		
7	0	0	0	108	135	238	468	135	288	0		
8	0	0	0	108	135	187.26	468	127.74	288	0		
9	0	0	90	108	0	187.89	468	129.11	288	0		
10	0	0	90	108	0	179.27	466.42	110.31	288	0		
11	0	0	90	108	0	171.96	444.67	94.37	288	0		
12	0	72	90	108	135	213.18	0	135	288	140.82		
13	0	72	90	108	135	205.77	0	135	288	120.23		
14	0	72	90	108	135	201.54	0	135	288	108.46		
15	0	0	90	108	135	216.88	0	135	288	151.12		
16	54	0	90	108	135	194.93	0	135	288	90.07		
17	54	0	90	108	135	188.48	0	130.38	288	72.14		
18	54	0	90	108	135	183.61	0	119.77	288	58.61		
19	0	0	90	108	0	217.94	0	135	288	154.06		
20	0	0	90	0	0	0	468	132	288	0		
21	0	0	90	0	0	0	468	117	288	0		
22	0	0	90	108	0	0	442.92	93.08	288	0		
23	0	0	90	108	0	0	468	127	288	0		
24	54	0	90	108	0	203.13	468	135	288	112.87		

NSGA-II and MNSGA-II produces the pareto-optimal solutions in a single simulation run. Figure 3 illustrates the best pareto front obtained using NSGA-II and MNSGA-II. The comparison with respect to reference Pareto front is also presented in the same figure. When compared to NSGA-II, the pareto front obtained in MNSGA-II is much better in terms of non-domination level. Also the solution obtained using NSGA-II and MNSGA-II are well distributed, whereas solution obtained by RGA are poorly distributed and is having less number of non-dominated solutions

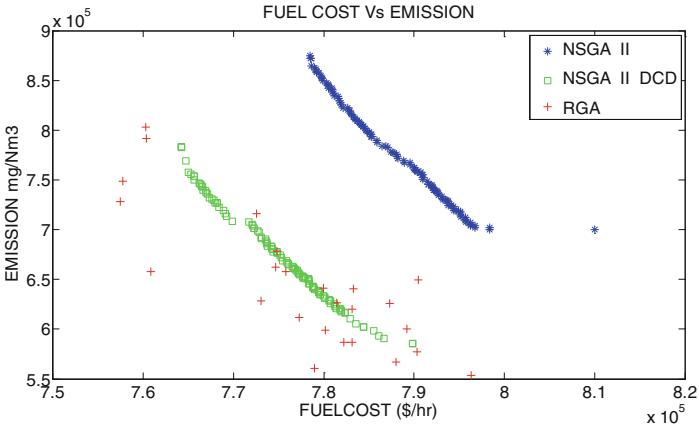

Fig. 3. Pareto optimal solutions for the 10 unit 24 h test system using NSGA-II, MNSGA-II and RGA

6 Conclusion

Multi-objective generation scheduling problem is considered with objectives of minimization of total operating cost and total emission release using modified NSGA-II algorithm. Intelligent coding scheme is employed to effectively satisfy minimum up/down time constraints. To demonstrate the effectiveness of MNSGA-II and intelligent coding scheme, 10 units 24-hour test system is taken. The reference Pareto front is generated using weighted sum method with RGA. The results obtained shows that the MNSGA-II is an effective tool for handling MOGS problem to generate a pareto front in a single simulation with the best computational time. Results also show that, pareto front obtained using MNSGA-II is well distributed with more number of non-dominated solutions as compared to the obtained pareto front by reference and the NSGA-II.

References

1. Wood, A.J., Wollenberg, B.F.: Power Generation, Operation and Control, 2nd edn. Wiley, New York (1996)
2. Yamin, H.Y.: Review on methods of generation scheduling in electric power systems. J. Electr. Power Syst. Res. **69**, 227–248 (2004)
3. Padhy, N.P.: Unit commitment – a bibliographical survey. IEEE Trans. Power Syst. **19**, 1196–1205 (2004)
4. Lee, F.N.: Short-term unit commitment – a new method. IEEE Trans. Power Syst. **3**, 691–698 (1988)
5. Pang, C.K., Sheble, G.B., Albuyeh, F.: Evaluation of dynamic programming based methods and multiple area representation for thermal unit commitment. IEEE Trans. Power Apparatus syst. **100**, 1212–1218 (1981)
6. Virmani, S., Imhof, K., Mukherjee, S.: Implementation of lagrangian based unit commitment problem. IEEE Trans. Power Syst. **10**, 772–777 (1995)
7. Kazarlis, S.A., Bakirtzis, A.G., Petridis, J.: A genetic algorithm solution to the unit commitment problem. IEEE Trans. Power Syst. **11**, 83–92 (1996)
8. Orero, S.O., Irving, M.R.: A genetic algorithm for generation scheduling in power systems. Int. J. Electr. power Energy syst. **18**, 19–26 (1996)
9. Swarup, K.S., Yamashiro, S.: Unit commitment solution methodology using genetic algorithm. IEEE Trans. Power Syst. **17**, 87–91 (2002)
10. Dasgupta, D., Mcgregor, D.R.: Thermal unit commitment using genetic algorithms. IEE Proc. Gen Trans. Dist. **141**, 459–465 (1994)
11. Juste, K.A., Kita, H., Tanaka, E., et al.: An evolutionary programming solution to the unit commitment problem. IEEE Trans. Power Syst. **14**, 1452–1459 (1999)
12. Mantawy, A.H., Abdel-Magid, Y.L., Selim, S.Z.: A simulated annealing algorithm for unit commitment. IEEE Trans. Power Syst. **13**, 197–204 (1998)
13. Mantawy, A.H., Abdel-Magid, Y.L., Selim, S.Z.: Unit commitment by tabu search. Proc. Inst. Elect. Eng. Gen. Trans. Dist. **145**, 56–64 (1998)
14. Saneifard, S., Prasad, N.R., Smolleck, H.: A fuzzy logic approach to unit commitment. IEEE Trans. Power Syst. **12**, 988–995 (1997)
15. Ouyang, Z., Shahidehpour, S.M.: Heuristic muti-area unit commitment with economic dispatch. IEE Proc. **138**, 242–252 (1991)
16. Tong, S.K., Shahidehpour, S.M., Ouyang, Z.: A heuristic short-term unit commitment. IEEE Trans. Power Syst. **6**, 1210–1216 (1991)
17. Wang, C., Shahidehpour, S.M.: Effects of ramp-rate limits on unit commitment and economic dispatch. IEEE Trans. Power Syst. **8**, 1341–1350 (1993)
18. Ongsakul, W., Petcharaks, N.: Unit commitment by enhanced adaptive lagrangian relaxation. IEEE Tran. Power Syst. **19**, 620–628 (2004)
19. Cheng, C.P., Liu, C.W., Liu, C.C.: Unit commitment by lagrangian relaxation and genetic algorithms. IEEE Trans. power Syst. **15**, 707–714 (2002)
20. Mahadevan, K., Kannan, P.S.: Lagrangian relaxation based particle swarm optimization for unit commitment problem. J. Power Energy Syst. **27**(4), 320–329 (2007)
21. Bharathi, R., Kumar, M.J., Sunitha, D., Premalatha, S.: Optimization of combined economic and emission dispatch problem – a comparative study. In: Proceedings of Eighth International Power Engineering Conference, pp. 134–139 (2007)
22. Dhillon, J.S., Parti, S.C., Kothari, D.P.: Stochastic economic emission dispatch. Electr. Power Syst. Res. **26**, 197 (1993)

23. Deb, K.: Optimization using evolutionary algorithms, 2nd edn, pp. 171–280. Wiley, New York (2001)
24. Yokoyama, R., Bae, S.H., Morita, T., Sasaki, H.: Generation dispatch based on probability security criteria. IEEE Trans. Power Syst. **3**, 317–324 (1988)
25. Abido, M.A.: Evolutionary algorithms for electric power dispatch problem. IEEE Trans. Evol. Comput. **10**(3), 315–329 (2006). doi:10.1109/tevc.2005.857073
26. Zio, E., Baraldi, P., Pedroni, N.: Optimal power system generation scheduling by multi-objective genetic algorithms with preferences. Reliab. Eng. Syst. Saf. **94**, 432–444 (2009)
27. Li, Y.F., Pedroni, N., Zio, E.: A memetic evolutionary multi-objective optimization method for environmental power unit commitment. IEEE Trans. Power Syst. **28**(3), 2660–2669 (2013)
28. Luo, B., Zheng, J., Xie, J., Wu, J.: Dynamic crowding distance - A new diversity maintenance strategy for MOEAs. In: 4th International Conference on Natural Computation (ICNC 2008), vol. 1, pp. 580–585 (2008)
29. Dhanalakshmi, S., Kannan, S., Mahadevan, K., Baskar, S.: Application of modified NSGA-II algorithm to combined economic and emission dispatch problem. Int. J. Electr. Power Energy Syst. **33**(4), 992–1002 (2011)
30. Baskar, S., Subbaraj, P., Chidambaram, P.: Application of genetic algorithms to unit commitment problem. IE(I) J. **81**, 195–201 (2001)
31. Dhanalakshmi, S., Kannan, S., Baskar, S., Mahadevan, K.: Intelligent genetic algorithm for generation scheduling under deregulated environment. In: Panigrahi, B.K., Suganthan, P.N., Das, S., Satapathy, S.C. (eds.) SEMCCO 2011, Part I. LNCS, vol. 7076, pp. 282–289. Springer, Heidelberg (2011)
32. Manoharan, P.S., Kannan, P.S., Baskar, S., Iruthayarajan, M.W.: Penalty parameter-less constraint handling scheme based evolutionary algorithm solutions to economic dispatch. IET Gener. Transm. Distrib. **2**, 478–490 (2008)
33. Danaraj, R.M.S., Gajendran, F.: Quadratic programming solution to emission and economic dispatch problems. IE (I) J. **86**, 129–132 (2005)

Indian Road Traffic Surveillance System using Blob Tracking for ATIS Applications

Balaji Ganesh Rajagopal, Appavu alias Balamurugan Subramanian, and Midhun Kumar Ayyalraj

Abstract— **Intelligent Transportation System is an Emerging area to solve multiple transportation problems. Several forms of inputs are needed in order to solve ITS problems. Advanced Traveler Information System (ATIS) is a core and important ITS area of this modern era. This involves travel time forecasting, efficient road map analysis and cost based path selection, Detection of the vehicle in dynamic conditions and Traffic congestion state forecasting. This Article designs and provides an algorithm for traffic data generation which can be used for the above said ATIS application. By inputting the real world traffic situation in the form of video sequences, the algorithm determines the Traffic density in terms of congestion, number of vehicles in a given path which can be fed for various ATIS applications. The Algorithm deduces the key frame from the video sequences and follows the Blob detection, Identification and Tracking using connected components algorithm to determine the correlation between the vehicles moving in the real road scene.**

Keywords **– Traffic Transportation, Traffic Density estimation, Blob Identification and Tracking, Relative Velocity of vehicles, Correlation between vehicles.**

I. INTRODUCTION

INTELLIGENT Transportation System is an Emerging Area to Solve multiple transportation Issues. Advanced Travelers Information System is a core area of ITS which gives amenities to the traveler by providing valuable information which can be used by the traveler for path selection, travel time forecasting and time management.

Traffic flow monitoring and traffic analysis based on computer vision techniques, and especially traffic analysis and monitoring in a real-time mode raise precious and complicated demands to computer algorithms and technological solutions. Most convincing applications are vehicle tracking, and the crucial issue is initiating a track automatically. Traffic analysis then leads to reports of speed violations, traffic congestions, accidents, or illegal behavior of road users. Various approaches to these tasks were suggested by many scientists and researchers [1,3]

Balaji Ganesh Rajagopal, Assistant Professor in the Department of Computer Science and Engineering, Ramco Institute of Technology, Rajapalayam-626117, Tamilnadu, India (phone: +918220037222; e-mail:balajiganeshr@ gmail.com).

Dr.Appavu alias Balamurugan Subramanian, Professor and Head, Department of Information Technology, K.L.N. College of Information Technology, Pottapalayam 630611, Tamilnadu, India. (e-mail: app_s@yahoo.com)

Midhun Kumar Ayyalraj, Assistant Professor, Department of Information Technology, K.L.N. College of Information Technology, Pottapalayam 630611, Tamilnadu, India. (e-mail:midhuntce@gmail.com)

One of the main aspects was to modify these algorithms to fit to real-time road monitoring processes, and as a consequence the prototype of system for traffic analysis was developed. Technically this system is based on stationary video cameras as well as computers connected to wide area network.[2,4]

The application is utilizing image-processing and pattern recognition methods designed and modified to the needs and constraints of road traffic analysis. These are combined together gives functional capabilities of the system to monitor the road, to initiate automated vehicle tracking, to measure the speed. [6]

Image processing and object/pattern recognition of moving objects, chosen for the system, lead to complex mathematical, algorithmic and programming problems. Many articles have considered particular questions related to scene modeling, object geometry accounting, image contours processing. There is a lack of information on methods and algorithms used in digital monitoring technology, perhaps for commercial reasons. [7]

In the cell transmission model, a very simple model and yet it is able to recover most of the phenomena observed in real traffic. There are many other traffic flow models suggested in the literature that also reproduce traffic flow, in some cases with more precision than the cell transmission model. However, one of the challenges for real time on-ramp metering control consists on having calibrated traffic flow models. [3]

Grid method is the most common method in road density analysis. However, the determination of grid size, position and orientation is rather arbitrary. It also fails to provide information within grids, and may bring obstacles to road selection process, since grid boundaries may ‘split’ the roads into several parts and ultimately give rise to the loss of information about connectivity. [5]

Fractal geometry method is devised by introducing self-similar fractal concepts. This method splits the whole study area into self-similar grids iteratively and the algorithm stops when the features within grids are homogeneous. It has the setback that the initial grid size exerts too much influence on computed road density, and the information lost at larger grid may not be recovered. Mesh density based on sub-region avoids several of the aforementioned setbacks. However, it neglects geographical characteristics of road networks and may not reflect information about the area each road is serving and its relative importance. [5]

The problem of road monitoring as it is chosen in our research is presented as a sequence of independent processing steps intended to solve tasks logically connected to each other.

These steps are in hand of the following order of algorithmic processing: video stream input to computer (personal computer or specialized one), its conversion to a sequence of single frames, Key Frame Selection, Blob Identification, Blob Coloring, Blob Tracking, Analysis of relative velocities of the Blobs.

This paper mainly describes about the relative velocities of the moving blobs by utilizing the individual blobs velocity and draws the Probability Density Function (PDF) which then determines the density of the road surface.

The paper is organized as follows. Section 2 explains the Selection of Key frames from the input Video Sequence. Section 3 explains the extraction of Blobs. Section 4 outlines the blob spatial moment and the correlation among the blobs which includes centroid extraction. Section 5 discusses the experimental results and Section 6 presents the conclusion of proposed algorithm.

II. KEY FRAME SELECTION

A. Overview

For every video input to be processed, key frame selection is the initial step which selects the frames that best describes the important change detected in the input video. Here we propose a method to select the key frame based on color histogramming technique.

B. Color Histogramming

This technique detects the peak change in the RGB values of the pixel in each frame. The Frame's RGB values are appropriately sampled in the 64 bin space which derives the key frame. By sorting each frame against the RGB Pixel value, the frame which most deviates from the rest of the frames is obtained. In The Color Histogramming technique the Mean R,G,B Value of each frame is calculated which then sorted and the deviation of R,G,B Mean value with other frames is listed out as shown in Fig.1. The Frames with the highest deviation and lowest deviation are considered as key frames.

Our Experimental results show that this technique is cost effective in-terms of run time memory requirements. This approach also reduces the constraints on the input requirements when compared to other techniques like edge histogram and wavelets and distance descriptor matching. The Method of Color Histogramming is easy to implement and cost effective in terms of both Space and Time complexity. Around 100 sets of video are applied over this algorithm to test the accuracy of the results. Color Histogramming can be applied to a large volume of data since it uses n-bin technique to group the pixels by which pre-processing is done at an earlier stage to avoid keeping unwanted information through all phases of the algorithm.

Image Number	Red Mean Value	Green Mean Value	Blue Mean Value
img10.jpg	92.3166666	118.041025	109.735353
img11.jpg	92.3166666	118.041025	109.735353
img12.jpg	92.2833333	118.046153	109.711111
img14.jpg	92.2833333	118.046153	109.711111
img15.jpg	92.2385416	117.970256	109.670707
img16.jpg	92.2385416	117.970256	109.670707
img9.jpg	92.1916666	117.873846	109.586868
img8.jpg	92.1552083	117.869743	109.489898
img7.jpg	92.155208	117.869743	109.489898
img17.jpg	92.064583	117.710769	109.413131
img18.jpg	92.064583	117.710769	109.413131
img43.jpg	92.079166	117.817435	109.333333
img44.jpg	92.079166	117.817435	109.333333
img45.jpg	92.1	117.810256	109.370707
img47.jpg	92.1	117.810256	109.370707

Table.1. Showing the Color Histogram values for the individual frames which are sorted based on the Deviation Descriptor.

Figure.1. Showing the Best 2 Frames which are more deviated from each other based on the Color Histogram Value

III. BLOB DETECTION AND TRACKING

A. Overview

Here we propose an algorithm to detect each and every moving vehicle designated as blobs. A blob is defined to be a filled square and any square that can be reached from that square by moving horizontally or vertically. A blob is a connected region that can be found out by traversing through the pixels of the image.

B. Blob Detection

Here we designed and experimented with a kernel which can be moved over the image to find out all the connected components. A Connected component refers to an object which has coherency of features when compared to the rest of the objects. The kernel shown in Fig 2 is moved over the image to find the connected components. For position S in the kernel Neighbouring pixels A, B, C & D are checked for the least label value. The pixel with minimal Label value is added to the list of connected pixels. Similarly many groups of connected pixels are grouped.

A	B	C
D	S	

Figure.2. Blob Detection Kernel used to analyze the neighbourhood pixels for connected component S:Source Pixel, A,B,C,D:Neighbourhood Pixel

Algorithm

1. Read the Image Array
2. Initialize labelTable, xMinTable, xMaxTable, yMinTable, yMaxTable, massTable to 0

   Initialize labelBuffer to the no. of pixels in the image
3. For Each Pixel S the nearest pixels are verified

   A B C

   D S
4. Assign Labels for each Pixel and enter it into labelTable
5. Iterate through pixels looking for connected regions.
6. Find the neighbouring pixel with the least labelValue
7. If the found neighbour is a foreground pixel

   a. Set S Pixel Label value to min and assign the least labelValue to the pixel

   b. Update min & max X, Y values on the found neighbour into labelTable

   c. Increment the massTable value
8. If the found neighbour is not a foreground pixel

   a. Enter the min & max X, Y values into the xMinTable, xMaxTable, yMinTable, yMaxTable

   b. Increment the label value
9. Repeat Steps 3 to 8 for all pixels
10. Rearrange the labelValue of the each labelBuffer starting from 0
11. Assign color value to each labelValue (Blob)

The algorithm uses Five Tables (xMin, yMin, xMax, yMax, MassTable) to identify the nearest and least neighborhood pixel. The kernel is made to pass through the entire array set of images. For each neighbor pixel, the labels are assigned and it is compared with the rest of the neighbours.

If the found neighbor posses Label value less than the current pixel's Label value, then the neighbor pixel is designated as the new pixel and its x,y position in the array are entered into the corresponding tables.

To ensure the reliability of Blob Detection Algorithm, during the free flow traffic in which the vehicles can be passed through with greater velocity and to identify the missed vehicles between the two key frames, a Middle frame approach is suggested. This approach compares the no. of blobs with an intermediate frame that lies exactly in the middle of the two key frames. The frame is taken into account, so that a moving object with higher velocity gets out in between the key frames and can be neglected in the further processing.

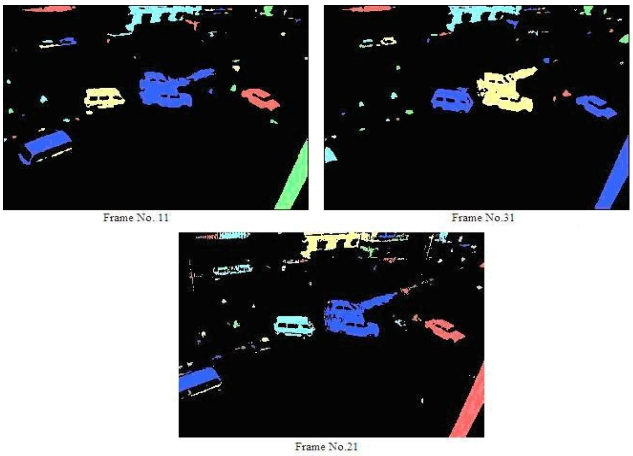

Figure.3. Result of Blob Detection Algorithm which Detects the Moving Foreground Pixels & Colours the Blobs (Key Frame1, Key Frame2, Middle Frame)

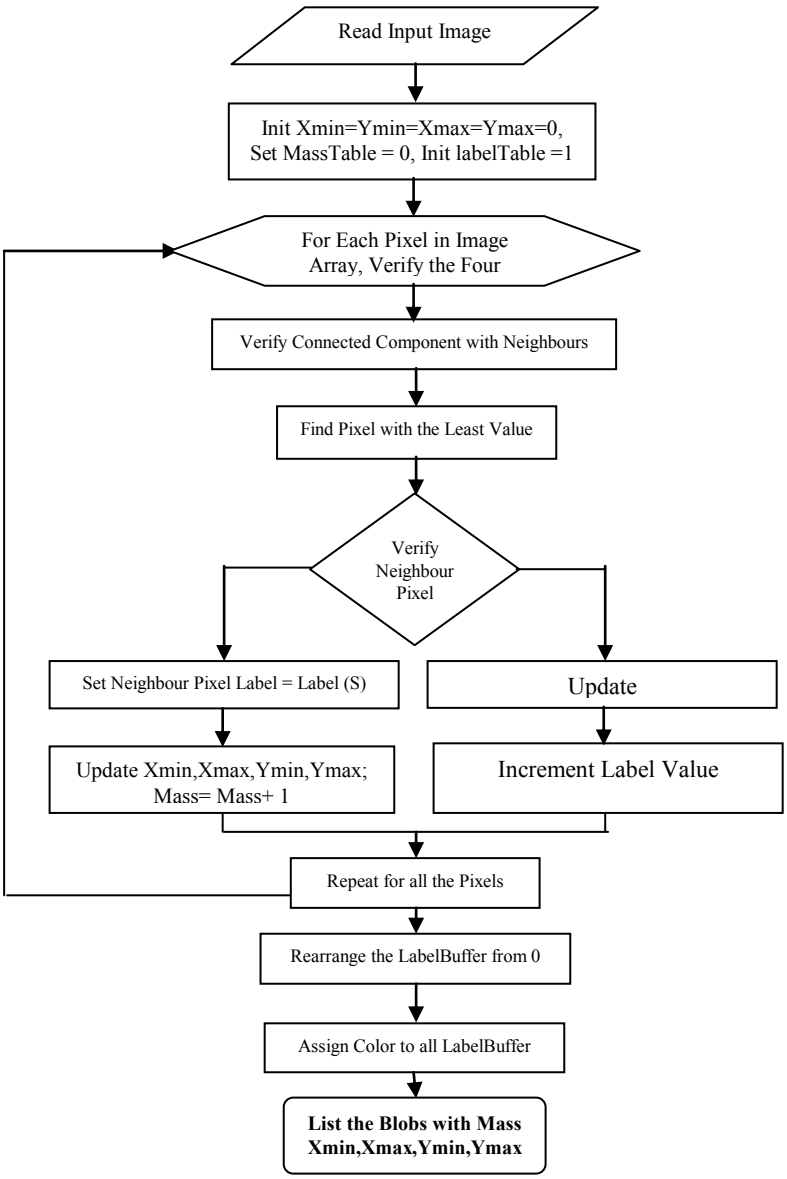

Figure. 4. Flow Chart Depicting Blob Detection Algorithm based on Connected Pixel Region.

C. Blob Filtering

In this Section, the identified Blobs are labelled from 1 to n Numbers. Each blob's X and Y position is calculated and the mass of each blob is calculated. The massTable in the above algorithm provides the value of each blob's spatial mass which can be calculated.

The blobs listed based on the algorithm in the previous section consists of all the blobs in the input frames. Blob filtering is carried out to filter out the stationary blobs which are basically the background pixels in the input frames. Three sets of conditions are applied over the blob list to find out the blobs which contain only the vehicles which are correlated between the two frames.

Blobs which are stationary over a set of frames and Blobs that are having mass less than the specified threshold, where the threshold is calculated based on trial and error basis.

Blobs whose change is very low, this is carried out to avoid erroneous blobs because of the internal movement of the camera and lightning conditions

The Blobs are Filtered using (1) and are sorted out. The filtered Blobs need to be tracked to find out the spatial movement of the blobs and their correlation between the frames. The correlation between the frames is found out to conclude whether the blobs have their movement independent or depend on some other blobs. This is found out by comparing the blobs that are having equal mass between the frames. The final list of blobs is analysed for their spatial movement. A rectangle is drawn over the blobs to track it across the frame.

$$\text{Bi}=\begin{cases}\mathbf{b_i} \; where & ((\mu(b_i)>th1)\,\&\& \\ & ((\delta(b_{i,f_a}(x),b_{i,f_b}(x))>th2)\,\&\& \\ & (\delta(b_{i,f_a}(y),b_{i,f_b}(y))>th2))\end{cases} \quad (1)$$

Where, μ =Mass of the Blob, f_a =Frame 1, f_b = Frame 2, δ =Difference in the position of the object between frame 1 and frame 2, Number of Blobs Detected (i) = 0 to n, th1, th2 = Threshold. B_i is the list of blobs from the set b_i which satisfies the threshold condition.

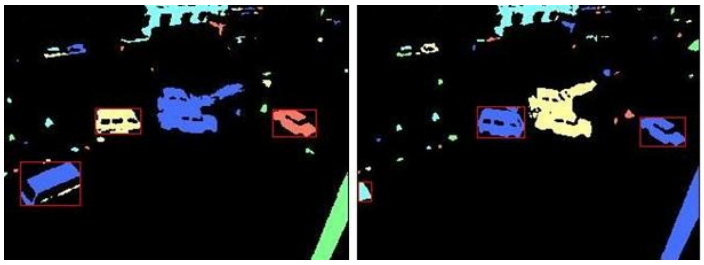

Figure 5 Blob Filtering Constraints Applied over the list of Blobs and Convex Hull Marked over Similar Moving Blobs

D. Blob Tracking

These moving blobs represent the vehicle motion in the images. It has asserted that the convex hull surrounding a vehicle in an image is a good approximation of the projection of a vehicle in the image. In the Blob Filtering, we exclude the blobs whose mass is less than 100 pixels. To characterize the moving blobs, we calculate the convex hull and calculate the centroid for the blobs. The area of each blob is calculated and is indexed by the vertical location of its centroid in the image. This area is an indicator of blob size relative to its location in the image.

Having located a vehicle in one image, the vehicle is tracked across images by enforcing co- linearity of the centroid of the convex hulls. The Figure 6 presents a representation of three convex hulls with centroid (x1, y1), (x2, y2), and (x3, y3).

E. Velocity Estimation

Figure.6. Moving Blobs Identified between Frame 1 and Frame 2 by applying Equation (1)

For a set of Two Blobs, Calculate the velocity of the blobs by fixing a reference point and calculate the displacement. Calculate the time difference between the frames and hence calculate the velocity of the individual blobs.

A point in the previous frame, p , will be associates with a point in the current frame based on the minimum Euclidean distance, However, in order to determine the Minimum distance, all the distance between reference point p and all other points c1 , c 2 ...c n must be established

$$E_d=\sqrt{(P_x-x_{cb})^2+(P_y-y_{cb})^2} \quad ;\forall b\in B \quad (2)$$

For every blob $b\in B_i$ in the image, the bounding box and centroid, λ = (x_{cb}, y_{cb}) are extracted where x_{cb} and y_{cb} denotes the points connecting the diagonal of the convex hull marked over the blob. Centroid is computed by calculating the blob's spatial moment and is given in (3) and (4). This centroid will be used for tracking object.

$$u_{pq}=\sum_{x_b=0}^{m-1}\sum_{y_b=0}^{n-1}{x_b}^p\,{y_b}^q:(x_b,y_b)\in b,\forall b\in B \quad (3)$$

$$x_{cb}=\frac{u_{10}}{u_{00}},y_{cb}=\frac{u_{01}}{u_{00}} \quad (4)$$

The ratio between the pixels and length in meters can then be defined by assuming that the ratio of world to pixel space is given as $\frac{\omega}{\zeta}$, which is calculated by determining the

Systems DPI with relative to the input image.

Further, we can derive the velocity in actual world unit using is given in (5) as

$$v_\tau = \frac{(\lambda_n - \lambda_{n-1})\frac{\omega}{\zeta}}{\tau_n - \tau_{n-1}} ms^{-1} \quad (5)$$

F. Speed-Flow-Density Relationship

Speed, flow, and density are all related to each other. The relationships between speed and density are not difficult to observe in the real world, while the effects of speed and density on flow are not quite as apparent.

Under uninterrupted flow conditions, speed, density, and flow are all related by the following equation:

$$q=k*v \quad (6)$$

Where q = Flow (vehicles/hour)
v = Speed (miles/hour, kilometers/hour)
k = Density (vehicles/mile, vehicles/kilometer)

Because flow is the product of speed and density, the flow is equal to zero when one or both of these terms is zero. It is also possible to deduce that the flow is maximized at some critical combination of speed and density.

Under Interrupted Flow Conditions, the Vehicle Speed, Density and Flow are related using a Gaussian PDF. The velocity of vehicles follows a normal distribution, the resulting PDF for the differential velocity v of two vehicles a and b is given by:

$$f_V(v) = \frac{1}{\sqrt{2\Pi}\sqrt{\sigma_a^2 + \sigma_b^2}} e^{-\frac{1}{2}\frac{(v-(v_a - v_b))^2}{\sigma_a^2 + \sigma_b^2}} \quad (7)$$

IV. Experimental Results

Experimental results of the proposed vehicle speed estimation are presented to demonstrate the real-time velocity estimation of random vehicles. The algorithm is implemented using Java Advanced Imaging Package, Java Media Framework and executes on a 2.6 GHz Pentium Intel dual core with 4 GB ram memory and 500 GB hard disk. The experiment was set up to monitor the speed of vehicles moving along the selected road lane. The real-world scene was recorded in 6 seconds.

The Proposed Method is tested over a range of videos taken at different scenarios like Bad Light, Rainy(or) Snow Days, Interrupted Traffic scene at Urban road side, Uninterrupted Traffic Scene at National Highways, Video Taken at Tunnels.

The Results of the various video scenario at various part of the Algorithm is given in Table.2.

Video Scenario	No. of Input Videos (120)	Frame Selection *	Blob Detection *	Blob Tracking*
At Bad Light	38	91.8	95.4	89.7
At Rain (or) Snow Days	20	95.67	91.43	90.25
Interrupted Traffic	22	98.4	99.32	97.646
Uninterrupted Traffic	27	99.21	99.98	98.89
At Tunnels	13	98.12	97	89.91

(* Accuracy in Percentage)

Table.2. Accuracy of the Piece-wise Algorithms under various dynamic video streams taken at different conditions

Since the key frame selection algorithm is used, the system is said to be in the state of intrinsic ie., the total input should be available before the start of the process.

The overall performance of the Algorithm with 2 sets of Input data at various locations and conditions are shown in Table.3 and Illustrated in Graph.1

Video Scenario	No. of Input Videos (120)	Accuracy of the Results (%)
At Bad Light	38	92.3
At Rain (or) Snow Days	20	92.45
Interrupted Traffic	22	98.45533
Uninterrupted Traffic	27	99.36
At Tunnels	13	95.01

Table.3. The Accuracy of the Overall System at various Dynamic Conditions.

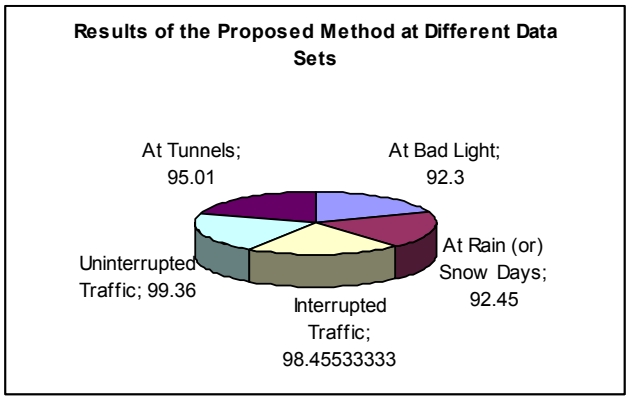

Graph 1. The Distribution of the System's Performance over Different Data Sets.

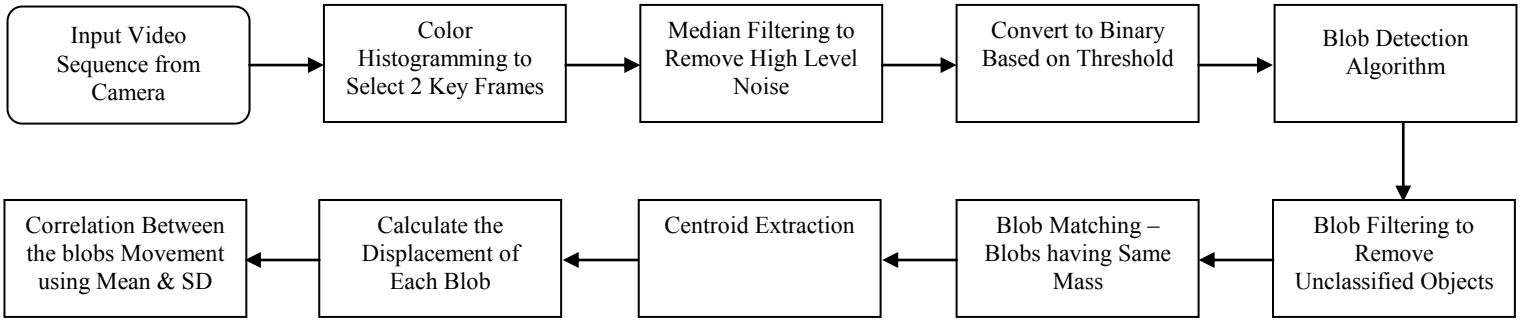

Figure.7. Overall Architecture of the System

Methods	Advantages (+), Short Comings(-)	
Lane Masking & Contour Extraction	+	Easy to Implement, Quick Results
	-	Applicable Only to Uninterrupted Traffic Situations on Highways with Lanes
Cell Transmission Model	+	Very Simple Model, Traffic is simulated based on Kinetic Theory
	-	Less Precision, Cant able to deduce traffic at high densities
Grid Method	+	Widely used Model, Earlier Conclusions
	-	Grid Size and Number of Grids within the picture are hard to apply
Point Based Method	+	Individual Analysis of Vehicles is Easy.
	-	Hard to implement at Interrupted Traffic Flow Junctions
Proposed Method	+	Easy to Implement, Good flow of Logic from Top to Bottom, Readapted to Different Density – Flow Correlation.
	-	Long Mathematical Steps, High Time Bound, Constraints in Input Video

Table.4. Shows the Comparative Study of Various Road Traffic Density Analysis Methods.

V. CONCLUSION

The Proposed Solution for the Analysis of the Traffic Situation is efficient and produces approximated results on all the video sequence. This Method deduces, whether the road traffic is congested or free flow. As this algorithm also detects the number of blobs in the given traffic scene, which makes further analysis of the road traffic. The method describes the step by step process in the analysis and so, there are several midterm results like key frame selection, Blob Detection in the proposed solution which can be useful in all video surveillance systems.

Traffic Situation, the proposed method plays a vital role for future enhancements The outputs of this system, can be a mandatory input for all kind of Advanced Traveler Information Systems and also for various domains of ITS applications.

The proposed solution is based on some input constrain including illumination effect of the video frames and camera angle. Future research work may be directed towards accounting the illumination changes as the object moves across the frame. The process can be extended to capture the video sequence in multiple lanes with the use of revolving camera instead of multiple stationary cameras.

REFERENCES

[1] Tomas Rodriguez, Narciso Garcia, "An adaptive, real-time, traffic monitoring system", Springer-Verlag 2010, Machine Vision and Applications (2010), 555–576

[2] Cheng-You Cui · Ji-Sun Shin · Fumihiro Shoji, Hee-Hyol Lee," Traffic signal control based on a predicted traffic jam distribution", IEEE transactions on Artificial Life Robotics (2009) 134–137

[3] Oscar Rosas-Jaimes , Luis Alvarez-Icaza," Vehicle density and velocity estimation on highways for on-ramp metering control", Springer - Nonlinear Dynamics (2007) 49:555–566

[4] E. Atkociunas, R. Blake , A. Juozapavicius , M. Kazimianec," Image Processing in Road Traffic Analysis", Nonlinear Analysis: Modelling and Control, 2005, Vol. 10, No. 4, 315–332.

[5] LIU Xingjian, AI Tinghua, LIU Yaolin," Road Density Analysis Based on Skeleton Partitioning for Road Generalization", Geo-spatial Information Science 12(2): Volume 12, Issue 2 June 2009, 110-116

[6] H. A. Rahim, R. B. Ahmad, A. S. M. Zain, U. U. Sheikh," An Adapted Point Based Tracking for Vehicle Speed Estimation in Linear Spacing", International Conference on Computer and Communication Engineering (ICCCE 2010), 11-13 May 2010, Kuala Lumpur, Malaysia

[7] Robert Nagel, "The Effect of Vehicular Distance Distributions and Mobility on VANET Communications", 2010 IEEE Intelligent Vehicles Symposium University of California, San Diego, CA, USA, June 21-24, 2010

Detecting Contrast Enhancement based Image forgeries by Parallel Approach

Ms.S.T Suryakanthi Sornalatha
Department of Computer science and Engineering
Mepco Schlenk Engineering College
Sivakasi,India
stsuryacse@gmail.com

Ms.S.Devi Mahalakshmi
Department of Computer science and Engineering
Mepco Schlenk Engineering College
Sivakasi,India
sdevi@mepcoeng.ac.in

Ms. Dr.K.Vijayalakshmi
Department of Computer science and Engineering
Ramco Institute of Technology
Rajapalayam,India

***Abstract*— Contrast and brightness of digital images can be adjusted by contrast enhancement. Mostly digital images are stored in Jpeg format in real application like Internet and Mobile phones. In order to reduce the size digital images are compressed with high, middle and low quality factor. Move and paste type of images are created by malicious person, in which contrast of one source image is enhanced to match the other source image. Detecting global contrast enhancement on previously Jpeg compressed images can identified using global contrast enhancement detection algorithm. Zero height gab bins of histogram used to identify the global contrast enhancement. Zero height gap bins/peaks are used to identify the composite images created by contrast enhancement. Contrast enhancement technique aimed at detecting image tampering has grown in different applications area such as law enforcement, surveillance. Composite detection algorithm and global contrast enhancement detection algorithms are presented here. In order to increase the image processing task parallel approach is used.**

Keywords **–** Contrast enhancement, Parallel approach, Zero height gab bins/peaks, Jpeg Compression.

I.INTRODUCTION

Now a days digital image editing skills becomes very popular and digital image manipulation becomes convenient and easy.Malevolent user may perform innocent manipulation to tinker the digital images.Information delivered in images might become no longer believable.In the application such as surveillance and news recording, it is necessary to certify the integrity and originality of images.

Primary goal of digital image forensics is the identification of image regions which was undergone some form of alteration[19-21]. Digital forensics techniques used to detect the image tinkering operations such as alteration, deletion etc.

Low contrast image quality globally improved when using global contrast enhancement. The enhanced output image, produced by this enhancement is free from noise and ringing artifacts. It may have more exposure on some part of the image and less exposure on some other part of the image when high contrast gain occurs.

The enhanced output image may lack in local details. Using local contrast enhancement, the local details of an image can be better defined. However, local contrast enhancement may produce the output image with noise when too much contrast gain occurs. Besides these, it may be poor in global contrast. For some images, applying the local contrast enhancement along with global contrast enhancement is much better than that of global contrast enhancement alone or local contrast enhancement alone.

Previous works deal with image manipulation detection with classifier based approaches and specific image manipulations. Each manipulation leaves distinct fingerprints on images, so it is feasible to test the enforced manipulation. Manipulation specific detection techniques used to recover the image processing history. Prior works focus on 2 different type of image alterations. 1. Non content changing operation includes resampling [4], contrast enhancement [7,8,9,12,13], compression [5], sharpening filtering [6], median filtering [10,11]. 2. Content changing operations includes splicing and composition[17,18]. Contrast enhancement including statistical intrinsic fingerprints[7,16], Gamma correction[8], reverse engineering of double Jpeg compressed images[9], noise features[15].

Prior contrast enhancement forensics algorithms works well under the assumption that the gray level histogram of original image shows a smooth contour. But digital images are stored in Jpeg format compressed with medium or low quality factor in real applications such as internet. Quality factor (Q=50) medium, less than 50 (<50) referred as low quality. Low quality Jpeg compression causes unsmoothness and generates thick peak bins in gray level histogram. In that case, prior works fail to detect the contrast enhancement in previously Jpeg compressed images. To solve such a problem Detection of global contrast enhancement algorithm is proposed.

An important application is to find the move and paste type of image forgeries. Composite images are created by 2 source images, in which contrast of one source image is enhanced to match the other source image. Single source and both source enhanced images are identified using the concept of zero height gab bins and peaks. Then composition region is located using difference between the similarity measures in different image blocks of regions.

This paper organized as follows. In Section II previous works on global contrast enhancement detection algorithm. In section III proposed global contrast enhancement detection algorithm has been discussed. In section IV proposed composite detection algorithm by parallel approach has been discussed. Result and discussions are presented in section V and conclusion is drawn in section VI.

II.PREVIOUS WORK

Stamm and Liu [3] proposed a contrast enhancement detection algorithm as follows.

Get the normalized histogram of image h(x).

Modified histogram g(l) is obtained by performing the element wise multiplication between h(l) and a "'pinch off" p(l) function so that

$$g(l) = p(l)\, h(l) \quad \text{where}$$

$$p(l) = \begin{cases} \frac{1}{2} - \frac{1}{2}\cos\left(\frac{\pi l}{N_p}\right) & l \le N_p \\ \frac{1}{2} + \frac{1}{2}\cos\left(\frac{\pi(l-255+N_p)}{N_p}\right) & l \ge 255 - N_p \\ 1 & else \end{cases}$$

where N_p is the width of the region over which p(l) decays from 1 to 0. The pinch off function is designed to both remove impulsive histogram components which may occur due to saturation effects as well as to minimize the frequency domain effects of multiplying h(l) by p(l), which behaves similar to a windowing function. Calculate E, a normalized measure of the energy in the high frequency components of the pixel value histogram, from g(l) according to the formula

$$E = \frac{1}{N}\sum_k |\mathcal{B}(k)G(k)|$$

where N is the total number of pixels in the image, $G(k)$ is the DCT of g(l), and $\mathcal{B}(l)$ is a weighting function which takes values between 0 and 1. The purpose of $\mathcal{B}(l)$ is to deemphasize low frequency regions of $G(k)$ is to deemphasize low frequency regions of where nonzero values do not necessarily correspond to contrast enhancement artifacts.

$$\mathcal{B}(k) = \begin{cases} 1, & c \le k \\ 0 & else \end{cases}$$

where c is the entry of the 256 point DFT corresponding to a desired cut off frequency. $\mathcal{B}(k)$ is zero for all values greater than k = 256 because symmetry properties inherent in the DFT of real valued signals make it unnecessary to measure these values. After E has been calculated, the decision rule δ_{ce} is used to classify an image as unaltered or contrast enhanced, such that

$$\delta_{ce} = \begin{cases} image\ is\ not\ contrast\ enhanced, & E < \delta_{ce} \\ image\ is\ contrast\ enhanced, & E \ge \delta_{ce} \end{cases}$$

Detection depends upon the presence or absence of an intrinsic fingerprint introduced into an image's histogram by a pixel value mapping. The intrinsic fingerprints of contrast enhancement operations add energy to the high frequency components of an image's pixel value histogram. It fails to detect contrast enhancement in the previously low quality JPEG-compressed images.

III. GLOBAL CONTRAST ENCHANCEMENT DETECTION

From the study of peak/gap artifacts from contrast enhancement [1], the zero height gap bins are absent in compressed images since there is absence of a distinct pixel value mapping applied to all pixels. A pixel value mapping relationship exists in flat regions, but not in other regions. Therefore, the zero-height gap feature can be used for detecting global contrast enhancement in both uncompressed and compressed images.

Algorithm:

1) Normalized gray level histogram of image is denoted by nh(x) where x = 1,2,….256.

2) Bin k is called as zero height gab bin if it satisfies

$$\begin{cases} nh(k) = 0 \\ \min\{nh(k-1), nh(k+1)\} > \mathrm{r} \\ \frac{1}{2\omega+1}\sum_{x=k-\omega}^{x=k+\omega} nh(x) > \mathrm{r} \end{cases}$$

first sub equation says that the current bin is null. The second sub-equation keeps two neighboring bins larger than the threshold τ. In the third sub equation the average of neighboring (2w1 + 1) bins are taken which should be larger than τ. Here w1 = 2 and τ = 0.00001. This algorithm focus on the detection of isolated zero-height gap bins which are rarely occurs in the middle of histograms.

3) Count the number of zero-height gap bins, denoted by N

4) If N is larger than the decision threshold, contrast enhancement is detected, else not.

Figure 1 shows the (a) raw image, (b) compressed image with quality factor 10 and (c) contrast enhanced compressed image with quality factor 10. Figure 2 shows the corresponding normalized histogram for images in figure 1.

IV. PROPOSED COMPOSITE DETECTION ALGORITHM

In this section, composite contrast enhanced image detection algorithm is proposed. Figure 3 shows the block diagram of composition detection algorithm.

A. Detection of Gap and Peak bins

Initially test image is divided into non overlapping blocks. The position of detected gab bins labelled as $[V_{gp}{}^{i}(0), V_{gp}{}^{i}(1) \ldots V_{gp}{}^{i}(k), \ldots , V_{gp}{}^{i}(255)]$ where $V_{gp}^{i}(k) = 1$ if the bins at k is a gap; $V_{gp}^{i}(k) = 0$ otherwise.Peak bins which behave as impulse noise can be locate by median filtering and labelled as

$$[V_{pk}{}^{i}(0), V_{pk}{}^{i}(1) \ldots V_{pk}{}^{i}(k), \ldots , V_{pk}{}^{i}(255)]$$

where $V_{pk}^{i}(k) = 1$ refers to peak ; $V_{pk}^{i}(k) = 0$ otherwise.
i = 1,2…N_b; N_b – Number of divided blocks.

Fig.1 (a) Raw image; (b) Compressed Raw image with quality factor Q=10; (c) Contrast enhanced compressed image

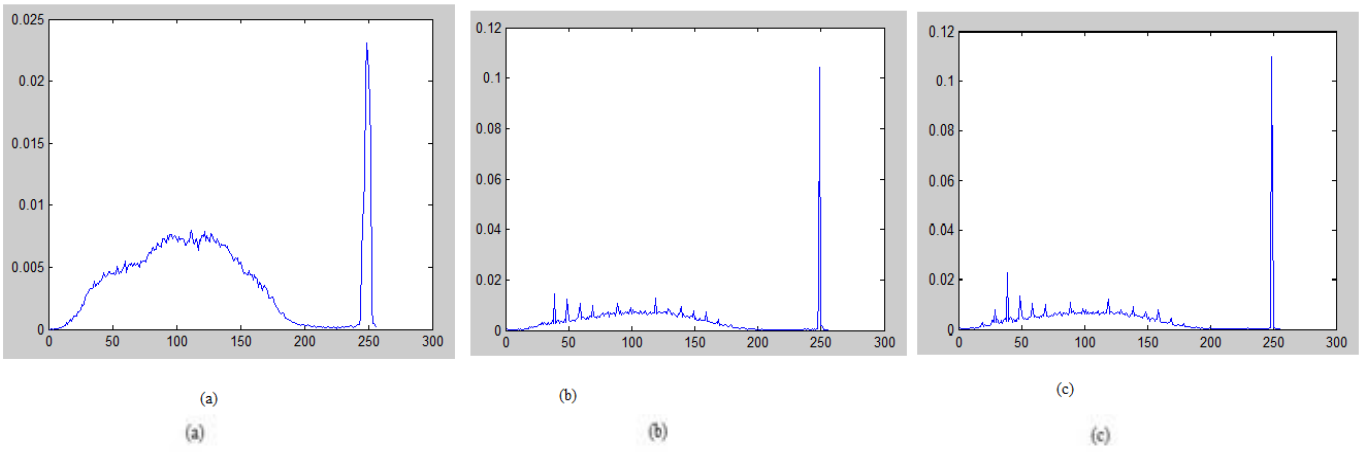

Fig.2 Normalized histogram of (a) Raw image; (b) Compressed Raw image with quality factor Q=10; (c) Contrast enhanced compressed image

To decrease detection errors, the extracted peak/gap positions are corrected by co-existing peak/gap positions.

$$C_{gp} = \sum_{i=1}^{N_b} \frac{V_{gp}^i}{N_b}$$

The detected co-existing gap positions as labelled as

$$V_{gp} = [V_{gp}(0),\ V_{gp}(1) \ldots\ V_{gp}(k), \ldots, V_{gp}(255)]\ .$$

$V_{gp}(k) = 1$ if $C_{gp}(k)$ is larger than the threshold, $V_{gp}(k) = 0$ otherwise. The corrected gap position vector, generated as

$$V_{gpc}^i = V_{gp}^i \odot V_{gp}$$

Similarly, the corrected peak position vector can also be calculated.

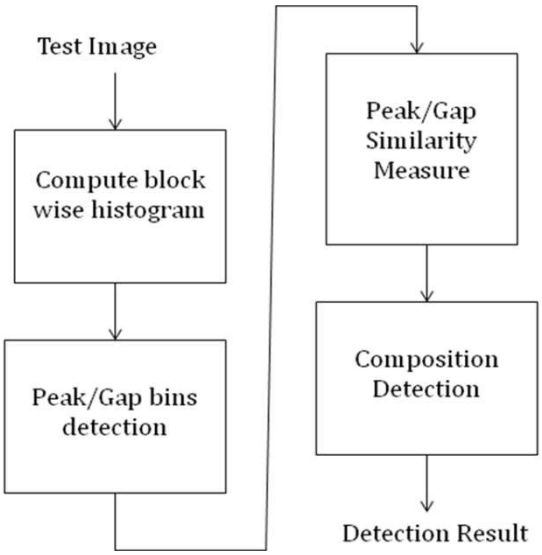

Fig.3 Block diagram of composite image detection.

B. Gab based similarity measure

To distinguish two source regions, calculate reference position vector. The reference gap position vector for located source region can be set as

$$V_{gpr} = {V_{gpc}}^k \text{ where}$$

$$k = {}^{\arg\ max}_{i\{1,2\ldots N_b\}} (|V_{gpc}^i|)$$

Effective Detection Range $\Omega_{gpr} = \Omega_k$. Similarity between V_{gpc}^i and V_{gpr} , denoted by Sm_g^i and calculated by

$$\frac{\sum_{k\in\Omega_i \cap \Omega_{gpr}} V_{gpc}^i(k).V_{gpr}(k)}{\sum_{k\in\Omega_i \cap \Omega_{gpr}} V_{gpc}^i(k).V_{gpr}(k)+\overline{V}_{gpc}^i(k).V_{gpr}(k)+V_{gpc}^i(k).\overline{V}_{gpr}(k)}$$

C. Peak based similarity measure

The reference peak position vector calculated by

$$V_{pkr}(k) = l\left(\sum_{n\in N_R} V_{pkc}^n(k) > 0\right)$$

Where k = 1,2...255 and

$$N_R = \{i | Sm_g^i > t_g\}$$

t_g is a threshold taken as 0.7. $\Omega_{pr} = U_{n\in N_R}\Omega_n$ .Similarity between V_{pkc}^i and V_{pkr}, denoted by Sm_p^i and calculated by

$$\frac{\sum_{k\in\Omega_i \cap \Omega_{pkr}} V_{pkc}^i(k).V_{pkr}(k)}{\sum_{k\in\Omega_i \cap \Omega_{pkr}} V_{pkc}^i(k).V_{pkr}(k)+\overline{V}_{pkc}^i(k).V_{pkr}(k)+V_{pkc}^i(k).\overline{V}_{pkr}(k)}$$

D. Fusion

Fusion value for each block denoted by m^i and calculated by

If $Sm_g^i \neq -1$ and $Sm_p^i \neq -1$ then

$$Sm^i = (Sm_g^i + Sm_p^i)/2$$

Otherwise

$$Sm^i = max(Sm_g^i, Sm_p^i)$$

for all blocks $m^i > t$ then it is identified as single source enhanced image. Otherwise m^i values classified as 2 sets. (i.e) $Sm^i \geq t$ in one set and $Sm^i < t$ in another set. It is identified as both source enhanced image. Figure 4(c) shows the detection result of this algorithm.

E. Parallel approach

Parallel processing improves the performance of the system by speeding up the execution[2]. Composition detection algorithm repeated for each block of image. So each block of image is processed in parallel manner. It increases the performance of image processing task.

V. RESULT

A. Test Data

Dataset 1:

Uncompressed Colour Image Database (UCID) [14]. It has 1338 uncompressed images.

Dataset 2:

CASIA1 Tampered Image Detection Evaluation Database. It has 921 spliced color images.

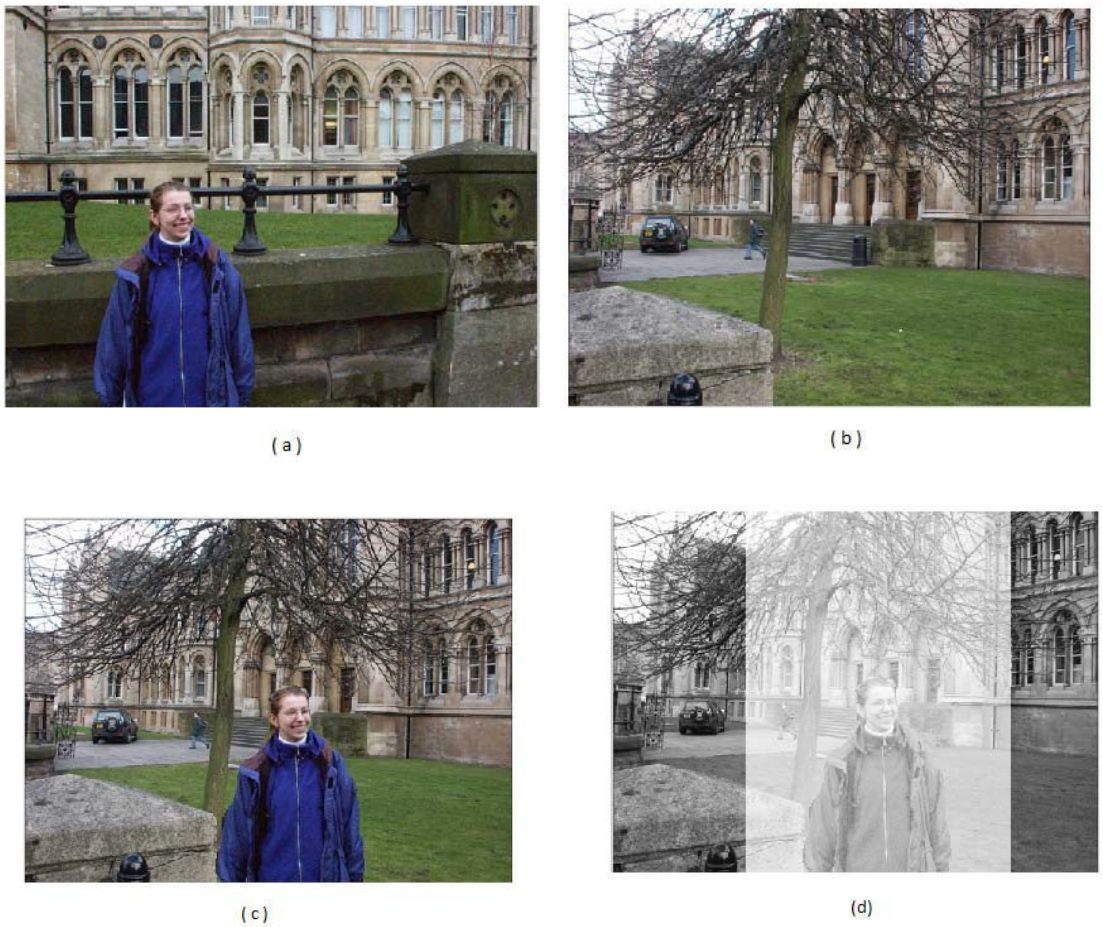

Fig. 4 (a) and (b) Source images;(c) Composite image created by contrast enhancement (d) Detection Result

B. Experimental Discussion

Proposed global contrast enhancement detection algorithm, works well for previously Jpeg compressed images with medium and low quality factor. It means that image enhancement techniques are applied after the Jpeg compression strategy. Prior works for composition detection fails to identify which type of manipulation was enforced. But proposed composite detection method identifies the manipulation using the similarity Sm^i values.

Splicing attack more or less similar to move-and- paste attack. Both techniques modifies the certain region of image. But move-and-paste attack uses portion of the original image as its source image. i.e the source and destination of the modified image originated from the same image. This algorithm also identifies the splicing attack. The future work is to identify the forgeries in double Jpeg compressed images

Dataset	UCID images	CASIA1 Spliced images
	True Positive Rate	True Positive Rate
Proposed Composite image detection	85%	80%
ExistingMethod Stamm and Liu [3	55%	75%

VI. CONCLUSION

In this paper, two contrast enhancements based algorithms have been proposed. These algorithms based on histogram bins and peaks analysis. Parallel approach used to increases the performance of the system. Zero height gap bins, similarity

measures are exploited as identifying features. Composition detection algorithm works well for previously Jpeg compressed images. In future this work extended to images undergone to post processing.

ACKNOWLEDGMENT

The authors would like to thank the Institutes for providing the databases. They also thank the anonymous reviewers and associate editor for their comments that greatly improved the manuscript.

REFERENCES

[1] Gang Cao, Yao Zhao, Rongrong Ni and Xuelong Li,"Contrast Enhancement-Based Forensics in Digital Images",IEEE Trans. Information forensics and security, vol. 9, No. 3 April 2013

[2] Eric Olmedo, Jorge de la Calleja, Antonio Benitez, and Ma. Auxilio Medina,"Point to point processing of digital images using parallel computing",IJCSI International Journal of Computer Science Issues, Vol. 9, Issue 3, No 3, May 2012

[3] M. C. Stamm and K. J. R. Liu, "Forensic detection of image manipulation using statistical intrinsic fingerprints," IEEE Trans. Inf. Forensics Security, vol. 5, no. 3, pp. 492–506, Sep. 2010.

[4] A. C. Popescu and H. Farid, "Exposing digital forgeries by detecting traces of resampling," *IEEE Trans. Signal Process.*, vol. 53, no. 2, pp. 758–767, Feb. 2005

[5] T. Bianchi and A. Piva, "Detection of non-aligned double JPEG compression based on integer periodicity maps," IEEE Trans. Inf. Forensics Security, vol. 7, no. 2, pp. 842–848, Apr. 2012.

[6] G. Cao, Y. Zhao, R. Ni, and A. C. Kot, "Unsharp masking sharpening detection via overshoot artifacts analysis," IEEE Signal Process. Lett., vol. 18, no. 10, pp. 603–606, Oct. 2011.

[7] M. C. Stamm and K. J. R. Liu, "Forensic estimation and reconstruction of a contrast enhancement mapping," in Proc. IEEE Int. Conf. Acoust., Speech Signal, Dallas, TX, USA, Mar. 2010, pp. 1698–1701.

[8] G. Cao, Y. Zhao, and R. Ni, "Forensic estimation of gamma correction in digital images," in Proc. 17th IEEE Int. Conf. Image Process., Hong Kong, 2010, pp. 2097–2100.

[9] P. Ferrara, T. Bianchiy, A. De Rosaz, and A. Piva, "Reverse engineering of double compressed images in the presence of contrast enhancement," in Proc. IEEE Workshop Multimedia Signal Process., Pula, Croatia, Sep./Oct. 2013, pp. 141–146.

[10] M. Kirchner and J. Fridrich, "On detection of median filtering in digital images," in Proc. SPIE, Electronic Imaging, Media Forensics and Security II, vol. 7541, San Jose, CA, USA, Jan. 2010, pp. 1–12.

[11] C. Chen, J. Ni, and J. Huang, "Blind detection of median filtering in digital images: A difference domain based approach," IEEE Trans. Image Process., vol. 22, no. 12, pp. 4699–4710, Dec. 2013.

[12] T. Arici, S. Dikbas, and Y. Altunbasak, "A histogram modification framework and its application for image contrast enhancement," IEEE Trans. Image Process., vol. 18, no. 9, pp. 1921–1935, Sep. 2009.

[13] S. Battiato, A. Bosco, A. Castorina, and G. Messina, "Automatic image enhancement by content dependent exposure correction," EURASIP J. Appl. Signal Process., vol. 12, pp. 1849–1860, Jan. 2004.

[14] G. Schaefer and M. Stich, "UCID—An uncompressed colour image database," in Proc. SPIE, Storage and Retrieval Methods and Applications for Multimedia, vol. 5307, San Jose, CA, USA, 2004, pp. 472–480.

[15] Fan, H. Cao, and A. C. Kot, "Estimating EXIF parameters based on noise features for image manipulation detection," IEEE Trans. Inf.Forensics Security, vol. 8, no. 4, pp. 608–618, Apr. 2013.

[16] A. Swaminathan, M. Wu, and K. J. R. Liu, "Digital image forensics via intrinsic fingerprints," IEEE Trans. Inf. Forensics Security, vol. 3, no. 1, pp. 101–117, Mar. 2008.

[17] D. Mahajan, R. Ramamoorthi, and B. Curless, "A theory of frequency domain invariants: Spherical harmonic identities for BRDF/lighting transfer and image consistency," IEEE Trans. Pattern Anal. Mach. Intell., vol. 30, no. 2, pp. 197–213, Feb. 2008.

[18] J. O'Brien and H. Farid, "Exposing photo manipulation with inconsistent reflections," ACM Trans. Graph., vol. 31, no. 1, pp. 1–11, 2012.

[19] H. Farid, "Image forgery detection," *IEEE Signal Process. Mag.*, vol. 26, no. 2, pp. 16–25, Mar. 2009.

[20] B. Mahdian and S. Saic, "A bibliography on blind methods for identifying image forgery," *Image Commun.*, vol. 25, no. 6, pp. 389–399, Jul. 2010.

[21] S. Bayram, I. Avcubas, B. Sankur, and N. Memon, "Image manipulation detection," *J. Electron. Imag.*, vol. 15, no. 4, pp. 04110201–04110217, 2006.

A PRODUCTION COST MODEL FOR REACTIVE POWER IN ELECTRICITY MARKET

D.Danalakshmi[1], S.Kannan[2]

[1]*Research Scholar, Kalasalingam University, Krishnankoil, Tamil Nadu, India*

[2]*Department of EEE, Ramco Institute of Technology, Rajapalayam, Tamil Nadu, India*

Abstract - In a restructured power market, supply of reactive power is an essential ancillary service provided by an Independent System Operator taking into account the voltage stability and reliability of the power system. The generators are the main producer of reactive power. The production cost of generator reactive power should be consideredfor reactive power pricing. In this paper, the production cost of real and reactive power was considered in the objective function of the optimal power flow problem.Different methods were presented to obtain the reactive power cost equation of the generator. The triangular method is based on generator power factor to allocate the cost for reactive power service. Real power based method and apparent power based method depends on the opportunity cost of the generator for reactive power cost allocation. These methods are illustrated with IEEE-14 bus power systems to show its validity andpracticability.

Keywords:Opportunity cost, optimal power flow, Reactive power cost functions, Restructuring.

I. INTRODUCTION

In a restructured power system, one of the most important issues of Independent System Operator (ISO) is to maintain the reactive power. Steady supply of reactive power improves the stability and reliability of the power system. Inadequate reactive power in the system leads to voltage collapses and has been a major cause of blackout across the world, e.g. United states and Canada in the year 2004 [1]. In a restructured electricity market, the ISO aims to utilize the available reactive power resources efficiently. It is essential to determine the price payment to market participants for providing the reactive power service in the system.

In deregulated power system, the reactive power service is separated from the real power services and is considered as one of the activity of system operator. The cost of reactive power service is recovered based on various methods in deregulated power system. In some power system, cost of reactive power is included in active power price. In some system, the power factor is used for calculation of cost of reactive power service[2]. In reactive power pricing based on load power factor, the generators have to produce necessary power at a specified range of power factor. If the power factor deviate the specified range, the reactive power has to be priced. In a pool type competitive electricity market, ISO constitutes the appropriate payment mechanism and market structure for reactive power services so that the reactive power producers are encouraged to participate in the electricity market.

Many researches have been carried out for pricing of reactive power service. Practical restructured power systems adopt different pricing strategies for reactive power. Dona and Paredes have proposed a reactive power pricing technique using decoupled OPF with an objective of minimization of operational cost as well as the

transmission losses [3]. Chu and Chen have proposed the reactive power cost allocation using modified Y-bus

matrix [4]. Rider and Paucar have introduced a reactive power pricing method which is solved by Interior point method [5]. Chung et al. have presented a reactive power pricing method in which the reactive power production cost by generators and capacitors are minimized in the objective function [6]. Deksnys and Staniulis have introduced a method for reactive power cost equation of generators, synchronous condenser and static reactive power sources [7].

Allocation of generator production cost and generator transmission cost using reactive power flow tracing method are determined in [8]. An electricity tracing method is used to charge the reactive power provider for the actual amount of transmission line loading and loads [9]. Ashutosh et al have proposed the application of power flow tracing method for reactive power pricing [10]. In this paper, we have compared the three methods for framing the reactive power cost equation and calculated the production cost of reactive power service in a power market.

The rest of the paper is organized as follows: Section II explains the methods for reactive power production cost model of the generator. Section III describes the formulation of OPF problem and Section IV analyses the results and compared the reactive power production cost allocation in IEEE 14 bus system. Finally Section V provides the conclusion.

II. REACTIVE POWER COST MODEL OF THE GENERATOR

The reactive power produced by a synchronous generator is composed of two cost components. They are explicit cost and the implicit cost [11]. Explicit cost is the investment costs and operating cost. Implicit cost refers to the opportunity cost which depends on the reduction in its active power generation. The following methods have been considered to evaluate the cost of generator reactive power.

A. Triangular method

The cost calculation of generator reactive power is based on the active power cost equation. The reactive power equation for the generators follows the same quadratic structure as active power using the power triangle relationship [2]. The reactive power cost function is represented as

$$C(Q) = a'Q^2 + b'Q + c' \tag{1}$$

where a', b', c' are cost coefficients which are derived from the active power cost coefficient (a_p, b_p and c_p) and generator power factor ($\cos\theta$). They are calculated as follows from power triangle relationship.

$$\left[a' = a_p \sin^2\theta,\ b' = b_p \sin\theta \text{ and } c' = c_p\right]$$

B. Maximum Apparent power based Opportunity cost method

Synchronous generators are rated in maximum MVA at specified voltage and power factor. The generator real power output is usually limited by the capability of its prime mover. The generator reactive power output is limited by armature current, field current and end region heating limit [12].The mutual relationship between real and reactive power output of synchronous generator are represented by capability curve as shown in Fig.1.

Let $V_t$is the generator terminal voltage

$I_a$is the steady state armature current.

$P_g$and Q_g are real and reactive power generation from the synchronous generator.

E_f is the excitation voltage and

X_s is the synchronous reactance of the generator.

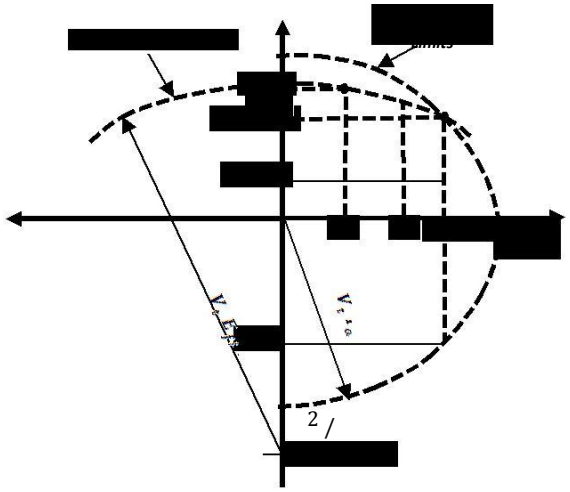

Fig. 1. Capability curve of synchronous generator

The production cost of generator reactive power is called opportunity cost. The production of reactive power reduces the active power output of the generator and may leads to financial loss to the generator. Opportunity cost can be approximately evaluated as [8]:

$$C_{qgi}(Q_{Gi}) = \left[C_{pgi} (S_{Gi,\max}) - C_{pgi} \sqrt{S^2_{Gi,\max} - Q^2_{Gi}} \right] K_{Gi} \quad (2)$$

where $C_{qgi}$is the reactive power production cost of the *i*-thgenerator, C_{pgi} is the active power production cost of the *i*-th generator, P_{Gi} and Q_{Gi} are the real and reactive power of generator i, $S_{Gi,max}$is the apparent power of generator, K_{Gi} is the profit rate of the active power, which is usually chosen between 0.05~0.1. In this paper, K_{Gi}= 0.1.

C. Maximum real power based opportunity cost method

If the generator is operating at its maximum active power P_{max} and there is no reactive power. In such situation S equals P_{max}. To generate reactive power from the generator, it is required to reduce the real power. Suppose the generator needs to produce the reactive power Q_A which has been operating at its maximum power, it is required to reduce the real power from P_{max} to P_A as shown in Fig. 1. Hence the generator reactive power production results in reduction of real power [2].

$$P_A = \sqrt{P_{\max} - Q_A^2} \quad (3)$$

$$\Delta P = P_{\max} - P_A \quad (4)$$

The opportunity cost of Q_A depends on the profit of $\Delta P = P_{\max} - P_A$. Hence the generator production cost of reactive power Q_A while the generator operating point is moved from P_{max} to P_A is as follows

$$Cost(Q_A) = Cost(\Delta P) \tag{5}$$

$$Cost(Q_A) = Cost(P_{\max}) - Cost(P_A) \tag{6}$$

$$Cost(Q_A) = Cost(P_{\max}) - Cost(P_{\max} - \Delta P) \tag{7}$$

Usingthe equations 3, 4 and 7, the cost value of reactive power is calculated for different values of $Q_A$with respect to P_A. The cost expression for reactive power is calculated by fitting a curve into a quadratic polynomial form as below

$$Cost(Q) = a'Q^2 + b'Q + c' \tag{8}$$

This reactive power cost equation is simple and can provide results for reactive power pricing.

III. Optimal Power Flow (OPF) problem formulation

The real and reactive power production cost of the generator is obtained by solving the OPF. The OPF problem is defined as minimizing the system objective function, i.e. summation of quadratic cost functions of active and reactive power cost of the system [2]. The OPF problem formulation is:

Objective function

$$\sum_{i \in g} C_{pgi}(P_{gi}) + C_{qgi}(Q_{gi}) \tag{9}$$

where g is the number of generators; $C_{pgi}(P_{gi})$ is the active power cost function of the *i*-th generator; $C_{qgi}(Q_{gi})$ is the reactive power cost function of the *i*-th generator respectively.

The constraints considered in this OPF problem are the set of equality and inequality constraints. The equality constraints are standard power flow equations and inequality constraints are the generation, voltage and line flowlimits of the system, as shown below:

Load flow equations:

$$P_{gi} - P_{di} - \sum_{j \in N} \left|V_i^{\bullet}\right| \left|V_j^{\bullet}\right| \left|Y_{ij}\right| \cos(\theta_{ij} + \delta_j - \delta_i) = 0 \tag{10}$$

$$Q_{gi} - Q_{di} + \sum_{j \in N} \left|V_i^{\bullet}\right| \left|V_j^{\bullet}\right| \left|Y_{ij}\right| \sin(\theta_{ij} + \delta_j - \delta_i) = 0 \tag{11}$$

where *N i*s the number of buses in the system; P_{gi} and Q_{gi} are the active and reactive power generation in *i*-th bus, respectively; P_{di} and $Q_{di}$are the active and reactive power demand in *i*-th bus, respectively; $Y_{ij} = Y_{ij} \angle \theta_{ij}$ is the element in the bus admittance matrix between bus i and j; $V_i^{\bullet} = V_i \angle \delta_i$ and $V_j^{\bullet} = V_j \angle \delta_j$ are the bus voltage at bus i and j, respectively.

Active and Reactive power generation limits:

$$P_{gi,\min} \le P_{gi} \le P_{gi,\max}$$

$$Q_{gi,\min} \le Q_{gi} \le Q_{gi,\max}$$

$$\leq Q_{gi,\max} \quad (12)$$

(13)

$$P_{gi}^2 + Q_{gi}^2 \le S_{gi,\max}^2 \tag{14}$$

where $P_{gi,\ min}$ and $P_{gi,\ max}$ are the minimum and maximum value of the active power generation at *i*-th bus; $Q_{gi,\ min}$ and $Q_{gi,\ max}$ are the minimum and maximum value of the reactive power generation at *i*-th bus; $S_{gi,max}$is the maximum apparent power at *i*-th bus, respectively.

Bus voltage limits:

$$V_{i,\min} \le |V_i| \le V_{i,\max} \tag{15}$$

where $V_{i,\ min}$ and $V_{i,\ max}$ are the minimum and maximum value of the voltage limit at *i*-th bus, respectively.

Transmission line limits:

$$S_l \le S_l^{\max}; l \in N_l \tag{16}$$

where S_l is line loading and $S_l^{\max}$ is maximum loading limit of *l*-th line and N_l is the total number of transmission line.

The optimization problem takes the form

$$\min_x \quad f(x) \tag{17}$$

Subject to

$$g(x) = 0$$
$$h(x) \le 0$$

The optimization problem is solved using MATPOWER [13]. The optimization vector x consist of voltage magnitude, voltage angle and the vector of generator real and reactive power respectively.

IV. Results and Discussion

To investigate validity of the methods, it has been applied to IEEE 14 bus system. The system has 5 generators and 20 transmission lines. Table I and Table II shows the generator characteristics and load characteristics with non capacitive load respectively. The base of generator apparent power is 100MVA. The voltage limit is $0.9\ p.u \le |V_i| \le 1.05\ p.u$ and swing bus voltage is $V_i = 1.05\ p.u$ *and* $\delta_i = 0$ .The generator power factor are taken as 0.97 and generator 3 with power factor of 0.85.

TABLE I

GENERATOR CHARACTERISTICS

Generator No.	Bus no.	P_{max}(MW)	P_{min}(MW)	Q_{max}(MVAr)	Q_{min}(MVAr)	Real Power coefficient		
						a_p	b_p	c_p
1	1	332	50	100	-100	0.0430	20	0
2	2	140	10	50	-50	0.25	20	0
3	3	100	12	100	-60	0.01	40	0
4	6	100	10	30	-30	0.01	40	0
5	8	100	10	30	-30	0.01	40	0

Three different cases have been analyzed. In the first case, the reactive power cost equations are framed using triangular method. In the second case, the reactive production cost equation are framed using apparent power based opportunity cost method and in the third case, the maximum real power based opportunity cost approach is used to frame the reactive power production cost equations of the IEEE-14 bus system. Table III shows the comparison of results for these three cases.

TABLE II

LOAD CHARACTERISTICS

Bus No	Active power(MW)	Reactive power (MVAr)
2	21.7	12.7
3	94.2	19.0
4	47.8	3.9
5	7.6	1.6
6	11.2	7.5
9	29.5	16.6
10	9.0	5.8
11	3.5	1.8
12	6.1	1.6
13	13.5	5.8
14	14.9	5.0

TABLE III

ANALYSIS OF RESULTS IN IEEE 14 BUS SYSTEM

	Bus. No	P_g (MW)	Q_g (MVAr)	Generator Actual real power production cost ($/h)	Generator actual reactive power production cost ($/h)	Total cost ($/h)
Case 1 (Triangular method)	1	33.2331	10.0177	712.2	42.3316	12656.33
	2	140.0	28.0272	7700	147.5069	
	3	53.1197	10.0167	2153	216.2728	
	6	13.2143	14.3828	530.3	112.9067	
	8	23.3083	13.2509	937.8	104.0155	
Case 2 (Apparent power based opportunity cost method)	1	33.2331	10.0216	712.2	20.4754	12282.12
	2	140	29.6654	7700	81.3318	
	3	53.1396	10.0170	2153.8	40.1682	
	6	10.1046	12.8339	405.2	51.5005	
	8	26.3773	13.7873	1062.1	55.3392	
Case 3 (Real power based opportunity cost method)	1	33.2331	10.0782	712.2	70.7204	12534.39
	2	140	7.9637	7700	20.7357	
	3	52.8162	10.0675	2140.5	133.9180	
	6	10.0171	30.0	401.7	186.4606	

	8	26.9906	20.0211	1086.9	81.2575	

From Table III, the following observations are made:

- The active power production cost at the generator bus changes slightly when the objective function changes.
- For each test case, the reactive power production cost fluctuates significantly at the generator buses.
- The active power production cost is much higher than the reactive power production cost at various generator buses.
- When the reactive power production cost is included in the objective function, the total production cost of the generator is increased.
- The total reactive power generation cost in triangular method is greater than that of apparent power based opportunity cost method and real power based opportunity cost method. This will encourage and motivate the reactive power provider to invest and provide reactive power service to keep the power system in a secure manner. On the other hand, in deregulated power markets where the reactive power is priced low, based on apparent power and real power based opportunity cost method. This will make less motivation among the reactive power suppliers to support for the reactive power service. Thus the modeling of reactive power production cost equation using triangular method seems to provide good pricing of reactive power. This will encourage the reactive power provider for their active participation to provide reactive power for enhancement of stable and reliable operation of power system.

V. CONCLUSION

In this paper, both active and reactive power production costs of the generators are considered in the objective function of the OPF problem. Three different methods are employed to obtain the reactive power cost equation for the generator. The IEEE 14 bus system is used to verify the validity of the method. Results confirm that the reactive power cost obtained through triangular method is higher than the cost obtained through real power based cost method and apparent power based method. Finally, based on motivating the generators to provide reactive power service and also providing good production cost for real and reactive power, the triangular method yields better production cost for generator real and reactive power.

ACKNOWLEDGMENT

The authors gratefully acknowledge the management of Kalasalingam University, Krishnankoil and Ramco Institute of Technology, Rajapalayam, Tamil Nadu, India for their constant support and encouragement during this research.

REFERENCES

[1] US-Canada Power System Outage Task Force,"Blackout in the United States and Canada: Causes and Recommendations," Issued in April 2004. Available: http://www.iwar.org.uk/cip/resources/blackout-03/ch1-3.pdf

[2] S. Hasanpour · R. Ghazi · M. H. Javidi, "A new approach for cost allocation and reactive power pricing in a deregulated environment" *Electrical Engineering*, vol. 91, issue.1, pp 27-34, Springer-Verlag 2009.

[3] Dona V.M. andParedes A.N., "Reactive power pricing in competitive electric markets using the transmission losses function," *Power Tech conference,* IEEE porto, vol.1,pp 1–6, 10-13 September, 2001.

[4] Chu. W and Chen. B, "Allocating the costs of reactive power purchased in an ancillary services market by modified Y-bus matrix method," *IEEE Transaction on Power System*, vol.19, issue. 1, pp.174-179,February 2004.

[5] Rider M.J. and Paucar V.L.,"Application of a nonlinear reactive power pricing model for competitive electric markets," *IEE Proc. Generation Transmission Distribution*,vol. 151,issue.3, pp.407-415,May2004.

[6] Chung CY, Chung TS, Yu CW and Lin XJ, "Cost-based reactive power pricing with voltage security consideration in restructured power systems," *Electric Power System Research*,vol. 70, issue.2, pp.85-92, July 2004.

[7] Deksnys R andStaniulis R,"Pricing of reactive power services," *Oil Shale Estonian Academy Publisher*, vol. 24, pp.363-376,2007.

[8] Dai ,Y., Liu, X. D., Ni,Y.X., Wen, F.S., Han, Z.X., Shen, C.M. Felix F. Wu, " A cost allocation method for reactive power service based on power flow tracing," *Electric power system research*,vol.64, issue.1, pp. 59-65, Jan. 2003.

[9] Mala De, Swapan and Goswami, K, "Reactive power cost allocation by power tracing based method", *Energy Conversion and Management*, vol. 64, pp. 43-51, December 2012.

[10] AshutoshTiwari and Ajjarapu. V, "Reactive Power Cost Allocation Based on Modified Power Flow Tracing Methodology," Power Engineering Society General meeting IEEE 2007, E-ISBN: 1-4244-1298-6, pp.1-7, June 2007.

[11] John Lamont , W., and Jian Fu, "Cost Analysis of Reactive Power Support," *IEEE Transactions on Power Systems*,vol.14, issue.3, pp. 890-898, August 1999.

[12] Bhattacharya, K., and Jin Zhong, "Reactive power as an ancillary service", *IEEE Transaction on Power Systems*, vol.16, issue.2, pp. 294-300, May 2001.

[13] Zimmerman.R and Gan.D. MATPOWER 4.0, A MATLAB power system simulation package, Cornell University, Available from: http://www.pserc.cornell.edu /matpower. Feb. 2011.

Asset Management in Smart Grids Using Improved Dissolved Gas Analysis

V. Srinivasan
Research Scholar
Department of Electrical and Electronics Engineering
Kalasalingam University
Krishnankoil, Srivilliputtur (via),
Virudhunagar District
Tamilnadu, India

B. Subathra, Seshadhri Srinivasan
Sr.Associate Professor, Professor
Kalasalingam University
Krishnankoil, Srivilliputtur (via),
Virudhunagar District
Tamilnadu, India

S.Kannan
Professor and Head,
Department of Electrical and Electronics Engineering
Ramco Institute of Technology
Virudhunagar District
Tamil Nadu, India

***Abstract*— Asset Management Systems (AMS) are pivotal to build reliable and safe smart grids. An important function of AMS is the monitoring and diagnosis of the power transformers. Various tests are performed on power transformers to detect incipient faults. Among the available methods, Dissolved Gas Analysis (DGA) has been widely used and shown promise. However, interpreting the results of the DGA is challenging due to the availability of wide variety of methods such as Rogers ratio, Doernenburg ratio, key gas procedure of IEEE, Basic gas ratio and Duval triangle methods of IEC. The accuracy of the interpretation methods influences AMS performance leading to reliability issues in the grid. This investigation compares the accuracy of Duval method and basic gas ratio method to detect transformer faults from real-time fault data obtained from power transformers. Our results on data obtained from Electrical Research and Development Association for seven transformer incipient faults shows that the Duval method is accurate than the basic gas ratio method for identifying incipient transformer fault based on DGA results. Further, the basic gas ratio was not able to detect two of the seven faults. These results illustrate the need to integrate Duval method to detect power transformer faults within AMS.**

Keywords—Transformer Condition Monitoring, Asset Management Systems, Dissolved Gas Analysis (DGA), Duval, basic gas ratio method.

I. INTRODUCTION

Power Transformers are vital equipment in the electric grid and their outage leads to significant economic loss. Further, replacement time of power transformer is quite high due to cost and logistics difficulties. Consequently, condition monitoring and fault-diagnosis of power transformers have received significant attention. The importance of power transformer condition monitoring can be understood from the various tests such as the insulation resistance, tan-delta, oil quality inspection, winding resistance test, dissolved gas analysis (DGA), and so on, that are conducted at regular intervals by utilities to avoid outages. Although, many tests are conducted on transformers, DGA has emerged as a promising solution, due to their ability to detect incipient faults and possible failures. However, interpreting DGA results is still challenging due to the availability of various methods such as Duval, basic gas ratio, Rogers ratio, Doernenburg ratio, and key gas procedure (see, [1]-[3] and references therein). Further, the accuracy of these methods differ for a given fault. For instance, the accuracy of the methods for the seven faults described in Table 1 has not been studied extensively in literature. However, such a comparison is required for building future Asset Management Systems (AMS). Therefore, the accuracy of these interpretation methods in detecting incipient faults and predicting failures for enhancing the capabilities of AMS needs to be studied.

TABLE 1

OCCURRED FAULTS

Tr. Case	Actual fault occurred
1	hot-spot on connecting lead due to bolted joint loose connection
2	melting of core-stamping bolt
3	arcing between high voltage leads
4	arcing between LT bus bars
5	inter-turn fault
6	arcing at OLTC (on-load tap changer) contact
7	arcing in diverter switch

The accuracy of DGA interpretation methods for diagnosing faults has been studied by researchers and some useful comparisons have been reported in literature. As reviewing the complete literature is not within the scope of this paper; here a brief idea on significant results is presented. The authors in [2], used key gas ratio and basic gas ratio methods for diagnosing power transformer faults using DGA results. Further, the investigation developed a fuzzy inference system for improving the fault-diagnosis and detection of thermal faults using fuzzy has been studied. Although, this method is an improvement in detecting multiple faults, the approach suffers from the efficacy of the DGA interpretation methods in detecting faults. The investigation in [4] studied the use of Rogers and IEC -ratio methods for power transformer fault detection using artificial neural network using data from 30 faulted transformers. The investigation concluded that both the ratio methods are effective and simple, as the volume of the oil involved in the dissolution of the gas is not required. Though, the method is a progress towards developing expert systems for transformer condition monitoring, accuracy of inference method has not been studied. Importance of inference method accuracy can be understood in the light of results of investigation [5], that used Roger's ratio to interpret

978-1-4799-8371-1/15/$31.00 ©2015 IEEE

DGA results, and concluded that the efficiency of the method in detecting incipient faults to be 45-52%. Reading the results of the investigation [4] and [5] in unison reveals that, while it is essential to harness the features of computational intelligence in building expert systems for transformer condition monitoring, their performance is however dictated by the accuracy of the DGA inference method. This necessitates studying the accuracy of the inference methods for various faults envisaged in a power transformer. Seeing, the potential of accuracy of inference methods in designing expert systems that can be used in building dependable AMS, the authors in [3], studied the accuracy for 92 common faults in power transformers. Further, the investigation concluded that Duval method showed good accuracy in detecting incipient faults. However, comparison of Duval and gas ratio method that have competing accuracies for detecting faults listed in Table 1, has not been studied in literature extensively. In particular, accuracy of these methods studying incipient and operating faults has not been studied. Motivated by this research gap, this investigation aims to determine the accuracy of two methods: Duval and basic gas ratio in detecting incipient and operating faults. The two methods have been selected due to their competing accuracies and absence of results comparing both these approaches.

To reach the objectives of this investigation, first DGA data from seven faulted transformer is collected. Then computations that perform Duval and gas ratio method are applied to the results to detect the faults. The obtained results are compared with the actual faults to draw conclusions on the accuracy of the interpretation approaches. Our results show that the accuracy of Duval method in detection of power transformer faults is quite high compared to gas ratio method.

The investigation is organized into five sections. Section II reviews the gas ratio and Duval method. The condition monitoring of transformer and the DGA data from faulted transformers is presented in section III. The fault-case studies and results are presented in section IV. Conclusions are drawn from the obtained results in Section V.

II. Review of Dissolved Gas by Basic Gas Ratio and Duval Triangle

The DGA results of the failed transformers obtained from the laboratory can be analyzed by both the IEC basic gas ratio method and Duval triangle method

A. IEC basic gas ratio method

In IEC basic gas ratio method, DGA results are used to determine the C_2H_2/C_2H_4, CH_4/H_2, C_2H_4/C_2H_6 gas ratios.
DGA interpretation in Table 2 can be used to detect faults based on the gas ratio from the failed transformers.

TABLE 2
DGA INTERPRETATION

Case	Characteristic fault	C_2H_2/C_2H_4 in ppm	CH_4/H_2 in ppm	C_2H_4/C_2H_6 in ppm
PD	Partial discharges	NS	<0.1	<0.2
D1	Discharges of low energy	>1	0.1-0.5	>1
D2	Discharges of high energy	0.6-2.5	0.1-1	>2
T1	Thermal fault t<300°C	NS	1 but NS	<1
T2	Thermal fault 300°C < t < 700°C	<0.1	>1	1-4
T3	Thermal fault t>700°C	<0.2	>1	>4
NS = Non-significant whatever the value				

B. IEC Duval triangle method:

In Duval method, the gas concentration values are used to construct the coordinates of the triangle shown in Figure 1. The Duval coordinates are computed by using (1-3).

$$\%C_2H_2 = (100\ x)/(x+y+z) \quad \text{for } x = [C_2H_2] \text{ in ppm.} \tag{1}$$
$$\%C_2H_4 = (100y)/(x+y+z) \quad \text{for } y = [C_2H_4] \text{ in ppm.} \tag{2}$$
$$\%CH_4 = (100\ z)/(x+y+z) \quad \text{for } z = [CH_4] \text{ in ppm.} \tag{3}$$

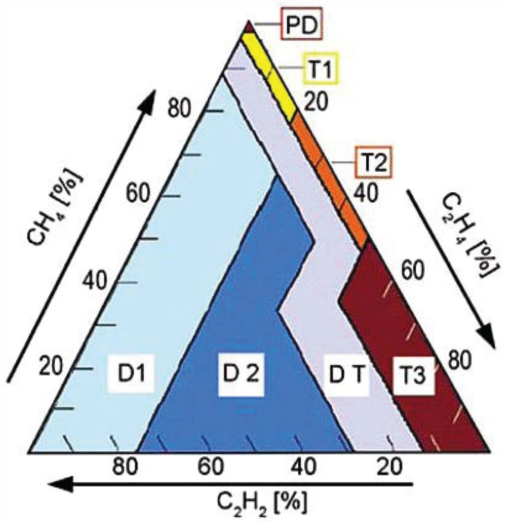

Figure 1: Duval triangle

After constructing the Duval triangle the faults are identified from the intersections of the coordinates computed from (1-3). This triangle forms the basis of analysis for the faults. The various faults that can be studied using Duval coordinates/gas ratio are defined in the standard IEC 60599 and are illustrated in Table 3, and Table 4, respectively.

TABLE 3
TYPICAL FAULTS IN POWER TRANSFORMERS

Type	Fault	Examples
PD	Partial discharges	Discharges in gas-filled cavities resulting from incomplete impregnation, high-humidity in paper, oil super saturation or cavitation, and leading to X-wax formation
D1	Discharges of low energy	Sparking or arcing between bad connections of different or floating energy potential, from shielding rings, toroids, adjacent disks or conductors of winding, broken brazing or closed loops in the corona Discharges between clamping parts, bushing and tank, high voltage and ground within windings, on tank walls Tracking in wooden blocks, glue of insulating beam, winding spacers, Breakdown of oil, selector breaking current
D2	Discharges of high energy	Flashover, tracking, or arcing of high local energy or with power follow-through Short circuits between low voltage and ground, connectors, windings, bushings and tank, copper bus and tank, windings and core, in oil duct, turret. Closed loops between two adjacent conductors around the main magnetic flux, insulated bolts of core, metal rings holding core legs
DT	Thermal and electrical faults	Mixture of thermal and electrical faults
T1	Thermal fault t<300°C	Overloading of the transformer in emergency situations Blocked item restricting oil flow in windings Stray flux in damping beams of yokes
T2	Thermal fault 300°C<t<700°C	Defective contacts between bolted connections (particularly between aluminium busbar), gliding contacts, contacts within selector switch (pyrolitic carbon formation), connections from cable and draw-rod of bushing Circulating currents between yoke clamps and bolts, clamps and laminations, in ground wiring, defective welds or clamps in magnetic shields Abraded insulation between adjacent parallel conductors in windings
T3	Thermal fault t>700°C	Large circulating currents in tank and core. Minor currents in tank walls created by a high uncompensated magnetic field Shorting links in core steel laminations

In addition to diagnosing transformer faults, DGA can be used to diagnose faults in switching equipment and accessories. The type of faults that are defined within the standard IEC 60599 is shown in Table 4.

TABLE 4
TYPICAL FAULTS IN SWITCHING DEVICES

Type	Fault	Examples
D1	Discharges of low energy	Normal operation of OLTC, selectors Arcing on off-load selector switch ring, OLTC connections
D2	Discharges of high energy	Switch contacts do not reach their final position but stop halfway, due to a failure of the rotating mechanism, inducing a spark over discharge Arcing on off-load selector switch ring, OLTC connections, of high energy or with power follow-through, with failure often transmitted to transformer windings
T3	Thermal fault	Increased resistance between contacts of OLTC or change-over selector, as a result of pyrolitic carbon growth, selector deficiency or a very large number of operations

III. Condition Monitoring and DGA Data

The transformer condition monitoring method using DGA test results is shown in Figure 2. The transformer oil collected from the transformer is the input to the DGA test, while the composition of dissolved gases in the transformer oil is the output. An analysis of the gas compositions gives information on possible transformer faults and gas ratio/Duval coordinates are used to this extent. This information is used by the diagnostic methods to detect the faults. As stated earlier, numerous methods are available in diagnosing the DGA results and their accuracy differs for a given fault. The DGA results and the gas ratios obtained from the laboratory for the

seven cases of faults studied in the investigation are given in Table 5 and Table 6, respectively. The gas ratios are analyzed with the DGA interpretation (Table 2) and the corresponding type of fault is determined as shown in Table 8.

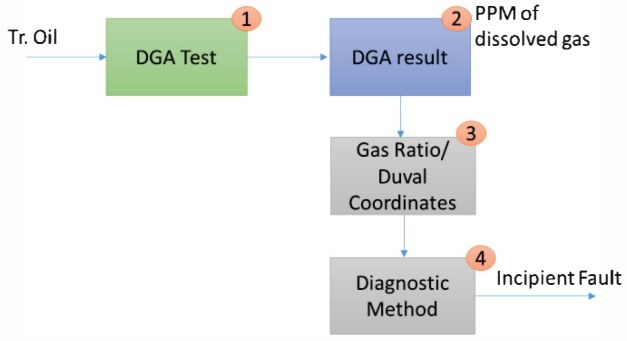

Figure 2: DGA based transformer condition monitoring system

TABLE 5
DGA RESULTS FROM THE FAULTED POWER TRANSFORMERS

Tr. Case	DGA results in ppm						
	H_2	CH_4	C_2H_2	C_2H_4	C_2H_6	CO	CO_2
1	1049	6986	1476	39998	6462	40773	949998
2	45	296	4	2228	1292	68	1458
3	2113	319	408	469	82	1632	4190
4	161	34	90	55	3	118	1151
5	821	1030	2	48	25	213	522
6	1064	1409	133	2046	1436	4779	1152
7	72	273	0	326	35	67	1383

TABLE 6
GAS RATIOS

Tr. Case	Gas ratios				
	C_2H_2/C_2H_4	CH_4/H_2	C_2H_4/C_2H_6	CO_2/CO	C_2H_2/H_2
1	0.04	6.6	6.19	2.3	1.407
2	0.002	6.58	1.72	21.44	0.088
3	0.87	0.151	5.72	2.57	0.193
4	1.63	0.211	18.33	9.75	0.56
5	0.042	1.25	1.92	2.45	0.003
6	0.065	1.32	1.42	0.24	0.125
7	0.0	3.79	9.3	20	0

The Duval coordinates constructed from the DGA test is shown in Table 7 and used as the basis to study transformer faults. These Gas ratios and Duval co-ordinates are analysed in the Duval triangle (Figure 1) and the corresponding type of fault is determined as shown in Table 8.

TABLE 7
DUVAL CO-ORDINATES

Tr. Case	Duval co-ordinates		
	% C_2H_2	% C_2H_4	%CH_4
1	3.05	82.54	14.4
2	0.16	88.14	11.7
3	34.11	39.21	26.67
4	50.27	30.72	18.99
5	0.185	4.44	95.37
6	4.12	63.38	32.5
7	0.16	54.33	45.5

TABLE 8
FAULTS

Tr. Case	Actual fault occurred	Fault found by gas ratio	Fault found by Duval triangle
1	Hot spot on one connecting leads due to joint loose connection	T3	T3
2	Bolt on stamping got melted	T2	T3
3	Sparking on HT leads	D2	D2
4	Arcing between LT busbars	D1	D2
5	Damaged winding	T2	T1
6	Arcing at contacts (OLTC)	T2	T3
7	Arcing in diverter switch (OLTC)	T1	T3

IV. FAULT ANALYSIS

This section computes the faults using the Duval and basic gas ratio method using the DGA results of seven faulted transformers from Electrical Research and Development Association (ERDA). Computations based on Duval and basic gas ratio methods were used to analyse the faults and the finding are reported in this section.

A. Case 1: Hot-spot in connecting lead due to bolted joint loose connection

The hot spot in one of the connecting lead due to joint loose connection causes power transformer failure. Further, it results in pitting and melting of the mild steel bolt. As the melting point of mild steel is greater than 700°C, the fault is in the T3 zone of the transformer. One can find from our analysis that both Duval and basic gas ratio methods were able to detect the faults as illustrated in Table 8.

B. Case 2: Melting of core stamping bolt

The second case of fault considered is the melting of core stamping bolt as shown in Figure 3. Since, the transformer grade stainless steel bolt melting point is above 1500°C; the fault region T3 identified by Duval suggests that the fault has been identified accurately. But, our computation with basic gas ratio reveals that the method cannot capture this type of fault accurately.

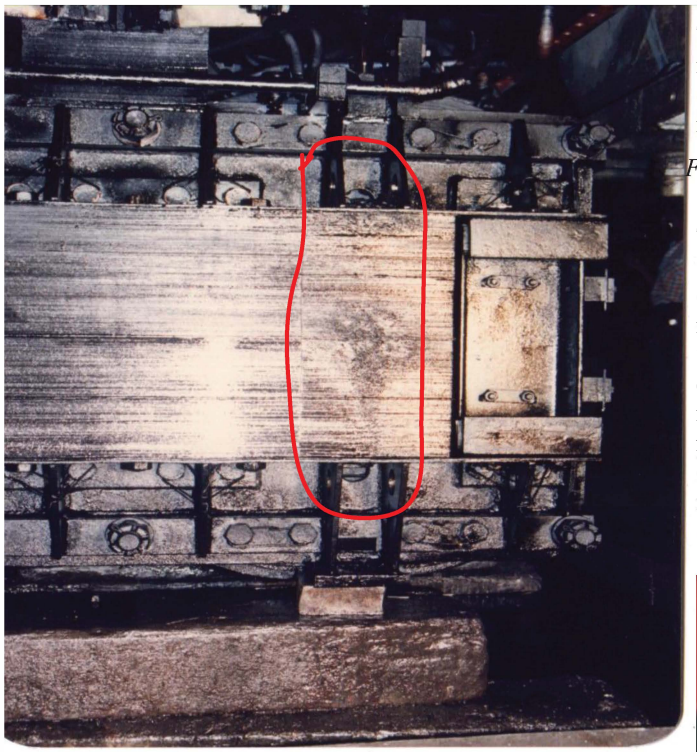

Figure 3: Melting of core stamping bolt

C. Case 3: Arcing between high voltage leads

The third case considered is the arcing between high voltage leads due to insulation failure resulting in a short circuit between two phases that is caused by heavy current flow which corresponds to high energy discharge D2 of Table 3. Our calculations with Duval and basic gas ratio illustrates that both these methods were able to detect the fault accurately as illustrated from Table 8.

D. Case 4: Arcing between LT bus bars

The fourth case of failure considered in our analysis is the arcing between the LT bus bars due to insulation failure. This results in increased current flow due to short circuiting of two phases with a high energy discharge. This fault corresponds to D2 of Table 3. Our computations with DGA results reveal that only Duval method is able to capture this fault, while basic gas ratio method fails to diagnose it.

E. Case 5: Inter-turn fault

The inter turn fault is most common in power transformers that leads to insulation of the winding to be overheated and decolorized. The fault results due to thermal breakdown in the insulation resistance of the oil immersed transformer windings (class-B insulation) which will withstand a temperature of up to 130°C. From our computations, one can find that the Duval method computed the fault to be in zone T1 is more appropriate that the T2 detected by gas ratio method. This illustrates that the Duval method is able to diagnose inter-turn fault more accurately than the basic gas ratio method.

F. Case 6: Arcing at OLTC contacts

The sixth fault analyzed is the improper contact at OLTC slider that happens due to switching of transformer taps (Figure 4). The faulted transformer is subjected to arcing and melting of copper contact surfaces. This leads to a thermal fault. The Duval method predicted the fault to be in T3 that corresponds to thermal fault. On the other hand, the basic gas ratio method predicted the failure to be in zone T2, which is not included in the switching and equipment accessories fault (Table 4). Therefore, our computations establish that Duval is more accurate and efficient in detecting arcing at OLTC contacts.

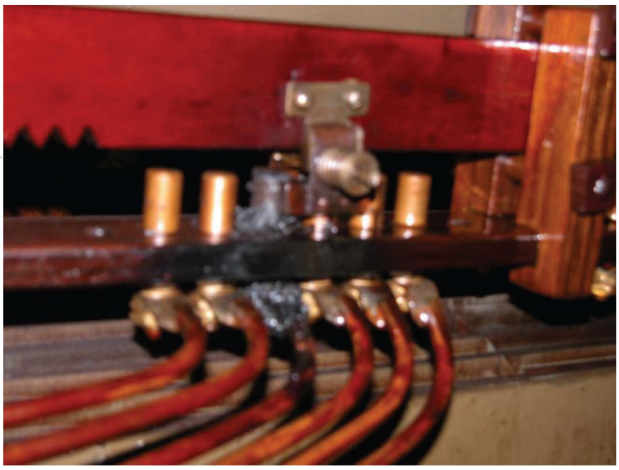

Figure 4: Arcing at OLTC contacts

G. Case 7: Arcing in diverter switch

Arcing in the diverter switch is an external fault that leads to thermal fault. This is an operation fault that can lead to failures. Our computations on power transformer indicated that, while Duval method was able to diagnose the fault, the basic gas ratio method failed to detect this fault. One can

conclude that the Duval method is more suitable for detecting such external faults from the DGA results.

Our analysis on the DGA data obtained from the transformer and computations performed using Duval and basic gas ratio method illustrated the accuracy of the methods. While, Duval was able to capture all seven faults successfully; the basic gas ratio was not able to capture five out of seven faults. It is to be noted here that, the case 6 of the fault is not even listed in the possible faults that can detected by basic gas ratio. However, Duval computed the fault accurately. This naturally suggests us to conclude that Duval is a more accurate method in detecting faults from DGA results and affirms the finding of the investigation [1]. Therefore, Duval method could well turn out to be the method required for building dependable AMS in future.

V. CONCLUSION

The paper compared the accuracy of two DGA interpretation methods in practice: Duval and basic gas ratio method. The study was based on seven faults (incipient, operational, and external) on the power transformers. The DGA results of the faulted transformers were obtained from Electrical Research and Development Association (ERDA) and studied in our investigation. Computations were performed on the DGA results using both Duval and basic gas ratio method. Our computations illustrated that Duval was successful in detecting the seven faults, while basic gas ratio failed in five cases as shown in Table 8. This leads us to the conclusion that Duval method is more accurate method in detecting the faults studied in the paper. Interpreting our results, one can conclude that the accuracy of Duval makes it the promising approach in interpreting DGA results for building dependable AMS. Combining Duval with measurements and other routine tests to diagnose power transformer faults and handling multiple faults are the future course of this investigation.

ACKNOWLEDGMENT

The authors thank Dr. Shrinet, ERDA, Govt. of India, for his valuable inputs.

REFERENCES

1. M. Duval, “A review of faults detectable by gas-in-oil analysis in transformers,” IEEE Electrical Insulation Magazine, 2002, 18(3), 8-17.

2. Q. Su, C. Mi, L.L. Lai and P. Austin, “A fuzzy dissolved gas analysis method for the diagnosis of multiple incipient faults in a transformer,” IEEE Trans. Power Syst., vol. 15(2), pp. 593-598, 2000.

3. N.A. Muhamad, B. T. Phung, T.R. Blackburn and K.X. Lai, “Comparative study and analysis of DGA methods for transformer mineral oil,” IEEE Lausanne Power Tech, pp. 45-50, July 2007.

4. D. V. S. S. Siva Sarma and G. N. S. Kalyani, “ANN approach for condition monitoring of power transformers using DGA,” IEEE Region 10 Conference Vol. 100, pp. 444-447, Nov. 2004.

5. N.A. Muhamad, B. T. Phung, and T. R. Blackburn, “Comparative study and analysis of DGA methods for mineral oil using fuzzy logic,” IEEE In Power Engineering Conference, pp. 1301-1306, Dec. 2007.

6. IEC Mineral oil impregnated electrical equipment in service- Guide to the interpretation of dissolved and free gas analysis, IEC Std. 60599, May 1999.

7. X. Zhang and E. Gockenbach, “ Asset-management of transformers based on condition monitoring and standard diagnosis,” IEEE Electrical Insulation Magazine, 24(4), 26-40, 2008.

8. A.E. Abu-Elanien and M.M.A. Salama, “Survey on the transformer condition monitoring,” IEEE In Power Engineering, Large Engineering Systems Conference pp. 187-191, Oct. 2007.

9. S. Kumar, P. Shukla, Y.R. Sood and R.K. Jarial, “An experimental study to know the behavior of transformer oil on ageing,” IEEE In Engineering and Systems Students Conference pp. 1-6, April 2013.

10. J. Singh, Y.R. Sood and R.K. Jarial, “Condition monitoring of power transformers-bibliography survey,” IEEE Electrical Insulation Magazine, 24(3), 11-25, 2008.

ICSCS 2016 Submission 53

Submission information updates are disabled.

For all questions related to processing your submission you should contact the conference organizers. Click here to see information about this conference.

All **reviews sent to you** can be found at the bottom of this page.

Paper 53	
Title:	Electricity Generation Planning for Tamil Nadu by Considering GHG Emission Using LEAP
Paper:	(Jan 13, 04:53 GMT)
Author keywords:	GHG Emissions Externality costs LEAP least cost Electricity Generation Tamil Nadu
EasyChair keyphrases:	technology simulation scenario (285), optimization scenario (190), leap model (170), electricity generation (167), tamil nadu (150), electrical energy (145), electrical energy shortage (95), least cost (80), least cost electricity generation (80), power plant (80), electrical energy output (79), natural gas (70), social cost (60), various electricity generation technology (60), renewable energy (60), energy demand (50), fuel cost (50), generating electricity (50), range energy alternative (47), energy alternative planning (47), various technology (40), base year (40), hydro only (40), generation technology (40)
Topics:	
Abstract:	This paper presents an application of Long-Range Energy Alternative Planning (LEAP) software to investigate a range of various technologies for generating electricity at least cost for Tamil Nadu. The cost of generating electricity includes the capital, fuel, operation and maintenance costs for those technologies that are considered. Detailed analyses are performed with and without the inclusion of externality costs of local air pollution in order to examine the cheapest option of electricity generation.The impact of imposing Green House Gases (GHG) emission limit on the change in generating technologies was analyzed, considering least cost of electricity generation. Moreover, the corresponding overall cost of electricity generation was found for each case. The LEAP model to estimate least cost Electricity Generation for Tamil Nadu is proposed. The electricity generation is predicted for future years until 2025, keeping 2015 as base year. This model can be further used for predictive electricity generation after 2025 also.
Submitted:	Jan 13, 04:53 GMT
Last update:	Jan 13, 04:53 GMT

Authors

first name	last name	email	country	organization	Web page	corresponding?
Bhuvanesh	A	bhuvanesh.ananthan@gmail.com	India	Mepco Schlenk Engineering College		✓
Jaya Christa	S.T	jayachrista@yahoo.com	India	Mepco Schlenk Engineering College		
Kannan	S	kannaneeeps@gmail.com	India	Ramco Institute of Technology		

Reviews

Review 1	
Overall evaluation:	**2**: (Accept with Revision)
Additional scores	
Level of Originality:	**2**: (Only Basic Review and Survey)
Abstract and Key Word:	**3**: (Given)
Standard of Quality Technical English:	**2**: (Satisfactory)
Structure of the Paper:	**2**: (Must be improved)
Relevance and Clarity of Flow Charts, Diagrams, Equations:	**3**: (Good)
Clarity of Table:	**3**: (Good)
Usage of References:	**3**: (Good - Recent literatures are reffered)
Review	
Review:	should maintain& use IEEE format(2 column)

Review 2	
Overall evaluation:	**3**: (Accept)
	Additional scores
Level of Originality:	**3**: (Novel / Good Work in the Current Area)
Abstract and Key Word:	**3**: (Given)
Standard of Quality Technical English:	**2**: (Satisfactory)
Structure of the Paper:	**2**: (Must be improved)
Relevance and Clarity of Flow Charts, Diagrams, Equations:	**3**: (Good)
Clarity of Table:	**3**: (Good)
Usage of References:	**2**: (Refer some more literatures)
	Review
Review:	Strictly follow the Journal format. Please check your paper for typical and editing errors. Improve the Technical English quality of your paper. Citations of all the references must be done. Texts and diagrams taken from other papers must be acknowledged and added to the reference. Result and discussion part must be made clear. Equations must be typed using equation editor and must be numbered. Add more number of recent references.

Electricity Generation Planning for Tamil Nadu by Considering GHG Emission Using LEAP

[1]A.Bhuvanesh, [2]S.T.Jaya Christa, [3]S.Kannan

[1]Research Scholar, [2]Associate Professor,
[1,2]Department of EEE, Mepco Schlenk Engineering College, Sivakasi
[3]Professor & Head, Department of EEE, Ramco Institute of Technology, Rajapalayam
E-mail: bhuvanesh.ananthan@gmail.com

Abstract. This paper presents an application of Long-Range Energy Alternative Planning (LEAP) software to investigate a range of various technologies for generating electricity at least cost for Tamil Nadu. The cost of generating electricity includes the capital, fuel, operation and maintenance costs for those technologies that are considered. Detailed analyses are performed with and without the inclusion of externality costs of local air pollution in order to examine the cheapest option of electricity generation. The impact of imposing Green House Gases (GHG) emission limit on the change in generating technologies was analyzed, considering least cost of electricity generation. Moreover, the corresponding overall cost of electricity generation was found for each case. The LEAP model to estimate least cost Electricity Generation for Tamil Nadu is proposed. The electricity generation is predicted for future years until 2025, keeping 2015 as base year. This model can be further used for predictive electricity generation after 2025 also.

Keywords. GHG Emissions, Externality costs, LEAP, least cost Electricity Generation and Tamil Nadu.

1 Introduction

Electricity plays an important role for the development of any country. It was reported that southern region of India had the highest peak demand and electrical energy shortage in 2013. Tamil Nadu, one of the states in southern region of India, had an average electrical energy shortage of 10.5 % in 2013. In the last few years Tamil Nadu is facing huge electrical energy shortage due to several reasons [1]. This problem of electrical energy shortage is being felt mainly by the industries, leading to a loss in production efficiency and heavy loss of income. This electrical energy shortage should be removed, because electrical energy is most important for socioeconomic development, particularly in the developing countries. In this era of globalization, a quick increase in urbanization, population and the energy demand show that electrical energy shortage will be the major problem in the developing countries as well as in the world in the coming years. Therefore, the electrical energy generation forecasting should be done effectively and economically. The first developed energy supply models were established on only one feature of the problem namely costs, environmental impacts, or energy supply security. The old energy supply models only reflect one energy sector or even one energy carrier.

They were developed based on econometric methods and they relate energy demand with some macroeconomic indicators such as Gross Domestic Product (GDP). Because those models were not able to take into consideration two differing goals of using low-cost electrical energy production and environment conservation, they did not have sufficient efficiency in facing the recent energy concerns [2].

In recent years, a great number of wide-ranging energy models have been developed which consider not only all energy consumption sectors and energy carriers, but also environmental aspects and the trend of energy utility's efficiency. LEAP has a significant impact in shaping energy and environmental polices worldwide. It had been successfully used in more than 150 countries worldwide for different purposes. For example, in California, (2001) LEAP was used for energy forecasting and identifying alternative fuels [3]. In Mexico, it was used to determine the feasibility of future scenarios based on moderate and high use of biofuels in the transportation and electricity generation sectors [4]. In Lebanon, mitigation options were assessed to reduce emissions from electricity generation with emphasis on the usage of renewable energy resources [5]. The energy consumption and various types of emissions in consumption sectors in Iran were analyzed by using LEAP model [6]. So far, for Tamil Nadu, an energy model of electricity is proposed using Energy and Power Evaluation Program (ENPEP-BALANCE) tool, with consideration of different RETs (Renewable Energy Technologies) for 30 years from 2013 to 2042 [7]. The various factors such as average capacity, Energy Not Served (ENS), energy consumption by demand sectors, ratio of supply and demand, average cost of energy generation, pollutants CO_2, SO_2 and Particulate Matter (PM) emitted by thermal plants are evaluated [7]. It is necessary to plan an economic future electricity generation method with low emission of GHG by concentrating the renewable energy sources (RES). The modeling studies carried out to demonstrate the impact of bringing in solar plants into the generating system as a technology alternative power plant is presented in [8]. Hence, in this paper, the application of LEAP software to investigate a range of various technologies for generating electricity in Tamil Nadu for two different cases namely single-technology simulation scenarios and optimization scenario is presented.

2 Leap and Its Features

Future prediction of electricity generation through various technologies is a challenging task. To assist the Power System Planning Engineer in this task, various tools are developed. LEAP is one such energy-planning tool developed by the Stockholm Environment Institute, Boston (SEI-B). It consists of an EDB (Environmental Database), which was also developed by SEI-B with additional support from the United Nations Environment Programme (UNEP), and is a joint UNEP/SEI activity [9]. LEAP is an accounting framework, within which the user can develop models of demand and supply. It is a long-term integrating and modelling tool. The LEAP model requires data for at least the base year and any of the future years. Then, using the function such as interpolation or extrapolation or the growth rate method, the future energy demand and emissions are

predictable for the other years. The fundamental concept in LEAP is an end-use driven scenario analysis [10].

LEAP model is mostly used for energy and environmental planning for both medium and long-term consideration. LEAP works with an unlimited time horizon with an annual time setup that can be extended up to 50 years. Different modeling approaches used by LEAP cover both the demand and supply side of energy. To model electricity generation planning and generation capacity expansion, LEAP offers a series of methodologies accompanied with accounting and simulation [11].

3 LEAP Model for Tamil Nadu

The LEAP model is developed for Tamil Nadu and the electricity is set as the only demand. The electricity can be generated by the plants namely Natural Gas (NGCC), RES, Coal, Hydro, Nuclear and Diesel. In addition, they are entered into the Process branch of LEAP model. The Carbon emitting substances to the environment are entered into the Effects branch of LEAP model.

The LEAP model for Tamil Nadu has been developed by setting the base values shown in Table 1. The model has been developed for the base year 2015 and extrapolated until 2025. The electricity demand for the year 2025 will be 200 Thousand GWh and it is one of the inputs for LEAP [7]. The electricity losses are taken as 18% for developing the model [12].

This data for various electricity generation technologies is taken from [13], [14] and [15] for January 2015. These data are entered into the Transformation module called Electricity Generation in the LEAP model, which include various electricity generation plants namely Coal, Gas, Diesel, Nuclear, Hydro and Renewable Energy Sources (RES) and its properties are fixed to Capital cost, Fixed Operation and Maintenance (OM) Cost, Variable OM Cost, Fuel cost, Capacity, Efficiency, Maximum availability, Capacity credit, Life time, system load curve and a planning reserve margin. The discount rate is set as 5% while entering the cost data.

Table 1. The Base Values of LEAP for The Year 2015 Including Various Electricity Generation Technologies

Name of the plant	Capacity (MW)	Efficiency (%)	Maximum availability (%)	Capacity credit (%)	Capital cost ($\times 10^3$ $/MW)	Fixed OM Cost ($/MW)	Variable OM Cost ($/MW)	Fuel Cost ($/MWh)	Life Time (years)
Coal	9688.10	35	90	90	2934	31.18	4.47	95.6	40
Gas	1026.30	38	90	90	917	13.17	3.60	75.8	40
Diesel	411.66	40	90	90	950	30	3.10	85	40

Nuclear	986.50	35	80	90	5530	93.28	2.14	96.1	50
Hydro	2182.20	90	90	50	2936	14.13	0	84.5	50
RES	8075.38	25	100	25	3000	52.00	0	100	50

4 Result and Discussions

The fossil fuels are expected to unavailable in 50 more years if the consumption rate remains to grow at high rate. With the unstable nature of international crude prices, it is important to reduce this dependence and look for alternatives. Therefore, the renewable energy technologies also be expanded to supply secure electrical energy at least cost and low GHG emission. The developed LEAP model for Tamil Nadu having two different cases namely Single-technology simulation scenario and Optimization scenario. In Single-technology simulation scenario the LEAP having various electricity generation technologies namely Coal Only, Diesel Only, Hydro Only, Natural Gas Only, RES Only and Nuclear Only. LEAP decides the types of power plants to be added and when to be added to meet out the demand by giving more preference to a single generation technology, based on its availability and fuel cost. The Optimization scenario is simulated to explore least cost electricity generation by considering GHG emission limit also.

4.1 Case 1: Single-Technology Simulation Scenario

In this case, a simple scenario using each of single generation technology have been simulated. They are namely, Coal only, Diesel only, Hydro only, Natural Gas only, RES only and Nuclear only. In the Coal only technology, LEAP automatically gives more preference to coal plant for generating electricity to meet out the electricity demand based on its availability. If the coal is not sufficient to generate the required electrical energy, then other sources for generating electrical energy are considered based on its fuel cost. Based on standard simulation calculations, LEAP decides the types of power plants to be added and when to be added to meet out electrical energy demand. This simulation is also carried out for all the other single generation technologies such as Diesel only, Hydro only, Natural Gas only, RES only and Nuclear only. The predicted values of capacity, Electrical energy output and Social cost in the year 2025 for various single technologies are shown in figures 1, 2 and 3 respectively.

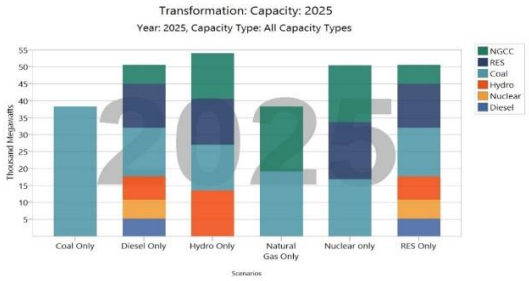

Fig. 1. Capacity values predicted by LEAP by single-technology simulation scenarios for the year 2025

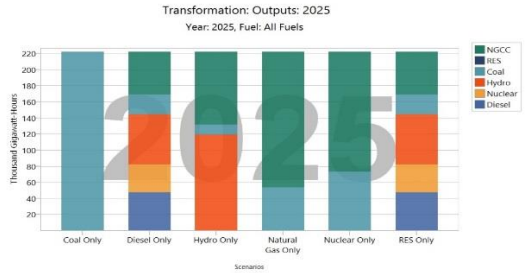

Fig. 2. Electrical Energy Output predicted by LEAP by single-technology simulation scenarios for the year 2025

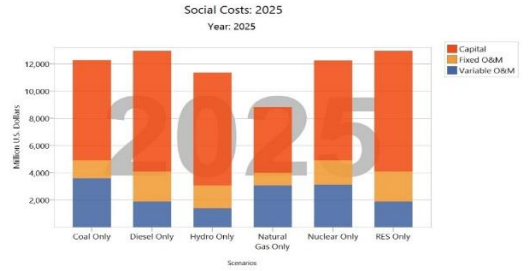

Fig. 3. Social Cost predicted by LEAP by single-technology simulation scenarios for the year 2025

The results from LEAP model show that for most of the single-technology simulation scenarios, Natural Gas technology is used to generate more amount of electrical energy and is shown in Figure 2. Figure 3 shows that the Natural Gas only generation technology will be the cheapest option for power generation in the year 2025, due to their low fuel cost.

4.2 Case 2: Optimization Scenario

The Optimization scenario allows LEAP to decide the combination of power plants which will meet demand at the lowest cost and lowest emission of GHG.

Evaluation of Least Cost Electricity Generation.

The LEAP model runs the OSeMOSYS optimization model, which is used to simulate the optimization scenario. The comparison of capacity, electrical energy output and social cost in the year 2025 using single-technology simulation scenarios and Optimization Scenario are shown in figures 4, 5 and 6 respectively.

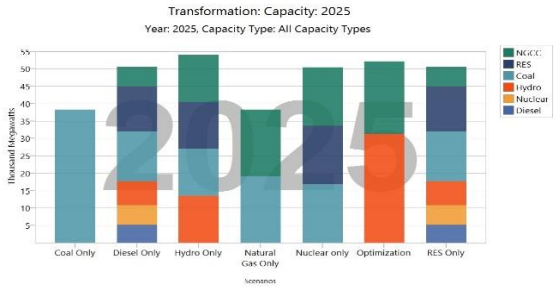

Fig. 4. Comparison of Capacity by single-technology simulation scenarios and Optimization Scenario predicted by LEAP for the year 2025

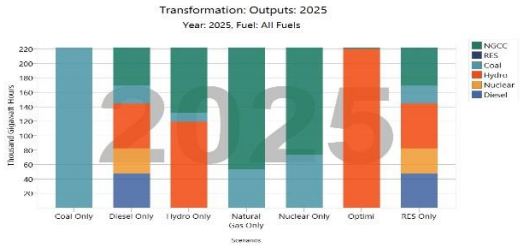

Fig. 5. Comparison of Electrical Energy Output by single-technology simulation scenarios and Optimization Scenario predicted by LEAP for the year 2025

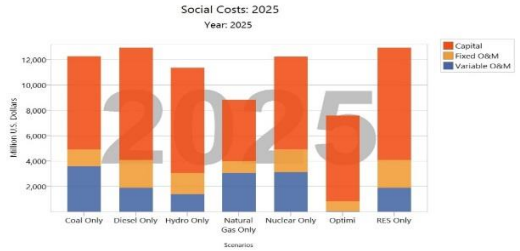

Fig. 6. Comparison of Social Cost by single-technology simulation scenarios and Optimization Scenario predicted by LEAP for the year 2025

Figure 5 shows that the LEAP has chosen a mix of power plants in the Optimization scenario, unlike the other single-technology simulation scenarios. The results show that peak load periods favor Natural Gas power plants that are relatively cheap to build but expensive to operate. Base load periods favor Hydro power plants that have higher capital cost but with low running costs. Figure 6 shows that, because of the low variable and fixed O&M cost, the total social costs of Optimization Scenario are slightly cheaper than even the cheapest of the other single-technology simulation scenarios which were created previously.

All the single-technology scenarios having maximum penetration of non-renewables in its fuel mix. So the fixed and variable O&M cost will be high. But the Optimization scenario penetrates renewables in more amount. So the fixed and variable O&M cost will be very low. So the overall cost will be minimum. The Optimization Scenario also shows a maximum level of GHG emissions is imposed on the system with least cost. The comparison of total GHG emission for generating electrical energy by single-technology simulation scenarios and Optimization Scenario predicted by LEAP for the year 2025 is shown in Figure 7.

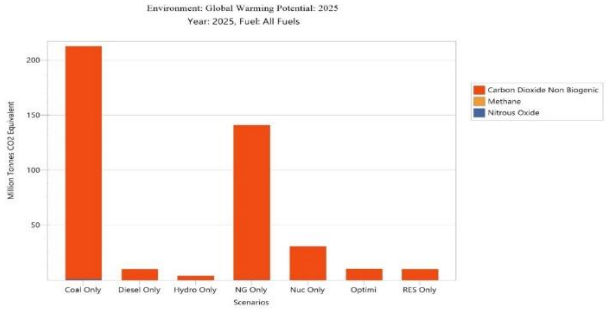

Fig. 7. Comparison of Total GHG Emission by single-technology simulation scenarios and Optimization Scenario predicted by LEAP for the year 2025

Figure 7 shows that the emission of GHG is less in Optimization Scenario next to Hydro Only single-technology simulation scenario, compared to other single-technology simulation scenarios.

5 Conclusion

The application of Long-Range Energy Alternative Planning (LEAP) software to investigate a range of various technologies for generating electricity, at least cost for Tamil Nadu is presented in this paper. The LEAP model was developed to estimate least cost Electric Generation by considering GHG emission factor for Tamil Nadu for the base year 2015 and extrapolated till 2025 for the future generation expansion planning. The LEAP model was developed for two different cases such as single-technology simulation scenario and optimization scenario. The predicted electrical energy output and social cost

values are obtained for the two cases. The results show that the optimization scenario gives the least cost generating capability to meet the demand with less emission of GHG.

References

[1] S.R.Rallapalli, S. Ghosh.: Forecasting monthly peak demand of electricity in India-A critique. Energy Policy, vol. 45. (2012) 516-520.

[2] M.A. Moradi, H. Shakouri, A.M. Aboutaleb.: Developing the Electricity Demand Model for Iran's Residential Sector; Based on LEAP. International Power System Conference, Tehran, Iran, (2013).

[3] Ghanadan, R., J.G. Koomey.: Using energy scenarios to explore alternative energy pathways in California. Energy Policy, vol. 33. (2005) 1117-1142.

[4] Islasa, J., F. Manzini., O. Masera.: A prospective study of bioenergy use in Mexico. Energy, vol. 32. (2007) 2306-2320.

[5] El-Fadel, M., M. Zeinati, N. Ghaddar., T. Mezher.: Mitigating energy-related GHG emissions through renewable energy. Energy Policy, vol. 29. (2001) 1031-1043.

[6] Awami, A., B. Farahmandpour.: Analysis of environmental emissions and greenhouse gases in Islamic Republic of Iran. International Institute for Energy Studies, vol. 4. (2008).

[7] B.R.Prabakar, K.Karunanithi, S.Kannan, C. Thangaraj.: Energy Model of Electric Sector for Tamil Nadu. International Journal of Applied Engineering Research, vol. 10. (2015) 5681-87.

[8] K. Rajesh, A. Bhuvanesh, S. Kannan, C. Thangaraj.: Least cost generation expansion planning with solar power plant using Differential Evolution algorithm. Elsevier Renewable Energy, vol. 85. (2016) 677-686.

[9] Long range energy alternatives planning system. Boston. SEI-Stockholm Environment Institute, Tellus Institute, (2008).

[10] Rabia Shabbir., Sheikh Saeed Ahmad.: Monitoring urban transport air pollution and energy demand in Rawalpindi and Islamabad using leap model. Elsevier Energy, vol. 35. (2010) 2323-2332.

[11] Syeda Shaima Meryem, Sheikh Saeed Ahmad, Neelam Aziz.: Evaluation of biomass potential for renewable energy in Pakistan using LEAP model. International Journal of Emerging Trends in Engineering and Development, vol.1. (2013) 243-249.

[12] Power Sector in Tamil Nadu: A Comparative Analysis. Athena Infonomics India Pvt. Ltd, (2011).

[13] Executive Summary Power Sector. Government of India Ministry of Power Central Electricity Authority New Delhi, (2015).

[14] Annual Energy Outlook. U.S. Energy Information Administration, (2015).

[15] Updated Capital Cost Estimates for Utility Scale Electricity Generating Plants. U.S. Energy Information Administration, (2013).

VEL TECH HIGH TECH
Dr.RANGARAJAN Dr.SAKUNTHALA
ENGINEERING COLLEGE
(Approved by AICTE, Affiliated to Anna University of Technology, Chennai & ISO 9000:2008 Certified Institution & Accredited by NBA)
#60, Avadi-Vel Tech Road, Avadi, Chennai - 600 062, Tamil Nadu, INDIA.

DEPARTMENT OF MECHANICAL ENGINEERING

1st National Conference

on

TECHNOLOGICAL ADVANCES IN MECHANICAL ENGINEERING

(TAME 2015)

20th August, 2015

9.00 a.m at Convention Center, Veltech North Campus.

in association with

IOSRD
International Organization of Scientific Research and Development
International Journals and Conferences

AENSI

Chief Guest

Mr.A.Rajan Babu

General Manager – HR & Operations

SIPCOT, NSK-ABC Bearings Ltd

Sriperumbudur

Presided By

Col. Prof. Dr. Vel R. Rangarajan, B.E.(Elec.), B.E.(Mech.), M.S.(Auto), D.Sc.,
Founder & Chairman

Dr. Mrs. Sakunthala Rangarajan, M.B.B.S.,
Founder & Vice Chairman

Dr. Mrs. Rangarajan Mahalakshmi, **K**., B.E., M.B.A.(UK), Ph.D.,
Chairperson and Managing Trustee

Mr. K.V.D. Kishore Kumar, B.E., M.B.A.(USA),
Vice President

Dr.K.Murugesan, M.E, Ph.D.,
Principal

Dr.K.Umanath, M.E, Ph.D.,
Coordinator

PROGRAMME SCHEDULE

09.00 a.m	PRAYER SONG	
09.10 a.m	LIGHTING OF LAMP	Dignitaries
09.15 a.m	MULTIMEDIA PRESENTATION	
09.30 a.m	WELCOME ADDRESS	Dr.K.Umanath, AP/Mech
09.40 a.m	ADDRESS BY ALUMINI	S.Bharani Deepak Trainee/ForEd Overseas
09.50 a.m	RELEASING OF PROCEEDINGS & CD	Mr.A.Rajan Babu Chief Guest
10.00 a.m	FELICITATION ADDRESS	Dr.K.Murugesan Principal
10.10 a.m	INTRODUCTION TO CHIEF GUEST	Mr.M.Karthigairajan HOD/Mech
10.15 a.m	ADDRESS BY CHIEF GUEST	Mr.A.Rajan Babu
10.45 a.m	TEA BREAK	
11.00 a.m	TECHNICAL SESSION – I	Dr.G.Deenadhayalan Prof/Mech
01.00 p.m	LUNCH BREAK	
01.30 p.m	TECHNICAL SESSION – II	Dr.R.Henry Xavier Prof/Mech
03.30 p.m	TEA BREAK	
03.45 p.m	VALEDICTORY FUNCTION	
04.00 p.m	VOTE OF THANKS	Mr.T.Raphael

TAME 2015 - TECHNICAL SESSION 1: DESIGN

HALL 1: AYYAPAN HALL TIME:11:00am-1:00pm

HALL INCHARGE: Dr. HENRY XAVIER

SLNO	PAPER CODE	TITLE	AUTHOR	AFFILIATION
1	M08	Fuzzy based optimization to reduce the blind spots in heavy transport vehicles	Pitchipoo P	P.S.R. Engineering College
			Vincent D.S	Thiruvannamalai
			Rajini N	Kalasalingam University
			Rajakarunakaran S	Ramco Institute of Technology
2	D01	Design,development of &analysis on landing gear of light weight fighter aircraft	Mr. K.S Naidu	MLR Institute of Technology
			Hari Krishna Yadav Veerla	
3	D02	Design of mechanical cruise control system in automobile	M.Arun Kumar	Anna University
			R.Balaji	
			J.Nishanth	
			N.Yuvaraju	
4	D03	Design of axle and disc brakes for installation in brakes in a trolley	Gaurav Sevda	VIT University
			E. Raj Kumar	
5	D05	Design And Analysis Of Door Harvesting Energy	Vasantha Prasath N	GRT Institure of engineering and technology
			S.Vignesh	
			M.M Ganesan	
6	D06	Evaluation Of Static Behavior Of Automobile Steering Knuckle Strut Arm Column	N.Gnanasekar	P.A.College of Engineering and Technology
			Rama Thirumurugan	Dr. Mahalingam College of Engineering and Technology
			S.Madhusuthanan	
7	D09	Diminutionof Drag Using Owl Feathers	Robinson Jerin.R	KCG College Of Technology
			Robinsonselva	
			Suresh	
			Prof.Karthick	
8	D12	Reduction of turn radius by Four wheel steering using sprocket and chain drive	B.Magesh kumar	Veltech Hightech Dr.Rangarajan Dr.Sakunthala Engineering College
			N.Vignesh	
			A.Manivasagam	
9	D15	Assembly Line Design For After Test And After Paint Assembly	R.DurgaPrasad	Anna University
			K.VishwaKumar	
			P.A.Jeeva	

Fuzzy based optimization to reduce the blind spots in heavy transport vehicles

Pitchipoo P[a]*, Vincent D.S[b], Rajini N[c] and Rajakarunakaran S[d]
[a] Department of Mechanical Engineering, P.S.R. Engineering College, Sivakasi, Tamil Nadu, India. Email: drpitchipoo@gmail.com
[b] Tamil Nadu State Transport Corporation Ltd., Thiruvannamalai, Tamil Nadu, India.
[c] Department of Mechanical Engineering, Kalasalingam University, Anand Nagar, Krishnankoil, Tamil Nadu, India.
[d] Department of Mechanical Engineering, Ramco Institute of Technology, Rajapalayam, Tamil Nadu, India

Abstract:
Blind spot is a key phenomenon related to the visibility of the driver while he is driving. It plays a vital role in road accidents. Reduction of the area of blind spot is very much required in order to reduce the accidents. In this paper an attempt is made to overcome the problems of blind spot by optimizing the design parameters used in the rear view mirror design of heavy transport vehicles. The blind spot of the existing body structure was studied in a public transport corporation of Tamilnadu, India. First the area of the blind spot of the existing body structure was studied and the optimal design parameters are ranked by Fuzzy Analytical Hierarchy Process (FAHP). FAHP was also used for the determination of the weights of the design parameters and ranking of the vehicle body structures.

Keywords: Blind spots, Rear view mirror, Optimization, FAHP

1. INTRODUCTION

Statistics revealed that most of the road accidents were happened due to vision related problems of the driver. Good driver visibility results safe road traffic (Hatamleh et al., 2013). A blind spot in a vehicle is the area around the vehicle that cannot be directly seen by the driver when he is in the seat. The heavy vehicle drivers can't see some areas on the roadway in the front, behind and on either sides of the vehicle. Front side blind spots are influenced by many design criteria such as vehicle body structure, human anthropometric data, road geometry, driver seat design etc., Among the main factors to be considered for driver seat design was identified as important factor. While designing the driver's seat, height of the seat from platform, total seat height, distance of seat back rest to windscreen glass and distance of seat back rest to steering wheel centre, to reduce blind spots, the distance between seat back rest to windscreen glass attracts major importance. A large enough blind spot in the rear or sides of the heavy vehicle can completely hide a portion of pedestrian / motor-cycle or even a full vehicle. Because, blind spots hide the road to verify them before making such maneuvers on roads while turning, reversing, changing lanes, or while overtaking other vehicles. This places the driver in a risky situation resulting sometimes in untoward incidents and accidents.

Blind spots exist in a wide range of vehicles such as cars, trucks, motorboats and aircraft. Figure 1 reveals the area of the blind spot existing in a heavy transport vehicle.

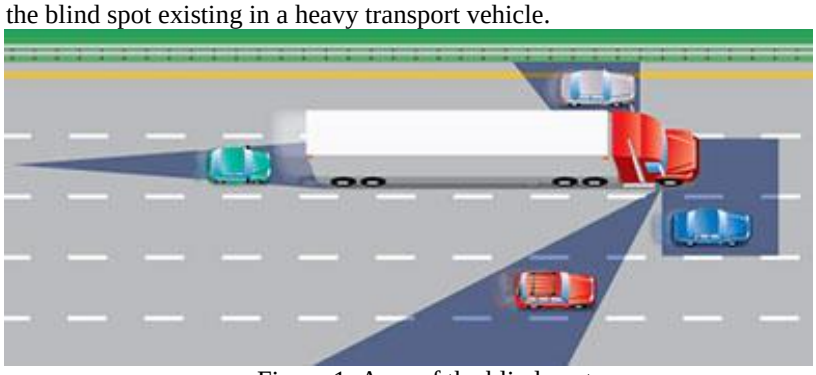

Figure 1. Area of the blind spot

In this paper the blind spot on either sides of the driver while driving is considered. Rear view mirrors reduce some area of the blind spots behind and on either sides of the heavy vehicle. Adjustment and installation or positioning of mirrors with larger fields-of-view will be helpful in reducing the blind spots. While considering the installation of mirrors, the distance between the driver and the pillar or frame structure to the left and right side of the front body structure, driver eye sight height while he is in the driver seat from the platform, and the centre height of the mirror from the ground level are all the important data.

Cho and Han (2010) stated that the vision of the driver is the most vital factor for an unusual driving situation. Burger (1974) analyzed the rear vision systems in twelve passenger vehicles and three trucks under actual driving conditions and predicted the critical zone in the rear side of the vehicle using expert's opinion. Ayres et al (2005) assessed the safety aspects during the usage of rear view mirrors and analyzed the research issues involved in the design of rear view mirrors. The rear view mirrors may not be related with any significant accident prevention, possibly they are not consistently used by all the drivers while driving. More over the major accidents were caused when the target vehicle appears in the driver's blind spot during lane change or crowded urban travelling and the driver has not carefully observed the approaching vehicle from the rear and side mirrors. Pardhy et al. (2000) introduced the concept of computer graphics display driven by differential global positioning system as a virtual mirror. This display was intended to be used as a rear or side view mirror in automobiles or trucks. Kojima et al. (2005) proposed a vision support system "NaviView" as visual assistance for safe driving. Llaneras et al (2005) developed driver interface criteria for a rear obstacle detection system and evaluated various interface approaches for presenting warning information to drivers.

Fuzzy based intelligent blind spot detecting system was presented by Qidwai (2009). In this system several ultrasonic sensors were used to monitor the chosen blind spots in a vehicle. Hughes et al (2009) discussed the use of electronic vision systems in vehicles. The benefits of using wide-angle lens camera systems to minimize the vehicle's blind-zones were described. The application of RFID and bluetooth technology in the blind zone area reduction was proposed by Lakshmi and Wahida Banu (2010). Kim et al. (2011) studied the surface flow around an automotive external rear view mirror and explained the visualizations over the mirror housing surface and the driver side vehicle skin. Computer based simulation method was also used to detect and warn of objects present within the blind spots in automobiles (Hatamleh et al., 2013).

Bao et al. (2010) developed a fuzzy TOPSIS decision model for road safety using performance index by incorporating experts' opinions. This approach effectively handled experts' linguistic expressions into account in the current index research. TOPSIS was used for evaluation of road safety measures focused on road users, vehicles, road infrastructure, and comprehensive measures by using a survey with a questionnaire. An intelligent decision support system (IDSS) was developed to evaluate the road safety performance in European countries (Bao et al., 2012). To develop the IDSS, an improved hierarchical fuzzy TOPSIS model was used. The experts' knowledge was incorporated in the proposed model. FAHP method was used in several multicriteria decision making problems such as supplier evaluation and selection (Pitchipoo et al , 2013), material handling equipment selection (Kulak, 2006), machine tool selection (Taha and Rostam, 2011) etc.,

From the study of literature, it is evident that the design parameters involved in the design and installation of rear view mirror should be in the optimal conditions to overcome the problems of blind spots on the either sides of the vehicle. The aim of this work is to optimize the blind spots for heavy transport vehicles by optimizing the design parameters used for the design and implementation of rear view mirrors. To achieve this, fuzzy based decision model is developed and the model is validated by a case study conducted in the transport corporation of Tamilnadu, India. The remaining part of this paper is organized as follows: Section 2 depicts the development of model, and the case study is explained in Section 3 and finally, Section 4 concludes the study and outlines some future research directions.

2. MODEL DEVELOPMENT

In this paper the weights of the criteria and the ranking of the vehicle body structures are determined by FAHP method FAHP is developed by integrating Saaty's (1990) analytical hierarchy process with fuzzy concept. Based on the opinion of the decision maker, the evaluation criteria are compared. The ranking of the criteria used for evaluation was collected. Based on that first the criteria matrix was formed based on the Saaty's nine point scale which is shown in Table 1.

The pair wise comparison matrix is called original matrix or criteria matrix which is given by matrix X_{cri} as shown below.

$$X_{Cri} = [a_{ij}]; 1 \leq i, j \leq m \quad (1)$$

where, a_{ij} = Pair wise comparison of i^{th} and j^{th} criteria. m = the number of alternatives

Table 1 Equivalent triangular fuzzy number for Saaty's nine point scale

Verbal judgment or preference	Saaty's scale of relative importance	Triangular fuzzy numbers
Extremely preferred	9	9,9,9
Very strongly to extremely preferred	8	7,8,9
Very strongly preferred	7	6,7,8
Strongly to very strongly preferred	6	5,6,7
Strongly preferred	5	4,5,6
Moderately to strongly preferred	4	3,4,5
Moderately preferred	3	2,3,4
Equally to moderately preferred	2	1,2,3

Equally preferred	1	1,1,1

This was converted into fuzzy original matrix using TFN prescribed by Mohamad et al. (2009) which is also shown in Table 1. The fuzzy number in a fuzzy set can be represented by equation (2).

$$F = \{x, \mu F(x), x \in R\} \quad (2)$$

where F is fuzzy set; x is fuzzy number; $R: -\propto \leq x \leq \propto$ and μF(x) is a continuous mapping from R in the interval [0, 1]. A TFN expresses the relative strength of each pair of elements in the same hierarchy and denoted as TFN (M) = (l, m, u) where $l \leq m \leq u$ in which l is the smallest possible value, m is the most promising value and u is the largest possible value in a fuzzy event. The triangular membership function of M fuzzy number can be described in equation (3). Then the fuzzy original matrix is normalized using equation (4).

$$\mu_A(x) = f(x) = \begin{cases} 0 & x < l \\ (x-l)/(m-l) & l \leq x \leq l \\ (u-x)/(u-m) & m \leq x \leq u \\ 0 & x > u \end{cases} \quad (3)$$

$$N_{ij} = \frac{a_{ij}}{T_j} \quad (4)$$

where a_{ij} is the cell value of i[th] row and j[th] column in the fuzzy original matrix; $1 \leq i, j \leq m$; and $T_j = \sum_{i=1}^{m} a_{ij}$

The weights were calculated by converting fuzzy numbers into crisp values by using defuzzification technique. The defuzzification has the capability to reduce a fuzzy to a crisp single-valued quantity. There are seven methods were used for defuzzification of the fuzzy output functions such as max-membership principle, centroid method, weighted average method,, mean–max membership, centre of sums, centre of largest area and first of maxima or last of maxima. In this study, centroid method was used for defuzzification which is given in equation (5).

$$\text{Weights (Crisp value)} \quad W_i = \frac{\sum_{i-1}^{k} D_p^i * O^i}{\sum_{i=1}^{k} D_p^i} \quad (5)$$

where k is the number of rules, O^i is the class generated by rule i (from 0, 1, …. L-1); L is the number of classes and

$$D_p^i = \prod_{i=1}^{n} m_{li} \quad (6)$$

where n is the number of inputs and m_{li} is the membership grade of feature l in the fuzzy regions that occupies the i[th] rule.

Since the pairwise comparison matrix is formulated based on human judgment, it is must to ensure that the values collected are accepted values. To check the consistency, the Consistency Ratio (CR) is calculated using equation (7)

$$CR = CI/RI \quad (7)$$

where CI is consistency index which is determined using equation (8) and RI is random indices for criteria size 'm'.

$$CI = \frac{\varphi_{max} - m}{m-1} \quad (8)$$

where φ_{max} is the maximum eigen value and m is the number of criteria

RI was approximated by Saaty (1990) which is shown in Table 2. If the CR is < 0.10 the decision maker's pairwise comparison matrix is acceptable.

Table 2. Random Indices

m	1	2	3	4	5	6	7	8	9	10	11	12
RI	0	0	0.58	0.90	1.12	1.24	1.32	1.41	1.45	1.49	1.51	1.58

Then all the alternatives are compared together using Saaty's nine point scale (Table 1) based on each criterion and the pairwise matrix for alternatives are developed. This matrix is converted into fuzzy matrix using the fuzzy numbers given in Table 1. Then the fuzzy matrix is normalized using equation (4) to formulate fuzzy normalized alternative matrix. From this the weights of the alternatives based on each criterion are computed. Finally overall priority matrix is determined using equation (9).

$$O = [C_{mn}] * [W_i] \quad (9)$$

where *Cmn* is the weights of the alternative 'm' for criterion 'n'.

From the overall priority, the higher value is selected as the best alternatives

3. CASE STUDY

To prove the effectiveness of the proposed model, a case study is conducted in a transport division located in the southern part of India. At present, four different types of vehicle bodies are used in that division. They are, body built in the same organization (in-sourcing – IS) and three outsourced (OS -1, OS – 2 & OS – 3) bodies. The following data variables such as the distance between the driver and the right side of the body pillar

or frame structure (A), the distance between the driver and the left side of the body pillar or frame structure (B), the distance of driver's eye right height from the platform (C) and the distance between the centre of the rear view mirror and the ground level (D) are identified as the influencing criteria for the design and implementation of rear view mirror in heavy vehicle. The data of influencing criteria for the design of driver seat are given in Table 3.

Table 3 Data of influencing criteria for the design of driver seat

Types of Vehicle	**A (cm)**	**B (cm)**	**C (cm)**	**D (cm)**
IS	36	178	122	242
OS – 1	34	181	123	240
OS – 2	34	182	123	224
OS - 3	34	177	119	204

After the data were collected, the comparisons of criteria were obtained from the transport corporation and the same is given in Table 4.

Table 4. Crisp original matrix

	A	B	C	D
A	1	2	5	3
B	1/2	1	4	2
C	1/5	1/4	1	1/4
D	1/3	1/2	4	1

The crisp matrix is converted into fuzzy matrix using triangular fuzzy numbers (Table 1) recommended by Alias et al (2009). The fuzzy criteria matrix is shown in Table 5. The fuzzy criteria matrix was normalized and shown in Table 6. The consistency ratio for this proposed FAHP model is calculated using equation (7) and is found as 0.091 which is less than 0.1. So this model is acceptable.

Table 5. Fuzzy criteria matrix

	A			B			C			D		
A	1.000	1.000	1.000	1.000	2.000	3.000	4.000	5.000	6.000	2.000	3.000	4.000
B	1.000	0.500	0.333	1.000	1.000	1.000	3.000	4.000	5.000	1.000	2.000	3.000
C	0.250	0.200	0.167	0.333	0.250	0.200	1.000	1.000	1.000	0.333	0.250	0.200
D	0.500	0.333	0.250	1.000	0.500	0.333	3.003	4.000	5.000	1.000	1.000	1.000

Table 6.The fuzzy normalized matrix

	A			B			C			D			Weights
A	0.364	0.492	0.571	0.300	0.533	0.662	0.364	0.357	0.353	0.462	0.480	0.488	0.459
B	0.364	0.246	0.190	0.300	0.267	0.221	0.273	0.286	0.294	0.231	0.320	0.366	0.281
C	0.091	0.098	0.095	0.100	0.067	0.044	0.091	0.071	0.059	0.077	0.040	0.024	0.075
D	0.182	0.164	0.143	0.300	0.133	0.074	0.273	0.286	0.294	0.231	0.160	0.122	0.210

Table 7. Fuzzy alternative matrix

		IS			OS - 1			OS - 2			OS - 3		
Based on A	IS	1.000	1.000	1.000	0.250	0.200	0.167	0.250	0.200	0.167	0.250	0.200	0.167
	OS - 1	4.000	5.000	5.988	1.000	1.000	1.000	1.000	1.000	1.000	1.000	1.000	1.000
	OS - 2	4.000	5.000	5.988	1.000	1.000	1.000	1.000	1.000	1.000	1.000	1.000	1.000
	OS - 3	4.000	5.000	5.988	1.000	1.000	1.000	1.000	1.000	1.000	1.000	1.000	1.000
Based on B	IS	1.000	1.000	1.000	0.500	0.333	0.250	0.250	0.200	0.167	2.000	3.000	4.000
	OS - 1	2.000	3.003	4.000	1.000	1.000	1.000	2.000	3.000	4.000	4.000	5.000	6.000
	OS - 2	4.000	5.000	5.988	0.500	0.333	0.250	1.000	1.000	1.000	6.000	7.000	8.000
	OS - 3	0.500	0.333	0.250	0.250	0.200	0.167	0.167	0.143	0.125	1.000	1.000	1.000
Based on C	IS	1.000	1.000	1.000	2.000	3.000	4.000	2.000	3.000	4.000	0.500	0.333	0.250
	OS - 1	0.500	0.333	0.250	1.000	1.000	1.000	1.000	1.000	1.000	0.250	0.200	0.167
	OS - 2	0.500	0.333	0.250	1.000	1.000	1.000	1.000	1.000	1.000	0.250	0.200	0.167
	OS - 3	2.000	3.003	4.000	4.000	5.000	5.988	4.000	5.000	5.988	1.000	1.000	1.000
Ba	IS	1.000	1.000	1.000	0.500	0.333	0.250	0.200	0.167	0.143	0.111	0.111	0.111

	OS - 1	2.000	3.003	4.000	1.000	1.000	1.000	0.250	0.200	0.167	0.111	0.111	0.111
	OS - 2	5.000	5.988	6.993	4.000	5.000	5.988	1.000	1.000	1.000	0.167	0.143	0.125
	OS - 3	9.009	9.009	9.009	9.009	9.009	9.009	6.000	7.000	8.000	1.000	1.000	1.000

After checking the consistency, the weights of the criteria are determined using equation (5) and shown in Table 6. Next all the alternatives are compared with each other based on all selected criteria which are shown in Table 7. Then these fuzzy matrixes are normalized and shown in Table 8. Finally the overall priority is determined using equation (9). From the overall priority the best alternative is selected. Table 9 depicts the overall priority for all the alternatives.

Table 8. Normalized alternative matrix

		IS			OS - 1			OS - 2			OS - 3			Score
Based on A	IS	0.077	0.063	0.053	0.077	0.063	0.053	0.077	0.063	0.053	0.077	0.063	0.053	0.064
	OS - 1	0.308	0.313	0.316	0.308	0.313	0.316	0.308	0.313	0.316	0.308	0.313	0.316	0.312
	OS - 2	0.308	0.313	0.316	0.308	0.313	0.316	0.308	0.313	0.316	0.308	0.313	0.316	0.312
	OS - 3	0.308	0.313	0.316	0.308	0.313	0.316	0.308	0.313	0.316	0.308	0.313	0.316	0.312
Based on B	IS	0.133	0.107	0.089	0.222	0.178	0.150	0.073	0.046	0.032	0.154	0.188	0.211	0.156
	OS - 1	0.267	0.322	0.356	0.444	0.536	0.600	0.585	0.691	0.756	0.308	0.313	0.316	0.509
	OS - 2	0.533	0.536	0.533	0.222	0.179	0.150	0.293	0.230	0.189	0.462	0.438	0.421	0.408
	OS - 3	0.067	0.036	0.022	0.111	0.107	0.100	0.049	0.033	0.024	0.077	0.063	0.053	0.074
Based on C	IS	0.250	0.214	0.182	0.250	0.300	0.334	0.250	0.300	0.334	0.250	0.192	0.158	0.259
	OS - 1	0.125	0.071	0.045	0.125	0.100	0.083	0.125	0.100	0.083	0.125	0.115	0.105	0.102
	OS - 2	0.125	0.071	0.045	0.125	0.100	0.083	0.125	0.100	0.083	0.125	0.115	0.105	0.102
	OS - 3	0.500	0.643	0.727	0.500	0.500	0.500	0.500	0.500	0.500	0.500	0.577	0.631	0.553
Based on D	IS	0.059	0.053	0.048	0.034	0.022	0.015	0.027	0.020	0.015	0.080	0.081	0.082	0.058
	OS - 1	0.118	0.158	0.190	0.069	0.065	0.062	0.034	0.024	0.018	0.080	0.081	0.082	0.109
	OS - 2	0.294	0.315	0.333	0.276	0.326	0.369	0.134	0.120	0.107	0.120	0.105	0.093	0.265
	OS - 3	0.530	0.474	0.429	0.621	0.587	0.555	0.805	0.837	0.859	0.720	0.733	0.742	0.686

Table 9 Overall priority score

	A	B	C	D	Overall Score
IS	0.029	0.044	0.020	0.012	0.105
OS - 1	0.143	0.143	0.008	0.023	0.317
OS - 2	0.143	0.114	0.008	0.056	0.321
OS - 3	0.143	0.021	0.042	0.144	0.350

From Table 9 & Figure 2, OS - 3 vehicle has the higher score (FAHP score) values followed by OS – 2, OS – 1 & IS body built vehicles.

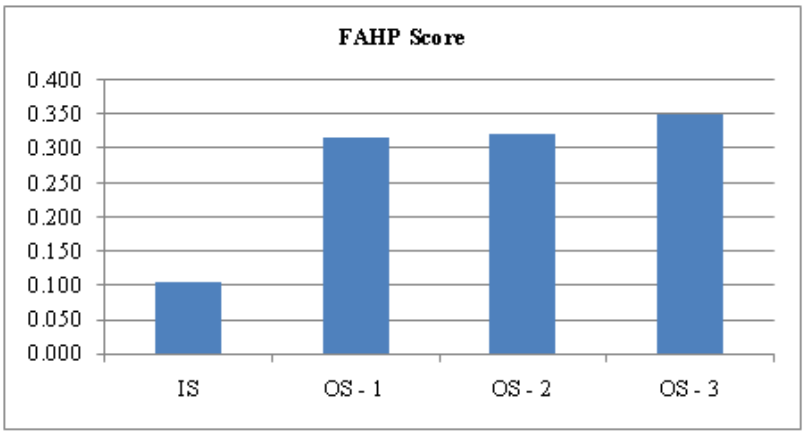

Figure 2. FAHP score

4. CONCLUSION

This paper discusses the elimination of blind spots in the sides and rear side of the heavy vehicle which is an important aspect of road safety. An intelligent multi criteria optimization model was proposed in the reduction of blind spot area in heavy transport vehicle. FAHP was used to determine the weights of the influencing criteria and the best alternative was also selected. In the model fuzzy concepts are combined with AHP. The model was tested by a case study and the effectiveness of the model was proved. FAHP is an effective tool which can accommodate both tangible and intangible factors. Based on the suggestion of optimized positioning of rear view mirror, there are great chances of reduction of area of blind spots in the sides and rear of the heavy vehicle.

REFERENCES

1. Hazem (Moh'd Said) Hatamleh, Ahmed A.M Sharadqeh, As'ad Mahmoud Alnaser, Omar Alheyasat and Ashraf Abdel-Karim Abu-Ein (2013). Computer simulation to detect the blind spots in automobiles. International Journal of Computer Science Issues, 10 (1), 453-456.
2. Burger W. (1974). Evaluation of innovative passenger car and truck rear vision system. SAE paper 1974 – 740965.
3. Thomas Ayres, Li Li, Doris Trachtman and Douglas Youn. (2005). Passenger-side rear-view mirrors: driver behavior and safety. International Journal of Industrial Ergonomics, 35, 157–162.
4. Pardhy S., Shankwitz C. and Donath M. (2000). A virtual mirror for assisting drivers. The Proceedings of IEEE symposium on Intelligent Vehicles, Dearborn, Michigan, USA: 255 – 260.
5. Kojima K., Sato A., Taya F., Kameda Y. and Ohta Y. (2005). Naviview: visual assistance by virtual mirrors at blind intersection. The Proceedings of IEEE Intelligent Transportation Systems, Vienna, Austria: 592 – 597.
6. Qidwai U. (2009). Fuzzy blind-spot scanner for automobiles. The Proceedings of IEEE Symposium on Industrial Electronics & Applications, Kuala Lumpur, Malaysia: 758 – 763.
7. Hughes C., Glavin M., Jones E. and Denny P. (2009). Wide-angle camera technology for automotive applications: A review. Intelligent Transport System, 3(1), 19-31.
8. Lakshmi S. and Wahida Banu R.S.D. (2010). Efficient realisation and rendering of images in blind zone. Journal of Computer Engineering, 1(1), 1-5.
9. Cho Y.H. and Han B.K. (2010). Application of slim a-pillar to improve driver's field of vision. International Journal of Automotive Technology, 1 (4), 517-524.
10. Kim J.H., Park B.H. and Han Y.O. (2011). Surface flow and wake characteristics of automotive external rear-view mirror. Proceedings of the Institution of Mechanical Engineers Part D - Journal of Automobile Engineering, 225 (12): 1605-1613.
11. Qiong Bao, Da Ruan, Yongjun Shen, and Elke Hermans. (2010). Creating a composite road safety performance index by a hierarchical fuzzy TOPSIS approach. The Proceedings of International Conference on Intelligent Systems and Knowledge Engineering, Hangzhou, China: 458-463.
12. Qiong Bao, Da Ruan, Yongjun Shen, Elke Hermans and Davy Janssens. (2012). Improved hierarchical fuzzy TOPSIS for road safety performance evaluation. Knowledge Based Systems, 32, 84-90.
13. Robert E. Llaneras, Charles A. Green, Raymond J. Kiefer, William J. Chundrlik Jr., Osman D. Altan and Jeremiah P. Singer. (2005). Design and evaluation of a prototype rear obstacle detection and driver warning system. Human Factors, 47 (1), 199-215.
14. Pitchipoo P., Venkumar P. and Rajakarunakaran S. (2013). Fuzzy hybrid decision model for supplier evaluation and selection. International Journal of Production Research, 51 (13), 3903-3919.
15. Osman Kulak. (2005). A decision support system for fuzzy multi-attribute selection of material handling equipments. Expert Systems with Applications, 29, 310–319.
16. Zahari Taha and Sarkawt Rostam. (2011). A fuzzy AHP–ANN-based decision support system for machine tool selection in a flexible manufacturing cell. International Journal of Advanced Manufacturing Technology, 57 (5-8), 719–733.
17. Thomas L. Saaty. (1990). How to make a decision: the analytic hierarchy process. European Journal of Operations Research, 48 (1), 9-26.
18. Mohamad Ashari Alias, Siti Zaiton Mohd Hashim and Supiah Samsudin. (2009). Using fuzzy analytic hierarchy process for southern Johor river ranking. International Journal of Advanced Soft Computing Applications, 1 (1), 62-76

CONTENTS

PEC-DM-232

DAMAGE DETECTION OF COST EFFECTIVE CFRP COMPOSTE STRUCTURE USING FIBER OPTIC SENSOR UNDER DYNAMIC LOAD

J. Jerold John Britto[1, a], A. Vasanthanathan[2, b], Dr. P. Nagaraj[3, c]

[1]Assistant Professor, Department of Mechanical Engineering, Ramco Institute of Technology,Rajapalayam, India

[2]Associate Professor, Department of Mechanical Engineering, Mepco Schlenk Engineering College, Sivakasi, India

[3]Sr. Professor & Head, Department of Mechanical Engineering, Mepco Schlenk Engineering College, Sivakasi, India

Abstract: Recent advances and cost reductions has simulated interest in fiber optical sensing. This technique helps to detect the damage in aircraft structure. Nowadays, most of the critical components of aircraft structure made up of composite structure. CFRP can significantly reduce the weight while increasing strength and durability. The weight reduction of the structure will increase the fuel efficiency. The composite structure subjected to static and dynamic loading during the running condition. This paper overviews the cost effective material selection (CFRP) and damage detection setup using fiber optic sensor under dynamic loading condition.The spectrum received from the damage detection setup is analysed to ensure the size, shape and damage condition. The intensity of spectrum depends on the damage size of the given component. The entire paper shows the damage detection under dynamic loading with various indenter for impact.

Keywords: Fiber optic sensor, Composite Laminate, CFRP, Impact.

I. Introduction

Carbon-fiber-reinforced polymers are composite materials. They have unique properties of relatively high strength at high temperatures coupled with low thermal expansion and low density[1] . The physical properties of composite materials are generally not isotropic in nature, but rather are typically anisotropic (different depending on the direction of the applied force or load). For instance, the stiffness of a composite panel will often depends upon the orientation of the applied forces and/or moments.

Static and Dynamic loads are known to induce damage to the composite in the form of matrix cracking delamination, debonding and fibre breakage (Serge Abrate, 2011). Research has shown that composites are capable of absorbing energy and dissipating it by various fracture and elastic processes when subjected to a loads. The ability of composite material is to absorb energy elastically depends on the mechanical properties of the matrix and fibres, the interfacial strength, the velocity of impact (Hualin Fan eLal, 2009) and the size of the component. Materials and structures, in addition to enabling technologies for future aeronautical andspace systems, continue to be the key elements in determining the reliability, performance,testability, and cost effectiveness of these systems. The focus of the present paper is ondevelopments damage identification using fiber optic sensor.

II. MATERIALS AND METHODS

1. MATERIALS

a. Carbon Fibre

Carbon fibers are commercially available with a variety of tensile modulus values ranging from 207 MPa on the low side to 1035 MPa on the high side. In general, the low-modulus fibers have lower density, lower cost, higher tensile and compressive strengths, and higher tensile strains-to-failure than the high-modulus fibers.

Carbon fibers are their exceptionally high tensile strength–weight ratios as well as tensile modulus–weight ratios, very low coefficient of linear thermal expansion high fatigue strengths, and high thermal conductivity. Their high cost has so far excluded them from widespread commercial applications. They are used mostly in the aerospace industry, where weight saving is considered more critical than cost.

b Epoxy Resin & Hardener

Epoxy resins are the most used just after polyesters, their price being the only limit to their usage. They have better mechanical characteristics in tension, compression, impact and others when compared with polyester resins, and so they are preferred in the manufacturing of high performance parts like those used in aeronautics and others. Besides they present good heat resistance up to 15^0 to 190^0 C, have good chemical resistance, [2] low retraction, good reinforcement wetting and an excellent adhesion to metallic materials. The hardener is used to cure the matrix materials in fibre as faster than usual curing time. From that we can get excellent adhesive bonding together and normally the proportion of hardener, epoxy resin is equal amount and equal to weight of fibre.

c. Fiber Optic Sensor

Fiber optic sensor technology has been a major user of technology associated with the optoelectronic and fiber optic communications industries. The ability of fiber optic sensors to displace traditional sensors (Shizhuo Yin, Paul B. Ruffin, Francis T. S. Yu 2008) for rotation, acceleration, electric and magnetic field measurement, temperature, pressure, acoustics, vibration, linear and angular position, strain, humidity, viscosity, chemical measurements, and a host of other sensor applications has been enhanced. The inherent advantages of fiber optic sensors, which include their ability to be lightweight, of very small size, passive, low power, and resistant to electromagnetic interference, high sensitivity [9].Fiber optic sensors are often loosely grouped into two basic classes referred to as extrinsic, or hybrid, fiber optic sensors and intrinsic, or all fiber, sensors.

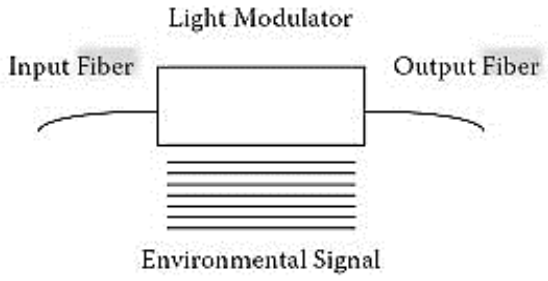

Fig. 1 Overview of Fiber Optic Sensors.

d. Material Properties

The following material properties from Test Data results [3,4] have been taken into account for analysis 1 Psi = 0.0069 MPa. Composites are the orthotropic material the property varies along the three directions. The stiffness of a composite panel will often depend upon the orientation of the applied forces and/or moments. Panel stiffness is also dependent on the design of the panel.

Table 1 Material Property of CFRP

Properties		**Carbon/epoxy**
E_a	(GPa)	125.485
E_b	(GPa)	8.067
E_c	(GPa)	8.067
G_{ab}	(GPa)	41.29
G_{bc}	(GPa)	2.42
G_{ca}	(GPa)	4.129
γ_{ba}		0.0176
γ_{cb}		0.0176
γ_{ca}		0.4657
Density	Kg/m^3	4.152

III. EXPERIMENTATION

3.1 Low velocity impact test Data

Damage in unidirectional carbon/fibre composite resulting from low velocity/energy impacts was evaluated embedded fiber optic sensor. [6] The value for conducting experiments based on the experimental results taken from the output of the experimental value the Impactor and energy consideration taken into account for the further improvement of the velocity impact energy. Initially low velocity impact was conducted by using two types of impactor shape [7]. The laminates used in the low velocity impact tests were manufactured from uni-directional carbon fibre/epoxy prepreg. The panels 200 mm ×90 mm × 3 mm.

1. Impactor for testing
   - Conical -167gm
   - Hemi Spherical -180 gm
2. Impact Energy for conducting test
   - 0.33 J with Corresponding velocity 1.3 m/s
   - 0.56 J with corresponding velocity 2.5 m/s
3. Formula for calculating the impact energy
   - E=W × h

$V=\sqrt{2gh}$ Where W- Weight of the Impactor (N),h- Vertical height,

Courtesy: "*Evaluating impact damage in CFRP using fibre optic sensors" A.R. Chambers a,*, M.C. Mowlem b, L. Dokos a*

V- velocity (m/s), E – Energy (J)

3.2 Experimental Setup

Figure 2 – 4 shows the configuration of the test specimen of impact detection with flat plat. The specimen is a quasi-isotropic laminate plate. A single mode fiber sensor was bonded to the specimen surface for impact damage detection. The following components are used for the experiments (a) Electrical Input Signal – 1MHz, (b) Optical Transmitter, (c) Single mode fiber cable, (d) Optical receiver, (e) Digital Oscilloscope with data acquisition system. The low velocity impact experimental setup was created for damage detection.

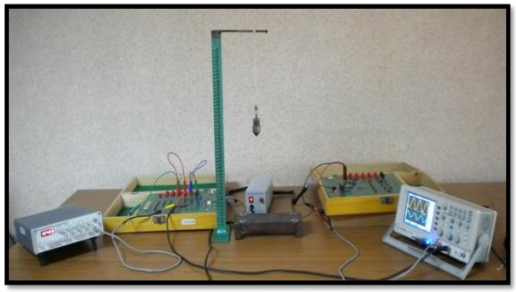

Fig. 2 Dynamic Load Test Setup Arrangement

Fig. 3 Test Setup arrangement

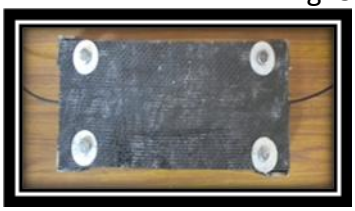

Fig. 4 Test Specimen with fiber optic sensor

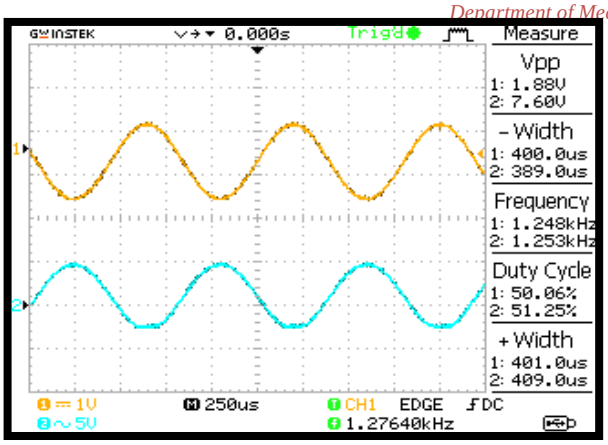

Fig (3) h= 186.88mm at 0.33J Hemi Spherical Impactor

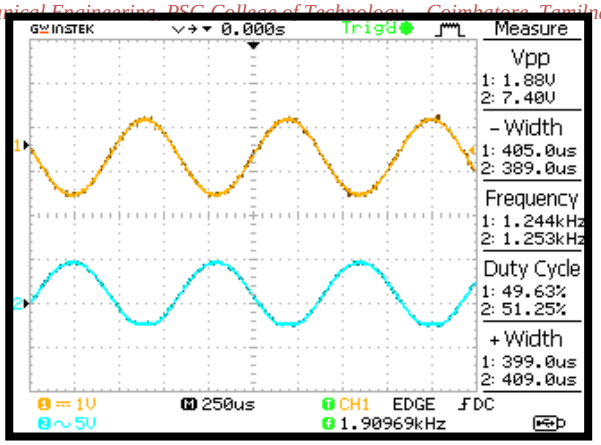

Fig (4) h= 317.1 mm at 0.56J Hemi Spherical Impactor

IV. **RESULTS AND DISCUSSIONS**

The following experimental result graph shows that the various impact energy with respect to the various height level [8]. Fig (1) h= 201.4mm at 0.33J Conical Impactor

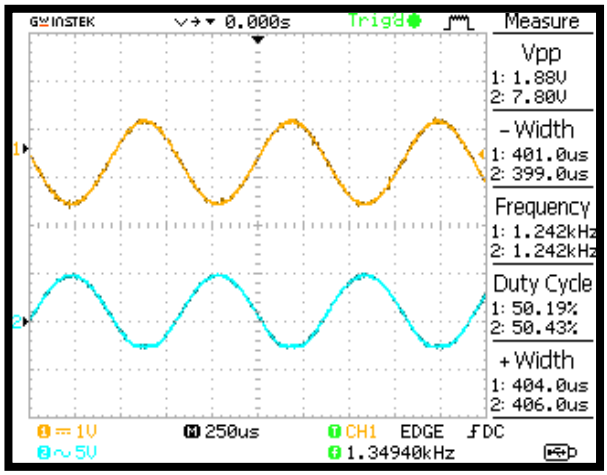

Fig (2) h= 341.4mm at 0.56J Conical Impactor

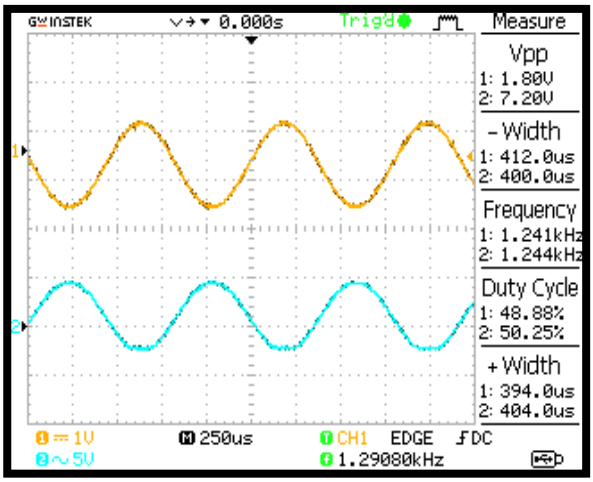

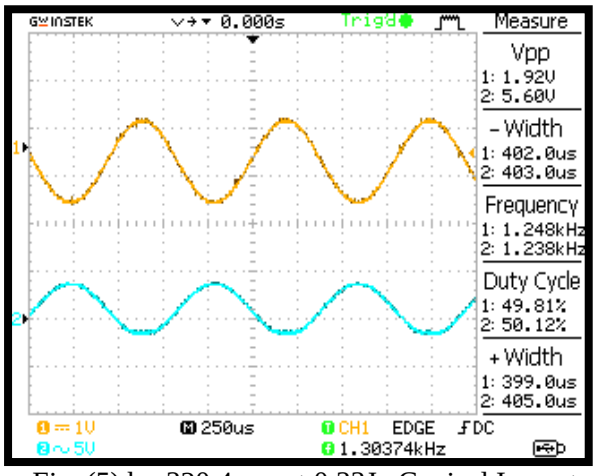

Fig (5) h= 320.4mm at 0.33J Conical Impactor (Ø 12mm)

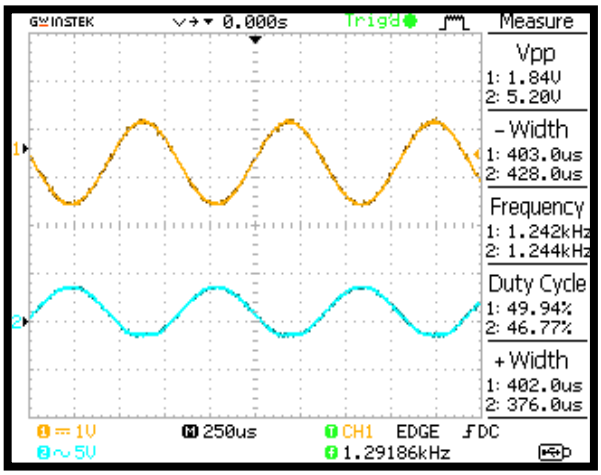

Fig (6) h= 543.66mm at 0.56J flat Impactor (Ø 12mm)

Fig. 5 Output Results for Dynamic Analysis

The damage detection principle of this system is based on the energy change of the received waveform. If a damaged section exists in the path of the elastic wave, the energy of the elastic wave will change. By detecting this change, the system can detect the damage in a composite structure. We could successfully detect the damage propagation by this system. Figure 5 [1-6] shows an output wave form of the impact load condition. We have conducted the impact detection test using a drop-weight type impact machine.

The weight of was 167 gm and its tip was a conical shape. The energy of the impact is 0.33 J at velocity 1.3 m/s. The figures 5 [1,3,5] shows the received waveform and the enlarged waveform of the elastic wave of fiber optic sensors under 0.33 J energy with height range of 201.6 mm, 186.88 mm and 320.4 mm. The figures 5 [2,4,6] shows the received waveform and the enlarged waveform of the elastic wave of fiber optic sensors under 0.56 J energy with height range of 341.4 mm, 317.1 mm and 543.6 mm. Based on this output wave the experimental setup detect the resulting damage. As the result of this study, it was revealed that two kind of detections, damage monitoring and impact detection, with the same system construction by the damage monitoring using single mode fiber sensor.

V. CONCLUDING REMARKS

The following conclusions were drawn from the present experimental investigations:

1. Carbon fibre is suitable material for absorbing more energy during the impact loading condition. Based on the material property.
2. For the constant input voltage of 1.88v the output voltage varies with respect to the impact [Fig. 5 (1 – 6)] load energy of 0.56 J, the output voltage is 5.20v.
3. The shape of the impactor in this experimental work: conical, Hemi spherical and flat shape.
4. In this paper, the low velocity impact load is applied in between the range of 1.3 to 2.5 m/s.

5. The figure 5 [1 – 5] shows the output of the impact load on the composite plate and it shows the energyabsorption capability of carbon fiber material.

ACKNOWLEDGEMENT

All the praise goes to Almighty God for his source of all inspirations, for showering his divine and merciful blessings on us. We express our heartiest gratitude and the authors would like to thank The Principal/RAMCO Institute of Technology, Rajapalayam and The Principal/MEPCO SCHLENK Engineering College, Sivakasi for providing facilities to carry out this research work.

REFERENCES

[1] Deborah D.L. Chung, "Composite Materials Functions and modern Technologies" composite materials laboratory, University of Buffalo, New York, 2009..

[2] P. K. Mallick, "Fiber-Reinforced Composites: Materials, Manufacturing and Design" – Taylor & Francis Group, LLC.

[3] G. C. Sih and S. E. Hsu, "Advanced Composite Materials and Structures" – Publisher VNU Science Press BV.

[4] Kersey AD, Davis MA, Patrick HJ, LeBlanc M, Koo KP, Askins CG, PutnamMA, and Friebele EJ. Fiber grating sensors, Journal of Lightwave Technol., Vol.15, No. 8, pp 1442-1463, 1997.

[5] Satori K, Fukuchi K, Kurosawa Y, Hongo A, and Takeda N. Polyimide-coatedsmall-diameter optical fiber sensors for embedding in composite laminatestructures, Proc. SPIE, Vol. 4328, pp 285-294, 2001.

[6] Okabe Y., Mizutani,T, Yashiro S, and Takeda N. Detection of microscopicdamages in composite laminates with embedded small-diameter fiber Brag grating sensors. Comp. Sci. Technol., Vol. 62, No. 7-8, pp 951-958, 2002.

[7] Guemes JA and Menendez JM. Response of Bragg grating fiber-optic sensorswhen embedded in composite laminates. Comp. Sci. Technol., Vol. 62, No. 7-8,pp 959-966, 2002.

[8] Taketa I, Amano M, Okabe Y, and Takeda N. Damage detection andsuppression system of CFRP laminates with FBG sensor and SMA actuator.Trans. Mater. Res. Soc. Japan, Vol. 28, No. 3, pp 675-678, 2003.

[9] Shizhuo Yin, Paul B. Ruffin and Francis T. S. Yu, "Fiber Optic Sensors", CRC Press, Taylor & Francis Group.

RAMCO INSTITUTE OF TECHNOLOGY

SECOND NATIONAL CONFERENCE ON INNOVATIONS IN ENGINEERING, SCIENCE AND TECHNOLOGY

CIVIL Stream

SL.NO	PAPER ID	TITLE
1.	CE101	FORENSIC ASSESSMENT OF CAUSES OF DISTRESS IN CONCRETE
2.	CE102	EXPERIMENTAL INVESTIGATION ON WASTE GLASS POWDER AS PARTIAL REPLACEMENT OF CEMENT IN CONCRETE
3.	CE103	STUDY ON PARTIAL REPLACEMENT OF COARSE AGGREGATE BY PLASTIC (POLYPROPYLENE)
4.	CE104	UTILIZATION OF DRY SOLID WASTE IN BRICKS
5.	CE105	CREATING AN ANDROID APPLICATION FOR WATER ESTIMATION OF AGRICULTURAL CROPS
6.	CE106	LABORATORY STUDY OF POROSITY AND STRENGTH PROPERTIES OF PERVIOUS CONCRETE
7.	CE107	COMPARATIVE STUDY AND ANALYSIS OF RCC & POST TENSIONED TRANSFER PLATE
8.	CE108	EXPERIMENTAL INVESTIGATION ON CONCRETE USING RECYCLED COARSE AGGREGATE
9.	CE109	SMART ENVIRONMENT USING ARCGIS
10.	CE110	THERMAL CONDUCTIVE CONCRETE USING SLAGS
11.	CE111	EXPERIMENTAL AND NUMERICAL STUDY OF WOOD AND UPVC JOINERY PROFILES
12.	CE112	NUMERICAL STUDIES OF AXIAL COMPRESSIVE BEHAVIOUR OF SLENDER I-SECTION COLUMN AND PARTIALLY ENCASED COMPOSITE COLUMN
13.	CE113	EXPERIMENTAL STUDY ON HYBRID FIBRE REINFORCED GEOPOLYMER CONCRETE

14.	CE114	UTILIZATION ASPECTS OF MARBLE CHIPS AND QUARRY SAND IN CONCRETE
15.	CE115	AROUND RIT THROUGH GIS
16.	CE116	EXPERIMENTAL STUDY ON STABILIZATION OF BLACK COTTON SOIL USING LIME AND COPPER SLAG
17.	CE117	ANALYTICAL MODELLING OF REINFORCED CONCRETE BEAM USING GFRP SANDWICH PANELS
18.	CE118	PERMEABLE PAVEMENT
19.	CE119	EXPERIMENTAL STUDY ON STRENGTH OF CONCRETE BY PARTIAL REPLACEMENT OF SAND WITH BOTTOM ASH

RAMCO INSTITUTE OF TECHNOLOGY

(Approved by AICTE, New Delhi and Affiliated to Anna University, Chennai)
North Venganallur Village, Rajapalayam - 626 117, Tamil Nadu.

National Conference on Innovations in Engineering, Science & Technology

CERTIFICATE

24th & 25th March, 2017

This is to certify that ~~Dr./Mr.~~/Ms. Subha C of Ramco Institute of Technology presented a paper entitled Utilization of dry solid waste in bricks

National Conference on Innovations in Engineering, Science and Technology - NCIEST, organised by Ramco Institute of Technology, Rajapalayam during 24th & 25th March, 2017.

G. Karthik
Organizing Secretary
NCIEST

Dr.R.V.Mahendra Gowda
Principal

UTILIZATION OF DRY SOLID WASTE IN BRICKS

C. Subha, V. Abinaya Sundhari, P. Navabharathi, S. Pavithra, M.Suveetha
Assistant Professor in Civil Engineering, Ramco Institute of Technology
B.E. student in Civil Engineering, Ramco Institute of Technology

Abstract: **There is an increasing demand on building materials especially in the recent years because of increasing population. The main challenge is to convert wastes to useful construction materials. Recycling of waste as raw material alternatives, may reduce the exhaustion of the natural resources and waste disposal costs. Bricks are commonly used building material around the world. Conventional bricks are produced from clay with high temperature kiln firing which emits nearly 1 ton of CO_2. For environmental protection and sustainable development, extensive research has been conducted on production of bricks from waste materials. The waste materials to be filled in the landfill is greatly reduced and thereby saving the environment. This project emphasizes on the use of waste materials like Flyash, marble dust, rice husk ash, quarry dust and egg shell powder replacing clay in bricks. The bricks are manufactured and tested as per IS standards.**

Keywords: waste materials, clay, environmental protection, kilns, hydraulic compression

I.INTRODUCTION

Brick is one of the oldest and commonly used building materials. In 8000 BC, the dried-clay bricks were used for the first time. The fired clay bricks were used as early as 4500 BC. The worldwide annual production of bricks and demand for bricks is continuously increasing in the recent years. Conventional bricks are produced from clay with high temperature kiln firing. The high temperature kiln firing not only consumes significant amount of energy, but releases large quantity of greenhouse gases. Clay bricks, on average, have an embodied energy of approximately 2.0 kWh and release about 0.41 kg of carbon dioxide (CO_2) per brick. The process of brick making has not changed since many centuries except some minor refinements. There have been hardly any efforts in the country to improve the brick-making process for enhancing the quality of bricks. The main reason for this attitude is that the production of bricks has been largely remained confined to the unorganized small sector. Some of the large mechanized brick plants came up in the past but they failed for some reason or other. The result is that the construction industry is largely dependent on the small sector which is unable to deliver high quality bricks in view of rising fuel cost, outdated technology and lower efficiency of production. Environmental concerns are also being raised against uncontrolled extraction of clay. The main concern is land degradation. Therefore, clay should be replaced in bricks with some other suitable materials.

Various attempts were made to incorporate various waste material in bricks production such as natural fibers, textile laundry wastewater sludge, foundry sand, granite sawing waste, perlite, processed waste tea, sewage sludge, structural glass waste, PC and TV waste, fly ash, sugarcane bagasse ash, organic residue, steel dust, bottom ash, rice husk ash, silica fume, marble and granite waste, municipal solid incineration fly ash slag.

II. MATERIALS USED

A. Clay

Clay soils are compounds of silica and alumina. Calcareous clays have calcium carbonate and will burn to a yellow or cream color. Non-calcareous typically contain feldspar and iron oxides, and will burn to a brown, pink or red, depending on the amount of iron oxide. The silica in the clay, when fired at 900-1200 degrees C, will turn to a glassy phase. This process, called vitrification, will turn the clay to a crystalline structure. Clay was replaced with the following materials such as fly ash, rice husk ash, marble dust, egg shell powder, quarry dust, cement.

B. Fly ash

Fly ash or pulverized fuel ash (PFA) is the residue from the combustion of pulverized coal collected by mechanical or electrostatic separators from the flue gases or power plants. It constitutes about 75% of the total ash produced. Fly ash is puzzolanic in nature, and contains less than 7% lime. The puzzolanic *property* coupled with lime reactivity makes it very suitable for cementitious / binding applications

C. Rice husk ash

Combustion of rice hulls affords rice husk ash. This ash is a potential source of amorphous reactive silica, which has a variety of applications in materials science. The amount of silica increases with increase in burning temperature. This ash is also a very good thermal insulation material and maintains temperature.

D. Marble Dust

The marble dust is a Very fine powder obtained during cutting or dressing of marble. 25% marble mass becomes marble dust. It is also used as an admixture, increases cohesiveness to the mixture and enhances good binding.

E. Egg Shell Powder

It is obtained by grinding of egg shells. Egg shell Contains lot of calcium and its chemical composition is similar to limestone It offers high density, compressive strength and durability.

F. Quarry dust

It is a byproduct of quarrying of rocks. It used as a substitute for fine aggregate and the construction cost reduces and in addition it increases the strength to a little.

G. Cement

Cement is a powdery substance made by calcining lime and clay.Cement is a great binding material and hence it is used in small quantity in the bricks for binding the waste materials.

III. CASTING OF BRICKS

Bricks made of waste materials were cast by means of hydraulics compression technique. The following steps were involved in the casting of bricks.The waste materials that were used in the manufacture of bricks were collected from various places and is shown in the Table I and the collected materials are shown in the Fig.1

TABLE I

MATERIALS COLLECTED

MATERIALS	PLACE OF COLLLECTION
Fly ash	Local dealer from Rajaplayam
Egg shell powder	Schools and hotels
Rice husk ash	Rice mills
Marble dust	Mandeep Marbles& Stones Private Limited, Madurai
Quarry dust	Local dealers from Rajapalayam
Cement	Local dealers from Rajapalayam

Fig1. Mixture of materials used

The collected materials are put in the mixer and water was added till it attains proper consistency. Comparatively for all the trials the quantity of water added was 3 to 4 litres for a weight of 21kg of materials. The weight of one brick was estimated to be around 3.5kg so that 6 bricks weigh around 21kg.The materials were allowed to mix in the pan mixer for 10 to 15 minutes until a uniform mixture was obtained. The mixed raw materials are taken to the compression machine through conveyor belt for casting and compaction. The pan mixer in which materials were mixed is shown in Fig.2

Figure 2: Cylindrical pan mixer

The bricks were produced finally from hydraulics pressing machine which runs at a rate of 2200Psi. The bricks were of size 23 x 11 x 7 cm. The produced bricks are taken and then stacked for curing for a period of at least 21 days to ensure good strong brick. The bricks were cast in five trials of various proportions as shown in Table II

TABLE II:
PROPORTION OF MATERIALS USED IN BRICK

MATERIALS	TRIAL 1 %	TRIAL 2 %	TRIAL 3 %
Flyash	40	40	40
Marble dust	10	10	10
Cement	5	5	5
RHA	2	2	2
ESA	3	5	10
Quarry dust	40	38	33

IV. RESULT AND DISCUSSION

The various tests were conducted and the results are shown in table. The bricks were tested for their compressive strength after 21 days of curing. The bricks were tested in the compression testing machine by providing two iron plates. The water absorption is found by immersing the brick

for 24 hours at room temperature. The difference between the dry and wet weight is calculated in percentage.

TABLE III

TEST RESULTS

TYPE OF TEST	TRIAL1	TRIAL 2	TRIAL 3
Weight	Around 3 Kg	Around 3 Kg	Around 3 Kg
Compressive strength	7.2 N/ mm^2	7.8 N/ mm^2	8.45 N/ mm^2
Water absorption	5.12 %	5.28 %	5.41 %
Efflorescence	Nil	Nil	Nil
Shape	Even	Even	Even
Structure	No pores/ honey comb	No pores/ honey comb	No pores/ honey comb
Soundness	Produces cling sound	Produces cling sound	Produces cling sound

The graph plotted with the compressive strength values is shown in Fig.3

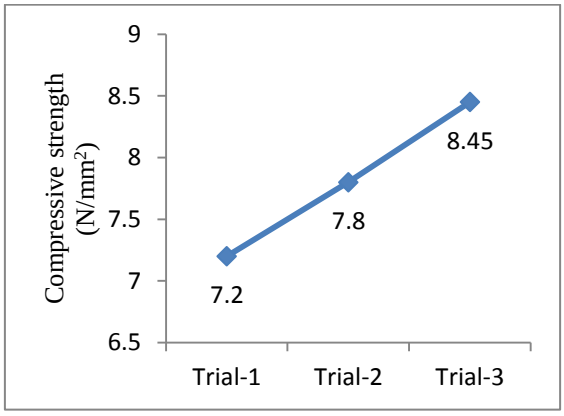

Fig 3. Compressive strength chart

The graph plotted with the water absorption values is shown in Fig.4

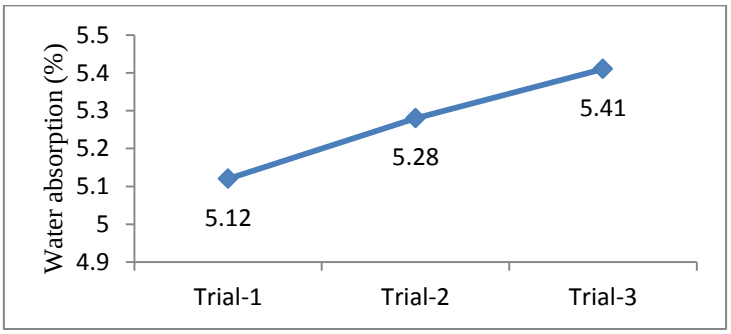

Figure 4: Water absorption chart

V.CONCLUSION

1. The compressive strength of the brick increases with increasing percentage of egg shell powder and decreasing percentage of quarry dust.
2. The maximum compressive strength value obtained is 8.45 N/mm^2.
3. The water absorption value is less than 7% for all the trials.
4. The optimum proportion of waste materials is fly ash 40 %, marble dust 10%, cement 5%, RHA 2%, Egg shell powder 10%, quarry dust 33%.

REFERENCES

[1] J. O. Akinyele , O. T. Olateju, O. K. Oikelome:"*Rice Husk As Filler In The Production Of Bricks Using GbokoClay" Nigerian Journal of Technology (NIJOTECH) , 2015*

[2] N. Bilgin, H.A. Yeprem , S. Arslan , A. Bilgin, E. Gunay, M. Mars_oglu : *"Use of waste marble powder in brick industry" Construction and building materials ,* 2012

[3] Francis Adogla, Peter Paa Kofi Yalley, Moses Arkoh: "*Improving Compressed Laterite Bricks using Powdered Eggshells"* The International Journal Of Engineering And Science (IJES) ISSN (e): 2319 – 1813, 2016

[4] R.Nithiya, Chris Anto L, K.R.Vinodh, Dr.C.Anbalagan: *"Experimental investigation on bricks by using various waste materials"* International Journal of Latest Trends in Engineering and Technology (IJLET), ISSN :2278-621X, 2016

[5] Obadakayali: "*High performance bricks from fly ash*" World of Coal Ash (WOCA), 2015

[6] H N Rajendra Prasad, H G Vivek Prasad, Chetana Hamsagar, D Yogesh Gowda , Nikitha Marina Lobo, SreePushpakGowda : "An approach for alternative solution in brick Manufacturing" International Journal of Science, Environment and Technology, ISSN 2278-3687 (O) , 2014

[7] Sarker Kamruzzaman, Nahid Sharmin, Md. Moniruzzaman, Md. Sagirul Islam : "Pilot Plant Study on Energy Saving Brick from Rice Husk Ash" International Journal of Emerging Technology and Advanced Engineering , ISSN 2250-2459, 2015

[8] SwaminathanDhanapandian, BalasubramaniGnanavel ,&ThirunavukkarasuRamkumar : "Utilization Of Granite And Marble Sawing Powder Wastes As Brick Materials " Carpathian Journal of Earth and Environmental Sciences, 2009

[9] N.Vamsi Mohan, Prof.P.V.V.Satyanarayana, Dr.K.Srinivasa Rao : "Performance Of Rice Husk Ash Bricks" International Journal of Engineering Research and Applications (IJERA) ISSN: 2248-9622 , 2012

RAMCO INSTITUTE OF TECHNOLOGY

(Approved by AICTE, New Delhi and Affiliated to Anna University, Chennai)
North Venganallur Village, Rajapalayam - 626 117, Tamil Nadu.

National Conference on Innovations in Engineering, Science & Technology

CERTIFICATE

24th & 25th March, 2017

This is to certify that ~~Dr./Mr./Ms.~~ MURUGANATHAM R of RAMCO INSTITUTE OF TECHNOLOGY presented a paper entitled THERMAL CONDUCTIVE CONCRETE USING SLAGS

National Conference on Innovations in Engineering , Science and Technology - NCIEST , organised by Ramco Institute of Technology ,Rajapalayam during 24th & 25th March, 2017.

Organizing Secretary
NCIEST

Dr.R.V.Mahendra Gowda
Principal

THERMAL CONDUCTIVE CONCRETE USING SLAGS

Keerthana.C, Pavithra.S, Subhalakshmi.LV, Muruganantham.R, Karthikeyan.N
U.G student, Department of Civil Engineering, Ramco Institute of Technology, Rajapalayam
Assistant Professor, Department of Civil Engineering, Ramco Institute of Technology, Rajapalayam
Assistant Professor (S.G), Department of Physics, Ramco Institute of Technology, Rapalayam

Abstract **- This paper examines the thermal conductivity of concrete. The thermal conductivity is increased by the addition of copper slag and steel slag. Many hit and trial methods have been done to identify the correct mix proportion of slag in concrete and also to find the compressive strength of the concrete. From the experiments that have been done, it has been inferred that 20% replacement of weight of concrete by slag is suitable without any compromise on strength. Thermal studies have been conducted on the controlled concrete M30 with and without adding slag separately. The results have been studied and have been found that the induction concrete attained high temperature faster than the normal concrete and the heat retaining capacity was also found to be much more than the normal concrete. The main application of this induction concrete is de-icing and anti-icing in bridge decks and highways**.

I. INTRODUCTION

Concrete bridge decks are prone to ice accumulation. The use of road salts and chemicals for deicing is an effective method for ice removal, but causes damage to concrete and corrosion of reinforcing steel in concrete bridge decks. This problem is a major concern to transportation officials and public works due to rapid degradation of existing concrete pavements and bridge decks. The use of insulation materials for ice control and electric or thermal heating for deicing have been attempted and met limited success. Conductive concrete may be defined as a cementitious composite that contains a certain amount of thermally conductive components to attain stable and relatively high thermal conductivity. When power supply is given to the light weight iron element which is embedded in concrete, heat is induced in it.

This is based on the principle of thermal conductivity. In physics, thermal conductivity (often denoted k, λ, or κ) is the property of a material to conduct heat. It is evaluated primarily in terms of Fourier's Law for heat conduction. Heat transfer occurs at a lower rate across materials of low thermal conductivity than across materials of high thermal conductivity. Correspondingly, materials of high thermal conductivity are widely used in heat sink applications and materials of low thermal conductivity are used as thermal insulation. The thermal conductivity of a material may depend on temperature. The reciprocal of thermal conductivity is called thermal resistivity.

Ongoing IRC research is now focused on optimizing conductive concrete formulations for the best combination of strength, electrical properties, and production methods at the lowest possible cost, leading ultimately to commercial development and widespread use.

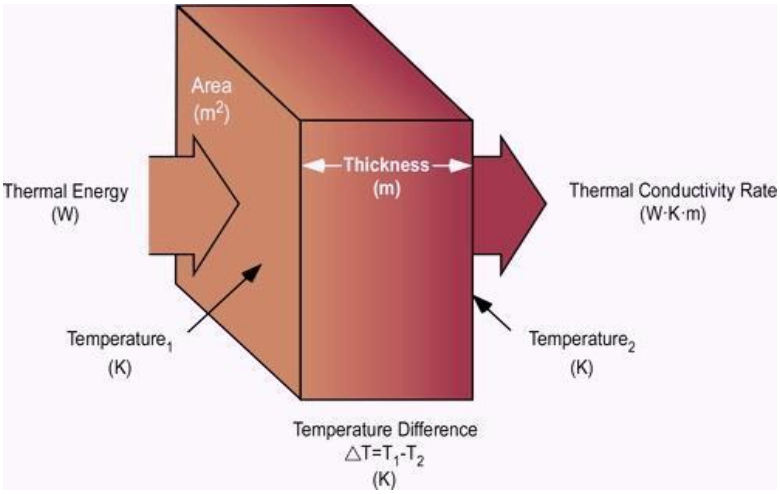

Fig 1 Principle of thermal conductivity

II. OBJECTIVES AND SCOPE

The main objective of this thesis is to prepare a conductive concrete mix specifically for cold regions, for deicing and anti-icing application and to increase the thermal conductivity of concrete by incorporating steel slag and copper slag in the concrete mix. The thermal conductivity of the copper and steel slag along with the concrete has been studied.

III. MATERIALS BACKGROUND

A.Copper Slag

Copper slag is a by-product of copper extraction by smelting. During smelting, impurities become slag which floats on the molten metal. Slag that is quenched in water produces angular granules which are disposed of as waste or utilized as discussed below Copper slag is one of the materials that is considered as a waste material that could have a promising future in construction industry as partial substitute of either cement or aggregates. Studies are already being carried out to increase the output by using copper slags and other materials as composites. From this project, it is evident that copper slag can be used to enhance the characteristics when used with other materials. Hence, it has a huge potential to be used for industrial applications.

Fig-2 Copper slag

TABLE I
PROPERTIES OF COPPER SLAG

Name	Thermal conductivity (W/mK)	Cost (Per Ton) (Rs.)
Copper slag	385	200/tonne

B.Steel Slag

Steel slag, a by-product of steel making, is produced during the separation of the molten steel from impurities in steel-making furnaces. The slag occurs as a molten liquid melt and is a complex solution of silicates and oxides that solidifies upon cooling.

Fig-3 Steel slag

TABLE 2
PROPERTIES OF STEEL SLAG

Name	Thermal Conductivity (W/mK)	Cost (Per Ton) Rs.
STEEL SLAG	50.2	650

IV. EXPERIMENTAL PROGRAMME

C.Compressive Strength Test

In order to find the compressive strength of concrete, specimens of size 15cm x 15cm x 15cm were casted for various proportions. The test were performed with a 2000kN compression testing which provided essentially fixed end condition to the bottom and the top was free end. Specimen end plates provide a uniform load distribution over the cross section. The cube was generally loaded at the rate of 99.9kN/s. Near and after failure, the load was manually controlled to allow visual observation. The load was applied to the specimen up to failure mode.

Fig-4 Compressive strength machine

From the experimental result, it has been found that the concrete cube which was formed by replacing 20% by weight of the concrete showed satisfiable results. The comparative study of the various mix proportions are tabulated.

TABLE 3

COMPRESSION TEST RESULTS

Mix proportion	Copper slag in %	Steel slag in %	Peak load in kN
M30	_	_	667.25
10% replacement	5	5	511.5
	7.5	2.5	545.3
20% replacement	10	10	634.25
	15	5	659.5
30% replacement	15	15	640.7
	22.5	7.5	602.6

Cracks are formed in the 30% replaced concrete cube, even though it has achieved the nearer strength as that of the 20% replaced concrete.

D. Thermal Study

After finding the correct mix proportion with the required strength, thermal studies were conducted on the concrete cubes .The temperature of the cubes were raised to about 10 degree Celsius from room temperature. It was

found that the concrete cube with the addition of slag attained the temperature 64.4 degree Celsius 13 minutes earlier than the concrete cube without the addition of the slag. After the supply of electricity is stopped the heat retaining capacity of the cubes were also found .From that it was inferred that the heat retaining capacity of the concrete with the addition of the slag was 2 hours more than that of the normal concrete. Graphs were drawn between the temperature and the time and results were found.

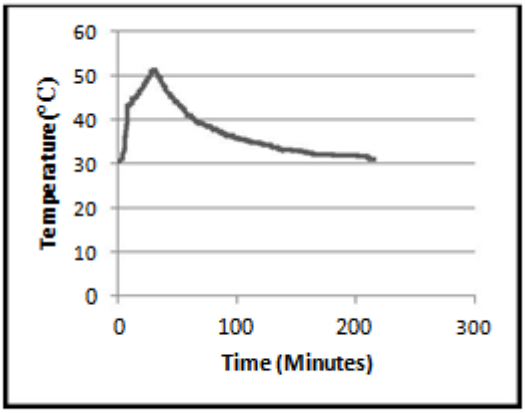

Fig-5 Experimental results of temperature Vs time graph (M30 concrete)

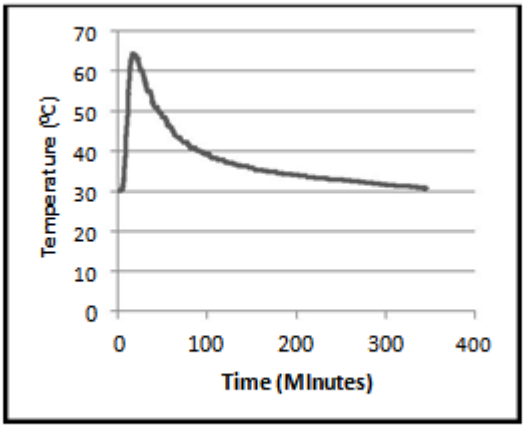

Fig-6 Experimental results of temperature Vs time graph (20% replaced concrete)

V.APPLICATIONS

- Conductive concrete has the potential to address a wide variety of applications, including grounding, heating, cathodic protection of reinforcing steel in concrete structures such as bridges and parking garages, and electromagnetic shielding.
- Electrical heating using conductive concrete has excellent potential for domestic and outdoor environments, especially for de-icing of parking garages, sidewalks, driveways, highway bridges, and airport runways.

VI.CONCLUSIONS

The thermal conductivity of copper and steel slag are studied. The heat retaining capacity of the conductive concrete proved to be a valuable asset for its de-icing and anti-icing applications. Research is also being made to implement the conductive concrete in the steam power plants.

REFERENCES

[1] K.S. Al-Jabri, A.W. Hago, A.S. Al-Nuaimi, A.H. Al-Saidy "Concrete blocks for thermal insulation in hot climate", Cement and Concrete Research 35 (2005) 1472 – 1479.
[2] K.Venkatraman , Dr.V.Tamizharasan "Electrically Conductive Concrete" International Journal of Innovative Research in Science Engineering and Technology, Vol. 4, Issue 8.
[3] Sherif Yehia and Christopher Y. Tuan "Conductive Concrete Overlay for Bridge Deck Deicing", ACI Structural Journal, volume: 96, pp.382-390.
[4] P. Xie and J. J. Beaudoin "Electrically conductive concrete and its application in deicing", ACI Structural Journal, volume: 154, pp.399-417.
[5] Mohd. Rosli Hainina, Md. Maniruzzaman A. Aziza,b*, Zulfiqar Alia, Ramadhansyah Putra Jayaa, Moetaz M. El-Sergany c, Haryati Yaacoba "Steel Slag as A Road Construction Material", Jurnal Teknologi, volume 73, pp. 33–38.

Experimental investigation on waste glass powder as partial replacement of cement in concrete

K.Mohamedmoulana, G.Nirmal Ganesh ,M.S.Vibu, R.Chitradevi
B.E. student in Civil Engineering, Ramco Institute of Technology.
Assistant Professor in Civil Engineering, Ramco Institute of Technology.

***Abstract*— Cement manufacturing industry is one of the carbon dioxide emitting sources besides deforestation and burning of fossil fuels. The global warming is caused by the emission of greenhouse gases, such as CO_2, to the atmosphere .Among the greenhouse gases; CO_2 contributes about 65% of global warming. The global cement industry contributes about 7% of greenhouse gas emission to the earth's atmosphere. In order to address environmental effects associated with cement manufacturing, there is a need to develop alternative binders to make concrete. Efforts have been made in the concrete industry to use waste glass as partial replacement of coarse or fine aggregates and cement. In this study, finely powdered waste glass is used as a partial replacement of cement in concrete and compared it with conventional concrete. This work examines the possibility of using Glass powder as a partial replacement of cement for new concrete. Glass powder was partially replaced as 5%, 10%, 15%, 20%, 25%and 30% and tested for its Compressive, Tensile and Flexural strength up to 28 days of age and were compared with those of conventional concrete. From the results obtained, it was found that 10% replacement of cement with glass powder as optimum;**

Keywords—powdered glass; workability, alkalinity, split tensile, pozzolanic

I. INTRODUCTION

A. Glass

Glass is a widely used manufactured product in our life in various forms such as sheet glass, bottles, glassware etc. Glass is an amorphous material with high silica content(SiO_2) i.e.72% waste glass when grounded to very fine powder (600 micron) reacts with alkali in cement (Pozzolana reaction) &cementations product that help to contribute to the strength development [Veena et al,2014].Since glass is a non-bio-degradable product, ideal for recycling. The physical and chemical properties of glass powder is mentioned in table I, II and III

B. Recycling of Glass

An enormous quantity of waste glass is generated all around the world. The land filling of waste glass is undesirable, since it is a non-biodegradable it is less environmental friendly. Use of recycled materials in construction is the most attractive option because of the large quantity due to widespread sites of construction. Thus there is a need of utilizing waste glass. There is huge potential for using waste glass in the concrete construction sector. Waste glasses when reused in making concrete products can decrease the cost of construction.

II. OBJETIVE OF THE WORK

The main objective of this research is to assess the properties of concrete when the cement was partially replaced by the waste glass powder of size less than 75μm.

a) To find the optimum replacement percentage of waste glass powder as the partial replacement of cement in concrete production.

b) To determine the strength characteristics of concrete like flexural strength, compressive strength and split tensile strength.

III. MATERIALS AND METHOD

C. Cement

In this research, locally available cement which is of the Ordinary Portland Cement type (53 grade) was used conforming to IS 8112 throughout the work.

D. Water

Water used was potable, fresh, colorless, odorless, and tasteless water that is free from organic matter of any type conforming to IS3025.

E. Fine Aggregates

The locally available sand confirming to zone II having the specific gravity 2.48 was used for this study. The coarse aggregate used for this research is 20mm size with specific gravity 2.8. The tests were done as per Indian Standard Specifications IS: 2386.

F. Waste Glass Powder

Waste glass locally available and it has been collected and made in to glass powder. Before adding glass powder in the concrete it has to be powdered to required size. In this experiments glass powder (GLP) having particle size less than 75µm was used.

Fig: 1 Waste Glass Powder

TABLE I
PHYSICAL PROPERTIES OF GLASS POWDER

S.No	Physical Properties of Glass Powder	
1	Specific gravity	2.6
2	Fineness Passing 150µm	99.5
3	Fineness Passing 90µm	98

TABLE II
CHEMICAL PROPERTIES OF GLASS POWDER

S.No	Chemical Properties of Glass Powder	
1	pH	10.25
2	Colour	Grayish white

TABLE III
CHEMICAL COMPOSITION OF GLASS POWDER

S. No	Chemical Properties of Glass Powder	% by mass
1	SiO_2	67.330
2	Al_2O_3	2.620
3	Fe_2O_3	1.420
4	TiO_2	0.157
5	CaO	12.450
6	MgO	2.738
7	Na_2O	12.050
8	K2O	0.638
9	ZrO2	0.019
10	ZnO	0.008
11	SrO	0.016
12	P2O5	0.051
13	NiO	0.014
14	CuO	0.009
15	Cr2O3	0.022

G. Experimental plan

Experiments were conducted on concrete prepared by partial replacement of cement by waste glass powder of particle size 75µm.The cement was replaced by waste glass powder as 5%,10%, 15%, 20%, 25% and 30%. Three specimens were prepared and tested for each replacement of cement.

H. Mix Design

The concrete mix design was prepared as per IS 456:2000 and IS 10262:2009. The grade of concrete used for this study is M35. The mixture was prepared with the cement content of 413.33 kg/m^3 with w/c ratio of 0.45. The mix proportion of materials is 1:1.63:2.94.Chemical admixture was not used here. The partial Replacement of cement by using glass powder is mention in table IV.

TABLE IV
PARTIAL REPLACEMENT OF CEMENT BY USING GLASS POWDER

S. No.	% of Replacement	Cement Kg/m^3	Glass powder Kg/m^3	Fine aggregate Kg/m^3	Coarse aggregate Kg/m^3
1	0%	413.33	-	673.712	1215
2	5%	389.33	20.67	673.712	1215
3	10%	372	41.33	673.712	1215
4	15%	351.33	62	673.712	1215
5	20%	330.66	82.67	673.712	1215
6	25%	310	103.34	673.712	1215
7	30%	289.33	124	673.712	1215

IV DURABILITY TEST

The concrete prepared with various percentage replacement of the cement such as 5%, 10%, 15%, 20%, 25% and 30%was cured under normal condition as per IS recommendation and were tested at 28 days for determining the compressive, tensile and flexural strength and also compared with the test results of conventional concrete

I. Compressive Strength

The specimen cubes of size 150mm x 150mmx 150mm were casted and the compressive strength test was carried out as per IS: 516 – 1959 AT 28th day using compression testing machine. The results obtained from the test have been tabulated in Table V. Compressive Strength of M35 Grade V/S % Of Glass Powder is mentioned in figure 2

TABLE V
COMPRESSIVE STRENGTH OF CONCRETE

Sl.no.	Percentage replacement of cement with glass powder	Number of cubes	Compressive strength N/mm^2
1	0	3	35.52
2	5	3	38.28

3	10	3	40.25
4	15	3	34.62
5	20	3	34.25
6	25	3	32.82
7	30	3	31.26

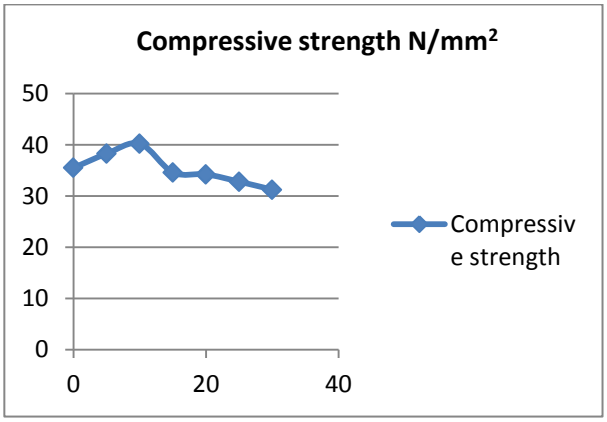

Fig 2: Compressive Strength of M35 Grade V/S % of Glass Powder

J. Tensile Strength

The specimen cylinders of diameter 150mm and height 300mm were casted and the tensile strength test was carried out as per IS: 516 – 1959 AT 28th day using compression testing machine. The results obtained from the test have been tabulated in Table VI. Tensile Strength of M35 Grade V/S % Of Glass Powder is mentioned in figure 3

TABLE VI
TENSILE STRENGTH OF CONCRETE

Sl.no.	Percentage replacement of cement with glass powder	Number of cylinders	Tensile strength N/mm^2
1	0	3	5.99
2	5	3	9.79
3	10	3	10.98
4	15	3	8.08
5	20	3	7.79
6	25	3	7.23
7	30	3	6.59

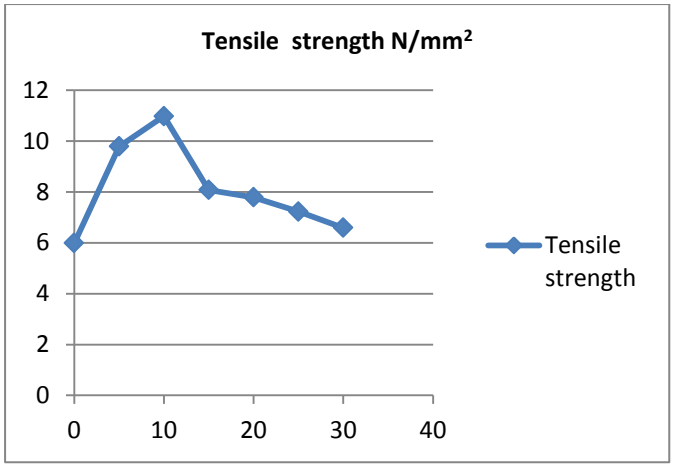

Fig 3: Tensile Strength of M35 Grade V/S % Of Glass Powder

K. Flexural Strength

The prism of size 100mm x 100mm x 500mm were casted and the flexural strength test was carried out as per IS: 516 – 1959 AT 28th day using compression testing machine. The results obtained from the test have been tabulated in Table VII. Flexural Strength of M35 Grade V/S % Of Glass Powder is mentioned in figure 4

TABLE VII
FLEXURAL STRENGTH OF CONCRETE

Sl.no.	Percentage replacement of cement with glass powder	Number of prism	Flexural strength N/mm^2
1	0	3	4.8
2	5	3	5.7
3	10	3	6.2
4	15	3	5.4
5	20	3	5.0
6	25	3	4.3
7	30	3	4.0

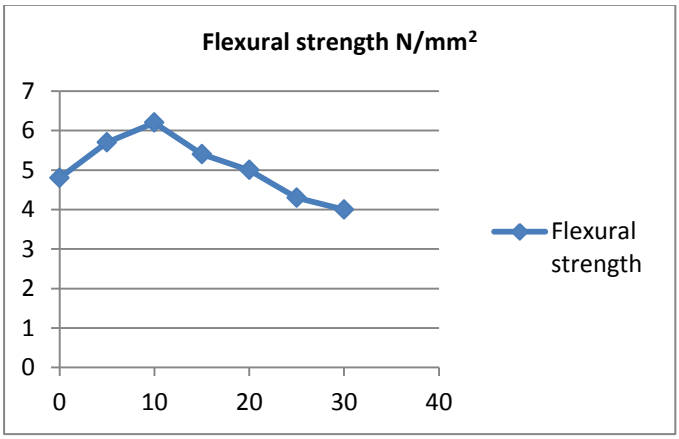

Fig 4: Flexural Strength of M35 Grade V/S % Of Glass Powder

L. Alkalinity test:

After 28 days curing the specimen are taken out from curing tank. Specimens are dried in oven at 105°C for 24 hours. The dry specimens are cooled to room temperature. Dry specimens are broken and separated the mortar from the concrete. Then the mortar is grinded into powder form. The powdered mortar is sieved in 150µ.

10 gm of mortar is taken and it is diluted in 50ml distilled water and completely stirred it. Then the pH meter immerse into the solution and pH value of the solution is noted Fig.4. The general pH value of the solution and the level of inducing corrosion in the concrete was noted and the results are shown in table VIII. Alkalinity test on Glass powder added concrete is mentioned in figure 5

Fig 5: Alkalinity test on Glass powder added concrete

TABLE VIII
THE ALKALINITY TEST VALUES FOR GLASS POWDER ADDED CONCRETE

% Replacement of Glass powder in concrete	pH Value
0	12.3
5	12.1
10	12.7
15	12.4
20	12.6
25	12.5
30	12.67

V. RESULT AND DISCUSSION

- The compressive strength test on both conventional and glass added concrete was performed on standard compression testing machine of 3000kN capacity, as per IS516-1959.cubicalspecimensofsize150mmX150mmX150mm was casted and tested for the compressive strength at the age of 28days . Each of the compressive strength test data corresponds to the mean value of the compressive strength of three cubes. At 28 days the glass powder shows a strength of 40.25N/mm2, strength at 10% cement replacement,
- The Tensile Strength test on both conventional and glass added concrete was performed on standard compression testing machine, as per IS: 516-1959prism specimens of size cylinders of diameter 150mm and height 300mm was casted, glass powder added concrete at the age of 28 days. At 28 days, in 10% replacement the strength has been increased to 10.98N/mm2 .
- The flexural strength test on both conventional and glass added concrete was performed on standard Universal testing machine,asperIS:516-1959prism specimens of size100mmX100mmX500mm was casted glass powder added concrete at the age of 28 days . At 28 days, in 10% replacement the strength has been increased to 6.2N/mm2

- The pH value observed from the alkalinity test showed that the specimen tested found to be more alkaline and hence more resistant towards corrosion.

VI. CONCLUSION

Conventional concrete shows at 28 days compressive strength as 40.25N/mm^2, split tensile strength of 10.98N/mm^2 and flexural strength of 6.2N/mm^2

1. Replacement of glass powder in cement by 10% increases the compressive strength by 13.32%, respectively.

2. Replacement of glass powder in cement by 10% increases the split tensile strength by 83..5% respectively

3. Replacement of glass powder in cement by 10% increases the flexural strength by 29.16% respectively.

4. Glass powder concrete increases the compressive, tensile and flexural strength effectively, when compared with conventional concrete

REFERENCES

[1] Bajad M.N. ,ModheraC.D.and Desai A.k.(2011) "Effect of Glass on Strength of Concrete Subjected to Sulphate Attack" International Journal of Civil Engineering Research and Development (IJCERD), ISSN 2228-9428(Print) ISSN 2248 – 9436(Online), Volume 1, Number 2.

[2] BhatVeena V, Rao N. Bhavanishankar "Influence of Glass Powder On The Properties Of Concrete" International Journal of Engineering Trends andTechnology (IJETT), ISSN: 2319 –8753, Volume- 16, Number-5, October 2016

[3] Chikhalikar S.M. and Tande S.N. (2012) "An Experimental Investigation On Characteristics Properties of Fibre Reinforced Concrete Containing Waste Glass Powder as Pozzolona" 37th Conference on Our World in Concrete and Structures, Singapore, August.

[4] Dali J.S. and Tande S.N. (2012) "Performance of Concrete Containing Mineral Admixtures Subjected to High Temperature" 37th Conference on Our World in Concrete and Structures, Singapore, August.

[5] JangidJitendra B. and Saoji A.C. (2014) "Experimental investigation of waste glass powder as the partial replacement of cement in concrete production" IOSR Journal of Mechanical and Civil Engineering (IOSR-JMCE) e-ISSN: 2278-1684, p-ISSN: 2320-334X [International Conference on Advances in Engineering and Technology –(ICAET-2014)].

[6] KRaghavendra, Virendra Kumara. K. N "Reusing Of Glass Powder And Industrial Waste Materials In Concrete" International Journal of Research in Engineering and Technology, eISSN: 2319-1163 | pISSN: 2321-7308, Volume: 04 Issue: 07 | July-2015)

[7] Khatib J.M., Sohl H.S., H.S. Sohl and Chileshe N. (2012) "Glass Powder Utilisation in Concrete Production" European Journal of Applied Sciences 4 (4): 173-176, 2012 ISSN 2079-2077 © IDOSI Publications.

[8] Kumarappan N.(2013) "Partial Replacement Cement in Concrete Using Waste Glass" International Journal of Engineering Research and Technology (IJERT) Vol. 2 Issue 10, ISSN: 2278-0181.

[9] PatilDhanraj Mohan and Dr.SangleKeshav K (2013) "Experimental Investigation of Waste Glass Powder as Partial Replacement of Cement in Concrete". International Journal of Advanced Technology in Civil Engineering, ISSN: 2231 –5721, Volume-2, Issue-1, 2013.

[10] RajuShilpa, Dr. Kumar P.R. "effect of using glass powder in concrete" International Journal of Innovative Research in Science, Engineering andTechnology, ISSN: 2319 –8753, Volume-3, Issue- 5, July 2014.

[11] SharmaAshutosh and SangamnerkarAshutosh "Glass Powder – A Partial Replacement For Concrete" International Journal of Core Engineering and Management (ISSN 2348 9510, Volume 1, Issue 11, February 2015)

[12] Singh ShekawatBhupendra and Dr. AggrawalVanita "Utlisationof Waste Glass Powder in Concrete – A Literature Review" International Journal of Innovative Research in Science, Engineering andTechnology, ISSN: 2319 –8753, Volume-3, Issue-7, July 2013.

[13] T Bhagyasri, U Prabhavathi and NVidya "Role of Glass Powder in Mechanical Strength of concrete" Proceedings of 39th IRF International Conference, 27th March, 2016, ISBN: 978-93-85973-81-9

RAMCO INSTITUTE OF TECHNOLOGY

(Approved by AICTE, New Delhi and Affiliated to Anna University, Chennai)
North Venganallur Village, Rajapalayam - 626 117, Tamil Nadu.

National Conference on Innovations in Engineering, Science & Technology

CERTIFICATE

24th & 25th March, 2017

This is to certify that ~~Dr./Mr./Ms.~~ Chockalingam. I of Ramco Institute of Technology presented a paper entitled Laboratory study of porosity and strength properties of pervious concrete

National Conference on Innovations in Engineering, Science and Technology - NCIEST, organised by Ramco Institute of Technology, Rajapalayam during 24th & 25th March, 2017.

Organizing Secretary
NCIEST

Dr.R.V.Mahendra Gowda
Principal

LABORATORY STUDY OF POROSITY AND STRENGTH PROPERTIES OF PERVIOUS CONCRETE

K.VISHALINI, T.SHEELARANI, S.YAMINI, T.CHOCKALINGAM
B.E. Student, Ramco Institute of Technology-Rajapalayam.
Assistant professor, Ramco Institute of Technology-Rajapalayam

Abstract: **The main aim of this project is to check the properties of pervious concrete without using any admixtures. Pervious concrete is a special type of concrete with high porosity used for concrete flat work applications that allow water from precipitation and other sources to pass directly through, thereby reducing the runoff from a site and allowing ground water recharge. This paper mainly focus on compressive strength, flexural strength, split tensile strength and porosity of pervious concrete. Consider to investigate the result of compressive strength, "cube" of size 150mm x 150mm x 150mm, for split tensile strength and "cylinder" of size 300mm x150mm are prepared and tested should be carried out at a regular interval of 7 ,14 and 28 days. Different concrete mix proportion such as 1:5, 1:4.5 , 1:3.2 and with size of coarse aggregate such as 12.5mm should be used to check the properties of pervious concrete.**
Keywords: Aggregates, Mix Proportion, Compressive strength, Porosity, Curing.

I. INTRODUCTION

Pervious concrete which is also known as the no-fines, porous ,gap-graded, and permeable concrete and enhance porosity concrete has been found to be a reliable storm water management tool. By definition, pervious concrete is a mixture of coarse aggregate, cement, water, little or no sand (fine aggregate) ,with or without admixtures. It has just enough cementitious paste to coat the coarse aggregate particles while preserving the interconnectivity of the voids.It consists of 15% to 35% voids, allowing for quick drainage.In late 1940s and early 1950s ,the no-fines concrete had been used for the construction of high rise buildings due to its light weight.Pervious concrete can be used in a wide range of applications, although its primary use is in pavements which are in: residential roads, alleys and driveways, low volume pavements, low water crossings, sidewalks and pathways, parking areas, tennis courts, slope stabilisation, sub-base for conventional concrete pavements etc. Pervious concrete has a lower compressive strength and a lower unit weight (approximately 70% of conventional concrete). However, pervious concrete has a greater advantage in many regards.

II.AIM AND OBJECTIVES

The aim of this research work is to study the properties of no-fines concrete with different mix proportion by varying aggregate-cement ratio. The main aim behind this research work was to produce a concrete block without fine aggregate particle which would result in lower density with sufficient strength thereby reducing production cost. The objectives are as follows:

- To investigate the performance characteristics of the pervious concrete such as Compressive strength and flexural strength, split tensile strength.
- To determine the effect of mix type on the engineering properties of thepervious concrete.

III. EXPERIMENTAL STUDY

Number of no-fines concrete mixes was prepared by varying aggregate-cement ratio and water-cement ratio were a/c ratio of 1:5, 4.5:1 & 3.2 :1 , w/c ratio of 0.4 and coarse aggregate of 12.5mm down size has been used in this study. Mixing of concrete was carried in concrete mixer for thorough mixing.

Firstly dry mix of coarse aggregate and cement was carried for about 1.5minutes and later calculated water was added to the dry mix and mixed for about 3minutes in the mixer. After thorough mixing, concrete mixture is then placed over a tray and then concrete was transferred into cube of size 150mm x150mmx150mm ,cylinder of size 300mm x 150mm and beam of size 500mmx100mmx100mm. Concrete specimens were de-molded after 24 hours and is cured by means of gunny bag curing. Then these cube and beam specimens were tested for compressive strength and flexural strength respectively at the age of 7 days, 14days and 28 days.

IV. MATERIALS AND METHODOLOGY

Constituent materials used for the study were cement, coarse aggregate, fine aggregate and water. Properties of the material used in this study are mentioned below.

- Cement: Ordinary Portland Cement of 53 grade was used in this study. The properties of cement are given below.
- Coarse aggregate: Crushed angular aggregate of 12.5mm down size obtained from local quarry was used in this study and its properties are given below.
- Water: Tap water available in concrete laboratory was used for mixing and curing of concrete .

TABLE 1
PHYSICAL PROPERTIES OF MATERIALS

S.No	Properties	Cement	Coarse aggregate
1.	Consistency	36%	-
2.	Initial setting time	35 minutes	-
3.	Final setting time	230 minutes	-
4.	Specific gravity	3.15	2.7
5.	Water absorption	-	0.5%
6.	Soundness	4 mm	-
7.	Fineness modulus	-	7.67%

V. CASTING OF SPECIMEN

Cubes of size 150x150x150mm, cylinder of size 300mm x 150mm and beams of size 500x100x100 mm were casted to carry out the compression, split tensile strength and flexural strength respectively. The fresh mix was placed in the mould . After demoulding they were cured by means of gunny bag curing for 7, 14 and 28 days respectively.

VI. TESTING OF CONCRETE

A. Compression Test

The compression test was studied in the CTM (Compression Testing Machine) 2000KN capacity. The load is applied at a uniform rate till failure.The compression test values are tabulated below:

TABLE 2
COMPRESSIVE STRENGTH OF SAMPLES

Size Of Aggregate	Mix Type	W/C Ratio	Compressive Strength	
			7 Days	28 Days
12.5	5:1	0.4	2.4	4.59
	4.5:1	0.4	3.91	6.12
	3.2:1	0.4	5.91	10.08

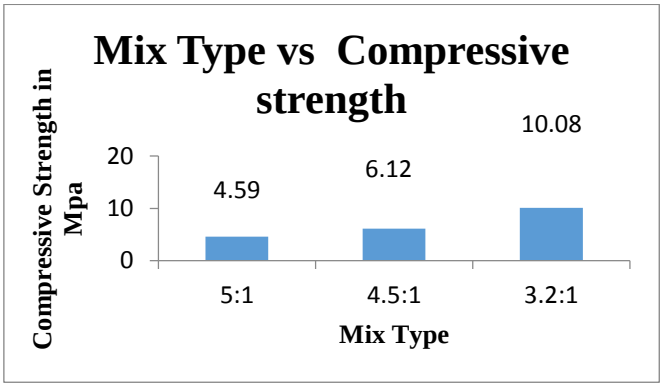

Fig 1.Mix Type vs Compressive Strength

B. Split Tensile Strength

The tensile strength of concrete is one of the basic and important properties. Splitting tensile strength test on concrete cylinder is a method to determine the tensile strength of concrete.The concrete is very weak in tension due to its brittle nature and is not expected to resist the direct tension. The concrete develops cracks when subjected to tensile forces. Thus, it is necessary to determine the tensile strength of concrete to determine the load at which the concrete members may crack.

$$\text{Split tensile strength } (T) = 2P/\pi DL$$

TABLE 3
SPLIT TENSILE STRENGTH OF SAMPLES

Size of Aggregate	Mix Type	W/C Ratio	Split Tensile Strength at the end of 28 Days
12.5	5:1	0.4	0.58
	4.5:1	0.4	0.654
	3.2:1	0.4	0.94

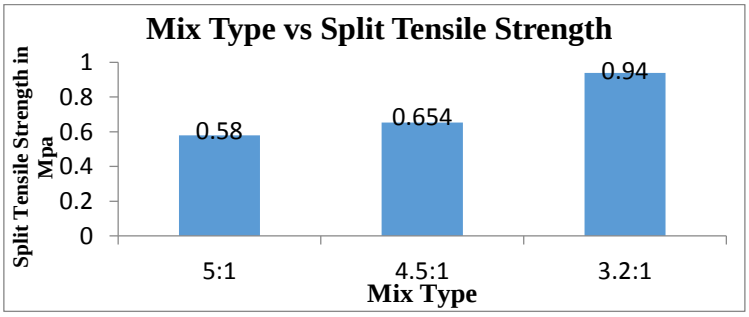

Fig 2.Mix Type vs Split Tensile Strength

C.Porosity

The porosity test was carried out at 28 day of age. The open porosity was measured as the percentage of pore volume or void space within the concrete that can contain water

$$v_r = [1-\frac{w_2-w_1}{\rho_w X\ vol}]\ 100\%$$

TABLE 4
POROSITY OF SAMPLES

Mix Type	Size of Aggregate (mm)	Weight of dry specimen(w_1)	Weight of saturated specimen(w_2)	Porosity in %
5:1	12.5	8.94	11.37	28
4.5:1		8.64	11.13	26.2
3.2:1		9.65	12.26	22.67

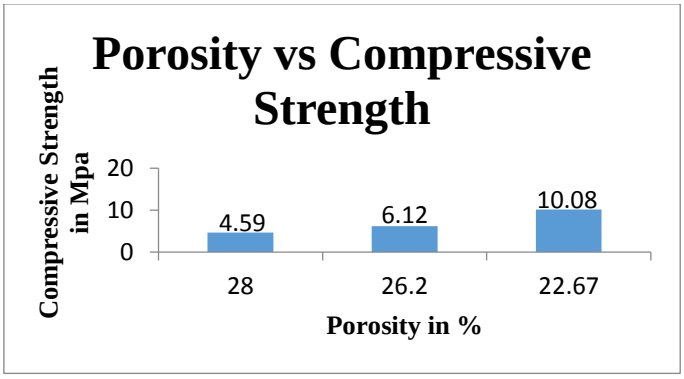

Fig 3.Porosity vs Compressive Strength

VII. RESULT &DISCUSSION

The following conclusion are based on the experimental study on no-fines concrete.

- From this study, for building application aggregate-cement ratio of 3.2 :1 without fines aggregate mix at 0.4 w/c ratio is recommended whose 28 day Compressive Strength was found to be 10.08 N/mm2.
- Strength properties of investigated no-fines concrete are found to be lower than that of conventional concrete but are sufficient enough for structural use such as sidewalks, roadways, tennis courts and low traffic areas.
- A decreases in porosity of the pervious concrete mixtures were found to be increasing in compressive strength. A reduction in compressive strength were observed when the pre sizes in the mixture were higher.

REFERENCES

[1] Cristian Gaedicke, Anthony Torres, Khanh C.T. Huynh, Armando Marines, A method of correlate splitting tensile strength and compressive strength of pervious concrete cylinders and cores, Construction and Building Materials 125 (2016) 271-278.

[2] Abdul Malik, An Experimental Study on properties of No- Fines Concrete, Imperial Journal of Interdisciplinary Research(IJIR) vol-2, Issue-10(2016), ISSN:2454-1362.

[3] P.Chindaprasirt, S.Hatanaka, T. Chareerat, N.Mishima, Y. Yuasa, Cement Paste Characteristics and Porous Concrete Properties, Construction and Building Materials 22 (2008) 894-901.

[4] Omkar Deo, Narayanan Neithalath, Construction and Building Materials 25 (2011) 4181-4189.

[5] Ahmed Ibrahim, Enad Mahmoud , Mohammed Yamin, Varun Chowdary Patibandla, Construction and Building Materials 50 (2014) 524-529.

SECOND NATIONAL CONFERENCE ON
INNOVATIONS IN
ENGINEERING, SCIENCE AND TECHNOLOGY

(NCIEST)
24-25 March 2017

BOOK OF ABSTRACTS

RAMCO INSTITUTE OF TECHNOLOGY
RAJAPALAYAM, TAMIL NADU

SECOND NATIONAL CONFERENCE ON
INNOVATIONS IN
ENGINEERING, SCIENCE AND TECHNOLOGY

(NCIEST)
24-25 March 2017

CHIEF PATRON
Shri. P. R. Ramasubrahmaneya Rajha
Chairman, Ramco Institute of Technology

PATRON
Shri. P. R. Venketrama Raja
Vice-Chairman, Ramco Institute of Technology

ORGANISING HEAD
Dr. R. V. Mahendra Gowda
Principal, Ramco Institute of Technology

RAMCO INSTITUTE OF TECHNOLOGY
RAJAPALAYAM, TAMIL NADU

vulnerabilities, and the presence of malicious threats. Smaller areas, such as vulnerability assessment and penetration testing, are also covered because they are very significant in the security of information. While vulnerability assessment is a necessity, penetration testing is purely an option to the security engineer. This paper aims to propose methods to avoid the cyber crimes.

CAREER DENDROGRAM

R. Venkatesh, N. Rajalakshmi, V. Priyadharshini, N. Siva Sakthi and K. Logeswari
Department of Computer Science and Engineering, Ramco Institute of Technology, Rajapalayam.

A national database of actual requirement of workforce, category-wise for both Government and Industry, the type of educational or skill qualification required, nature of job, eligibility criteria, salary, career development /progression in every field / sector of employment is urgently required. Employment is the greatest challenge these days. The problem is not that we do not have employment opportunities but that we do not get exposed to all the available opportunities. This is because there is no website application that can provide both career guidance and job opportunity to individuals at the same time. So the anticipated outcome of this paper is to build a website application that makes this type of website a reality. In this paper, the proposed scheme is not only efficient in providing career guidance and exposing individuals to all the job opportunities but it also helps in increasing the career development.

RANKING BASED ON SENSITIVITY SCORE AND DATA CLASSIFICATION

J. Sabthami, K. Esakki, K. Kandha Vivek Raj, M. Mathu Kumar and P. Muthu Manickam
Department of Computer Science and Engineering, Ramco Institute of Technology, Rajapalayam.

Large amount of data are used in our day to day life. To improve the security and find the category name of the document, all documents need to be assigned with a sensitivity value that properly indicates their business value and criticality to the organization. The system proposed in this paper aims to semi-automatically measure the sensitivity levels of data assets. The categories of data in the organization and their sensitivity levels are initially determined by Subject Matter Experts (SMEs). From the set of documents of different category, the features (Unique words in the document) are extracted using pre-processing like Bag of Words (BOW) Extraction, Stop Word Removal, POS Tagging, Noun phrase identification. The useful feature from pre-processed document is selected by Term Frequency and Inverse Document Frequency (TF-IDF). The categories of the documents are identified using the classification algorithm like Naïve Bayesian Algorithm (NB). Finally, based on the classification result to the sensitivity of the assets is calculated.

PREDICTING EMPLOYABILITY OF A STUDENT IN R PROGRAMMING

V. Manjula, M. Devi Uma Sankari, A. Periya Nayaki and R. Saranya
Department of Computer Science and Engineering, Kamaraj College of Engineering and Technology, Virudhunagar.

The students employability is a major concern for the institutions offering higher education and a method for early prediction of employability of the students is always desirable to take timely action. The company invests huge time & money (budget) on training the fresh engineering graduates to make them ready for work. Various classification techniques of data

SECOND NATIONAL CONFERENCE ON
INNOVATIONS IN
ENGINEERING, SCIENCE AND TECHNOLOGY

(NCIEST)
24-25 March 2017

BOOK OF ABSTRACTS

RAMCO INSTITUTE OF TECHNOLOGY
RAJAPALAYAM, TAMIL NADU

SECOND NATIONAL CONFERENCE ON
INNOVATIONS IN
ENGINEERING, SCIENCE AND TECHNOLOGY

(NCIEST)
24-25 March 2017

CHIEF PATRON
Shri. P. R. Ramasubrahmaneya Rajha
Chairman, Ramco Institute of Technology

PATRON
Shri. P. R. Venketrama Raja
Vice-Chairman, Ramco Institute of Technology

ORGANISING HEAD
Dr. R. V. Mahendra Gowda
Principal, Ramco Institute of Technology

RAMCO INSTITUTE OF TECHNOLOGY
RAJAPALAYAM, TAMIL NADU

TWO LEVEL QR CODE USING PRIVATE MESSAGE SHARING AND DOCUMENT AUTHENTICATION

P. Vasantha, M. Sangeetha, P. Rajeswari and P. Gopikannan
Department of Computer Science and Engineering, P.S.R Rengasamy College of Engineering for Women, Sivakasi.

The quick response (QR) code was designed for storage information and for high speeds reading application. In this paper we present a new rich QR code that has two storage levels and used for document authentication. The two level QR code means private level and public level. The public level QR code is same as the standard QR code storage level and it is readable by any classical QR code applications. The private level QR code allows us not only to increase the storage capacity of the QR code but also distinguish the original document from a copy. The experimental results show a perfect restoration of private information. It also highlights the possibility of using this new rich QR code for document authentication.

A COMPARATIVE STUDY BETWEEN SUPPORT VECTOR MACHINE AND NAIVE BAYES ALGORITHMS FOR CARDIOTOCOGRAM DATA CLASSIFICATION

D. Jagannathan
Department of Computer Science, Dr. C.V Raman University, Chhatisgarh

Cardiotocography (CTG) is a simultaneous recording of Fetal Heart Rate (FHR) and Uterine Contractions (UC). It is one of the most common diagnostic techniques to evaluate maternal and fetal well being during pregnancy and before delivery. By observing the Cardiotocography trace patterns doctors can understand the state of the fetus. There are several signal processing and computer programming based techniques for interpreting a typical Cardiotocography data. Even few decades after the introduction of Cardiotocography into clinical practice, the predictive capacity of these methods remains controversial and still inaccurate. In this paper, a model based CTG data classification system using a supervised SVM and Naive Bayes is implemented which can classify the CTG data based on its training data. According to the arrived results, the performance of the supervised machine learning based classification approach provided significant performance. In this paper, we have used Accuracy, Specificity, NPV, Precision, Recall and ROC are used as the metric to evaluate the performance. It was found that, the SVM based classifier was capable of identifying Normal, Suspicious and Pathologic condition, from the nature of CTG data with very good accuracy.

SECURE DE-DUPLICATION IN HYBRID CLOUD

R. Venkatesh, L. Ramesh, M. Siva, S. Manikandan and C. Manojkumar
Department of Computer Science and Engineering, Ramco Institute of Technology, Rajapalayam.

Data de-duplication is a data compression technique for eliminating duplicate copies of repeating data (file formats) and has been widely used in cloud storage to reduce the amount of storage space and efficient access. To protect the privacy of sensitive data while supporting de-duplication, the convergent encryption technique has been used to encrypt the data before outsourcing. To maintain data security, formally address the problem of certified data de-duplication. Unlike other traditional de-duplication systems, the differential privileges of users are further considered in duplicate check besides in data. We also present several new de-duplication structures supporting authorized duplicate check in hybrid cloud architecture.

KALASALINGAM
ACADEMY OF RESEARCH & EDUCATION
(DEEMED TO BE UNIVERSITY)

Under sec. 3 of UGC Act 1956. Accredited by NAAC with "A" Grade

Anand Nagar, Krishnankoil - 626126. Srivilliputtur (Via), Virudhunagar (Dt), Tamil Nadu | info@kalasalingam.ac.in | www.kalasalingam.ac.in

School of Environmental and Construction Technology

DEPARTMENT OF CIVIL ENGINEERING

ASCE
AMERICAN SOCIETY OF CIVIL ENGINEERS

Certificate of Participation

This is to certify that Dr. / Mr. / Ms. C. SUBHA

of RAMCO INSTITUTE OF TECHNOLOGY has participated and presented a paper entitiled as POWER PRODUCTION FROM WASTEWATER BY MICROBIAL FUELCELL

in one day National Conference on "SUSTAINABILITY IN CONSTRUCTION - NACSIC 2018" organized by the Department of Civil Engineering, Kalasalingam Academy of Research and Education, Krishnankoil dated 13th April 2018.

N. [illegible]
Organizing Secretary

C. [illegible]
Organizing Chair

Dean SECT

POWER PRODUCTION FROM WASTEWATER BY MICROBIAL FUEL CELL

[1] M.Chinthamani, [2]G.Daniel, [3]M.Ganapathisubramanian, [4]C.Subha
[1]U.G student, [4]Assistant professor
Department of Civil Engineering
Ramco Institute of Technology, Rajapalayam, Tamil Nadu
civilchinthamani@gmail.com, williamdanielgp@gmail.com, ganapathisubramanian090@gmail.com

Abstract **- Microbial fuel cell (MFC) is a new technology that not only generates energy but treats wastewater as well. A air-cathode MFC was operated under laboratory conditions. Wastewater samples from chemical industries were collected and treated for 312 h in MFC. The treatment efficiency for COD removal in MFC was in range of 85–90% at hydraulic retention time (HRT) of 310 h and had significant impact on wastewater treatment as well. The maximum voltage of 1130 mV was generated .The minimum voltage was produced in wastewater which was 139 mV. There was positive significant co-relation between COD concentration and generated voltage. Further research should be focused on the organic contents of wastewater and various ionic species affecting voltage generation in MFC**.

I. INTRODUCTION

Microbial fuel cells (MFCs) are a promising technology for sustainable wastewater treatment. In an MFC, biochemical reactions are carried out by electro genic bacteria in an anaerobic anode chamber, generating electrons and protons through the degradation of the organic substrates embedded in wastewater; concurrently, electrochemical reactions occur in the aerobic cathode chamber, whereby electrons and protons are accepted through an oxygen reduction reaction (ORR). Anaerobic treatment of wastewaters is substantially less energy intensive than aerobic treatment, however it takes longer to accomplish due to the inherently slow growth process of anaerobic microorganisms. Because of this, there has been little interest in applying anaerobic processes to dilute wastewaters (e.g., domestic wastewater).

MFC systems operate on the fundamental mechanisms of microbiology (e.g. biofilm growth on electrode), biochemistry (e.g. COD removal inside biofilms), and electrochemistry (e.g. electron generation and transfer on anodes and cathodes), which make it truly challenging to achieve effective power generation simultaneously with effective wastewater treatment.

Microbial fuel cell is found to be an alternative technology for direct power generation. It is clean power generation technique which does not generate secondary e pollutants. Power generation of an MFC is affected by many factors including microbe type, ionic strength, pH, temperature, and reactor configuration. These operating parameters can be regulated to decrease the polarizations in order to enhance the performance of an MFC. Use of wastewater in the anode chamber reduces the cost of treatment and reduces the problem of sludge deposal. Other than power generation application of MFC it has many other application such production of bio hydrogen from MFC and used as biosensor offset the large power demand from aerobic treatment, it is important that cost-effective processes be developed that can convert the contaminant loads in domestic wastewater to useable forms of energy. Over the past several years, a great amount of effort has been invested in testing MFCs at bench-scale, successfully converting the organic substrates inherent in the wastewater treatment to power.

II. MATERIALS AND METHODS

1.SURGICAL WASTEWATER

Surgical wastewater from chemical industry is one of the most difficult industrial wastewaters to treat since Surgical wastewater are degradation organic molecules. It adversely affects environment due to its immense colour and toxicities.

Chemical industry generates high-volumes of wastewater containing various chemical used is bleaching and Drycleaning. Since, effluents of Bleaching units are highly polluted and dangerous, they have to be treated with right technologies to nullify its harmful effect on the environment. Since characteristics of effluents varies with the type of raw materials used in the Bleaching process, adopting right wastewater treatment technology is a challenge.

2.ELECTRODE

Zhang et al., (2009) described the electrode materials in MFC have some general characters and also its self-characteristic. For all the types of electrodes, their base materials must generally of good conduction, good chemical stability, high mechanical strength, and low cost. Carbon materials and non-corrosive metals, which can basically meet the general requirements above, are currently the most-widely used base materials. In addition, there are some specific requirements for each group of electrodes. Bio-electrodes function not only as a conductor, but also as a carrier of bacteria, and some special surface characteristics of electrode materials, such as high surface roughness, good biocompatibility, and efficient electron transfer between bacteria and electrode surface, are essential for high bio-catalytic activity. In order to improve bacterial adhesion and electron transfer, electrode surface modification has become a new topic of interest in the research field of MFCs. The electrode material for air–cathodes with a catalyst is composed of a base material, a catalyst, a binder, and a waterproof coating. Material characteristics and functions are specific for each part. The base material generally only serves as supporting material and current collector. High conductivity and mechanical strength are critical for it. But there is no special requirement for bacteria adhesion. A catalyst is important for air–cathodes, but not absolutely necessary.

If necessary, the catalyst is immobilized on the substrate surface with a binder, and a hydrophobic coating is regularly added onto the cathode to avoid water loss. To reduce the cost of air–cathodes, several highly specific materials, such as activated carbon, that do not require a catalyst have been developed and reported. For aqueous air–cathode, only base material, catalyst and binder are needed.

Another great challenge in making MFCs a high performance and scalable technology is electrode configuration. Commonly used electrodes can be classified according to their configurations: the plane electrode and the three-dimensional electrode. A good configuration for bio-electrodes must provide a large surface area for bacterial adhesion and ensure efficient current collection. Plane electrode is more common for air–electrode. When the air–electrode contains a chemical catalyst, an effective configuration is necessary to ensure the oxygen reduction into a three-phase reaction involving the catalyst, the air, and water.

3.MICROBIAL FUEL CELL

B.E.Logan, (2008) clarified that microbial fuel cells (MFCs) are devices that use bacteria as a catalyst for the conversion of

organic matter into electricity. An MFC typically consists of anode (anaerobic) and cathode (aerobic or aerated). In MFCs, microbes on the anode surface oxidize substrates (organic matter) and generate electrons and protons. These electrons are transferred to the anode and pass towards the cathode through an external circuit to generate electricity. The generated protons diffuse through the solution towards the cathode.

S.No	Parameter	Test results
1	pH	10.58 ± 0.2
2	Total solids	8130 ± 150
3	Total dissolved soilds	3135 ± 100
4	Total susbended soilds	681 ± 20
5	Chemical oxygen demend	4000 ± 50
6	Total alkalinity	1200 ± 50

Mfc Operation

Several disadvantages of batch operation for the purpose of power generation in MFCs. The nutrients available in the working volume become depleted in batch mode. The substrate depletion in batch MFCs results in a decrease in bioelectricity production with respect to time. This problem is solved in continuous MFCs that are more suitable than batch systems for practical applications. The advantages of continuous culture are that the cell density, substrate and product concentrations remain constant while the culture is diluted with fresh media. The fresh media is sterilized or filtered and there are no cells in the inlet stream. The batch operation was switched over to continuous operation mode by constantly injection of the prepared substrate to the anode compartment. The other factors were kept constant based on optimum conditions determined from the batch operation.. The system was operated for 314 h with the fixed HRT. Produced power and current were recorded after 12, 24, 36 up to 302 h. The obtained data had no significant improvement in power and cell condition for any time after 120 h. Production of bioelectricity reached to steady-state condition after 4 HRT.

Electrochemical measurment

Chong yang Gao et al., (2014) reported that the Current (I) was calculated from I = U/R, and cell power output (P) was calculated from P = U * I. The power density (P_V) was calculated using the equation: P_V (W m^{-3}) = P/V, where P is cell power output, V is the volume of the anodic chamber.

4.Result and discussion

COD removal

The Surgical cotton wastewater is often complex with high COD concentration. COD removals at the MFC were measured at different HRTs. 120 h of HRT, 65% COD was removed at the MFC .The Surgical cotton wastewater was treated anaerobically in the anode chamber where the anaerobic bacteria degraded biodegradable organic– inorganic materials and the high COD removal was achieved because the cathode process acted as an additional aerobic polishing step following the standard anodic treatment. MFC anodes do not have ability to thoroughly remove slowly biodegradable COD.

EFFECT OF COD CONSUMPTION RATE ON POWER GENERATION

The power generation in the Air cathode MFC was analysed by varying different

HRT from 24 days to 7 days. Surgical cotton wastewater COD was in the range of 4000 ± 300 mg L^{-1}., voltage of 1130mV was achieved in MFC. At the starting HRT of 24 days, voltage was at 139mV.The highest voltage of 1130mV was achieved at 6 days HRT. The Surgical cotton wastewater is often complex with high COD concentration. COD removals at the MFC were measured at different HRTs. The Surgical cotton wastewater was primarily treated anaerobically in the anode chamber where the anaerobic bacteria degraded biodegradable organic– inorganic materials and the high COD removal was achieved because the cathode process acted as an additional aerobic polishing step following the standard anodic treatment. When a higher output power density is produced, more energy is derived from the respiratory chain. This compels microorganisms to consume more carbon sources to maintain their rate of metabolism.

Figure 4.3 shows the maximum COD removal of 71% obtained at 12 days HRT. At the time of 24 days HRT, organic loading was sufficient therefore the microorganisms consumed enough carbon as their food. So at 24 days HRT the COD removal was high as 66%. Overall COD removal decreased from 66% to 30% with an increase in Surgical cotton concentration and organic loading. In this experiment increase in the HRT from 24d to 7 d enhanced the performance of total COD removal from 66% to 30%. At the time of 7 days, organic loading was high compare to 24 days HRT, so the removal decreased to 30%.

COULOMBIC EFFICIENCY

The Coulombic efficiency or charge acceptance is a measure of how much usable energy is available during discharging compared with the energy used to charge the cell. The coulombic efficiency was increased due to the presence of electro genic bacteria, but it may decrease due to high saturation condition in anode surface. At the time of 24 days HRT the coulombic efficiency is low, because at the time production of power density is low. Figure 4.6 shows the coulombic efficiency at different HRT with power density. Due to the effective role of electro genic bacteria at the anode chamber. The power generation was maximum at the HRT of 6 days with the coulombic efficiency of 45%. The minimum efficiency obtained at the HRT of 7 d was found to be 14 %.

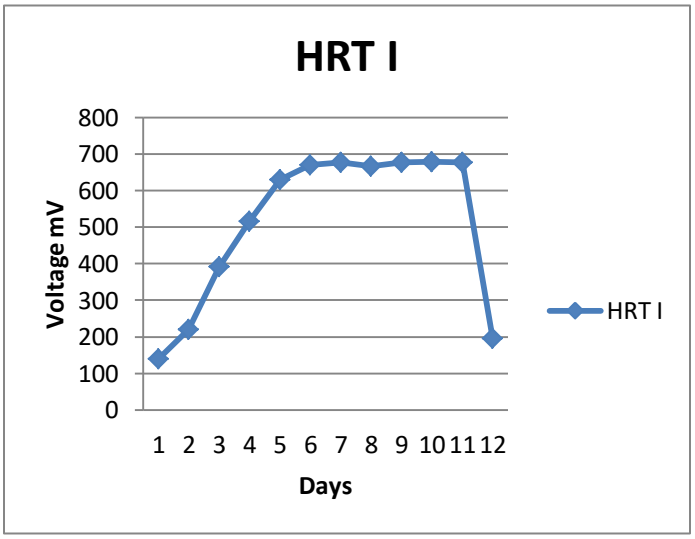

Organic loading rate for 1000mg/l of cod

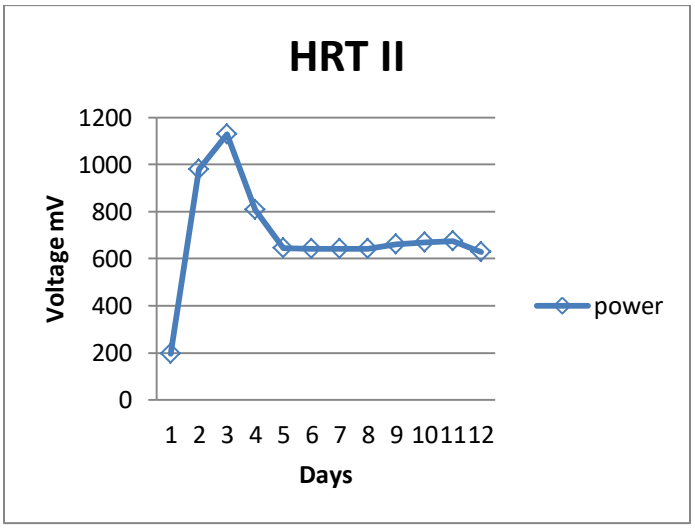

Organic loading rate for2000mg/l of cod

CONCULSION

The present study explains that air cathode MFC operated in continuous mode with surgical cotton industry waste water proved to be efficient for generating electricity.the continuous air cathode MFC achived maximum efficiency at OLR 1000gCOD/l where the highest power density of 34.63 Mv/cm^2 and maximum cod removal of 66% was observed . Hence it is concluded that MFC could be feasible obtion as primary treatment to treat and generate electricity from surgical cotton industry wastewater.

REFERENCES

1. APHA/AWWA/WEF, 2005. In: Eaton, A.D., Clescri, L.S., Rice, E.W., Greenberg, A.E.(Eds.), Standard Methods for the Examination of water and wastewater, Twenty-first ed. DC. American Public Health Association/American water works Association/ Water Environment Federation, Washington.
2. B.E. Logan, K. Rabaey, Conversion of waste into bioelectricity and chemicals by using microbial electrochemical technologies,science.Vol.337 (2012).,pp 686-690.
3. Cheng, S., Liu H., Logan, B.E.,2006. Power densities using different cathode catalysts (Pt and CoTMPP) and polymer binders (Nafion and PTFE) in single chamber microbial fuel cell. Environ. Sci. Technol. Vol.40., pp.364-369.
4. C. Jayashree, S. Singh, P. Arulazhagan, S. Adish Kumar, J. Rajesh Banu, Electricity generation from retting wastewater consisting of recalcitrant compounds using continuous upflow microbial fuel cell Electricity production from retting wastewater, Biotechnol, Bioprocess Eng.,Vol.20 (2015)., pp 753-759.
5. Chaundhury, S.K., Lovely, D.R., 2005. Electricity generation by direct oxidation of Glucose in mediator-less microbial fuel cell. Nature Biotechnology, Vol 21. Pp.1229-1232.
6. C. Jayashree, K. Tamilarasan, M. Rajkumar, P. Arulazhagan, K.N. Yogalakshmi, M. Srikanth, J. Rajesh Banu., Treatment of Seafood processing wastewater using Up-flow microbial fuel cell for power generation and Identification of bacterial community in anodic bio-film, Environ. Management, Vol.180(2016)., pp.351-358.
7. H.j. Kim, H.S. Park, M.S. Hyun, I.S. Chang, M. Kim, B.H. Kim, A mediator-less microbial cell using a metal reducing bacterium, Shewella putrefactions, Enzyme Microb. Techno., Vol.30 (2002)., pp. 145-152.
8. In Seop, C., Hyunsoo, m., Jae kyung, J., Byung Hong, K., 2005. Improvement of microbial fuel cell performance as a BOD sensor using respiratory inhibitors. Bioses. Bioelectron. Vol.20 ., pp. 1856-1859.
9. Kumlanghan, A., Liu, J., Thavarungkul, p., Kanatharana, P., Mattiasson, B., 2007. Microbial fuel cell based biosensor for fat analysis of biodegradable organic matter. Biosens. Bioelectron. 22(12), 2939-2944.

10. K.Tamilarasan, J.Rajesh Banu, C.Jayashree,K.N.Yogalakshmi, K. Gokulakrishnan 2017. Effect of organic loading rate on electricity generating potential of up-flow anaerobic microbial fuel cell treating surgical cotton industry wastewater. Environ. Chemical engg. Vol 5., pp. 1021-1026.
11. Logan, B.E., Hamelers, B., Rozendal, R.A., Schrorder, U., Keller, j., Freguia, S., Aelterman, P., Verstraete, W., Rabaey, K., 2006a. Microbial fuel cell: Methodology and technology. Environ. Sci. technology., Vol. 40,pp 5181-5192.
12. Liu, H., Ramnarayan, R., Logan B.E., 2004. Production of electricity during wastewater treatment using single chamber microbial fuel cell. Environ. Sci. Technology., Vol 38.,pp. 2281-2285.
13. Moon H, Chang IS, Kim BH.(2006), 'Continuous electricity production from artificial wastewater using a mediator-less microbial fuel cell. Bioresource Technol Vol.97, pp.621–627.
14. Min B, Kim JR, Oh SE, Regan JM, Logan BE.(2005), 'Electricity generation from swine wastewater using microbial fuel cells.' Water Res., Vol.39, pp.4961–4968.
15. Oh, S.E., Logan, B.E., 2005. Hydrogen and electricity production from a food processing wastewater using fermentation microbial fuel cell technologies. Water resource. Vol.39., pp. 4693- 4692.
16. VenkataMohan S.,Veer Raghavalu., Srikanth S., and Sarma.P.N., (2007), 'Bioelectricity production by mediator-less microbial fuel cell under acidophilic condition using wastewater as substrate : Influence of substrate loading rate', Current Science. Vol.92, pp. 12-25.

17.Zhuwei du, Haoran Li, TingyueGu (2011) 'A state of the review on microbial fuel cells: A promising technology for wastewater treatment and bioenergy' biotechnology advances, Vol 25, pp. 464-482

KALASALINGAM
ACADEMY OF RESEARCH & EDUCATION
(DEEMED TO BE UNIVERSITY)

Under sec. 3 of UGC Act 1956. Accredited by NAAC with "A" Grade

Anand Nagar, Krishnankoil - 626126. Srivilliputtur (Via), Virudhunagar (Dt), Tamil Nadu | info@kalasalingam.ac.in | www.kalasalingam.ac.in

School of Environmental and Construction Technology

DEPARTMENT OF CIVIL ENGINEERING

ASCE
AMERICAN SOCIETY OF CIVIL ENGINEERS

Certificate of Participation

This is to certify that Dr. / Mr. / Ms. R. MURUGANANTHAM

of RAMCO INSTITUTE OF TECHNOLOGY has participated

and presented a paper entitiled as EFFECT OF HARIKATI AS A RETARDING A WATER REDUCING ADMIXTURE FOR CONCRETE

in one day National Conference on "SUSTAINABILITY IN CONSTRUCTION - NACSIC 2018" organized by the Department of Civil Engineering, Kalasalingam Academy of Research and Education, Krishnankoil dated 13th April 2018.

Organizing Secretary | Organizing Chair | Dean SECT

EFFECT OF HARITAKI AS A RETARDING AND WATER REDUCING ADMIXTURE FOR CONCRETE

A.A.MUTHU JANANI*, M.SARANYA*, R.MURUGANANTHAM**

B.E – Department of Civil Engineering, Ramco Institute of Technology, Rajapalayam.

Assistant Professor, Ramco Institute of Technology, Rajapalayam.

jananianand96@gmail.com, sarancivil1997@gmail.com, murugananthamr@ritrjpm.ac.in

Abstract - Concrete is one of the most important composite materials in construction industry. This paper deals with the study of concrete in hot weather condition and aims to increase the performance of concrete and its workability. To improve the workability and to retard the setting time of concrete, the paper suggests using an admixture called Haritaki which is eco-friendly to environment. The thesis also deals with the properties and reaction of another retarding agent called sulphonated naphthalene formaldehyde (CPLAST 144) and a comparison study is carried out. Setting times of cement pastes prepared with Haritaki at different dosages were determined and it was found that Haritaki addition causes considerable increase in both initial and final setting times. Split tensile and compressive strength were determined on hardened concretes at both early ages (7 days and 28 days). Further the respective tests are proposed to find the optimum content of retarders on the basis of Setting time, Compressive strength and Split tensile test.

1. INTRODUCTION

Concrete is a material composed of coarse granular material embedded in a hard matrix of material that fills the space among the aggregate particles and glues them together. Globally, the ready-mix concrete industry, the largest segment of the concrete market, is projected to exceed $150 billion in revenue by 2017. A large number of retarding admixture products are available in the market. Overdosing of retarders may result in decrease in strength of concrete or failure of structures. Most of the constructions require pumpable and workable concrete. Thus, chemical admixtures are required to be added to the fresh concrete mix. To increase the setting time, achieve high workability in fresh state and desired compressive strength in hardened state of normal concretes, Sulphonated naphthalene formaldehyde and Haritaki based admixture has been incorporated. The setting behavior varies significantly from one brand of cement to another. Hence, it is required to study the compatibility between the retarder and Haritaki replaced concrete before a suitable combination is used, especially when increase in time, high workability, slump retention and required strength are to be obtained.

2. PROPERTIES OF MATERIALS

2.1 *Haritaki*

Haritaki (*Terminalia chebula*) possesses a great therapeutic value and is widely distributed in India. It is an admixture used in medicinary plant. This plant leaves powder, which can be replaced partially with cement. Detail Experimental investigation is done in the laboratory to determine the optimum usage of these herbal products in Concrete, Reinforced concrete structures as well as in prestressed concrete.

Table 2.1 Properties of Haritaki

pH Value	3.5 to 4.1
Cost of Haritaki	50 per kg

2.2 *Sulphonated Napthalene Formaldehyde*

Sulphonated Napthalene formaldehyde is a major ingredient of super plasticizers. It takes role in neutralizing the surface charges on the cement particles and enhancing water tied up in the cement agglomerations and thereafter reducing the viscosity of the paste and concrete. It promotes dispersing of cement particles and reduce water requirements without affecting the workability, thus resulting high strength concrete and lower permeability.

Table 2.2 Properties of Sulphonated Napthalene Formaldehyde

pH value	7.0 to 9.0
Appearance	Brownish colour
Specific gravity	1.19 to 1.24
Cost	190 per litre

2.3 *M-Sand*

Manufactured sand (M-Sand) is a substitute of river sand for concrete construction. It is used as a partial replacement of fine aggregate. It is produced from hard granite stone by crushing. The crushed sand is of cubical shape with grounded edges, washed and graded.

Table 2.3 Properties of M-sand

Bulk density	1.75kg/m³
Specific gravity	2.73 to 4.66
Slump value	55 mm
Sieve size	150 micron to 4.5 mm
Water absorption	2.2

3. MATERIAL TESTING

3.1 S*pecific Gravity*

Specific gravity is the ratio of the density of a substance to the density of a reference substance; equivalently, it is the ratio of the mass of a substance to the mass of a reference substance for the same given volume.

$$G = \frac{M_2 - M_1}{(M_2 - M_1) - (M_3 - M_4)}$$

1.	Fine Aggregate	**2.94**
2.	Coarse Aggregate	**2.85**
3.	Cement	**2.9**

3.2 Water Absorption

Water absorption is the amount of water taken up by the fine or coarse aggregate to achieve the desired consistency or optimal end result.

Water absorption = [(B – A)/B] x 100%

Water Absorption of Coarse Aggregate = **0.5%**

3.3 Particle Size Distribution

Particle size distribution also known as gradation refers to the proportions by dry mass

of a soil distributed over specified particle size ranges. Gradation is used to classify soils for engineering and agricultural purposes.

Fineness Modulus = **8.14**

4. MIX DESIGN

In this study, mix of concrete grade (M_{30}) were produced with partial replacement of Haritaki with water (5%,10%,15%,20% and 25%) The mix design process adopted was the Indian Standard Method. However, a certain amount of water was replaced with Haritaki by its weight of cement. Mix design for M_{30} as per IS 10262:2009 and IS 456:2000 is **1 : 1.58 : 2.71**

5. REPLACEMENT PROPORTIONS OF SETTING TIME TEST

5.1 Haritaki

Replacement (%)	5	10	15	20	25
Initial Setting Time (mins)	30	45	55	75	95

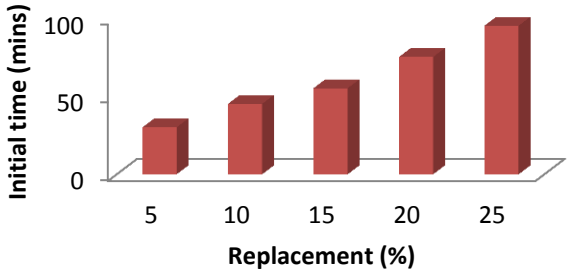

Fig 5.1 Replcement vs Initial Setting time of Haritkai replaced concrete

5.2 Sulphonated Napthalene Formaldehyde

Replacement (%)	0.4	0.6	0.8	1.0	1.2
Initial Setting Time (mins)	45	50	50	80	95

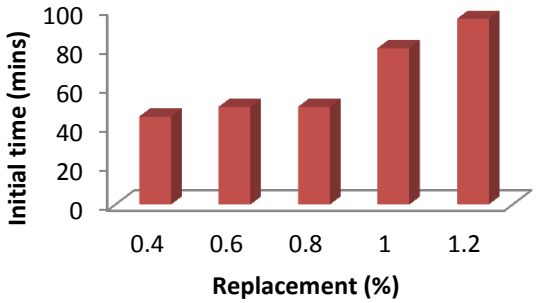

Fig 5.2 Replacement vs Initial Setting Time of retarder replaced concrete

6. REPLACEMENT PROPORTIONS OF COMPRESSION TEST

6.1 Haritaki

Replacement (%)	*Average Compressive Strength of 3 cubes (N/mm²)*	
	7 days	*28 days*
5	20.49	33.93
10	21.6	34.9
15	20.2	31.8
20	19.1	31.3

6.2 Sulphonated Napthalene Formaldehyde

Replacement (%)	*Average Compressive Strength of 3 cubes (N/mm²)*	
	7 days	*28 days*
0.8	23.55	34.48

7. REPLACEMENT PROPORTIONS OF SPLIT TENSILE STRENGTH TEST

7.1 Haritaki

Replacement (%)	*Average Split Tensile Strength of 3 cylinders (N/mm²)*	
	7 days	*28 days*
5	2.56	4.12
10	2.76	4.26
15	2.23	3.84
20	2.14	3.58

7.2 Sulphonated Napthalene Formaldehyde

Replacement (%)	*Average Split Tensile Strength of 3 cylinders (N/mm²)*	
	7 days	*28 days*
0.8	2.86	4.15

8. EXPERIMENTAL INVESTIGATION

8.1 Compressive strength

The cube specimens were tested in the compression testing machine with the capacity of 200 tonnes. The load is applied constantly at increased rate until the specimen is broken. The 28 days strength of cubes with various proportions is compared below. Cube of size 150 mm x 150 mm x 150 mm concrete specimens were casting**.**

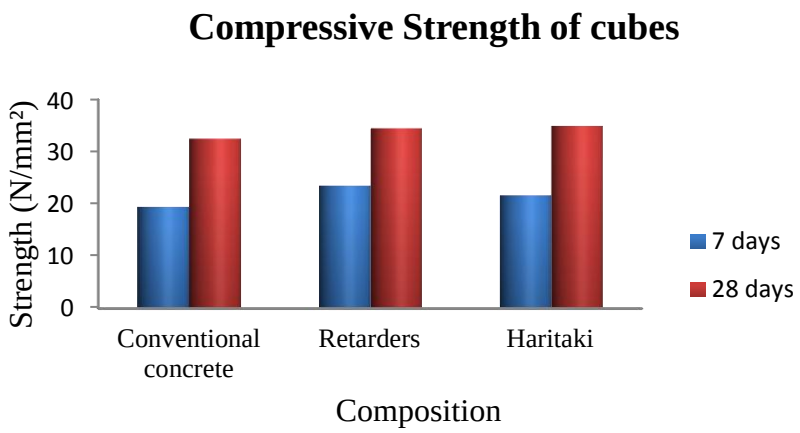

Fig 8.1 Comparison graph for compressive strength of cubes

8.2 Spilt tensile strength

Split tensile strength of concrete is usually found by testing plain concrete cylinders. Cylinders of size 150 mm x 300 mm were casting using M_{30} grade concrete.

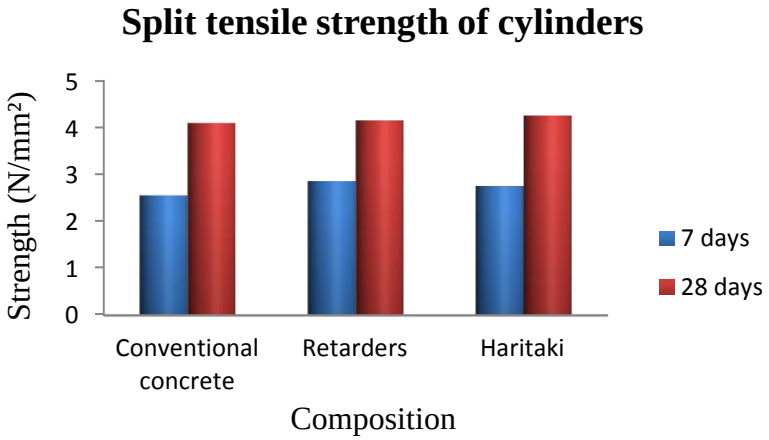

Fig 8.2 Comparison graph for split tensile strength of cylinders

8.3 Setting time

Within the hardening time of cement, it continues to react with water and slowly starts losing its plasticity. This complete cycle is called Setting time of cement. Retarders and Haritaki shows increase in setting time.

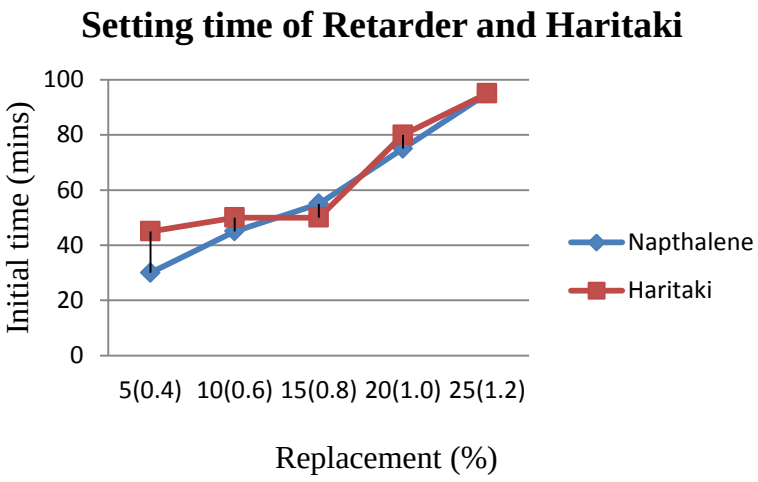

Fig 8.3 Comparison graph for setting time

9. DISCUSSION

- M_{30} concrete mix was designed.
- Consistency and setting time for various replacement of retarders and Haritaki based on mass of cement was determined.
- Compressive strength and split tensile strength was checked for the M_{30} concrete, retarders and Haritaki replaced concrete cubes which was found to be satisfiable.
- Comparison graphs were drawn on the setting time study between the various replaced concrete cubes.
- From the comparison it was inferred that the setting time of concrete gets increasing but 10% replaced concrete has a high strength capacity.
- Hence 10% - 15% replacement of concrete is found to be the Optimum content from all the trial methods carried out.

10. CONCLUSION

The retarder was used as an admixture in concrete at hot weather condition to extend the initial setting time of concrete. The properties of specifications are studied carefully to manufacture the concrete with retarding admixtures. The initial setting time was extended and the improvement in compressive strength was also achieved at an appropriate level of using the retarders. The setting time of Haritaki is gradually increasing for each 5% replacement, but 10% is suitable for achieving the required high strength of concrete. Hence the optimum dosage of Haritaki in replacement with water is found to be 10% - 15%. It is evident that the over dosage of admixture results in the decrease in strength of concrete.

11. REFERENCES

[1] IS 4031:1988(Part V) "***Determination of initial and final setting time of cement***"

[2] IS 2386:1963(Part IV) "***Determination of mechanical properties of concrete"***

[3] IS 10086:1982 "**Determination of the size of cube in concrete**"

[4] IS 10262:2009 and IS 456:2000 **"Concrete mix design"**

[5] Amanmyrat Jumadurdiyev, M. HulusiOzkul, Ali R. Saglam, NazmiyeParlak **"The utilization of beet molasses as a retarding and water-reducing admixture for concrete"** *Science direct - Cement and Concrete Research 35 (2005) 874-882.*

[6] R.Greesan and P.Prathap, R.Vijayakumar *"***Manufacturing of Concrete with Retarders**" *International journal of scientific and Engineering Research, Volume 5,Issue 4,April 2014 1636 ISSN 2229-5518.*

[7] Yadav Babita, Keshi peddi Sandhya Rani, Bhat Sulochana, Singh Mamta "**A Perspective study of Haritaki"** *IJRAP 2011, 2 (5) 1466- 1470.*

[8] Janardhana Maganti and V.Siva Prasada Raju "**Compatibility of Sulphonated Napthalene Formaldehyde and Lignosulphates based superplasticizer with Portland slag cement"***Third International Conference on Sustainable Construction Materials and Technologies.*

[9] M. Jirásek , P. Havlásek "**Accurate approximations of concrete creep compliance functions based on continuous retardation spectra"***Computers and Structures 135(2014)155 – 168*

[10] N.Bhanumathidas and N.Kalidas "**Dual role of gypsum: Set retarder and strength accelerator"**

[11] W.P.S Dias and C.G.Jayathunga **"Effects of large retarder overdosage on concrete strength development"***ENGINEER Vol.XXXXIII,No.3,2010.*

[12] Yan-Rong Zhang, Xiang-Ming Kong , Zhen-Bao Lu, Zi-Chen Lu, "**Effects of the charge characteristics of polycarboxylate superplasticizers on the adsorption and the retardation in cement"***Cement and Concrete Research 67(2015)184 - 196*

[13] **Properties of Sulphonated Napthalene Formaldehyde,** *Avh pvt.ltd*

[14] **Sulphonated Napthalene Formaldehyde Liquid,** *Meha chemicals.*

KALASALINGAM
ACADEMY OF RESEARCH & EDUCATION
(DEEMED TO BE UNIVERSITY)

Under sec. 3 of UGC Act 1956. Accredited by NAAC with "A" Grade

Anand Nagar, Krishnankoil - 626126. Srivilliputtur (Via), Virudhunagar (Dt), Tamil Nadu | info@kalasalingam.ac.in | www.kalasalingam.ac.in

School of Environmental and Construction Technology

DEPARTMENT OF CIVIL ENGINEERING

ASCE
AMERICAN SOCIETY OF CIVIL ENGINEERS

Certificate of Participation

This is to certify that Dr. / Mr. / ~~Ms~~. T. CHOCKALINGAM

of RAMCO INSTITUTE OF TECHNOLOGY has participated

and presented a paper entitiled as SHAPE AND SIZE EFFECT ON THE MECHANICAL PROPERTIES OF PERVIOUS CONCRETE

in one day National Conference on "SUSTAINABILITY IN CONSTRUCTION - NACSIC 2018" organized by the Department of Civil Engineering, Kalasalingam Academy of Research and Education, Krishnankoil dated 13th April 2018.

Organizing Secretary

Organizing Chair

Dean SECT

Shape and Size effect on Mechanical Properties of Pervious Concrete

LogaGanesh.S*, Mahalakshmi.S*, MuthuSelvi.R*, Chockalingam.T**
*B.E. Student, Ramco Institute of Technology – Rajapalayam.
**Assistant Professor, Ramco Institute of Technology – Rajapalayam

Abstract-In this paper, influence of the different shape and size of specimens on the properties such as compressive strength, split tensile strength and flexural strength of pervious concrete was investigated. The value of aggregate-cement ratio and water-cement ratio was kept constant as 3.2 and 0.4. It also focuses on permeability of pervious concrete. In order to find out the result of specimen size on mechanical properties, "cubes" of size 100 x 100 x 100 mm, 150 x 150 x 150 mm, 200 x 200 x 200 mm, "cylinders" of size 50 x 100 mm, 100 x 200 mm, 150 x 300 mm were casted. Beams" of size 100 x 100 x 200 mm, 150 x 150 x 300 mm, 200 x 200 x 400 mm were also casted to check the size effect on flexural strength. Testing was carried out at a period of 28 days. Size of the aggregate used was 10 mm. The slenderness ratio of 1, 2, and 2 was adopted for cube, cylinder, and prism respectively. Experimental results indicate that smaller the size of specimen compressive strength, split tensile strength and flexural strength increases. The reduction aspect of properties of pervious concrete, particularly with increasing the slenderness ratio (L/D) was seen as a matter of great worry. With the results achieved the correction factor has been developed for the further experimental investigations in pervious concrete.

Keywords: Size effect, Specimen Shape, Pervious Concrete, Slenderness ratio

1 Introduction

Pervious concrete which is also known as the no-fines, porous, gap-graded, and permeable concrete and enhance porosity concrete has been found to be a reliable storm water management tool. By definition, pervious concrete is a mixture of coarse aggregate, cement, water, little to no sand (fine aggregate) ,with or without admixtures. It has just enough cementitious paste to coat the coarse aggregate particles while preserving the interconnectivity of the voids. It consists of 15% to 35% voids, allowing for quick drainage. Due to increased void ratio, water is conveyed through the surface and allowed to infiltrate and evaporate whereas conventional surfaces will not do so. In late 1940s and early 1950s the no-fines concrete had been used for the construction of high rise buildings due to its light weight. For porous concrete, water permeability is the main specification requirement instead of its strength and continuity of the open porous is the main concern in the production of porous concrete. The high water permeability of porous concrete makes it to be considered as an environmentally friendly concrete.

Pervious concrete can be used in a wide range of applications, although its primary use is in pavements which are in: residential roads, alleys and driveways, low volume pavements, low

water crossings, sidewalks and pathways, parking areas, tennis courts, slope stabilization, sub-base for conventional concrete pavements etc.

The proposed laboratory work is intended to study the effect of specimen size and shape on the mechanical properties of the pervious concrete. Specimens of various sizes and shapes were cast with square and circular cross sections i.e, cube, prism, cylinder to investigate the compressive strength, flexural strength, split tensile strength at 28 days. Subsequently the compressive strength will decrease with increase in the size of the specimen.

2 Experimental Program

2.1 Physical Properties of materials

Pervious concrete mixes with aggregate cement ratio of 3.2:1 and water cement ratio of 0.4 were prepared containing Portland pozzalano cement (PPC), aggregate of 10 mm, water in a stable form. The physical properties of aggregate were studied experimentally and it is tabulated below.

Table 1. Physical properties of aggregate

Specific gravity, G	2.39
Impact value	13.46%
Crushing Strength	24.46%
Abrasion value	57.2%
Water Content	0.5%
Fineness Modulus	7.93%

2.2 Specimens

Three different shapes of specimen (cube, cylinder, and prism) with l/d of 1, 2, 2 respectively with mix ratio 1:3.2 and the water cement ratio 0.4. Three sizes of specimen were cast for each shape of specimen which is listed in the table below.

Table 2. Size of Specimen

Cube	100x100x100 mm, 150x150x150 mm, 200x200x200 mm
Cylinder	50x100 mm, 100x200 mm, 150x300 mm
Prism	100x100x200 mm, 150x150x300 mm, 200x200x400 mm

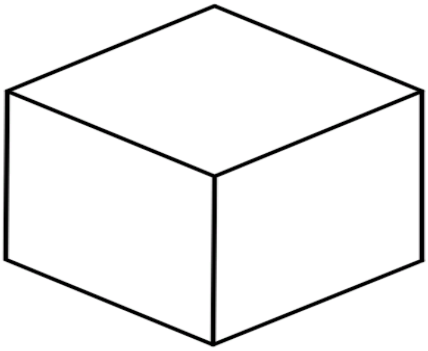

(a) 200x200x200 mm

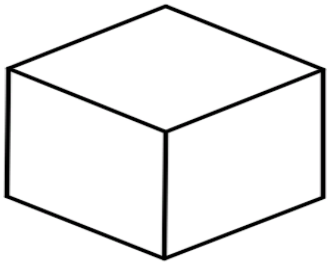

(b) 150x150x150 mm

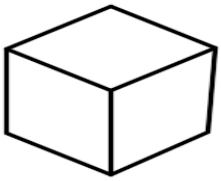

(c) 100x100x100 mm

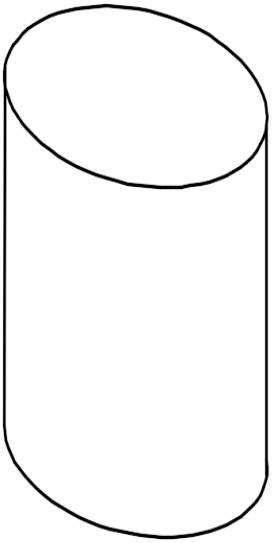

(d) 150x300 mm

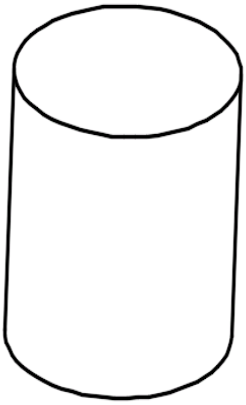

(e) 100x200 mm

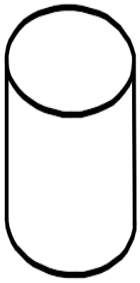

(f) 50x100 mm

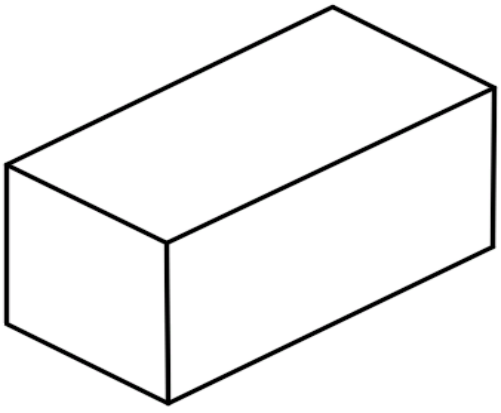

(g) 200x200x400 mm

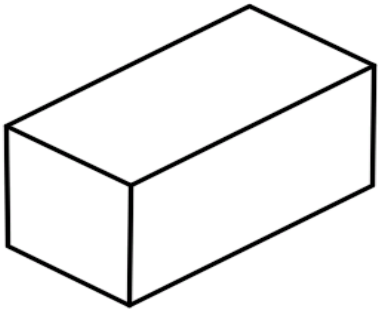

(h) 150x150x300 mm

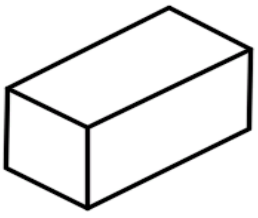

(i) 100x100x200 mm

2.3 Curing

After demoulding, samples were wrapped with the gunny bag and water was sprayed five times a day (as shown in figure 2). Samples were unwrapped on day 27(28 day strength) and it is allowed to dry under sunlight for 24 hours before the samples are tested.

Figure 2. Samples wrapped in gunny bag for curing

3 Results and Discussions

The compression test was carried out in accordance with MS 26: Part 2: 1991. Testing was carried out in the compression testing machine (Figure 3) with a loading rate of 0.3 N/ (mm^2.s)

Figure 3. Compression testing machine, with 2000 kN loading capacity

Table 3.Experimental results for the samples

Shape	Specimen Size in mm	Density in kg/m^3	Load in kN	Compressive Strength at 28 days in N/mm^2
Cube	100 x 100 x 100	2010	73.1	7.31
	150 x 150 x 150	1822	115.2	5.12
	200 x 200 x 200	1694	181.6	4.54
Cylinder	50 x 100	2280	14.78	7.53
	100 x 200	2095	49.22	6.27
	150 x 300	1821	95.73	5.42
Prism	100 x 100 x 200	2450	27.33	5.47
	150 x 150 x 300	2320	49.48	4.40
	200 x 200 x 400	2041	75.71	3.78

Table 4. Compressive Strength comparison between Samples A

SAMPLE A	Cube 100	Cube 150	Cube 200	Cylinder 50	Cylinder 100	Cylinder 150
Cube 150	-29.96%		+12.78%	-32.01%	-18.34%	-5.54%
Cylinder 150	-25.85%	+5.86%	+19.38%	-28.02%	-13.56%	

Inference:

From Table 4, there is 5.54% compressive strength increases, when the l/d ratio of cube and cylinder increased from 1.0 to 2.0. For comparison of same l/d ratio 29.96% compressive strength increases for 100 mm cube and 12.78% compressive strength reduction in 200 mm cube with respect to standard size of cube (150 mm cube). There is 5.86% compressive strength reduction, when the l/d ratio of cylinder and cube reduced from 2.0 to 1.0. For comparison of same l/d ratio 28.02% and 13.56% compressive strength increases for both 50 mm cylinder and 100 mm cylinder respectively with respect to 150 mm cylinder.

Table 5. Correction Factor for Cube

S.No	Specimen Size in mm	Average Compressive Strength in N/mm^2	Correction Factor
1.	100 x 100 x 100	7.31	1.43
2.	150 x 150 x 150	5.12	1
3.	200 x 200 x 200	4.54	0.89

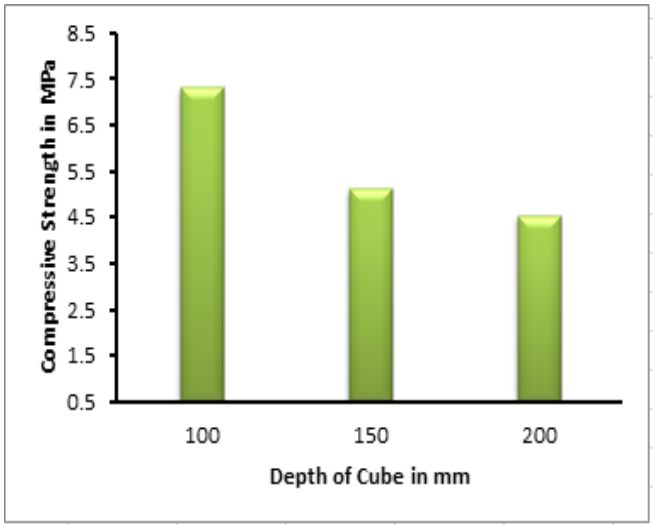

Figure 4. Decreases of compressive strength with the increase of depth

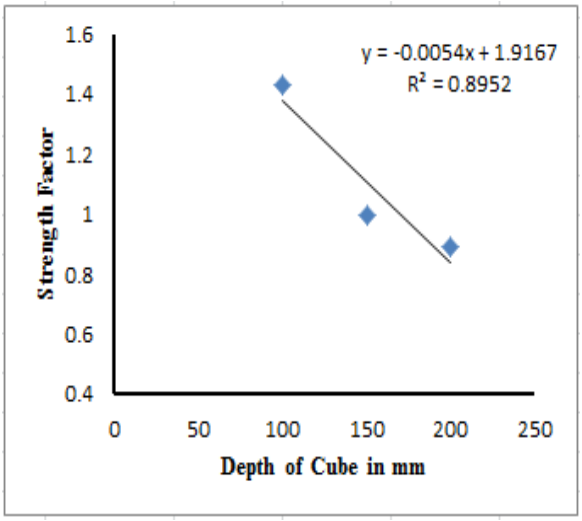

Figure 5. Strength Factor (w.r.t., 150 mm cube) vs Depth of cube

Inference:

From Figure 4 and Figure 5, it can be concluded that the compressive strength of concrete decreases linearly with the increase of cube depth. This also confirms the presence of a size effect where the nominal compressive strength at failure decreases with the specimen size increases. From Figure 5, the following empirical equation can be proposed:

$$y = -0.0054\ x + 1.9167$$

Where,

y = the ratio of the given sample strength to 150 mm cube strength

x = Depth of cube in mm

Table 6. Correction Factor for Cylinder

S.No	Specimen Size in mm	Average Compressive Strength in N/mm^2	Correction Factor
1.	50 x 100	7.53	1.39
2.	100 x 200	6.27	1.16
3.	150 x 300	5.42	1

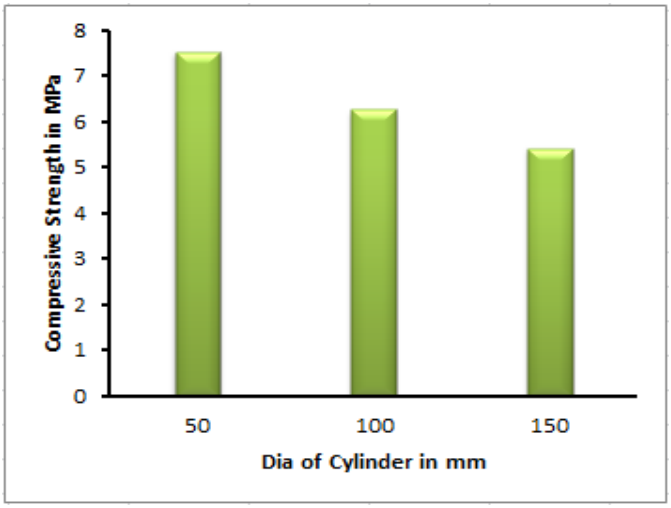

Figure 4. Decreases of compressive strength with the increase of depth

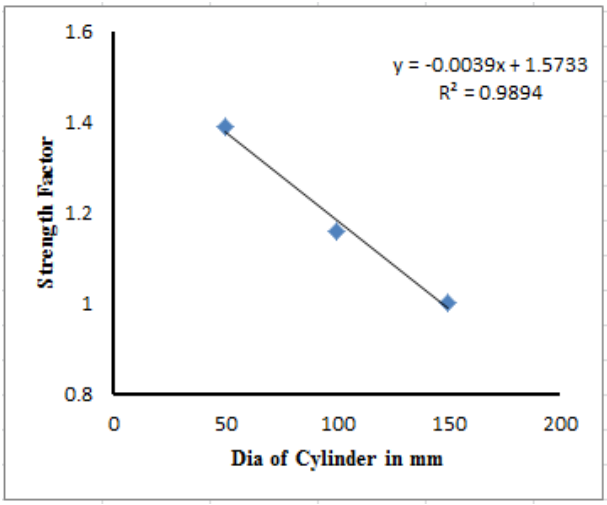

Figure 5. Strength Factor (w.r.t., 150 mm cube) vs Depth of cube

Inference:

From Figure 4 and Figure 5, it can be concluded that the compressive strength of concrete decreases linearly with the increase of cylinder diameter. This also confirms the presence of a size effect where the nominal compressive strength at failure decreases with the specimen size increases. From Figure 5, the following empirical equation can be proposed:

$$y = -0.0039\ x + 1.5733$$

Where,

y = the ratio of the given sample strength to 150 mm cylinder strength

x = Diameter of cylinder in mm

4 Conclusions

The effect of size and shape of a specimen on the pervious concrete compressive strength was examined. From the experimental test results, the following conclusions may be derived:

1. The strength of cube specimens increases with the decrease of specimen sizes of same slenderness ratio due to frictional effect.
2. The strength of cylinder specimens increases with the decrease of specimen sizes of same slenderness ratio due to frictional effect.
3. The ratio of the 28 days compressive strength of non –standard cubes compared that of standard 150 x 150 x150 mmcubes varied from 0.89 to1.43
4. The ratio of the 28 days compressive strength of non –standard cylinders compared that of standard 150 x300 mm cylinders varied from 1 to1.39

5. Specimen sizes decreases with increases the compressive strength, split tensile strength and flexural strength.

5 References

1. M.Dehestani Et al, Effect of Specimen shape and Size on the compressive strength of self consolidation concrete, Construction and building materials 66 (2014) 685-691
2. J.R.del Viso Et al, Shape and Size effects on the compressive strength of high strength concrete, Cement and Concrete Research 38 (2008) 386-395
3. E.L.Al-Sahawneh, Size Effect and Strength Correction factor for normal weight concrete Specimens under Uniaxial compression stress, Vol. 6,2013, no2,57-68
4. Ahi Jihad Hamad, Size and Shape effect of specimen on the compressive strength of HPLWFC reinforced with glass fibres, Journal of king sand University-Engineering Sciences (2017) 29, 373-380
5. T.Krauthammer Et al, Size effect for high-strength concrete cylinders subjected to axial impact, International journal of Impact Engineering 28 (2003) 1001-1016
6. M.Tokyay and M.Ozdemire, Specimen Shape and size effect on the compressive strength of higher strength concrete, PII S008-8846 (97) 00104-X

IEEE

Certificate of Participation

This is to certify that

Dr. Mahalakshmi,

has successfully presented a paper entitled

Network intrusion detection system using machine learning algorithms.

in the Second International Conference on Electronics, Communication and Aerospace Technology (ICECA 2018), held during 29-31, March 2018, at the RVS Technical Campus, Coimbatore, Tamilnadu, India.

Session Chair **Conference Chair** **Director**

Technical Sponsor

IEEE ELECTRON DEVICES SOCIETY

NETWORK INTRUSION DETECTION SYSYEM USING MACHINE LEARNING ALGORITHMS

G.Mahalakshmi,
Assistant Professor,
Department of Computer Science,
Ramco Institute of Technology,
Rajapalayam, India

Kaleeswari M, Ponthamarai S, Sangeetha K,
Vyshali Rajeswari G V
Final year, Computer Science,
Ramco Institute of Technology,
Rajaplayam, India

Abstract-Security of computers and the networks that connect them is increasingly becoming of great significance. Computer security is defined as the protection of computing systems against threats to confidentiality, integrity, and availability. The proposed system has a machine learning based data classification algorithm which is applied to network intrusion detection. The classification of network is done by combining Support Vector Machine (SVM) and Ant Colony Network (AC).By using CSVAC (Combined Support Vector and Ant Colony Network), the overall detection rate, false positive and false negative are obtained. This algorithm is implemented and evaluated using a standard NSLKDD data set. This increases the performance on both classification rate and run-time efficiency.

Keywords-Intrusion Detection System, Support Vector Machine, Ant Clustering, NSLKDD Dataset.

I.INTRODUCTION

An **intrusion detection system (IDS)** is a network security technology originally built for detecting vulnerability exploits against a target application or computer. In other words intrusion detection system is a device or software application that monitors network or system activities for malicious activities or policy violations and produces electronic reports to a management station. Intrusion Prevention System extended IDS solutions by adding the ability to block threats in addition to detecting them and has become the dominant deployment option for IDS/IPS technologies. It is a type of security software designed to automatically alert administrators when someone or something is trying to compromise information system through malicious activities or through security policy violations.

An IDS works by monitoring system activity through examining vulnerabilities in the system, the integrity of files and conducting an analysis of pattern based on already known attacks. It also automatically monitors the internet to search for any of the latest threats which could result in a future attack. More specifically, the goal of intrusion detection is to identify entities attempting to subvert in-place Security controls. There are two types of intrusion detection systems such as,

NIDS - **N**etwork **I**ntrusion **D**etection **S**ystems.
HIDS - **H**ost **I**ntrusion **D**etection **S**ystems.

A .Network Intrusion Detection Systems

Network Intrusion Detection Systems (NIDS) are placed at a strategic point or points within the network to monitor traffic to and from all devices on the network. It performs an analysis of passing traffic on the entire subnet, and matches the traffic that is passed on the subnets to the library of known attacks. Once an attack is identified, or abnormal behavior is sensed, the alert can be sent to the administrator. While classifying the design of the NIDS according to the system interactivity property, there are two types: on-line and off-line NIDS. On-line NIDS deals with the network in real time. It analyses the Ethernet packets and applies some rules, to decide if it is an attack or not. Off-line NIDS deals with stored data and passes it through some processes to decide if it is an attack or not.

B. Host Intrusion Detection Systems

Host Intrusion Detection Systems (HIDS) run on individual hosts or devices on the network. A HIDS monitors the inbound and outbound packets from the device only and will alert the user or administrator if suspicious activity is detected. It takes a snapshot of existing system files and matches it to the previous snapshot. If the critical system files were modified or deleted, an alert is sent to the administrator to investigate.

II.RELATED WORK

Security is an important issue for all the

networks of companies and institutions at the present time and all the intrusions are trying in ways that unsuccessful access to the data network of these companies and Web services and despite the development of multiple ways to ensure that the infiltration of intrusion to the infrastructure of the network via the Internet, through the use of firewalls, encryption, etc. But IDS is a relatively new technology of the techniques for intrusion detection methods that have emerged in recent years. Intrusion detection system's main role in a network is to help computer systems to prepare and deal with the network attacks.

Intrusion detection functions include:

1. Monitoring and analyzing both user and system activities.
2. Analyzing system configurations and vulnerabilities.
3. Assessing system and file integrity.
4. Ability to recognize patterns typical of attacks.
5. Analysis of abnormal activity patterns.
6. Tracking user policy violations

III.METHODOLOGY

A new machine-learning based data classification algorithm is applied to network intrusion detection system. Here the combination of the SVM method and Ant Colony Network (CSVAC) is used. Due to this modeling, the problem should be described in terms of some standard mathematical objects. In a CSVAC, ant moves the object on two dimensional grids so as to cluster similar objects into same region. In this process objects and ants are the two basic entities. This algorithm is implemented and evaluated using a standard NSLKDD data set.

The advantage of this system is that the there is a high performance in classification rate and run-time efficiency.

A. Normalizing data

The raw data set is given as input and it needs to be normalized to avoid biasing.

B. SVM training phase

The SVM training is repeated upon different training data sets. An SVM classifier is trained by using only small amount of data sets from the whole training data set and it is classified as normal and abnormal.

C. Ant clustering phase

The clustering process is divided into several periods by clustering around certain objects each time. The objects for each clustering period are support vectors marked by the last SVM training phase.

D. Constructing classifier

A binary classifier based on intrusion detection can be constructed by the result generated by SVM

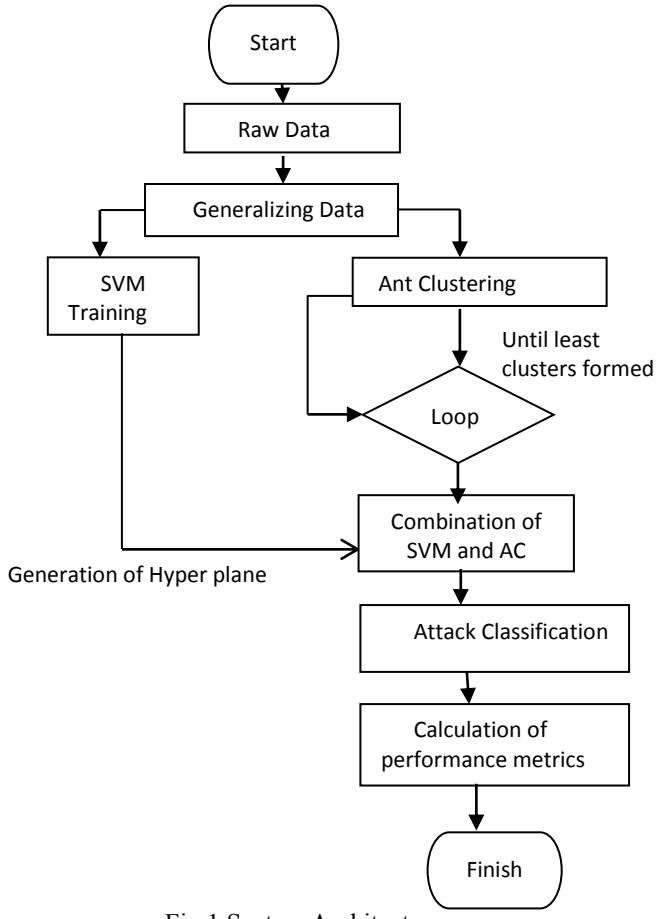

Fig 1.System Architecture

training phase. For the normal data, the centers of the clusters which include the support vectors are computed, the computing times for normal data are decreased. For the abnormal data, when the amount of training data from each abnormal class is small, the cluster centers of each data can be computed quickly. The SVM is used to minimize the reduction of detection rate which may be caused by the partial clustering process.

E. Classifier modification

The classifiers can be modified gradually by repeating the three steps,

- SVM training phase
- Ant clustering phase
- Constructing the classifier

The repeating loops will terminate when both of the two classifiers (SVM and AC classifiers) obtain a satisfying detection rate upon the entire training data.

IV. SVM TRAINING

SVM is a learning method for the Classification and Regression analysis of both linear and nonlinear data. It uses a hypothesis space of linear functions and maps input feature vectors into a higher dimensional space all the way through some nonlinear mapping. The SVM training is repeated upon different training data sets. The training data for each SVM training iteration are objects selected randomly.

SVM testing is done based on the records in SVM training data set. SVM constructs a hyper plane or set of hyper planes only the good separation is achieved by the hyper plane. The hyper plane searching process in SVM is achieved by the leading margin.

A network connecting record can be described by several features of the connection and is represented as a data point for SVM training. The traditional SVM algorithm is operated over the entire training data set. The number of training data points determines the dimension of the matrix for computing the kernel functions, which influences the time of solving the QP problems. However, SVMs have the property that the points that do not lie on the margin do not need to be involved in the computation. The same decision function is obtained if some of the training data points, excepting the support vectors, are removed. Hence, the number of training data points can be reduced without losing accuracy. An active learning SVM has to reduce the amount of training data. Initially, an SVM classifier was trained by using only small amount of data points from the whole training data set. The SVM classifier was then gradually modified by adding new data points for the training. After each training process, the output classifier is used to separate the entire data. The recurrence of training a new classifier can stop when a required correct classification rate is obtained.

V. ANT CLUSTERING

The ant clustering algorithm can used for intrusion detection problem. In natural the ants have the intellective character. This algorithm describes the Ant system manner based on such nature of ants and it produced great result.

The ant colony algorithm classify the objects into different classes the first one is normal and the remaining classes are different kind of intrusions. The intrusion detection classifier can be built based on anomaly and misuse detection pattern.

The heuristic features of this algorithm are robustness, distributed and parallel computing feature and positive feedback characteristic. The clustering process is divided into several periods by clustering around certain objects each time. The objects for each clustering period are support vectors marked by the last SVM training phase.

Algorithm 1: **Ant Clustering**

Input: Number of Trails and Ants
1 begin
2 Randomly choose data points from each class
3 **While** number of agents added to the cluster Do
4 **While** each ant completes the tour Do
5 update the local trail
6 **End**
7 Analyze the tour for each Ants
8 Globally update the trail
9 **end**
10 **end**

VI.SVM WITH ANT CLUSTERING

A new machine learning algorithm has been introduced namely combine support vector and ant colony (CSVAC**).** It is based on a mixture of customized version of SVM and AC algorithm. The interactive algorithm SVM and AC are taken multiple times for intrusion detection system. At first SVM finds the support vectors and then generate hyper plane that is used to separate normal and as well as for each class of abnormal data while an AC is used to discover data added to the SVM training set. At last Ant colony create models for normal data and abnormal data.

Algorithm 2: SVM with clustering.
1 begin
2 Randomly select data points from each class.
3 Generate a SVM classifier.
4 while more points to add to training set do
5 Find support vectors among the selected points;
6 Apply CSOACN clustering around the support vectors;
7 Add the points in the clusters to the training set;
8 Retrain the SVM classifier using the updated training set;
9 end
10 end

VII. DATA SET

The data set used in this process is NSL-KDD. But the existing system used KDDCUP'99 data set. KDDCUP'99 data set is not preferred in our proposed system as it creates many inherent problems such as very poor evaluation of anomaly detection. Some of

the advantages of NSL-KDD over the original KDD data set are mentioned below,

NSL KDD data set does not include redundant records in the train set, so the classifiers will not be biased towards more frequent records. The number of selected records from each difficulty level group is inversely proportional to the percentage of records in the original KDD dataset. As a result, the classification rates of distinct machine learning methods vary in a wider range, which makes it more efficient to have an accurate evaluation of different learning techniques.

The number of records in the train and test sets is reasonable, which makes it affordable to run the experiments on the complete set without the need to randomly select a small portion.

VIII.ATTACK CLASSIFICATION

In this phase the new machine learning algorithm has been introduced namely Combined Support Vector and Ant Colony (CSVAC).It is based on a mixture of the customized version of the two algorithms discussed above (SVM and AC). The interactive algorithm SVM and AC are taken multiple times at this phase for intrusion detection. At first SVM finds the support vectors and then generate hyper plane that is used to separate normal and as well as for each class of abnormal data while an AC is used to discover data added to the SVM training set.

At last ant colony create models for normal data and abnormal data. It establishes the CSVAC based classifier, which is a hybrid of the SVM classifier and the Ant clustering classifier. By repeating the processes of SVM training and Ant clustering, the classifier is established.

CATEGORY	**ATTACK TYPE**
Normal	Normal
Probe	Saten, IPsweep, Nmap, Portsweep, Mscan, Saint.
DOS	Back, Land, Neptune, Pod, Smurf, Teardrop, Mailbomb, Processtable, Udpstorm, Apache2,Worm
U2R	Buffer_overflow, Loadmodule, Rootkit, PErl, Sqlattack, Xterm, Ps
R2L	Guess_password, Ftp_Write, Imap, Phf, Multihop, Warezmasster, Xlock, Xsnop, Snpguess, Snmpgetattack, Httptunnnel, Sendmail, Named

Table 1. Types of Attacks

Attacks are classified based on,

Probe**,** Dos, U2R, R2L

Four types of attacks, those features are derived as the following four categories,

1. Basic features of individual TCP connection.
2. Traffic features computed using a 2s time window.
3. Host-based traffic features.
4. Content features within a connection suggested by domain knowledge

Attacks in testing dataset:

A. Probe

Probe is an attempt to gain access to a Computer and its files through a known or probable weak point in the computer system.

In this type of attack, an attacker examines a network to gather information or discover well-known vulnerabilities.

B. Dos: Denial Of Service

DOS is performed against an information system to prevent legitimate users from accessing the compromised system for service.

It makes the system to slows down or shut down so it interrupt the service and rebuff the indented authorized user. Due to this attack high network traffic occurs.

C**.** U2R: User To Root

Attacker has local access to the victim machine and tries to gain super user privileges.

In this attack, the attacker starts at client level like snatching the password, dictionary attack and at last attacker achieves the root to access the system.

D**.** R2L: Remote To Local

Attacker does not have an account on the victim machine but tries to gain access.

In this attack, the attacker can produce vulnerability over a network and have the ability to send a packet over a network which does not have an account on that machine.

Algorithm 3: Attack classification

Input: Training set with each data labeled as normal or abnormal

1 begin
2 Randomly choose data points from each class
3 Generate a SVM Classifier
4 **While** n number of data points added to training set **Do**
5 Locate support vector among the chosen point;
6 Apply Ant clustering around support vectors;
7 Add the points in the cluster to the training set;

8 Retain the SVM classifier using the updated training set;
9 Classification based on the attack types
10 **end**
11 **end**

XI.CALCULATION OF PERFORMANCE METRICS

Compares the system performance under the three different modes (SVM, AC, CSVAC), the classifiers generated by them should be tested separately by the same testing data set. The CSVAC mode can be used to balance the performance of IDS in terms of efficiency and accuracy. The following measurements which are often used to evaluate the efficiency of the classifier, is used in this research.

True positive: The number of sample that is correctly classified into the class.

False positive: The number of samples being wrongly classified into the class.

True negative: The number of outer samples that is correctly classified.

False negative: The number of the class samples which is wrongly classified into the other classes.

X.RESULTS AND DISCUSSION

By applying CSVAC Algorithm on selected features it finds the attacks accurately, From the exceeding implementation we have effectively produce some rules those categorize the declared attack connection, The training phase and testing phase are executed by two independent modules. The new algorithm processes the training and testing phases parallel in the new IDS. This is an important ability of IDSs that are intended for real- time detection.

XI.CONCLUSION

In this proposed system, a new algorithm (CSVAC) for generating classifiers with clustering is designed and applied to the intrusion detection problem. This process combines the SVM and Ant colony networks to classify the network data as normal and abnormal. Due to modeling, the problem should be described in terms of some standard mathematical. The experimental result shows the better performance in both detection accuracy rate and faster running time.

X.FUTURE WORK

As future work, there is a consideration for integrating the privacy preserving OLAP with the proposed framework in order to improve the effectiveness and the flexibility of IDS system. There is a plan to enhance the CSVAC algorithm to generate more SVM classifiers to handle multiclass cases and find ways to convert a nonlinear classification problem to a linear one by applying the recently proposed Maximum Information Coefficient (MIC) method.

References

[1] Muamer N. Mohammed et al, An approach for IDS by Combining SVM and Ant Colony Algorithm, in: proceedings of International Journal of Research in Engineering and Technology, 2014, pp. 120-132

[2] Y. Li et al., Evaluating Performance of Intrusion Detection System using Support Vector Machine, in: Proceedings of International Journal Of Security and its Applications, 2015, pp. 225-234.

[3] Yogita B. Bhavsar et al, An Effective Hybrid Intrusion Detection system based on C5.0 and SVM, im: proceedings of International Journal of Database Theory and Application, 2014, pp.59-70.

[4] G.Zhao et al., Some Studies in Intrusion Detection Using Data Mining Techniques, in: proceedings of International Journal of Innovative Research in Science Engineering and Technology, 2015, pp.617-631.

[5] W. Feng et al, Mining Network data for intrusion detection through combining SVM with Ant colony Network, in: proceedings of International Journal Of Computer Applications, 2014, pp. 13–24.

[6] Wun-Hwa Chen, Sheng-Hsun Hsu, Hwang-Pin Shen., Application of SVM and ANN for Intrusion Detection, in: proceedings of International Journal Of Computer Applications,2013,pp.441-453.

[7] D. Duan, S. Chen, W. Yang, Intrusion detection system based on support vector machine active learning, Computer Engineering 33 (1) (2007) 153–155.

[8] M. Dorigo, E. Bonabeau, G. Theralulaz, Ant algorithms and stigmergetic, Future Generation Computer Systems 16 (9) (2000) 851–871.

[9] V. Ramos, A. Abraham, Evolving a stigmergic self-organized data-mining, in: Proceedings of the 4th International Conference on Intelligent Systems, Design, and Applications, 2004, pp. 725–730.

[10] R. Rifkin, A. Klautau, in defense of one-vs-all classification, Journal of Machine Learning Research 5 (2004) 101–141.

[11] V. Vapnik, the Nature of Statistical Learning Theory, Springer, 1999.

[12] C.-H. Tsang, S. Kwong, Ant colony clustering and feature extraction for anomaly intrusion detection, in: Swarm Intelligence in Data Mining,In: Studies in Computational Intelligence, vol. 34, Springer, 2006, pp. 101–123

2nd International Conference on

Recent Trends in Engineering, Computers, Information Technology and Applications

ICRTECITA-2018

23rd March 2018

Organized by

PSNA COLLEGE OF ENGINEERING AND TECHNOLOGY

(Approved by AICTE & Affiliated to Anna University, Chennai All UG programmes and MBA are accredited by NBA, New Delhi & Accredited by NAAC With 'A' Grade)

Kothandaraman nagar, Dindigul-624622, Tamilnadu, India.

Department of Computer Applications and Department of Computer Science & Engineering

In Association with

SSRG

Seventh Sense Research Group®

Trichy Division, Website: www.internationaljournalssrg.org

Proceedings of
INTERNATIONAL CONFERENCE

ICRTECITA - 2018

2ND INTERNATIONAL CONFERENCE ON RECENT TRENDS IN ENGINEERING, COMPUTERS, INFORMATION TECHNOLOGY AND APPLICATIONS

23rd March 2018

Organized by

Estd : 1984

PSNA College of Engineering and Technology

Kothandaraman Nagar, Dindigul-624622, Tamilnadu, India.

(Approved by AICTE & Affiliated to Anna University, Chennai All UG Programmes and MBA are accredited by NBA, New Delhi & Accredited by NAAC with 'A' Grade)

Department of Computer Applications and Department of Computer Science and Engineering

In Association With

Seventh Sense Research Group®

Data Mining Approach for Anomaly Detection in Social Network Analysis

M.Swarna Sudha
Assistant Professor (Sr. Grade), Department of CSE
Ramco Institute of Technology
Rajapalayam, India

K.Arun Priya, A.Kanaka Lakshmi, A.Kruthika, D.Lakshmi Priya
IV year B.E. CSE
Ramco Institute of Technology
Rajapalayam, India

Abstract- *With the booming trends in various domains of the online social network; there is a need for security and privacy concerns. As there is a massive population of online social network users, it is difficult to detect anomalous behavior of the users. The present study aims at detecting the abnormal activities exhibiting different behaviors in social media application using Behavior-based anomaly detection approach. Anomaly detection is a technique to identify the anomalous activities from the social media. In this paper, we have used the unsupervised method to detect anomalies. For detecting such anomalies, we group the users into clusters using K-Means clustering algorithm. From the graph, the abnormalities have been detected. The Risk score is estimated by the Expectation Maximization algorithm to identify the abnormal activities of the user. This analysis is carried out using Facebook dataset.*

Keywords-*Online Social Network, Data Mining, Anomaly Detection, Clustering, Risk Analysis, Facebook.*

I. INTRODUCTION

The popularity of online social network is ever increasing. The social media are exposed to many security and privacy concerns because of the threats and attacks in it. These attacks exploit the infrastructure to collect and expose personal information of users. Lack of knowledge about the social media leads public to suffer. To prevent this, we prepare a framework to analyze the abnormal user in the online social network. Our paper proposes a solution to predict the abnormal behavior of the user whose behavior diverges from the normal user. An anomaly is a set of activities that deviate from the normal behavior of the user. Anomalies are also called as outliers, abnormities. Anomaly detection is the processing technique for removing anomalous data from the dataset. Therefore, in this paper technique to analyze and detect the anomalous behavior is covered. The paper is organized into various sections. In section II data mining topic is discussed. In section III related works are discussed. In section IV data mining approaches to anomaly detection are discussed. Section V will discuss the anomaly detection techniques available. Section VI presents the risk assessment based on user behavior. Section VII risky behaviors in online social networks are discussed. Section VIII tells how the system is implemented. Section IX Clustering approaches is discussed. Section X conclusion for the paper is discussed.

II. DATA MINING

Data mining is the process of discovering the patterns, associations, changes, anomalies from large amounts of data stored in datasets. The discovery process consists of an iterative sequence of the following steps:

Data cleaning – This handles noisy, erroneous, missing or irrelevant data from the collection.

Data integration – In this stage multiple, heterogeneous are combined in a common source.

Data selection – The data relevant to the analysis task are retrieved from the dataset.

Data transformation – Where the data are transformed are consolidated into forms appropriate for mining by performing aggregations operations.

Data mining – It is a crucial step, where intelligent methods are applied to extract data patterns.

Pattern evaluation – In this step, interesting patterns representing knowledge are identified based on given measures.

Knowledge representation – It is a final phase, where visualization and knowledge representation techniques are used to present the mined knowledge to the user.

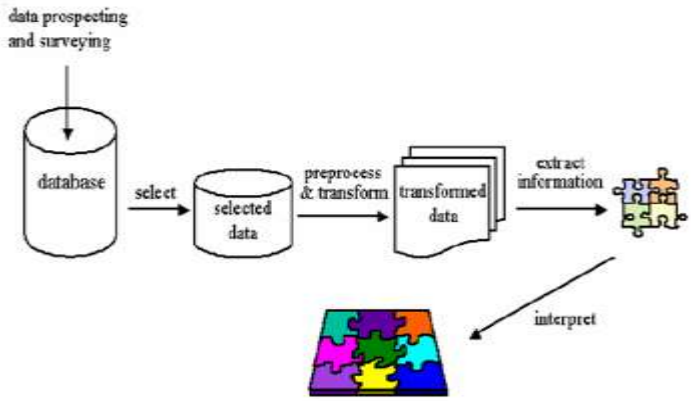

Fig II: Data mining process

III. RELATED WORK

Since information can spread rapidly and widely more than ever on online social network, they have become new hot beds of false rumor diffusion. Due to the potential harm this false information may bring to the public, false rumor detection has become a significant but challenging research topic. While previous research work mostly views it as a classification task, we treat it as an anomaly detection problem. The false rumors are viewed as anomalies and we perform factor analysis of mixed data on our proposed features to detect these anomalies. Two strategies based on Euclidean distance and cosine similarity are proposed to describe the deviation degree. A rank based on deviation degree is computed which can facilitate further rumor detection. We show our method can achieve good performance and can shed light on automatic detection of false rumors on online social networks.

IV. DATA MINING APPROACHES TO ANOMALY DETECTION

Anomaly detection is defined as "an observation that deviates so much from the other observation". From data mining perspectives, anomaly detection is classified into the following categories:

- Supervised method
- Semi-supervised method
- Unsupervised method

A) SUPERVISED METHOD

It involves studying anomaly detection as a classification problem with the pre-labeled data, labeled either as normal or as anomalous. These methods model both the normal and abnormal behaviors. There are two applicable approaches for it.

- One, experts may pre-label the normal data and any such data which is not analogous to this model is considered anomalous.

The other way is to do the opposite i.e. have the predefined set of anomalous data and any objects not corresponding to the set of anomalous data are considered as normal.

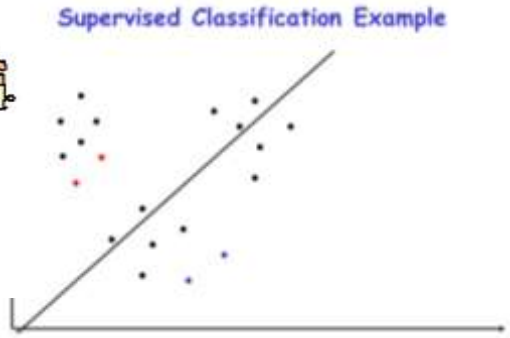

Fig IV: A(1) Supervised method

B) SEMI-SUPERVISED METHOD

Semi-supervised method, where the model is trained using the normal data, only to build the profile of normal activity. Semi-supervised methods work with two sets of data, labeled and unlabeled. So, these methods are used when out of the complete data set only few instances of data labeled as normal are available. Using the small amount of labeled data a classifier can be constructed which then tries to label the unlabeled data. Hence, a model for normal data objects is built which is used to detect the anomalies in a way that the objects not fitting the normal model are classified as anomalies. This is the simplest approach called self-training used under semi-supervised model.

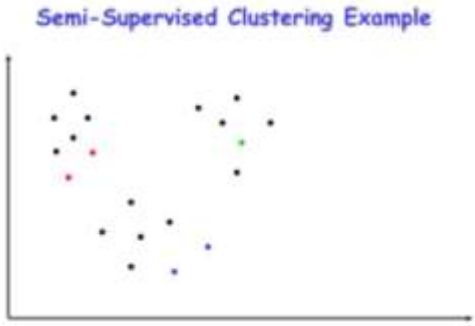

Fig IV: B(1) Semi-supervised method

C) UNSUPERVISED METHOD

Unsupervised methods, where the anomaly detection model is trained using unlabeled data that consists of both normal as well as abnormal data. Unsupervised anomaly detection methods are used when labeled data objects are not available i.e. no predefined labels as "anomalies" or "normal" are attached to the data objects. Unsupervised methods are usually studied as a clustering problem.
Finding the group of objects such that the objects in the group will be similar to one another and different from the objects in other group. Two major

challenges faced by unsupervised methods are as follows:

- First, a data object not belonging to any cluster is considered as anomalous but many times this deliberation can be false because, such a data object can be a noise rather than an anomaly.
- Secondly, what is usually practiced is to firstly find the clusters and then the anomalies. But this methodology seems to be quite expensive as number of anomalies present in a data set is pretty less than normal data objects.

Fig IV: C(1) Unsupervised method

V. ANOMALY DETECTION TECHNIQUES

In social networks, the node disobeying these similarity measures by following behavior which is deviates from the other nodes are detect as anomalous. Anomaly detection techniques in social networks can be categorized as follows:

- Behavior based techniques
- Structural (graph) based techniques
- Spectral based techniques

A) BEHAVIOR BASED TECHNIQUES

Behavior based techniques handle the behavioral properties of the users such as number and content of message, content of the items shared, number of likes or comments on a post and duration of a conversation.

B) STRUCTURAL BASED TECHNIQUES

Structural based methods work on the basic principle of using structural properties to check the characteristics of normal and anomalous users. A particular graph metric is figured out for different nodes and structure and the nodes showing different values than other users are considered as anomalous. Just like supervised approach, here also a predefined normal pattern is already known and any deviation from that known pattern depicts the anomalous behavior. These techniques help to identify dynamic unlabeled anomalies by predicting future events and analyzing previous network behavior which is a precondition for dynamic anomalies.

C) SPECTRAL BASED TECHNIQUES

Spectral anomaly detection techniques help in detecting anomalies using some spectral characteristic in the spectral space of the graph.

VI. RISK ASSESSMENT BASED ON USER BEHAVIOR

Our main goal is to associate a risk score with the user based how he/she behaves in online social networks. The key idea is that the more the user behavior diverges from what is considered to be a normal behavior, more it should considered being risky. Therefore we first define a user behavioral profile.

In an online social network variety of activity are possible, such as post, comment, share, like and different types of interaction. In designing this behavioral profile, there is no need for monitoring all the users' activities. But only those that might reveal risky behavior is monitored. For example, writing more comments/posts without receiving any likes on them. Can we consider as a warning and they might be victim of an attack. On the contrary, having huge number of friends, posts, comments, likes in a short period is also consider as risky. The online social network population is heterogeneous in observed behavior, so it is not possible to define unique standard behavioral model that fits all online social network user behaviors.

However, we expect similar people tend to follow similar rules which results in similar behavioral model. For this reason, we propose risk assessment organized into two phases: The first phase aims at identifying the groups in online social network. This is achieved by clustering techniques. The second phase aims at creating behavioral model for each group identified by first phase.

VII. RISKY BEHAVIORS IN ONLINE SOCIAL NETWORKS

Due to the popularity of social network sites, cyber criminals or attackers started to exploit them in propagating malwares and carry out scams. The discrepancy is defined in terms of frequency, number, as well as type of activities.

In general, attackers use online social network infrastructure to collect and expose personal information about a user and their friends by making the user to click on some specific malicious links so as to propagate them in the network. In the following, we illustrate the most notable types of attacks:

Sybil attack: Sybil attack is one of the practical attacks in online social networks. As an example

there are more than thousand social bots has been detected on Facebook. To launch this attack, a malicious user has to create multiple fake identities known as Sybil's, with the purpose to legitimate his/her identity. After that, the attackers initiate their work by sending friend requests to users in the community. Once the request has been accepted, the social bot can gather the user's private data.

Identity clone attack: In this attack, malicious user creates similar or identical profiles. The key goal is to obtain personal information about the victim's friend after successfully forging the victim and established an increased level of trust with the victim's social circle. Afterwards, he/she sends friend requests to the victim's contacts. Once the friend requests have been accepted, he builds the victim's friend network and gains access to the profiles of the victim's friends.

Socware attacks: In this attack, an adversary creates malware items, called socware, in the form of applications, pages or events containing malicious link to be propagated in the online social networks. This attack lures victims by offering false rewards to who will install/accept the socware. Once users have installed the socware, it is not only gets access to the user's personal information but also gains ability to post them on the victim's wall. As a consequence the users unknowingly end up sending socware messages or post to their friends, essentially assisting the socware's viral spread.

VIII. METHODOLOGY

Our Methodology flows through the concepts of the collection of the dataset, removing the null values, categorizing the data, clustering, risk analysis.

1. A dataset is a collection of data corresponds to the content of single database table.
2. From the dataset remove the null values.
3. Risk assessment approach is based on the idea of estimating the user's risk on the basis of how much his\her behavior deviates from the normal user. Risk assessment is composed of two phase clustering :
    a. The first phase consists of organizing the users according to group identification features.
    b. In the second phase, users are categorized using behavioral features using K-means and Expectation Maximization algorithm.
4. The risk score is estimated using Membership probability based on a value of group identification features.
    a. High membership probability-normal user.
    b. Low membership probability-abnormal user.

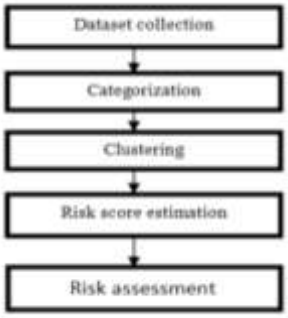

Fig VIII: Methodology

IX. CLUSTERING

- Clustering is a task of partitioning a set of data based on their characteristics into clusters.
- It is used for pattern recognition; image processing and data analysis. It discovers structures and patterns in high dimensional data.

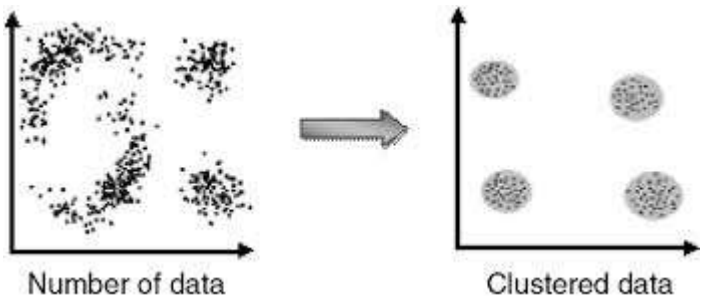

Fig IX: Clustering

A) K-Means Clustering Algorithm

- K-Means is one of the simplest unsupervised learning algorithm to cluster n objects based on attributes into k partitions where k>n.
- The goal is to find groups in data, with the number of groups represented by variable K.

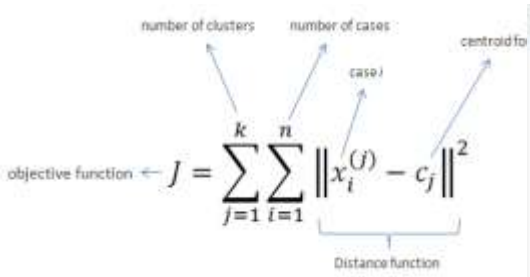

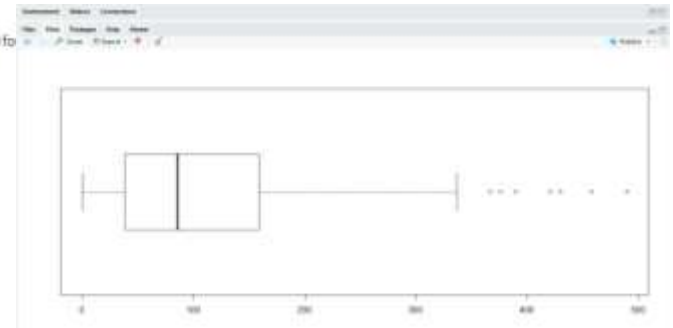

Fig IX: A(2) Removing of outliers

- Step1 - **Initialization:** Randomly choose k vectors from the dataset and make them initial cluster centers.
- Step2 - **Assignment:** Assign each vector to its closest center.
- Step3 - **Updating:** Replace each center with a mean of its members.
- Step4 - **Iteration:** Repeat step 2 and 3, until there is no more updating.

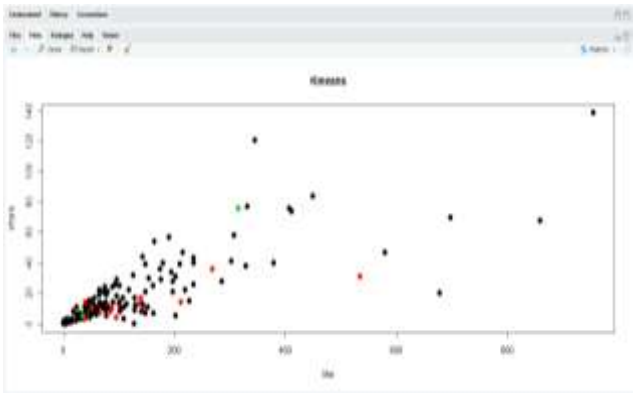

Fig IX: A(3) K-Means Clustering

IX.A (1) BOX PLOT

It is method of representing statistical data on a plot in rectangle for depicting groups of numerical data through their quartiles and vertical line inside to indicate the median value.

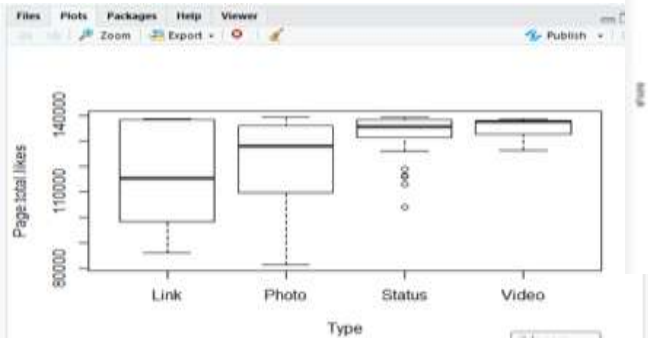

Fig IX: A(1) Box plot

Fig IX: A(4) K-Means Clustering

IX.A(2) OUTLIERS

It is an observation point that is distant from other observations.It may indicate experimental error or variability in the measurement.It can cause problem in statistical analysis.

B) Expectation Maximization Algorithm

It is a iterative method to find the maximum likelihood function that estimates for model parameters when your data is incomplete or has unobserved latent variables.

- Step 1 - Parameters are initialized by random positive values.
- Step 2a - The membership probability for each user in each cluster is calculated using **Expectation step**.

$$w_l^j(\vec{u}) = \frac{w_l^j . p_l(\vec{u}|\theta_l^j)}{\sum_{i=1}^{K} w_i^j . p_i(\vec{u}|\theta_i^j)}$$

- Step 2b – The parameter is optimized based on current membership property using **Maximization step**.

$$w_l^{j+1} = \sum_{\vec{u} \in N} w_l^j(\vec{u})$$

$$\vec{\mu}_l^{j+1} = \frac{\sum_{\vec{u} \in N} w_l^j(\vec{u}).\vec{u}}{\sum_{\vec{u} \in N} w_l^j(\vec{u})}$$

$$\Sigma_l^{j+1} = \frac{\sum_{\vec{u} \in N} w_l^j(\vec{u})(\vec{u} - \vec{\mu}_l^{j+1})(\vec{u} - \vec{\mu}_l^{j+1})^T}{\sum_{\vec{u} \in N} w_l^j(\vec{u})}$$

IX.A (5) HISTOGRAM

A histogram is an accurate representation of distribution of numerical data. It is an estimate of the probability distribution of a continuous variable.

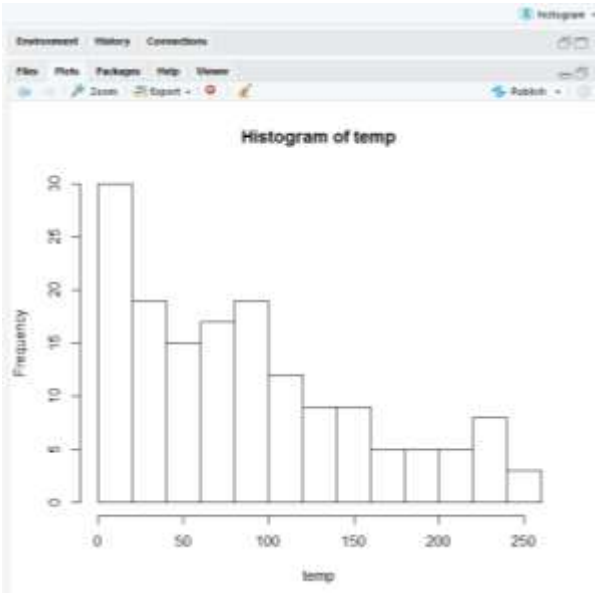

Fig IX: A(5) Histogram

X. CONCLUSION

In this paper, we proposed risk assessment approach to assign risk score to each OSN user. This assessment is based on user behavior under idea more user behavior diverge, it is considered to be risky. This analysis is carried out in Facebook dataset for effectiveness of our estimation.

REFERENCES

[1] Naeimeh Laleh, Barbara Carminati and Elena Ferrari. Risk Assessment in Social Networks based on User Anomalous Behaviours.2014.
[2] Ravneet kaur, Sarbjeet Singh. A survey of data mining and social network analysis based on anomaly detection techniques.2015
[3] Flora Amato, Giovanni Cozzolino, Antonino Mazzeo, and Sara Romano. Detecting anomalies in twitter stream for public security issues.2016.
[4] Naeimeh Laleh, Barbara Carminati and Elena Ferrari. Anomalous change detection in time-evolving OSNs.2016.
[5] Renjun Hut, Charu C.Aggarwal, Shuai Mat and Jinpeng Huait.An embedding approach to anomaly detection.2016.
[6] Weiling Chen, Chan Kiat Yeo, Chiew Tong Lau,Bu Sung Lee,Behavior Deviation:An Anomaly Detection View of Rumor Preemption 2016.
[7]Shan-Hung Wu, Man-Ju Chou, Chun-Hsiung Tseng, Yuh-Jye Lee, and Kuan-Ta Chen, Senior Member, IEEE.

IEEE

PSES
Product Safety Engineering Society

8TH INTERNATIONAL CONFERENCE ON ENGINEERING AND ADVANCEMENT IN TECHNOLOGY-2018

ORGANIZED BY

ORGANIZATION OF SCIENCE & INNOVATIVE ENGINEERING AND TECHNOLOGY (OSIET). CHENNAI, INDIA.

IN ASSOCIATION WITH

SRI KRISHNA
COLLEGE OF TECHNOLOGY
An Autonomous Institution | Accredited by NBA & NAAC with A Grade

SRI KRISHNA INSTITUTIONS

Department of Electronics and Communication Engineering
&
Department of Electrical and Electronics Engineering

Certificate of Presentation

This is to certify that .....T. RAMPRAKASH..... *from* RAMCO INSTITUTE OF TECHNOLOGY..... *has presented a paper titled* SMART DOOR LOCK SYSTEM USING QUICK RESPONSE CODE ENCRYPTION AND BLUETOOTH TECHNOLOGY..... *in the "International conference on Engineering and Advancement in Technology" held on 22nd & 23rd, March 2018.*

Dr. P. Aravinthan, M.E., Ph.D.
Technical Head, OSIET
Secretary

Prof. A. Krishnamoorthy, M.E., (Ph.D)
Technical Head, OSIET
Administrator

Dr. S.Vijayakumar, M.Tech., Ph.D
Vice Chairman
IEEE Product Safety Engineering Society, Madras Chapter

K.Janani, M.Tech.,
CEO, OSIET
Director

SMART DOOR LOCK SYSTEM USING QUICK RESPONSE CODE ENCRYPTION AND BLUETOOTH TECHNOLOGY

T.Ramprakash[1], B.Veeramani Viswanathan[2], T.Subash Chandra Bose[3] and K.Satheesh Kumar[4]

[1] Assistant professor, Department of ECE, Ramco Institute of Technology.
[2, 3, 4] UG Students, Department of ECE, Ramco Institute of Technology.
(ramprakasht@ritrjpm.ac.in, viswanathanv96@gmail.com, bosetamilselvan@gmail.com, satheesh1419kumar@gmail.com)

***Abstract*—Smart door lock system aims at developing a smart and safe security system using QR code encryption, Bluetooth and GSM Technology. In this system, a mobile application is created in which the users name and details are taken as input. Once the data is input, a QR code scanner from the app opens. With the help of the scanner, the QR code affixed to the main door, is scanned. If the reference key in the owner's mobile phone is same as that of the code in the door, the app sends a signal along with the user's detail to the microcontroller, via Bluetooth. If the details are verified correct, the microcontroller opens the door and sends an SMS along with the user's detail to the owner's mobile using GSM technology. The code on the door is generated using ESP32 and OLED display.**

Keywords—Bluetooth, GSM technology, Microcontroller, Quick Response Code, Mobile Application, ESP32, OLED

I. INTRODUCTION

In some high security areas, the gateways and entrance are not so secured. In spite of high security, they are easily breached without any acknowledgement. In order to overcome the disadvantages, we have designed a smart security lock. The main aim of the project is to develop a smart and safe door lock system which uses QR code encryption and GSM Technology. In this project, a mobile application is created in which the users name and details are taken as input. Once the data is input, a QR code scanner from the app opens. With the help of the scanner, the QR code affixed to the main door, is scanned. If the reference key in the owner's mobile phone is same as that of the code in the door, the app sends a signal along with the user's detail to the microcontroller, via Bluetooth. If the details are verified correct, the microcontroller opens the door and sends an SMS along with the user's detail to the owner's mobile using GSM technology. The code on the door is generated using ESP32 development board and OLED display [1] [2] [3].

II. COMPONENTS

A. *Arduino:*

Arduino is an open source, computer hardware and software company, project, and user community that designs and manufactures microcontroller kits for building digital devices and interactive objects that can sense and control objects in the physical world. The project's products are distributed as open-source hardware and software, which are licensed under the GNU Lesser General Public License (LGPL) or the GNU General Public License (GPL), permitting the manufacture of Arduino boards and software distribution by anyone. Arduino board designs use a variety of microprocessors and controllers. The boards are equipped with sets of digital and analog input/output (I/O) pins that may be interfaced to various expansion boards (shields) and other circuits. The boards feature serial communications interfaces, including Universal Serial Bus (USB) on some models, which are also used for loading programs from personal computers. The microcontrollers are typically programmed using a dialect of features from the programming languages C and C++the Arduino project provides an Integrated Development Environment (IDE) based on the Processing language project.
Arduino microcontrollers are pre-programmed with a boot loader that simplifies uploading of programs to the on-chip flash memory. The default boot loader of the Arduino UNO is the optiboot loader. Boards are loaded with program code via a serial connection to another computer.Some serial Arduino boards contain a level shifter circuit to convert between RS-232 logic levels and transistor–transistor logic (TTL) level signals. Current Arduino boards are programmed via Universal Serial Bus (USB), implemented using USB-to-serial adapter chips such as the FTDI FT232. Some boards, such as later-model Uno boards, substitute the FTDI chip with a separate AVR chip containing USB-to-serial firmware, which is reprogrammable via its own ICSP header. Other variants, such as the Arduino Mini and the unofficial BoArduino, use a detachable USB-to-serial adapter board or cable, Bluetooth or other methods, when used with traditional microcontroller tools instead of the Arduino IDE, standard AVR in-system programming is used.

B. *Arduino Software:*

A program for Arduino may be written in any programming language for a compiler that produces binary machine code for the target processor. Atmel provides a development environment for their microcontrollers, AVR Studio and the newer Atmel Studio. The Arduino project provides the Arduino integrated development environment (IDE), which is a cross-platform application written in the programming language Java. It originated from the IDE for the languages Processing and Wiring. It includes a code editor with features such as text cutting and pasting, searching and replacing text, automatic indenting, brace matching, and syntax highlighting, and provides simple one-click mechanisms to compile and upload programs to an Arduino board. It also contains a message area, a text console, a toolbar with buttons for common functions and a hierarchy of operation menus.
A program written with the IDE for Arduino is called a sketch. Sketches are saved on the development computer as text files with the file extension.ino. Arduino Software (IDE) pre-1.0 saved sketches with the extension .pde. The Arduino IDE

supports the languages C and C++ using special rules of code structuring. The Arduino IDE supplies a software library from the Wiring project, which provides many common input and output procedures. User-written code only requires two basic functions, for starting the sketch and the main program loop, that are compiled and linked with a program stub main() into an executable cyclic executive program with the GNU tool chain, also included with the IDE distribution. The Arduino IDE employs the program avrdude to convert the executable code into a text file in hexadecimal encoding that is loaded into the Arduino board by a loader program in the board's firmware.

A minimal Arduino C/C++ sketch, as seen by the Arduino IDE programmer, consist of only two functions:

• Setup: This function is called once when a sketch starts after power-up or reset. It is used to initialize variables, input and output pin modes, and other libraries needed in the sketch.

• Loop: After setup has been called, function loop is executed repeatedly in the main program. It controls the board until the board is powered off or is reset.

Thus the Arduino helps to interface Bluetooth with the application in the mobile phone. It also helps in the process of interfacing GSM with the door locking system for sending SMS to the owners.

C. MIT App Inventor 2:

App Inventor for Android is an open-source web application originally provided by Google, and now maintained by the Massachusetts Institute of Technology (MIT).It allows newcomers to computer programming to create software applications for the Android operating system (OS). It uses a graphical interface, very similar to Scratch and the StarLogo TNG user interface, which allows users to drag-and-drop visual objects to create an application that can run on Android devices. App Inventor and the projects on which it is based are informed by constructionist learning theories, which emphasizes that programming can be a vehicle for engaging powerful ideas through active learning. As such, it is part of an ongoing movement in computers and education that began with the work of Seymour Papert and the MIT Logo Group in the 1960s and has also manifested itself with Mitchel Resnick's work on Lego Mindstorms and StarLogo. This software is used for the purpose of creating the mobile application required for the scanning of QR codes.

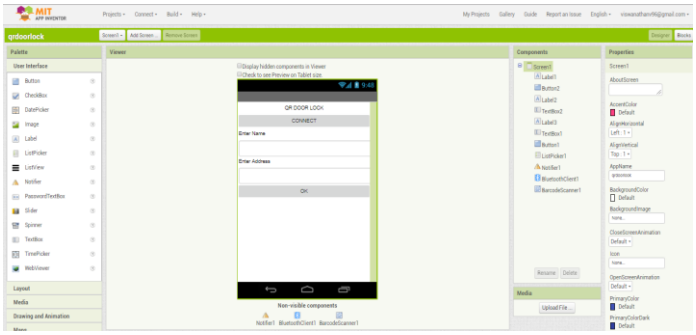

FIGURE. 1 (*MIT APP INVENTOR 2*)

D. Global System for Mobile Communications:

GSM (Global System for Mobile Communications) is a standard developed by the European Telecommunications Standards Institute (ETSI) to describe protocols for second-generation (2G) digital cellular networks used by mobile phones .The GSM module is interfaced with the Arduino for sending messages at time of opening the door. The port number 9, which is TX port of Arduino, is interfaced to GSM module via RX port of GSM and the GND port of GSM is grounded.

E. Relay:

A relay is an electrically operated switch. Many relays use an electromagnet to mechanically operate a switch, but other operating principles are also used, such as solid-state relays. Relays are used where it is necessary to control a circuit by a separate low-power signal, or where several circuits must be controlled by one signal. The first relays were used in long distance telegraph circuits as amplifiers: they repeated the signal coming from one circuit and re-transmitted it to another circuit. Relays were used extensively in telephone exchanges and early computers to perform logical operations. This relay switch is used for the purpose of controlling the actions of the door lock using the signals from the Arduino.

F. Solenoid Door Lock:

In physics, the term solenoid refers to a coil whose length is substantially greater than its diameter, often wrapped around a metallic core, which produces a uniform magnetic field in a volume of space (where some experiment might be carried out) when an electric current is passed through it. A solenoid is a type of electromagnet when the purpose is to generate a controlled magnetic field. If the purpose of the solenoid is instead to impede changes in the electric current, a solenoid can be more specifically classified as an inductor rather than an electromagnet. Here, the same principle of solenoid is employed in electric locks to control the opening and closing of lock levers.

G. Bluetooth Module HC-05:

HC-05 module is an easy to use Bluetooth SPP (Serial Port Protocol) module, designed for transparent wireless serial connection setup.

Serial port Bluetooth module is fully qualified Bluetooth V2.0+EDR (Enhanced Data Rate) 3Mbps Modulation with complete 2.4GHz radio transceiver and baseband. It uses CSR Blue core 04-External single chip Bluetooth system with CMOS technology and with AFH (Adaptive Frequency Hopping Feature). It has the footprint as small as 12.7mmx27mm. Using this module, the mobile app communicates with the Arduino microcontroller [4].

H. ESP32 development board:

SP32 is a series of low cost, low power system on a chip microcontrollers with integrated Wi-Fi and dual-mode Bluetooth. The ESP32 series employs a Tensilica Xtensa LX6 microprocessor in both dual-core and single-core variations and includes in-built antenna switches, RF balun, power amplifier, low-noise receive amplifier, filters, and power management modules. It is a successor to the ESP8266

microcontroller. [6]The ESP32 module gives input to the OLED Display to generate the required QR Code.

I. OLED display (SSD1306):

An organic light-emitting diode (OLED) is a light-emitting diode (LED) in which the emissive electroluminescent layer is a film of organic compound that emits light in response to an electric current. This layer of organic semiconductor is situated between two electrodes; typically, at least one of these electrodes is transparent. OLEDs are used to create digital displays in devices such as television screens, computer monitors, and portable systems such as mobile phones, handheld game consoles and PDAs. A major area of research is the development of white OLED devices for use in solid-state lighting applications.Thus, the OLED display converts the input from ESP32 into visible QR Code in it [6].

III. BLOCK DIAGRAM DESCRIPTION OF THE SYSTEM

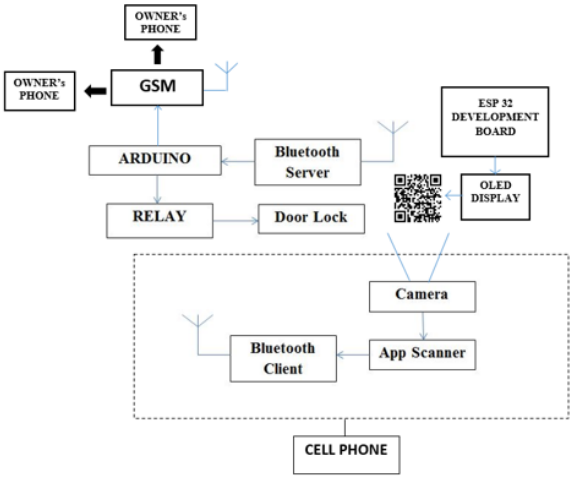

FIGURE. 2 (*BLOCK DIADRAM*)

The block diagram shows the connection of Arduino, Bluetooth module, Relay, GSM module, ESP32, OLED display and Solenoid Door lock. The working of the system, can be divided into 3 stages:

A. User details input stage:

Once the Bluetooth connection is set up with HC-05, the user who has to open the door has to input the username and his set password or address in the mobile application created. After typing OK button is pressed. Once the button is pressed, the user details are sent to the Arduino through Bluetooth for registration. Following the user details input stage, scanning of QR codes take place.

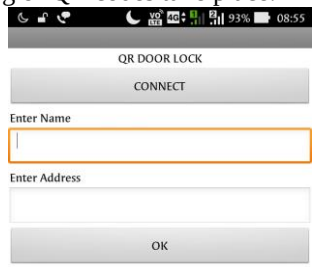

FIGURE. 3 (APP *INPUT STAGE*)

B. Scanning of QR Code:

Once the QR scanner from the app opens, the QR code affixed to the door is scanned. The app decodes the QR code and verifies it with the key in the app. If the verification is correct, the app sends a string key to the Arduino via Bluetooth.

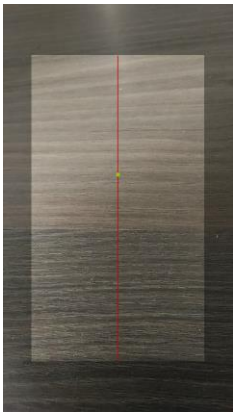

FIGURE. 4 (*QR CODE SCANNER*)

C. Verification and Intimation using GSM:

In the Arduino, the code developed verifies the sent string from the app. After verification, the code sets the AT commands for GSM to send SMS intimation to the owners. For each user who is accessing the door, a separate SMS along with the input details is sent to the owners [5].

FIGURE. 5 (*INTIMATION USING GSM*)

D. QR Code Generation Unit:

Using ESP32, QR codes can be generated through Arduino programming. The output from this development board can be displayed by using an OLED display [6].

E. Operation of solenoid lock:

Once after the verification is finished, the relay input is given high and hence relay opens up the solenoid lock according to the delay set. Once the delay ends, the lock closes automatically.

IV. FLOWCHART

A. *Mobile application flowchart:*

The flow of process happening in the Mobile application created is explained in this flowchart,

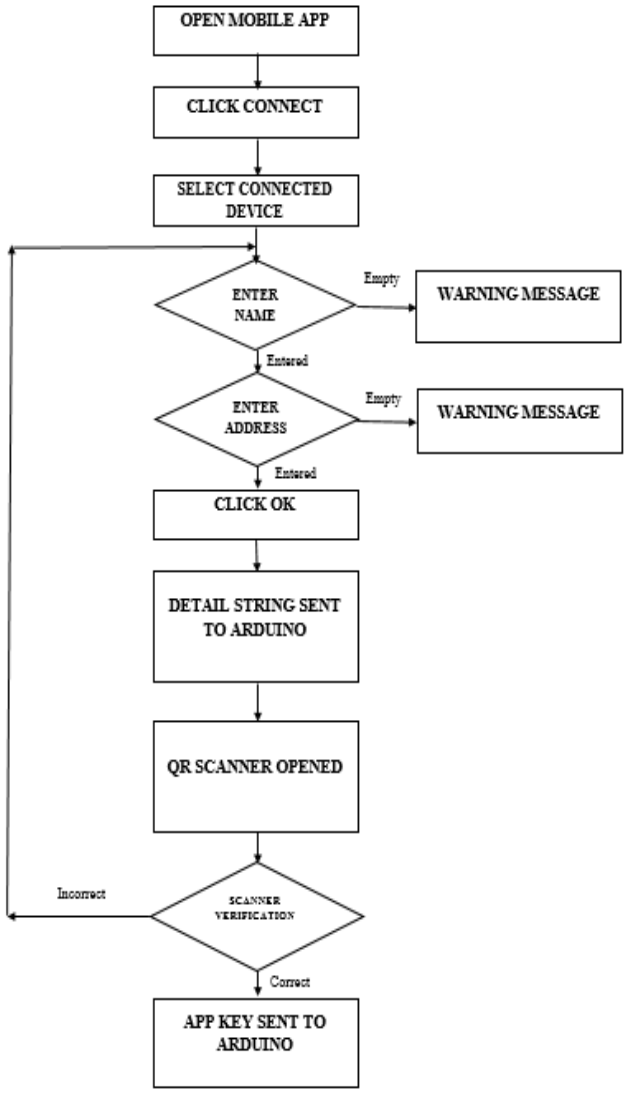

FIGURE. 6 (*Mobile app flowchart*)

First, the mobile application is opened. Following this a connection is set between the mobile phone and the Bluetooth module of Arduino.

After connecting, the name and address of the user is typed in the app and 'OK' is pressed.

Once 'OK' is pressed, the details are sent to the Arduino and a QR scanner opens up.

The QR Scanner is capable of scanning the QR code on the OLED display. The decoded data is verified with a string already present in the app.

If the verification is correct, a special unique key is sent to the Arduino via Bluetooth.

B. *Arduino flowchart:*

The flow of process happening in Arduino is explained in the below flowchart,

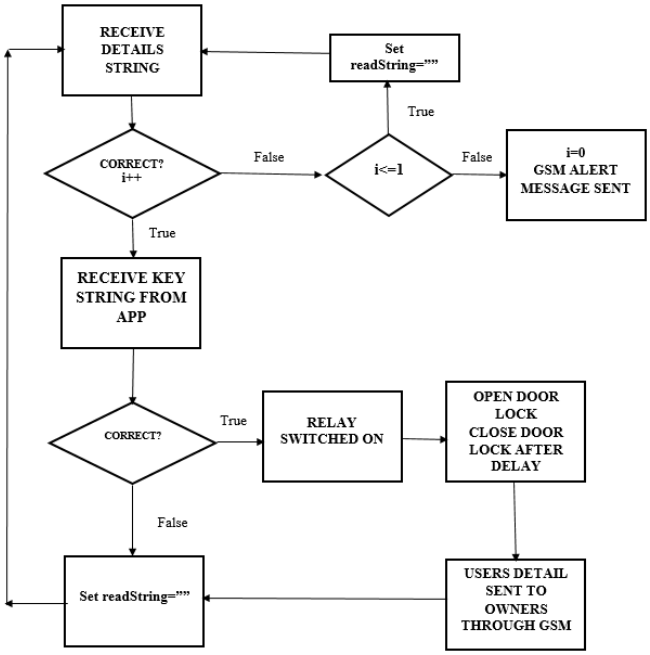

FIGURE. 7 (*Arduino flowchart*)

Set i=0

Once the details string from the app is received, the details are verified with the set strings in the arduino.

If correct, the second key is evaluated.

If wrong, second chance is given.

If both the chances goes wrong, intruder alert message is sent to the owners.

If the second key is correct, the relay switch is turned ON and the user details are sent through SMS to the owners.

The relay switch controls the opening and closing of the lock lever.

V. RESULTS AND CONCLUSION

QR code encryption used in security systems has enormous uses compared to old bar code systems, GSM based systems[5][7], Wi-Fi systems[8], NFC systems[9] and RFID systems like, they can store lots of data in a single QR code which can't be generated or decrypted easily without verification. As every systems has some pros and cons, this system has cons in terms of cost, even though in the recent years the cost has reduced. While RFID tags have issues for end users privacy especially in case of health care which is concerned with transmission frequency and access to unauthorized people, QR codes along with the mobile app can maintain access to specific authorized people only.

VI. Future Scope

Along with the system, an acknowledgement based control of the lock system can be introduced. The QR code displayed can be made different from time to time so as to improve the security.

References

[1] Kun Xie; Sebastien Gaboury; Sylvian Halle; Real Time Streaming Communication with Optical Codes; IEEE Access, Volume 4,pp.284-298,Jan 2016

[2] Pei-Yu Lin; Distributed Secret Sharing Approach with Cheater prevention Based on QR Code; IEEE Transactions on Industrial Informatics, Volume 12, No.1,pp.384-392

[3] Iiliia Tkachenko, William Puech, Christophe Destruel, Olivier Strauss, Jean-Marc Gaudin, Christian Guichard; Two-Level QR code for Private Message Sharing and Document Authentication; IEEE Transaction on Information Forensics and Security; Volume 11,No.3,pp.571-583

[4] Anisha Cotta, Naik Trupti Devidas, Varda Kalidas Naik Ekoskar; Wireless Communication using HC-05 Module Interfaced with Arduino; IJSETR, Volume 5, Issue 4,pp.869-872

[5] Amruta Patil, Pooja Potnis, Karishma Katkar; SMS Based Home Automation System using arduino ATMEG328 with GSM; International Journal of Engineering Trends and Technology (IJETT) – Volume 47 Number 7; pp.369-374

[6] Ravi Kishore Kodali and Kopulwar Shishir Mahesh; Smart Emergency Response System; Proc. of the 2017 IEEE Region 10 Conference (TENCON); pp. 712-717

[7] Adnan Ibrahim, Afhal Paravath, Aswin P. K., Shijin Mohammed Iqbal and Shaeez Usman Abdulla; GSM Based Digital Door Lock Security System; 2015 IEEE International Conference on Power, Instrumentation, Control and Computing (PICC);

[8] Abdallah Kassem and Sami El Murr; A Smart Lock System using Wi-Fi Security; 2016 3rd International Conference on Advances in Computational Tools for Engineering Applications (ACTEA); pp.222-225

[9] Chi-Huang Hung , Ying-Wen Bai, Je-Hong Ren; Design and Implementation of a Door Lock Control Based on a near Field Communication of a Smartphone; 2015 International Conference on Consumer Electronics-Taiwan (ICCE-TW); pp.44,45

Proceedings of the First National Conference on

ADVANCED TECHNOLOGIES IN ROBOTICS AND INDUSTRIAL AUTOMATION (ATRIA 2018)

Editor In-Chief

Dr. S. POORNACHANDRA
DEAN EIE & BME
SNS College of Technology

Editors

Ms. Poorani .V, Assistant Professor/EIE
Mr. Samba Siva Rao. K, Assistant Professor/ EIE
Ms. Brindha. M, Assistant Professor/ EIE

Organized by

Department of Electronics and Instrumentation Engineering
SNS College of Technology
Coimbatore - 641 035

INDEX

7076

AUTOMATIC GAS LEAKAGE DETECTION, ALERTING AND BOOKING SYSTEM USING GSM

Anupriya M, Jeyaselvi S, Kalaiarasi Rand Ramalakshmi R
Ramco Institute of Technology, Rajapalayam

ABSTRACT

Gas stoves are now very common in all houses including rural and remote areas. The main source of energy for gas stoves are either LPG or Biogas. Therefore safety plays a major role in today's world and it is necessary that good safety system is to be implemented in homes. The leakage of hazardous gases like LPG and propane are sensed using gas sensors (MQ-6). If these gases exceed the threshold level, the alarm is generated immediately and an alert message is sent to the authorized person using GSM. In order to avoid explosion the regulator is automatically turned off and also the relay switch is used to trip the main power supply off which will prevent electrical sparks. In this project a smart gas system is proposed, that will automatically turn ON the gas cylinder's regulator when the vessel is present on the stove holder and in the absence of vessel, the knob will be turned to OFF position. Continuous weight measurement of cylinder is done using a load cell which is interfaced with a Microcontroller. When the gas cylinder reaches lower weight threshold, SMS is sent automatically to the gas provider using GSM.

Key words: GSM, Load cell, Relay, Arduino, Gas leakage detection, Smart Alerting Techniques.

SNS COLLEGE OF TECHNOLOGY

(An Autonomous Institution)

Approved by AICTE, Affiliated to Anna University & Accredited by NAAC with A+ Grade

Sathy main road, saravanampatti(post), Coimbatore-35.

DEPARTMENT OF ELECTRONICS AND INSTRUMENTATION ENGINEERING

NATIONAL CONFERENCE ON

ADVANCED TECHNOLOGIES IN ROBOTICS AND INDUSTRIAL AUTOMATION

This is to certify that ~~Dr./Prof./Mr./Ms.~~ R. RAMALAKSHMI ASST. PROF. / ECE

of RAMCO INSTITUTE OF TECHNOLOGY

has presented a paper entitled AUTOMATIC GAS LEAKAGE DETECTION, ALERTING AND BOOKING SYSTEM In the National Conference on Advanced Technologies In Robotics and Industrial Automation ATRIA 2018 held at SNS College Of Technology, Coimbatore on 22 March 2018.

Organizing Secretary	Convenor	Chair	Principal
(Ms.V.Poorani)	(Dr.S.Poornachandra)	(Mr.J.VishnuVardhan) (MD,TREND Instrumentation and Automation Pvt.Ltd.)	(Dr.S.Chenthur Pandian)

RAMCO INSTITUTE OF TECHNOLOGY

(Approved by AICTE, New Delhi and Affiliated to Anna University, Chennai)

Rajapalayam - 626 117, Tamil Nadu.

National Conference on
Innovations in Communication Technology for Social Development

ICTSD-2018

CERTIFICATE

This is to certify that ~~Dr./Mr./Ms.~~ ...D..GOPINATH..... *of* ..RAMCO....INSTITUTE ..OF...TECHNOLOGY..... *presented a paper entitled* .WIRELESS....HEALTH..MONITORING ..SYSTEM...USING...MOBILE.....PHONE.....*in the National Conference on Innovations in Communication Technology for Social Development - ICTSD, organised by Department of Electronics and Communication Engineering in association with IETE student forum on 23rd March, 2018.*

Convenor

Principal

RAMCO INSTITUTE OF TECHNOLOGY

(Approved by AICTE, Affiliated to Anna University, Chennai)
Rajapalayam – 626117, Virudhunagar Dist.

National Conference on

Innovations in Communication Technology for Social Development

ICTSD-2018

CHIEF PATRON

Shri.P.R.Venketrama Raja
Chairman, Ramco Group

PATRON

Dr.R.Venkatraj
Chief Educational Officer

Dr.R.V.Mahendra Gowda
Principal
Ramco Institute of Technology

CONVENOR

Dr.S.Periyanayagi
Associate Professor/ECE

CO-ORDINATORS

Mrs.R.Ramalakshmi, Asst. Prof.
Mr.D.Gopinath, Asst. Prof.

A WIRELESS HEALTH MONITORING SYSTEM USING MOBILE PHONE ACCESSORIES

D.Gopinath*, S.E.Padma Gokila, M.Shenbagavalli and P.Umamaheswari
Department of Electronics and Communication Engineering, Ramco Institute of Technology, Rajapalayam.

Health monitoring system is commonly implemented to continuously track human health condition. Heart rate and body temperature are two important parameters to maintain a vital life. The prototype of the wireless health monitoring is to focus on measuring real time ECG and temperature. In this paper describes the development and software to enable the use of android mobile phones equipped with Bluetooth to receive the incoming electrocardiogram(ECG) signal and temperature values from a user. The proposed hardware system consists of single chip microcontroller Arduino, ECG sensor , LM35 sensor , BLE module HC-05.

AUTOMATED GRASPING DISTALS

S.Nirmal Kumar, S.Padmasubash, M.Paulraj and S.Valai Ganesh*
Department of Mechanical Engineering, Ramco Institute of Technology, Rajapalayam.

Achieving development in end effectors to grasp the object and getting motion as like a human hand for material handling application which will be flexible with our requirement in different environment by means of programming and exploring Mechatronics knowledge.

SMART HELMET BY USING ARDUINO FOR TWO WHEELERS

R.Dineshkumar, R.Kanaga Raj, Kishore Kumar, M.Manicka Raj, Mr.M.Sivagaminathan* and T.Ramprakash*
Department of Mechanical Engineering, Ramco Institute of Technology, Rajapalayam.

Smart helmet is the idea that has been developed for the social responsibility towards the society. In current trends, two wheelers are increasing tremendously in which Helmet is most popular form of head protection. Smart Helmet is the adding of features for safety purpose in helmet. The smart helmet consists of ultrasonic sensor for the safety measurements if any obstacles are present while driving. The GPS and GSM900a module for finding the two wheeler's location after the accidents occurred. These sensors are connected with microcontroller which set in the helmet. The camera is used for the investigation purpose if any accident happens .The transparent visor has the better vision during fog conditions.

MODIFIED CASCADED MULTILEVEL INVERTER FOR HOUSEHOLD APPLIANCES

Dr.K.Karthikeyan*, P.Moses Stephen, M.Ponraj,N.Sathesh and K.Balamurugan
Department of Electrical and Electronics Engineering, *Ramco Institute of Technology, Rajapalayam.*

The inverter is used for DC to AC conversion. A multilevel inverter is one in which a complete cycle of output waveform contains more than three DC levels. Increasing the number of voltage levels in the inverter output can increase the power rating without requiring higher ratings on individual devices. These multilevel inverters requires split sources depending on the voltage levels that are meant to be produced. This project is mainly focused on the development of single phase cascaded type multilevel inverter for a domestic application using Pulse Width Modulation (PWM) technique and elimination of harmonic distortion and its effects.